Sheffield Hallam University

A Sheffield Hallam University thesis

REFERENCE

ProQuest Number: 10697370

ProQuest 10697370

Synthesis and Characterisation of Some Solvatochromic Betaine Systems

Joanne Patricia Louise Mifflin (BSc Hons)

A thesis submitted in partial fulfilment of the
requirements of Sheffield Hallam University
for the degree of Doctor of Philosophy

October 1998

ABSTRACT

This thesis is concerned with the synthesis and characterisation of five new types of solvatochromic systems and preliminary investigations into the synthesis of some new systems involving several such chromophoric units. Confirmation of the structure of these systems was carried out by NMR (^{31}P and ^{1}H), and mass spectral analysis, together with the results of microanalysis. The solvatochromic behaviour was investigated in detail, by dissolution in a range of solvents and measurement of their longest-wavelength absorption bands using UV/Visible spectroscopy.

A range of long chain phosphoniophenyl-imidazolide betaine systems and long chain 4-N-(o-phosphoniobenzylidene) iminophenolate betaines has been prepared and their properties compared to the respective triphenylphosphonio analogues already reported in the literature. The formation of Langmuir Blodgett (LB) films by three of the amphiphilic betaines has been studied in collaboration with the University of Cranfield.

The effects of annelation of a benzene ring in the triphenylphosphoniophenyl-imidazolide and -benzylidene iminophenolate systems has been investigated and the effects on the solvatochromism of the resulting compounds has been explored. As part of this study two N-hexadecylquinolinium iminophenolate betaines have been prepared and their solvatochromism compared to that of the pyridinium counterparts. LB film formation of one of the quinolinium betaines has been studied, and nonlinear optical properties observed, together with other properties that may form the basis of sensor techniques.

The first solvatochromic arsonium and stibonium iminophenolate betaines have been prepared by a new synthetic procedure, and compared to their phosphonium counterparts.

All of the betaines studied display negative solvatochromism as the solvent polarity increases and their absorption maxima are linearly related with the standard E_T^N values for the Reichardt betaine dye, which suggests a possible application of these betaines as indicators of solvent polarity.

A new family of triphenylphosphonium salts employing different donor groups has been synthesised and converted into related phosphine oxides. The compounds were found not to be greatly solvatochromic.

Attempts to synthesise a range of "3-D" multi-chromophoric iminophenolate betaines have been carried out. However, at the present time the level of chromophore substitution is unknown, and the insolubility of the precursor salts has made isolation of the betaines very difficult. *In situ* formation of the betaines in the UV cell in a few solvents has shown the systems to be solvatochromic.

A quinolinium iminophenolate betaine has been covalently attached to a soluble polystyrene support. An LB film of the polymer bound betaine was formed at Cranfield University; however subsequent Surface Plasmon Resonance (SPR) studies were unsuccessful.

ACKNOWLEDGEMENTS

CONTENTS

CHAPTER 1

Introduction

CHAPTER 2

The Synthesis and the Characterisation of Phosphonium and Quinolinium Betaine Systems

CHAPTER 3

The Synthesis of Solvatochromic Aryl-arsonium and -stibonium Iminophenolate Betaines

CHAPTER 4

The Synthesis and the Characterisation of Push-Pull Triphenylphosphonium Salt Systems and their Respective Phosphine Oxides

CHAPTER 5

Preliminary Investigations of Multi-Chromophoric Systems

CHAPTER 6

Conclusions and Overview

1.0 Introduction

Of all known substances, water was the first to be considered as a solvent, and the Greek Alchemists gave all chemically active liquids or anything that was dissolved the name "Divine Water".

Between the 15th and 18th centuries it was believed that a substance disappeared upon dissolution. This theory was first opposed by Van Helmont who claimed that the nature of the substance was not lost, but present in solution, although in aqueous form and could be recovered.[1]

1.1 Solvent Polarity

It has long been known that solvents have a strong influence on reaction rates and chemical equilibria, as well as on the position of spectral absorption maxima. In 1862 Bérthelot and Péan de Saint-Gilles first observed the influence of solvents on the rates of chemical reactions whilst studying the esterification of acetic acid with ethanol.[2] Additionally, in 1890, Menschutkin concluded that "a chemical reaction cannot be separated from the medium with which it is performed".[3]

The influence of solvents on the position of chemical equilibria was reported in 1896 by Claisen,[4] Knorr,[5] Wislicenus[6] and Hantzch[7] simultaneously, at the same time as the discovery of keto-enol tautomerism in 1,3-dicarbonyl compounds. Solvents were, at this point, divided into two groups according to their ability to isomerise tautomeric compounds, and the classification by Stobbe[8] is very similar to some extent to the modern division into protic and aprotic solvents.

It is well known that the UV/Visible absorption spectra of certain compounds are influenced by the phase (liquid or gas) and that the solvent can bring about a change in the position, intensity, and shape of the absorption band. This was later termed *solvatochromism* by Hantzch,[9] although the meaning differs slightly from today's meaning.

The effect of the solvent on the rate of a chemical reaction has been considered in terms of *solvent polarity*, which is a parameter that cannot be defined in simple terms, or expressed quantitatively. The simplicity of idealised electrostatic solvation models has led to the use of physical parameters such as refractive index (n), permanent dipole moment (μ) and the static dielectric constant (ϵ_r) to determine the polarity of a solvent.

However, in practice, intermolecular interactions in solvent media are much more complicated than in theory. In addition to electrostatic forces arising from coloumbic effects between charged ions and dipolar molecules, (i.e. ion-ion, ion-dipole, dipole-dipole interactions)[10,11] and polarisation forces arising from dipole moments induced in molecules by nearby ions or dipolar molecules, (i.e. ion-nonpolar molecule, dipolar-nondipolar molecule, nonpolar-nonpolar molecules),[12] specific interactions such as hydrogen bonding,[13] electron-pair donor (EPD) and electron-pair acceptor (EPA) forces exist.[14,15] Mulliken described the latter as charge-transfer (CT) absorptions.[16]

Over the years, there have been many attempts at the classification of solvents. Five of these are as follows:-

- According to their chemical bonds
- Using physical constants
- Acid-base behaviour
- Specific solute/solvent interactions
- Multivariate statistical methods

More recently, Reichardt defined solvent polarity as *"the overall solvation capability (or solvation power) of a solvent"*.[17] The solvation capability is dependent on the action of all possible specific and non-specific intermolecular interactions between solute ions or molecules and solvent molecules, which excludes interactions leading to definite chemical alterations of the solute molecules or ions.

1.2 Solvatochromism

The well documented term *solvatochromism* refers to the shift of an electronic absorption band of a solute when the polarity of the solvent is varied. It is caused by differential solvation of the ground and first excited state of the light absorbing molecule or its chromophore. The solvatochromism of a compound is observed by means of UV/Visible measurements in solution. There are two types of solvatochromism which are:

Negative Solvatochromism.

The molecule undergoes a *hypsochromic* shift in which the longest wavelength charge–transfer absorption band increases in lower polarity solvents. With increasing polarity,

2

the ground state molecule is better stabilised by solvation than the molecule in the first excited state. This is also commonly known as a *"blue shift"*.

Positive Solvatochromism.

The molecule undergoes a *bathochromic* shift and the longest wavelength charge–transfer absorption band moves to a shorter wavelength in lower polarity solvents. There is better stabilisation of the molecule in the first excited state relative to that in the ground state, with increasing solvent polarity. This is also commonly known as a *"red shift"*.

The first excited state is the Franck-Condon excited state. The Franck-Condon principle states that a molecule gets electronically excited in a much shorter time than that required for a molecule to excite vibrations or rotations (about 10^{-15} s rather than 10^{-12}–10^{-10} s). The nucleii of the absorbing molecule and solvation shell do not appreciably alter their positions during an electronic transition.

Hence, the first excited state of a solvated molecule (Franck-Condon excited state), has the same solvation pattern as the corresponding ground state, and the ground state corresponds to an equilibrium ground state.

The observed solvatochromism depends on the physical properties and the chemical structure of the chromophore and the solvent. Strong solvatochromism is observed when the molecule exhibits a large change in its permanent dipole moment upon excitation; this is usually seen amongst compounds that are dyes.

If the solute dipole moment increases upon excitation, positive solvatochromism usually results ($\mu_g < \mu_e$), and negative solvatochromism is usually observed if the solute dipole moment decreases upon excitation ($\mu_g > \mu_e$).

The existence of *reverse solvatochromism* has also been observed among some molecules.[18,19] In solution, the solute molecule exhibits a bathochromic shift in polar solvents and a hypsochromic shift in non-polar solvents, or vice-versa. An example of this is the merocyanine dye 4-[2-methyl-4-pyridino)ethenyl]phenolate (1) which exhibits a hypsochromic shift of 178 nm from water (442 nm) to chloroform (620 nm) and then a bathochromic shift of 28 nm from chloroform (620 nm) to cyclohexane (592 nm).[20]

This reversed solvatochromism indicates that in solvents of low polarity the quinoid structure (1A) will predominate ($\mu_g < \mu_e$), and the benzenoid form (1B) only becomes the more stable structure in solvents of high polarity ($\mu_g > \mu_e$).

Me—N⬡=⬡=O   ⟷   Me—N⁺⬡—⬡—O⁻

<div align="center">

(1A)   (1B)

</div>
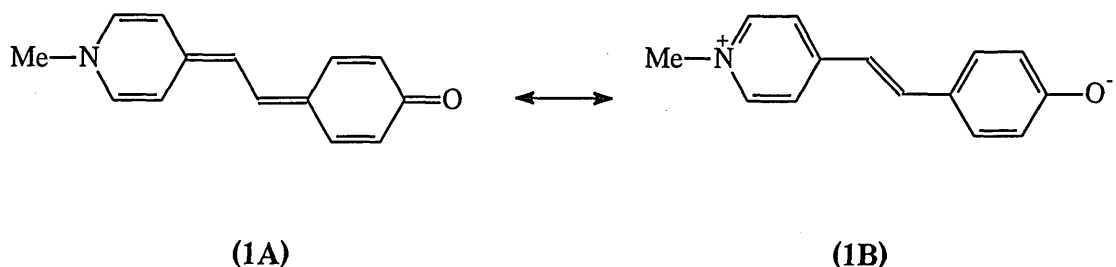
1.3   Empirical Scales of Solvent Polarity

Empirical scales of solvent polarity have been established due to the problem of defining *'solvent polarity'* in terms of simple physical parameters. Many solvent polarity scales have been developed over the years, and some are more reliable than others. This has been achieved by investigating the solvatochromism of various compounds. Some of the more useful scales are shown in table 1.

Name	Scale
Brooker *et al*[21,22]	X_R and X_B
Kosower *et al*[23]	Z
Kamlet *et al*[24,25]	π^*
Dahne *et al*[26]	RPM
Buncel *et al*[27]	π^*_{azo}
Middleton *et al*[28]	P_s
Reichardt and Dimroth[29]	E_T (30)
Walther[30]	E_K
Dubois *et al*[31]	ϕ
Zelinskii *et al*[32]	S
Wrona[33]	E_B

<div align="center">

Table 1 Selected scales of solvent polarity.

</div>

Brooker *et al* were the first to suggest that solvatochromic dyes should be used as indicators of solvent polarity[21,22] and the X_B (blue shift) and X_R (red shift) scales were defined. However Kosower was the first to establish an empirical solvent scale (Z scale).[23] Kosower suggested that the merocyanine dyes should not be used as solvent polarity indicators as the "dye molecules possess large π-electron systems which are

subject to specific interaction with solvent molecules, especially in the low polarity region". Also the "maxima change less in position with solvent change than the 1-alkylpyridinium complexes" which he used as his reference polarity indicator.[23]

Only four of the scales in table 1 are good models for solvent polarity as the compound used for each scale has significant solvatochromic properties. Most of the other scales are based on the spectral data of a single standard probe molecule, and so are limited in value when correlated against other solvent-dependant processes. This is because they correspond to a combination of specific and nonspecific solute/solvent interactions, which are only typical of the probe molecule.

The Z scale.

This scale was established in 1958,[23] using 1-ethyl-4-methoxycarbonyl pyridinium iodide (2) as the reference compound. The salt is negatively solvatochromic, and the longest wavelength band of the ground state ion-pair complex corresponds to the intermolecular transfer of an electron from the iodide ion to the pyridinium ion. The compound has a hypsochromic shift of 88 nm ranging from 342 nm in methanol to 430 nm in pyridine.

Unfortunately the pyridinium iodide indicator is almost completely insoluble in non-polar solvents (such as the hydrocarbons).

(2)
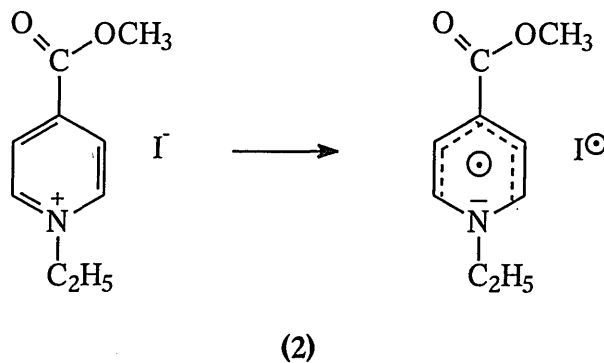
The π^* scale.

Kamlet based his scale on seven solvatochromic nitroaromatic indicators such as 4-methoxynitrobenzene (3) and 4-(diethylamino)-nitrobenzene (4), and is based on the solvent induced shifts of the longest wavelength $\pi - \pi^*$ absorption bands. The electronic transition in these compounds is due to the intramolecular charge-transfer (CT) from the electron-donor part of the molecule (OMe, NR_2, alkyl) to the electron-acceptor part (NO_2, COC_6H_5) via the aromatic system.

5

The longest intramolecular absorption band undergoes a bathochromic shift of 22 nm on going from dimethylsulphoxide (315 nm) to cyclohexane (293 nm) indicating that the first excited state is more polar than the ground state.

(3)   (4)
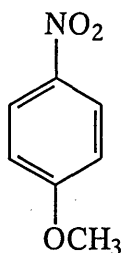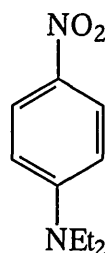
The π^*_{azo} scale.

The six indicators used were the positively solvatochromic azomerocyanine dyes, for example the 4-(1-methylpyridiniumazo)-2,6-disubstitutedphenolate (5) and the related benzothiazolium system (6). These azomerocyanine dyes seemed to be more appropriate than the nitroaromatic indicators used by Kamlet and coworkers. The positions of the absorption bands of the azomerocyanine dyes are in the region 440-590 nm which is further away from the cut off points of most solvents compared to the nitroaromatic indicators. This scale gave different values to the π^* scale of Kamlet but they were seen to correlate linearly with each other.[17] The π^*_{azo} scale correlates better with scales based on structurally similar dyes and dyes that are structurally similar to the azo merocyanines.

R = C$_6$H$_5$ or H

(5)

(6)

R = C$_6$H$_5$ or H
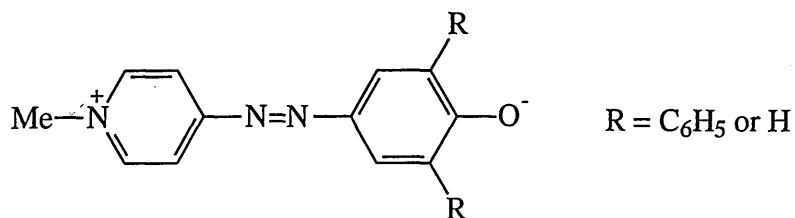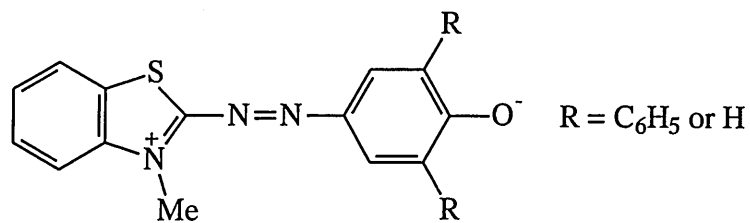
The E$_T$(30) scale.

This is by far the most important and well used scale, and was developed using the negatively solvatochromic pyridinium N-phenoxide dyes (7)[29] and (8).[34] The name E$_T$(30) was employed as dye (7) was listed as compound (30) in the first publication. Dye (7) is more commonly known as Reichardt's dye, which exhibits the largest solvatochromic shift ever observed to date. Its longest intramolecular charge-transfer band is shifted by 357 nm on going from water (453 nm) to diphenyl ether (810 nm).

Solutions of the dye are red in methanol, violet in ethanol, blue in isoamyl alcohol, green in acetone, and green-yellow in ethyl acetate, ranging over the whole visible region.

(7A)   (7B)
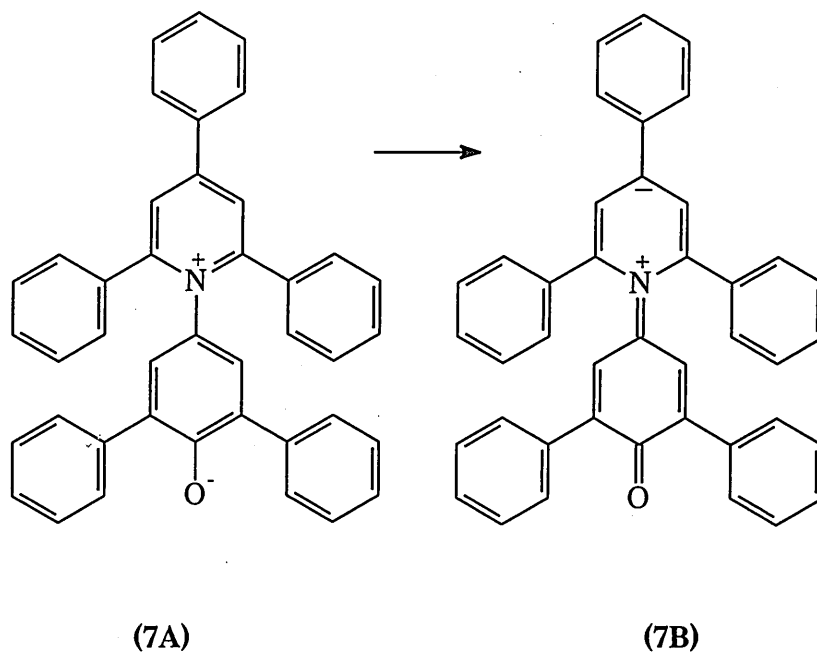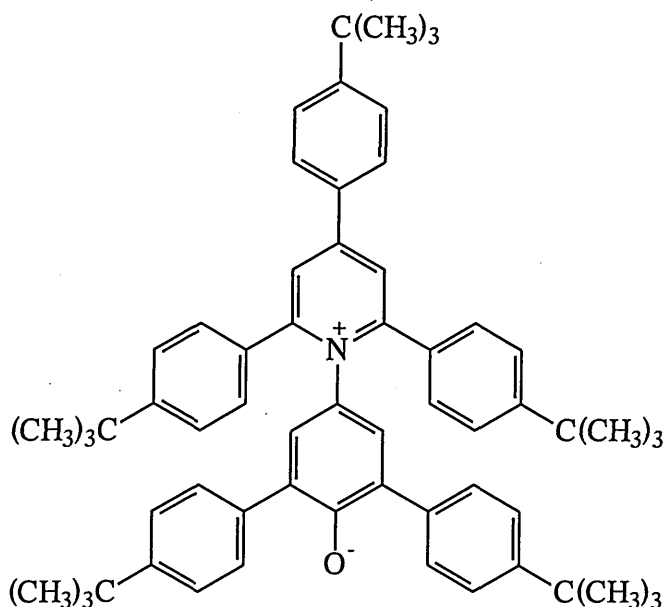
(8)

Reichardt's betaine dyes make good solvent polarity indicators because:-

- They exhibit large permanent dipole moments [(7) = 15 D in the ground state and 6 D in the excited state], suitable for dipole-dipole and dipole-induced dipole interactions between solvent and solute.

- There are 42-π electrons available for dispersion reactions.

- The phenolic oxygen atom is a highly basic electron-pair donor suitable for specific hydrogen-bond interactions with protic solvents.

The very large negative solvatochromism of (7) [and (8)] is due to the unequal differential solvation of its highly dipolar zwitterionic ground state e.g. (7A) relative to its less dipolar first excited (Franck-Condon) state e.g. (7B) with increasing solvent polarity. This is due to the considerable charge-transfer from the negatively charged phenolate moiety to the positive pyridinium part of the molecule.

Dye (8) is used as the indicator in extremely non-polar solvents as (7) is not soluble enough. There is excellent correlation between the E_T values of (7) and (8) in the twenty solvents in which they are both soluble. Subsequently, the $E_T(30)$ values have been calculated from the absorption maxima of both dyes and are defined as the molar electronic transition energies of the dyes, dissolved in the solvent, and measured in Kcal mol^{-1} at room temperature (25 °C) and normal pressure (1 bar) according to equation 1.

$$E_T(30)(Kcal\ mol^{-1}) = hc\nu_{max}N_A$$

$$= (2.8591 \times 10^{-3})\nu_{max}\ (cm^{-1})$$

$$= 28591/\lambda_{max}\ (nm) \qquad\qquad \text{(Equ. 1)}$$

where:-

h = Planck's constant = 6.62618×10^{-34} J s

c = speed of light in a vacuum = 2.99792×10^8 m s^{-1}

N_A = Avogadro's number = 6.02204×10^{23} mol^{-1}

ν_{max} = frequency of intramolecular charge-transfer absorption band ($\pi \rightarrow \pi^*$)

λ_{max} = wavelength of intramolecular charge-transfer absorption band ($\pi \rightarrow \pi^*$)

Equation 2 shows the calculation of the $E_T(30)$ values from dye (8).

$$E_T(30)(Kcal\ mol^{-1}) = ([28591/\lambda_{max}\ (nm)] - 1.808)/0.9424 \qquad \text{(Equ. 2)}$$

The $E_T(30)$ values range from 63.1 Kcal mol^{-1} for water (the most polar solvent) to 30.7 Kcal mol^{-1} for tetramethylsilane (TMS) (the least polar solvent). A normalised and dimensionless value (E_T^N),[34] was introduced as seen in equation 3, to avoid conversion from Kcal mol^{-1} to KJ mol^{-1}, using tetramethylsilane (TMS) and water as the extreme nonpolar and polar reference solvents, respectively. The E_T^N scale ranges from 0.000 (TMS) to 1.000 (water), and, as with the $E_T(30)$ scale, the higher the E_T^N value, the more polar the solvent.

The only drawback of this scale of solvent polarity is that the dyes (7) and (8) are not stable in strongly acidic solutions, such as acetic acid, as the phenolate oxygen atom is protonated, causing the solvatochromic charge-transfer absorption band to disappear, and the colour of the solution changes to pale yellow.

$$E_T^N = E_T(solvent) - E_T(TMS)\ /\ E_T(water) - E_T(TMS)$$

$$= (E_T(solvent) - 30.7)/\ 32.4 \qquad\qquad \text{(Equ. 3)}$$

Although there are many solvatochromic compounds, not all of them can be used as potential polarity indicators. A solvatochromic compound used to establish solvent polarity scales should meet the following requirements:-

- It should be easily available.

- It should be a crystalline compound of definite chemical structure.

- It should be sufficiently soluble in most solvents, which enables the indicator to be studied in non-polar through to polar solvents.

- No chemical reactions should occur with the solvent.

- The longest wavelength UV/Visible absorption band should be shifted hypsochromically or bathochromically with increasing solvent polarity to as great an extent as possible.

- The solvatochromic absorption band should be located preferably within the visible region of the electromagnetic spectrum.

- The molar extinction coefficient of the solvatochromic absorption band should be reasonably large, and not altered too much by different solvents. The Beer-Lambert law should also be followed in all solvents.

- The chemical structure of the indicator molecule should be of the kind to be involved in all important nonspecific and specific solvent interactions.

The E_T^N as well as the $E_T(30)$ values can be equally used; however the $E_T(30)$ values give an immediate indication of the solvent polarity whereas the E_T^N values are easier to use, especially in multiparameter correlation equations.

According to these two sets of values, organic solvents can be divided into several sets:-

- **HBD (Hydrogen-bonding donor) or "protic"**

  $E_T(30)$ 47-63 Kcal mol^{-1}; E_T^N 0.5-1.0

  E.g. methanol, ethanol

- **Dipolar non-HBD or "aprotic"**

  $E_T(30)$ 40-47 Kcal mol^{-1}; E_T^N 0.3-0.5

  E.g. acetonitrile, acetone

- **Apolar non-HBD**

  $E_T(30)$ 30-40 Kcal mol^{-1}; E_T^N 0.0-0.3

  E.g. ethyl acetate, toluene

1.4   Solvatochromic Compounds

Excluding the compounds used as solvent polarity indicators there are a large number of solvatochromic compounds that have been, and are still continuing to be reported in the literature, and it would be impossible to mention them all.

There have been many structural modifications of Reichardt's dye (7), with the aim of improving the solubility in hydrocarbons and water.[35] In all cases the negative charge of the betaine structure usually appears at an oxygen atom, as the result of proton removal from a phenolic hydroxy group.

However, the oxygen atom of (7) has been replaced by sulphur[36] leading to the thiophenolate betaine (9) which displays almost the same solvatochromism properties as (7); unfortunately it has been found to be very oxygen-sensitive. Gompper et al[37] were able to synthesise (10), only because proton removal from the corresponding acid was facilitated by the presence of the two electron withdrawing cyano groups.

(9)   (10)
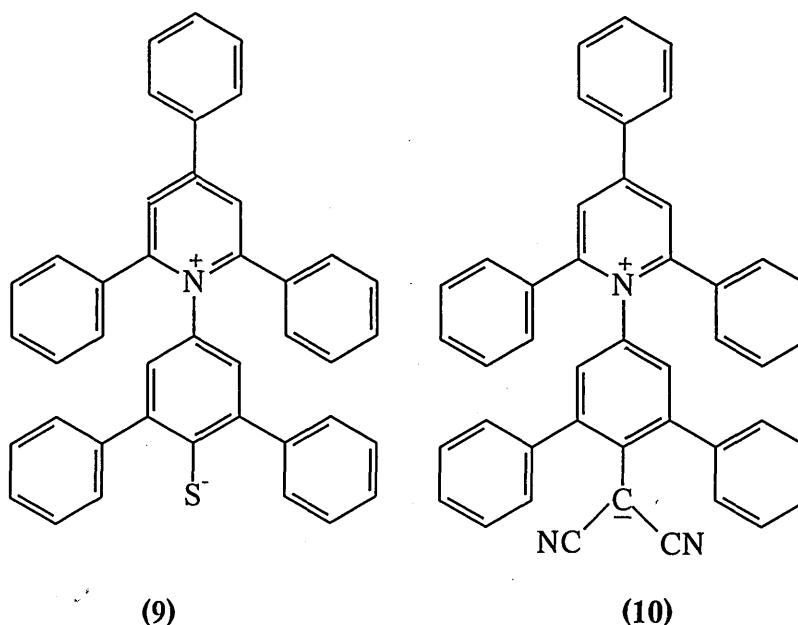
Milart et al[38] synthesised a new betaine (11) based on Reichardt's dye (7) with a positive and negative charge at two nitrogen atoms separated by an aromatic ring. The dye was found to be not quite as solvatochromic as (7) and its absorption maximum was 423 nm in methanol, compared to 515 nm for (7) and 545 nm in chloroform compared to 730 nm for (7). The hypsochromic shift observed is due to the intramolecular CT transition from the aminide moiety to the pyridinium ring.
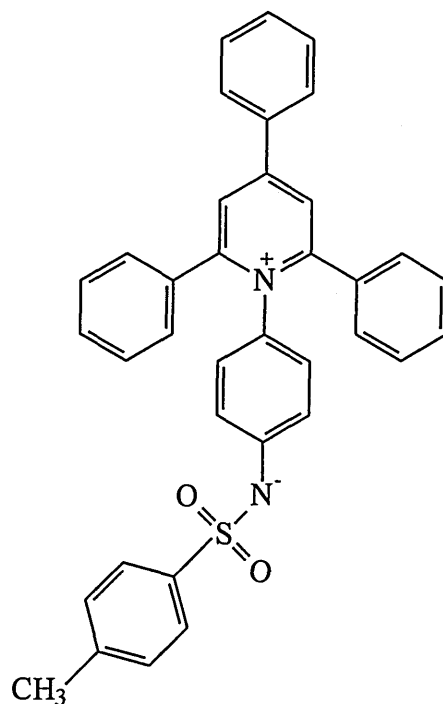
(11)

N^+N^- betaine dyes such as **(12)** with a direct bonding between the N^+ and the N^- moieties,[39,40,41] have been reported previously in the literature. However, when X = Ph (deep violet in solution) only a moderate hypsochromic shift was observed (λ_{max} = 588 nm in benzene and λ_{max} = 538 nm in methanol), as well as the solution being thermolabile and photochemically unstable.
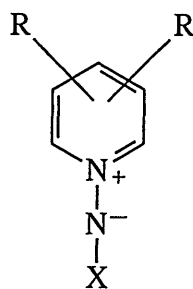
(12)

Introducing the electron-accepting substituents (X = -SO$_2$Ph,[42] -SO$_2$C$_6$H$_4$Me-p[43] and 2-py [44]) resulted in colourless betaines which underwent reactions resulting in cleavage of the N-N bond.

Merocyanine dyes constitute a class of compounds that have attracted great interest in past decades both from the theoretical, as well as from a practical point of view. As discussed earlier, Brooker et al [21] described the first merocyanine dye over

forty years ago, which was the starting point for structure variations that included modifications of the pyridinium or phenoxide rings, and that of the ethylene bridge.

Large *blue shifts* are shown by merocyanines of high polarity with long conjugated chains (insoluble in low polarity solvents), and *red shifts* are shown by certain less polar merocyanines (which are soluble in solvents of low polarity).

Buncel exchanged the stilbene linkage for the azo functionality,[27] in the process forming the π^*_{azo} scale, and more recently the linkage has been exchanged for an imino functionality[19] as in (13).

$$CH_3-N^+-CH=N-O^-$$
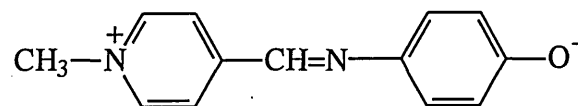
(13)

The isomers (14) and (15) were seen not to be as solvatochromic as (13), but still exhibited reverse solvatochromism. Compound (15) was insoluble in the non-polar solvents and was the least solvatochromic of the three isomers.
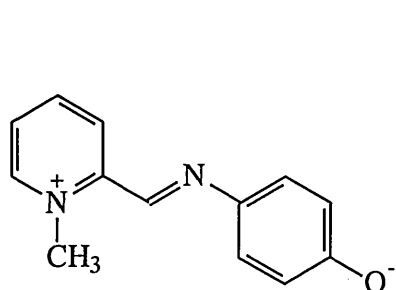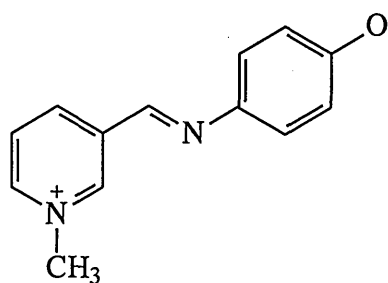
(14)   **(15)**

A range of stilbazolium merocyanine type dyes containing a benzo[a]quinolizinium ring[45] (16) and a benzo[c]quinolizinium[46] (17) ring have been reported and shown to exhibit a fair degree of solvatochromism.
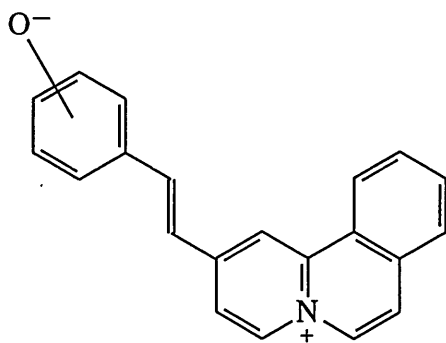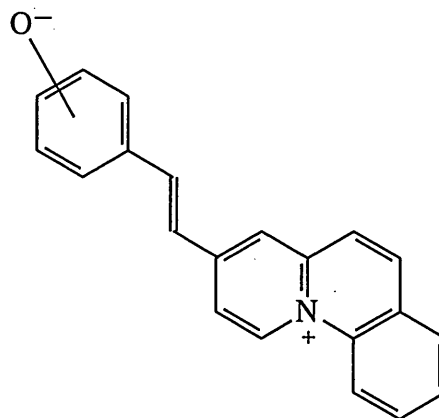
(16)   **(17)**

The longest intramolecular wavelength charge-transfer absorption bands of the betaines exhibited a hypsochromic shift, which extended almost over the whole visible region. The dyes containing the benzo[c]quinolizinium ring **(17)** were found to be more solvatochromic than the dyes containing the benzo[a]quinolizinium ring **(16)**.

For example, **(19)** had a λ_{max} ranging from 494 nm in methanol to 571 nm in acetone compared to **(18)**, which exhibited a λ_{max} of 485 nm in methanol and 556 nm in acetone.
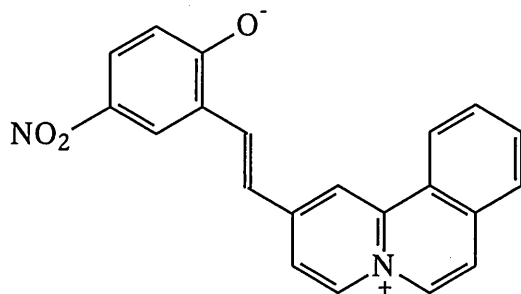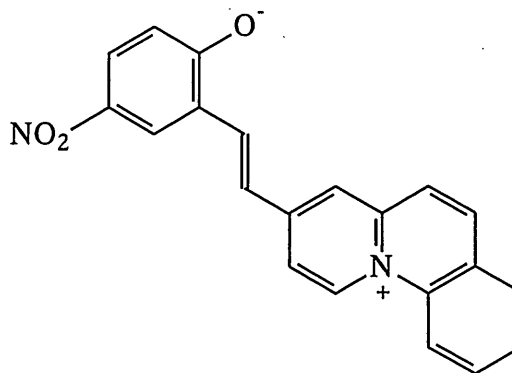
(18)   **(19)**

It was seen that increasing the electron-withdrawing ability of the substituents *para* to the phenoxide oxygen shifted the absorption maxima hypsochromically. This implies that the electron withdrawing group stabilises the polar ground state **(20A)** compared to the non-polar excited state **(20B)**.

14

(20A)   (20B)
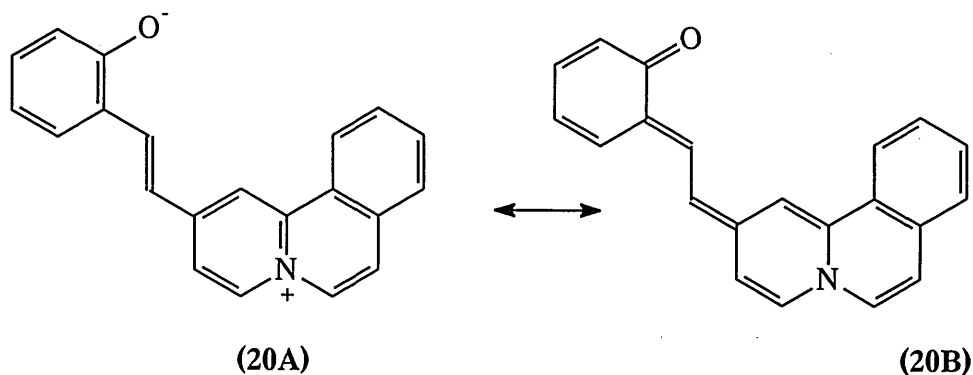
.In 1990 Reichardt and coworkers synthesised the γ-pyridone (21) and compared it to (7).[47] Although it behaved in a similar manner to (7), it was not nearly as solvatochromic due to the introduction of an unsaturated link between the pyridine acceptor and the phenoxide donor moieties.[48]

(21)   (22)
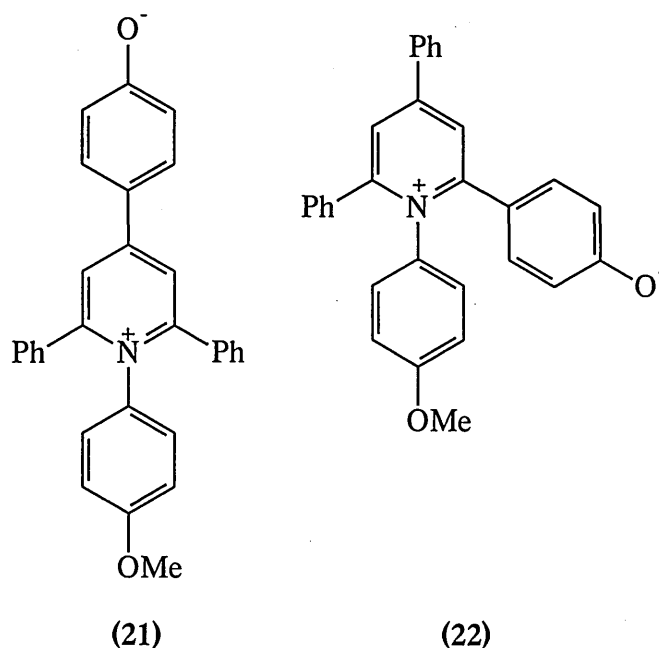
The analogous vinylogous α-isomer (22) has been compared to (21),[49] and was seen to be slightly more sensitive to solvent medium changes than the γ-isomer. In solvents of medium polarity the α-isomer absorbed at a longer wavelength and was shifted hypsochromically by about 20-30 nm. However, as the solvent polarity increases, the CT absorption band of both isomers converges to the same values in methanol.

The benzimidazole-based pyridinium betaine dye (IBI) (23), based on Reichardt's dye (7) has been shown to exhibit solvatochromism.[50] A hypsochromic shift was observed, smaller than that of (7), which was supported by the measurement of its dipole moment, which is 13 D in the polar ground state, and 3 D in the non-polar

15

excited state, compared to (7) which has a dipole moment of 15 D in the ground state, and 6 D in the excited state.
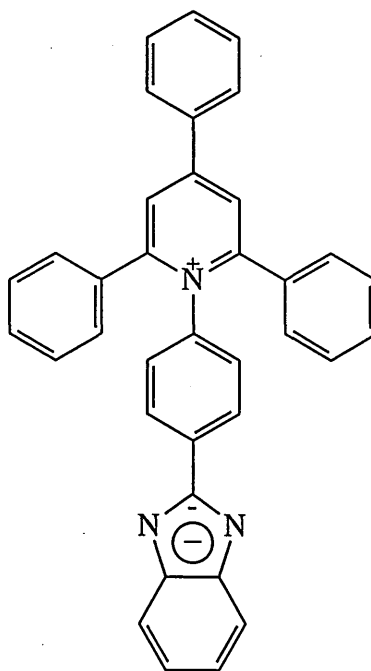
(23)

Solvatochromic studies have been conducted on 2-[(2-hydroxyphenyl)azo]-4,5-diphenylimidazole (HAI) (24) in various solvents.[51] In the basic solvent DMF, the imidazole absorbs essentially at 600 nm with two shorter wavelength bands at 430 nm and 460 nm, which increase in ratio with increase in concentration.

However, in the other less basic solvents (e.g. methanol, acetonitrile, acetone and chloroform) the band at 600 nm is absent, and only the two shorter wavelength absorptions are observed. It is thought that the two shorter wavelength bands arise from the existence of this compound in a tautomeric equilibrium of the azo ↔ hydrazone type as seen in figure 1.

The longer wavelength visible band appearing in DMF was assigned to the absorption by the ionised form of the compound: HAI +S ↔ AI⁻ + HS⁺.

(24)

16
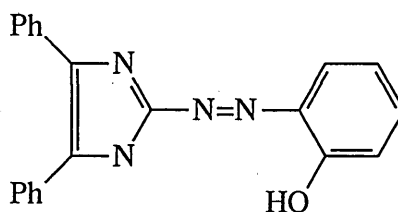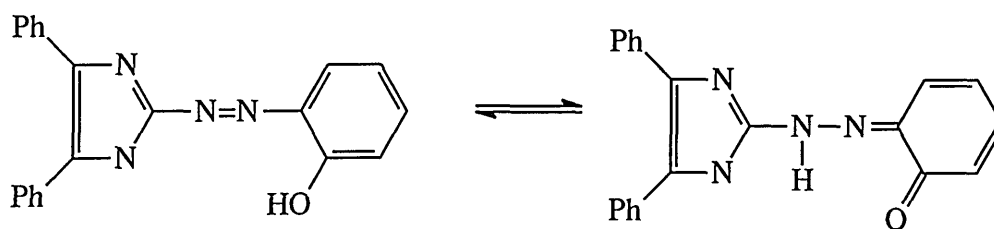
Figure 1

Some of the other solvatochromic compounds in the literature include phosphonium salts[52,53] and phosphine oxides[54,55] along with *the* newer and increasingly important organometallic compounds.[56] These are discussed in the introductory parts of later chapters.

1.5   Applications of Reichardt's Betaine Dye

The empirical parameter $E_T(30)$ has found many applications in addition to the study of solvent effects of pure solvents. For example there have been many studies on the solvent effects of binary solvent mixtures,[57] aqueous and non-aqueous electrolyte solutions,[58] microheterogeneous solutions[59] such as micelles, surfactants and bilayers, and for the characterisation of the polarity of polymers[60] and of chromatographic materials.[61]

The dye has been used as a probe for the surface polarity of chemically and thermally treated silicas[62] and alumina,[63] whereas Hubert *et al* have developed a solvatochromic dye-doped polymer for the detection of polar additives in hydrocarbon blends.[64] The polymer film (PMMA) is doped with Reichardt's betaine dye by spin-coating onto glass slides and the doped polymer has a high sensitivity to methanol, *tert*-butyl alcohol, and *tert*-butyl methyl ether in hydrocarbons. This makes them potential candidates for solvatochromic-based fibre optic chemical sensor (FOCS) for *in situ* monitoring of octane improvers in gasoline.

Reichardt's dye has also been used in optical sensors for humidity and gaseous ammonia.[65] Additionally it has been immobilised on silica gel and proposed as a sensitive optical chemical sensor,[66] producing significant shifts of λ_{max} when the liquid environment of the sensor was changed, although the shifts observed were smaller than those seen for the free dye in solution.

1.6   Thermochromism, Piezochromism, Halochromism

If a compound is solvatochromic, in theory it should also exhibit thermo-solvatochromism (thermochromism), piezo-solvatochromism (piezochromism) and halochromism. As well as exhibiting pronounced solvatochromism, Reichardt's betaine dye **(7)** also exhibits the above mentioned properties.[67]

In thermochromism (usually negative), the position of the long wavelength charge-transfer absorption band of the dissolved compound does not only depend on the polarity of the solvent, but also on the temperature of the solution.[67] Thermochromism is caused by the differential stabilisation of the dipolar electronic ground state relative to the less polar excited state with decreasing solution temperature. This is because the lower the solution temperature, the higher the corresponding $E_T(30)$ values, leading to the better solvation capability of the solvent.

Piezochromism is caused by the differential stabilisation of the solvated betaine ground state relative to its less polar excited state, with increasing external pressure. The $E_T(30)$ value is increased the higher the applied external pressure.[67]

The term halochromism was first introduced by Baeyer and Villiger in 1902,[68] and was initially used to describe the change in colour of a dissolved compound on the addition of an acid or a base.

$$\text{E.g. } (C_6H_5)_3C\text{-OH} + H_3O^+ \rightarrow (C_6H_5)_3C^+ + 2H_2O$$

colourless   yellow
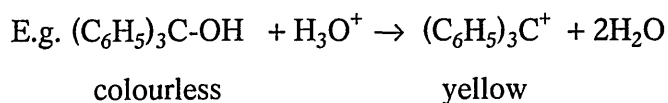
Nowadays the term is used to describe the hypsochromic shift of the charge-transfer absorption band of a betaine by the addition of salts [KI, NaI, LI, BaI_2, $Mg(ClO_4)_2$ etc.] to the solution of the betaine. Unlike the old terminology, this "true" halochromism is not accompanied by a chemical alteration of the chromophore.

Reichardt suggested the term negative halochromism for a hypsochromic shift of the UV/Visible absorption band of a dissolved substance on increasing the electrolyte concentration.[67]

The shift of the charge-transfer absorption band depends on the nature and the concentration of the salt added. The shift increases with increasing the effective cation charge (ionic charge/ionic radius). Furthermore, the shift depends on the ionisation energy of the electron-donor and electron affinity of the electron-acceptor.

Thus, the cations of the salts added increase the ionization energy of the electron-donor part because of the electrostatic O^-M^+ interaction. This corresponds to an increase in charge-transfer excitation energy and results in a salt-induced hypsochromic shift. If an electron withdrawing substituent is introduced into the acceptor part causing an increase in its electron affinity, it will cause a bathochromic shift of the charge-transfer absorption band.

1.7 Non-Linear Optics

Molecular electronics has been an active part of research for the last three decades, although it has evolved rapidly during the 1980's as scientists have become aware of the potential applications for organic materials in electronics. Examples of the materials studied are liquid crystals, conductive polymers, and low molecular weight synthetic materials.

Another class of organic materials, which has been the focus of recent attention, is that of nonlinear optical (NLO) materials. Two classes of materials have been studied, those with a large quadratic term in the response to applied electric fields (second order nonlinearity), and secondly those with a large third order (electric field cubed) response. The second order nonlinearity of organic molecules is easily predicted using simple quantum mechanical calculations of the first and second excited electronic states of the molecule. Prediction of the third order nonlinearity is more difficult to calculate.

The area of nonlinear optics evolved with the discovery of lasers. Franken and Hill demonstrated that when a beam of red light from a ruby laser was illuminated in a quartz crystal, the frequency of the emerging ultraviolet light component was doubled compared with the incoming red light.[69] This double-frequency phenomenon was termed the "second harmonic".

For molecules to be capable of exhibiting second harmonic generation (SHG) i.e. the ability of doubling the frequency of light applied (e.g. from an infrared laser),[70] they must consist of a donor part linked via an extended conjugated π-electron bridge to an acceptor part and have large molecular first (hyper)polarisabilities (β). Molecular structures that have large β values are often highly solvatochromic.[29,71] Therefore, in addition to their applications in the study of solvent polarity, betaine dyes have also been researched for NLO properties such as second harmonic generation. Such systems

can be described by one dominant hyperpolarisability component lying in the direction of charge-transfer.

Initial studies in the area of nonlinear optics centred mainly on inorganic materials such as $LiNbO_3$, $KTiOPO_4$ (KTP), $Ba_2NaNb_5O_{15}$, $NH_4H_2PO_4$ (ADP), HIO_3, LiB_2O_5, CdSe, $AgGaSe_2$, Te and SiO_2 etc. However, as the source of nonlinearity lies in the polarisability of the π-electron cloud of conjugated systems, it has become clear recently that organic molecules have an advantage over inorganic molecules. Organic molecules have an inherent tunability, faster nonlinear responses in the Visible/IR region, and the possibility of better fabrication, processing and varied molecular architecture. As well as larger SHG coefficients, organic materials have lower relative permittivities, and higher laser damage thresholds.

Additionally inorganic crystals such as lithium niobate ($LiNbO_3$) which are already on the market, have several drawbacks, as high quality single crystals are difficult to grow, are expensive, and are not easy to incorporate into electronic devices.

The second order nonlinear hyperpolarisability of the individual molecules in an organic solid is measured in terms of the β coefficient and its SI units are $[Cm^3V^{-2}]$ (x 2.7×10^{20} for esu), whilst the macroscopic manifestation of the individual molecular contributions (bulk material) is measured as the second-order nonlinear susceptibility $\chi^{(2)}$ and its SI units are $[CV^{-2}]$ (x 2.7×10^{14} for esu).

Other important quantities are the linear electro-optic coefficient r, $[mV^{-1}]$ and the second harmonic coefficient d $[mV^{-1}]$ which are related to $\chi^{(2)}$ by equations (4) and (5).

$$\chi^{(2)} (-\omega_a;\omega_b,0) = E_0 n^2_\omega n^2_0 r (-\omega_a;\omega_b,0) / 2 \qquad \textbf{(Equ. 4)}$$

$$\chi^{(2)} (-2\omega_a;\omega_b;0) = 2_{E0} d \qquad \textbf{(Equ. 5)}$$

where:-

n_ω = refractive index at frequency ω

ω_b = frequency of the applied field

ω_a = frequency of emitted field

Equation (6) gives the polarisation P of a molecule as the sum of the ground state polarisation P_0 and the induced polarisation by an **external electric field** E, expressed as a power series. There is a redistribution of electron density, which results in a change in the dipole moment.

$$P = P_0 + \alpha E + \beta EE + \gamma EEE + \cdots \quad \text{(Equ. 6)}$$

where:-

α = linear polarisability

β = quadratic hyperpolarisability (which must be optimised for SHG)

γ = cubic hyperpolarisability (important for a variety of other NLO properties)

This equation only offers a little insight into how to proceed in designing organic molecules with optimal properties. Therefore, $\beta_{CT,}$ which is the charge-transfer component and an approximation of β can also be calculated. This was obtained by Oudar[71] and is shown in equation (7).

$$\beta_{CT} = (3e^2h^2Wf\Delta\mu)/2m[W^2-(2h\omega^2][W^2-(h\omega)^2] \quad \text{(Equ. 7)}$$

where:-

$h\omega$ = laser fundamental photon energy

e = electron charge

m = mass

W = spectroscopic energy gap

f = oscillator strength of the charge-transfer transition of the molecule, and the change in the dipole moment $\Delta\mu$ involved in the transition.

For β to be at its maximum, molecules should have an electronic transition with a small energy gap near, (but not including) 2ω, accompanied by a large oscillator strength and change in dipole moment. W (the spectroscopic energy gap) is related to the frequency (or wavelength) of absorptions found in the UV/Visible spectra of the molecule and the oscillator strength is related to the extinction coefficient ε of the absorption. The induced dipole moment $\Delta\mu$, which is the change in dipole moment between the ground (μ_g) and excited states (μ_e) as seen in equation 8, must be as large as possible.

$$\Delta\mu = \mu_e - \mu_g \quad \text{(Equ. 8)}$$

Usually $\mu_e > \mu_g$ and β is positive.

In the presence of the high electromagnetic field of a laser beam, P is the polarisation induced in a macroscopic medium, and can be written as a power series of the applied field E as in equation (9).

$$P = P_0 + \chi^{(1)}E + \chi^{(2)}EE + \chi^{(3)}EEE + \cdots \cdots \quad \text{(Equ. 9)}$$

$\chi^{(1)}$, $\chi^{(2)}$ and $\chi^{(3)}$ are the first-order, second-order and third-order susceptibilities of the molecule. $\chi^{(1)}$ is a tensor which follows the symmetry properties of the crystal, which is termed "linear optics". The tensor $\chi^{(2)}$ causes second harmonic generation (SHG) and $\chi^{(3)}$ gives rise to third harmonic generation (THG).

As $\chi^{(n)}$ are tensor properties, the orientation of the molecule in a crystal lattice is of great importance and if the molecule has a centre of symmetry, $\chi^{(2)}$ will be zero and no nonlinear effects are observed.

Simply because a compound has a large β, however, does not ensure that it will be useful for SHG. The quantity β is a molecular property; it indicates that a single isolated molecule of the same compound is capable of SHG, but does not guarantee effectiveness of the compound for SHG in bulk form, either in the crystalline state or when present in a poled polymer film.[70]

For a medium to be capable of SHG, it must first be noncentrosymmetric.[70] Unfortunately, many compounds with large β's crystallise in centrosymmetric space groups; the very structural features that enhance β (i.e. polarity) often increase the likelihood of the molecules packing in a centrosymmetric crystal.

An example of a compound that exhibits a large β is Reichardt's betaine dye. The bulk material crystallises in a centrosymmetric manner even though β is large at 34 x 10^{-30} esu.[70] However, β values do provide initial information that assists in designing new organic systems with large NLO properties.

Numerous strategies have been reported in the literature for forming acentric crystal structures and have been found useful for ensuring a noncentrosymmetric dipolar alignment favouring SHG activity, these are:-

- Chirality
- Steric hindrance
- Langmuir Blodgett films

- Guest Host systems

- Electrical poling

There are several techniques used to measure β and $\chi^{(2)}$, these are:-

EFISH Technique (Electric Field Induced Second-Harmonic Generation)[73,74]

This is the traditional method of measuring the hyperpolarisability in solution. A strong static electric field is applied to the NLO chromophore in solution. A bias in the average orientation of the molecules is caused due to the interaction of the electric field. Second-harmonic generation is produced due to partial removal of the isotropy, and $\mu\beta$ is determined from the intensity of the second-harmonic light. This value only represents the scalar product of the permanent dipole moment and the vectorial part of the hyperpolarisability. A separate measurement of the permanent dipole is necessary to extract β. The drawback of this technique is that only polar and nonionic molecules can be measured due to the *dc* electric field.

Hyper Raleigh Scattering (HRS)[75,76]

This technique was developed in 1991, and as with EFISH, it measures the hyperpolarisability of the compound in solution. However, unlike EFISH, the technique measures both apolar and dipolar nonlinear molecules due to the absence of the orientating electric field.

An intense laser beam is focused on an isotropic solution containing nonlinear molecules and measures the intensity of scattered frequency-doubled light. The second-order optical processes are able to occur in a centrosymmetric solution due to fluctuations in molecular orientations that instantly break the centrosymmetry of the solution.

A disadvantage of this technique is that multiphoton fluorescence often interferes with the signal, and this can sometimes lead to serious experimental errors,[77] although there are some approaches that have been developed which can overcome this problem.[78]

Organometallic compounds were first studied by this technique. A laser is directed onto a powdered sample and the magnitude of SH intensity yielded from the sample is compared with the SH intensity of a standard reference sample such as urea or quartz.

The results are dependent on the particle size, and the recrystallisation from a different range of solvents can lead to different SHG efficiencies. This method is only really semiquantitative, and is not reliable for information on the structure-property relationships.

Materials exhibiting NLO properties could be useful for data storage systems in the future, using shorter wavelength sources than are at present available in order to increase the information density. Harmonic generation is also one possible route to short wavelength lasers. A great demand is therefore envisaged for devices that can perform these operations using only low power lasers and small supply voltages. Fibre telecommunications systems will offer the largest area of use for nonlinear optical devices.

1.8   Langmuir Blodgett (LB) Films

Langmuir Blodgett (LB) films have been the subject of scientific study for most of the twentieth century. The Langmuir-Blodgett technique was first introduced by Irving Langmuir in the 1920's[80] and then extensively applied by Katharine Blodgett.[81] As a direct result of the work by Hans Kuhn and colleagues on energy transfer in multilayer systems in the 1970's, the interest in LB films has greatly increased.

The LB technique is important as a means of imposing a noncentrosymmetric structure (as a film) onto a solid substrate (such as glass or quartz). It provides a means of controlling precisely the film thickness as well as aligning the molecules which are capable of displaying SHG activity. Although the LB technique was originally developed using materials such as fatty acids which have very low NLO coefficients, the technique has been extended to aromatic organic molecules such as charge-transfer systems, and is now the most common method of studying NLO properties of new organic materials.

A monolayer (monomolecular layer) is a surface film of one molecule thickness, which is formed from the orientation of certain organic molecules at the interface between a gaseous and liquid phase (or two liquid phases) to minimise free energy. Most molecules that form monolayers are amphiphiles and are composed of a hydrophilic (water-loving) part which is soluble with water and a hydrophobic (water-hating) tail which is insoluble with water.

Most monolayer materials are applied to the subphase surface (water) by dissolving them in a suitable solvent, which is immiscible with water (usually chloroform). When the solvent has evaporated, the organic molecules are compressed to form the floating film. The individual molecules are aligned in the same way due to the hydrophilic end pointing towards the water surface and the hydrophobic tail pointing away.

Spreading of the film is carried out until the surface pressure of the film has risen to an equilibrium value. The *equilibrium spreading pressure* is defined as that spontaneously generated when the bulk solid is placed in contact with a water surface.[82] Hence, the monolayer is expected to form crystals if its surface pressure is greater than the equilibrium spreading pressure.

As the monolayer is compressed on the water surface it undergoes several phase transformations. In the gaseous state **(G)**, the molecules are far enough apart on the water surface that they exert little force on each other (fig. 2). As the surface area of the monolayer is reduced the hydrocarbon chains begin to interact, and the "liquid" state that is formed is generally termed the *expanded monolayer phase* **(E)** (fig. 2). The hydrocarbon chains of the molecules are random in the film rather than in a regular orientation with their polar groups in contact with the subphase. As the molecular area is reduced further, condensed **(C)** phases may occur (fig. 2). These region(s) are associated with enthalpy changes in the monolayer. The molecules are tightly packed and are orientated with the hydrocarbon chain pointing away from the surface. The area per molecule in a condensed state will be similar to the cross-sectional area of the hydrocarbon chain.

Condensed phase **C** Expanded monolayer phase **E** Gaseous phase **G**
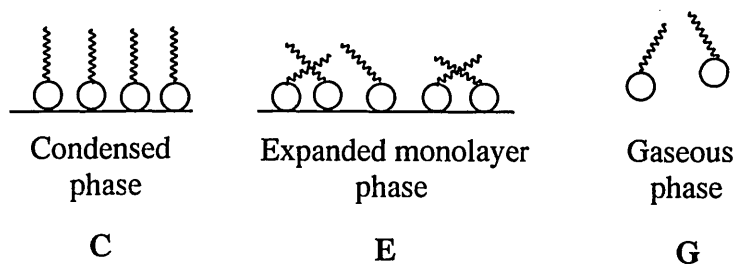
Figure 2

Monolayers can be compressed to pressures considerably higher than the equilibrium spreading pressure. The surface pressure continues to increase with decreasing surface area, until a point is reached at which it is not possible to increase the pressure any further. The area of the film decreases if the pressure is kept constant, or the pressure falls if the area is kept constant, and at this point the film collapses and the molecules are forced out of the monolayer. The forces acting on the monolayer at this point are quite high and the point of collapse depends on many factors including the rate at which the monolayer was being compressed and the history of the film.

An example of a surface pressure versus area per molecule isotherm for a long chain organic molecule is shown in figure 3. To be a meaningful pressure value, the exact conditions should be given at collapse.
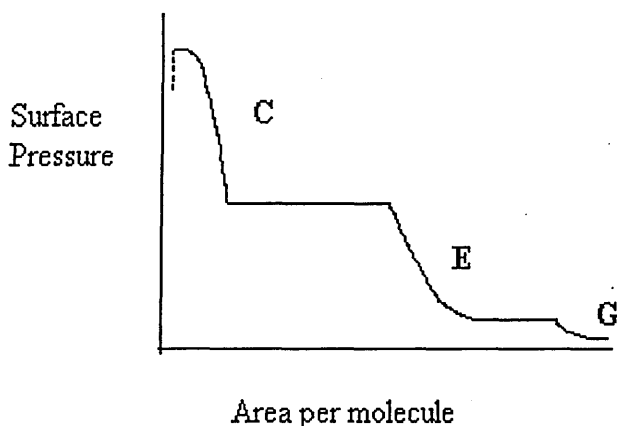
C = condensed phase, E = expanded monolayer (liquid) phase, G = gaseous phase

Figure 3 Surface pressure versus area isotherm.

There are three different types of film deposition :-

For the **Y-type**, which is the most common, the first monolayer is transferred as the substrate is raised through the water; subsequently a monolayer is deposited on each traversal of the monolayer/air interface. The molecular stack is in a head to head and tail to tail fashion as sh
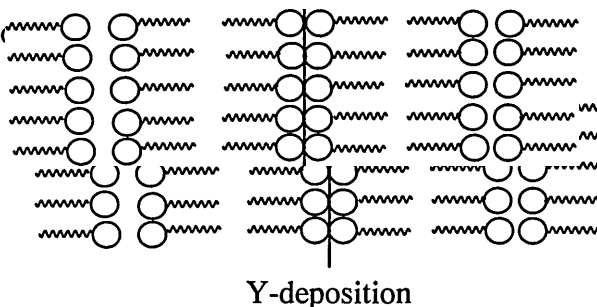
Y-deposition

Figure 4   Y-type Langmuir-Blodgett film deposition

For the **X** and **Z-type** depositions the floating monolayer is only transferred to the substrate as it is being inserted into the subphase, or as it is being removed. For the **X-type** the monolayer transfer is on the down stroke only (fig. 5) and for the **Z-type** the monolayer transfer is on the upstroke only (fig. 5). Sometimes mixed deposition modes are used and the deposition type can change as the LB film is being built up (multilayer films).

X-deposition
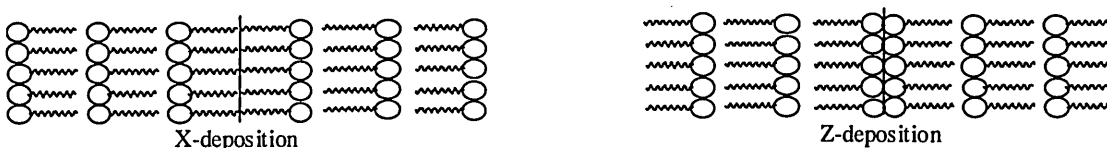
Z-deposition

Figure 5   X and Z-type deposition.

Fatty acid and fatty acid salt monolayers normally deposit as Y-type films, although X-type deposition is possible with suitable changes in the dipping conditions, such as increasing the pH. Aromatic molecules with short (or even no) hydrocarbon chains are deposited as Z-type films but they do not form true monolayers at the air/water interface.

Conventional Y-type films are symmetrical in character and are therefore unlikely to yield non-linear effects. An alternative approach to producing noncentrosymmetric structures is to use alternate layers of two different materials where the contributions of adjacent molecules do not cancel.[83] In the simplest case, alternate

27

layer films can be produced by raising the substrate through a monolayer of one material (A) and then lowering the substrate through a monolayer of a second compound (B) forming the multilayer structure ABABAB as in figure 6.
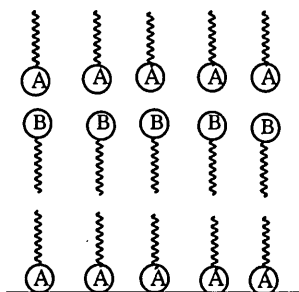
Figure 6   An alternate-layer Langmuir-Blodgett film built up from monolayers of compound (A) and monolayers of compound (B).

The final molecular arrangements in an LB layer is not always as first intended (figs. 4 and 5) for X, Y, and Z-type depositions, and the molecules can re-arrange themselves once the film has been formed. This originates from the interactions of :-

- Polar heads between hydrocarbon tails.

- Between head groups of one layer and hydrocarbon tails of another.

- Between heads and tails of molecules and the water subphase.

LB films are formed using a LB trough, which is usually made from a PTFE copolymer, as it is inert to the organic solvents used. The trough, which need only be a few millimetres deep basically consists of the monolayer barrier and a "well" which allows for the transfer of the floating layer onto the substrate.

1.9   Compounds Exhibiting NLO Properties

In general, SHG studies on organic materials have been performed on single crystals, LB films, NLO-dye functionalised polymer films, liquid crystals and guest host systems.

The number of organic crystals which have useful NLO properties are limited, as they crystallise into centrosymmetric space groups. However, compounds such as urea[69] and 2-methyl-4-nitro-aniline[69] have been found to exhibit large SHG values.

Nonlinear optical chromophores can be incorporated into a macroscopic environment in a variety of ways. The most widespread, and probably the most important is the incorporation of dipolar chromophores into a polymeric material as:- *guest host systems*-this simply involves dissolving the chromophore into the polymer, *side chain polymers*-covalently attaching the chromophore to a polymeric backbone and *main chain polymers*-incorporating the chromophores into the backbone of the polymer.[84]

Noncentrosymmetry is achieved by aligning the dipolar chromophores in the polymer matrix (poling) with a strong orientating electric field, whilst heating the polymer to near its glass transition temperature. The orientation of the chromophores is frozen by cooling the system in the presence of the field.

The nonlinear compound (25) which on its own has a $\mu\beta(0)$ of 4146×10^{-48} esu has been incoroporated into a polyquinoline matrix and has an electro-optic coefficient of 26 pmV^{-1} which is comparable with lithium niobate.[85]
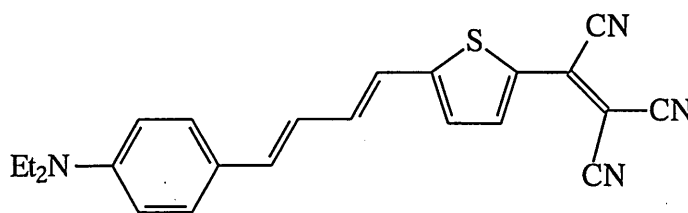

(25)

The advantage of poled polymers is that it is relatively easy to make thin films by spin coating, and they are compatible with the existing semiconductor technology. However, there are disadvantages, which include their instability at high temperatures, and the chromophores in the polymer tend to relax overtime forming centrosymmetric systems. This can be overcome though by crosslinking and using polymers with high glass transition temperatures. Poled polymers are almost ready for electro-optic market applications.

During the 1980's, several one dimensional charge-transfer systems were developed with reasonably good SHG values, and measured by the EFISH technique. These included dimethylaminonitrostilbene (DANS) (26) and p-nitroaniline (PNA) (27). DANS was considered to be quite nonlinear at the time, but is now only used as a comparison for new materials being tested.[86]

CH_3 and CH_3 —N— ... —NO_2 NH_2 ... NO_2

(26)   (27)
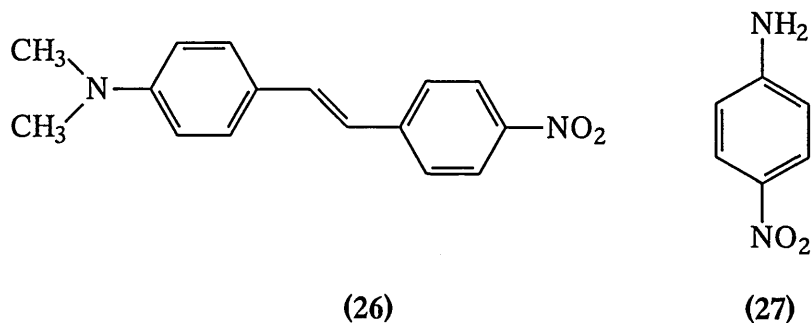
Attempts have been made to increase the non-linearities of DANS type systems by increasing the donor/acceptor strength, and increasing the length of the conjugation bridge.[87] Other conjugation bridges such as substituted benzenes, biphenyls, stilbenes, azostilbenes and tolanes have been employed.[88,89]

In the early 1990's, Marder *et al* found that, for a given conjugation bridge, there is an optimal combination of donor and acceptor strengths to maximise $\mu\beta$, and that beyond that point an increase in the donor/acceptor strength will attenuate $\mu\beta$.[90]

It was also observed that the average difference in length between single and double bonds in a molecule (bond length alternation) is a relevant parameter in maximising β.[91]

A high degree of bond length alternation in such molecules is indicative of an insufficient contribution of the charge separated resonance form to the ground state configuration of molecules. It is a direct consequence of the loss of aromatic stabilisation in the charge separated form.

Therefore molecules have been designed with less aromatic character in the ground state or where loss of aromaticity in the ground state is compensated for by a gain in aromaticity in the charge separated form as in (28).[92]
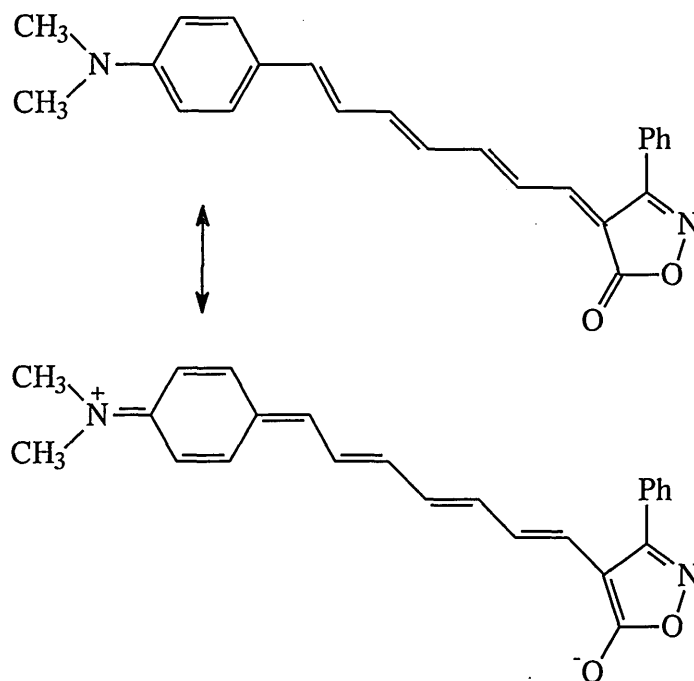
(28)

The hyperpolarisability $\mu\beta(0)$ of **(28)** is 4969×10^{-48} esu compared to 363×10^{-48} esu for DANS. Replacing benzene rings in stilbene derivatives by heterocyclic rings such as thiophene or furan decreases the aromatic character of the ground state and have led to extremely high hyperpolarisabilities.[93,94]

Compounds must not only have high nonlinearities, but also good thermal and chemical stability and high transparency (low optical loss). Many compounds have to exhibit a trade off between nonlinearity and the other properties. Achieving thermal stability in chromophores can be achieved by replacing the aliphatic part of the structure by an aromatic moiety, along the conjugation path, but as already discussed, doing this decreases β.

Moylan *et al* overcame this by synthesising **(29)** replacing dialkylamino with the diarylamino moiety, and increasing the thermal stability.[95,96] The chromophore exhibited high nonlinear properties as the new aryl groups were not involved in the charge-transfer process. Compound **(29)** has also been incorporated into a polyamide matrix directly onto the backbone via the donor group. The SHG was 7 pmV^{-1} and the poled polymer exhibited long term stability.[97]

31
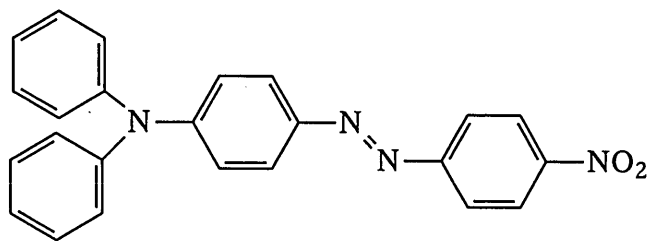
(29)

One of the most interesting candidates at the moment for NLO/transparency trade offs, with extremely stable chromophores, are analogues of 4-(dicyanomethylene-2-methyl-6-(4-dimethylaminostyryl)-4-pyran. Compound **(30)** contains a dicyanomethylene pyran acceptor attached to two carbazole donors.[98] The shape of the chromophore means that it is less susceptible to the loss of nonlinearity in poled polymer films.
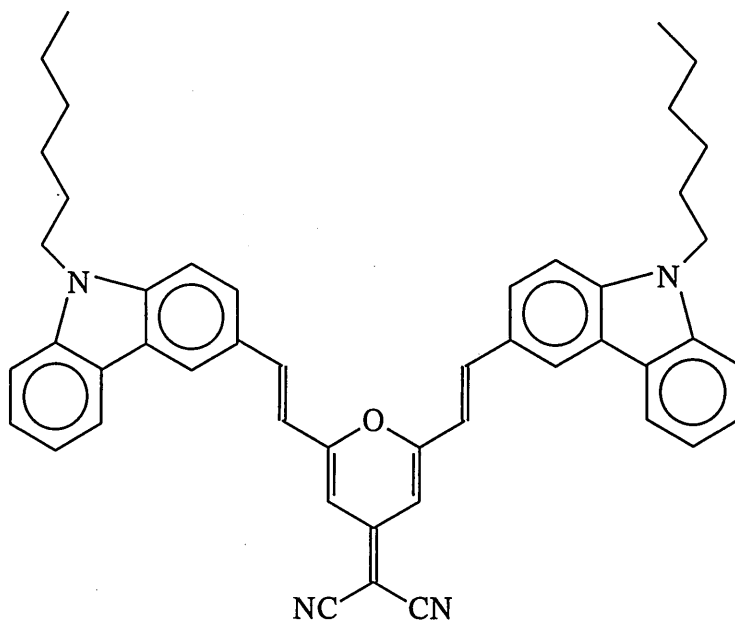
(30)

Ashwell *and coworkers* at Cranfield have greatly contributed to the area of NLO activity in LB films, especially in the area of unconventional organic chromophores. For SHG it is necessary for the LB film structure to be noncentrosymmetric (Z-type), and although SHG intensities have been obtained from monolayer films, the signal usually diminishes for the bilayer and all subsequent even layers.

This has been overcome to an extent by introducing a spacer such as a fatty acid between layers,[99,100,101] although there is usually phase separation, and for films of more than twenty layers the SH intensity is less than expected.

32

Ashwell overcame this problem by the introduction of a spacer, which is a "two legged" amphiphilic molecule (31),[83] so that the single leg of the hemicyanine dye (NLO chromophore) (32) would penetrate and fasten the interleaving LB layers forming a "molecular zip".
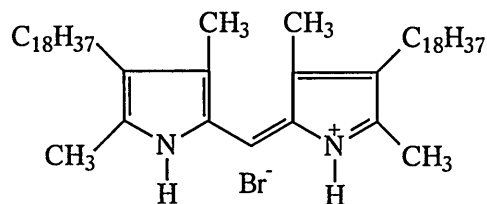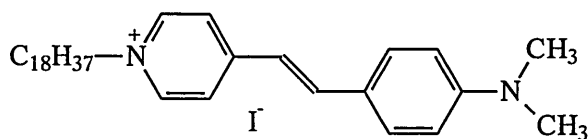
(31)   (32)

The SH intensity obtained from a two hundred layer film is 18,300 times the signal obtained by Girling *et al* for the monolayer of (32).[102,103]

The second harmonic generation of the hemicyanine dye (32) has been improved by exchanging the iodide anion for the amphiphilic anion octadecyl sulphate which was effectively used as the spacer.[104] The SH intensity of (33) was 500–1,500 pmV^{-1} compared to 90–150 pmV^{-1} for the iodide anion. It was seen that the amphiphilic anion and cation packed side by side with the negatively charged OSO_3^- group interleaving the positively charged pyridinium ring.
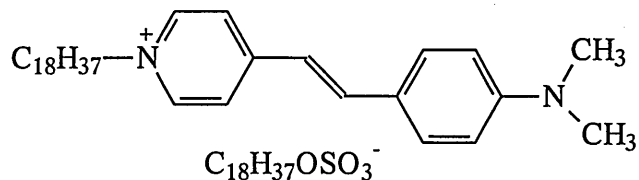
(33)

The SHG of the "two legged" benzothiazolium octadecylsulphate dye (34) was found to increase with film thickness (Z-type), and the intensity of a two hundred layer film was six hundred times that of the monolayer.[105,106]
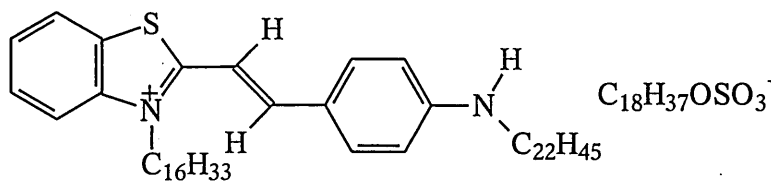
(34)

The dye consisted of two hydrophobic groups, but only one of the groups was at the end of the chromophore, unlike the other two legged dyes where they were at each

end of the molecule.[107] The dye which was initially thought to form a "U" shaped configuration [105] formed a stretched configuration in the film.

Ashwell's recent interest is in the surprising nonlinear optic squaraine dyes.[108-113] These molecules exhibit strong second order non-linearities, even though they form centrosymmetric films.

The squaraine dye (35) was SHG active but produced a poor quality film. However, the hexyl derivative (36) produced better and more reproducible films.[108]

(35)

(36)
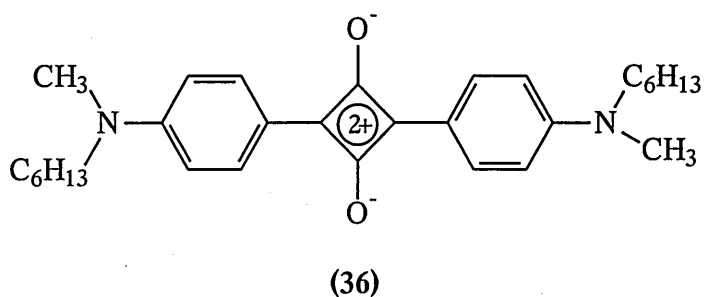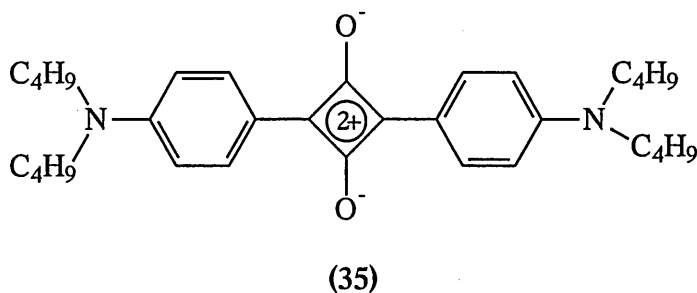
The exhibited SHG was attributed to an intermolecular rather than an intramolecular charge-transfer in noncentrosymmetric aggregates (dimers) in the LB films.[111] An X-ray crystal structure of the butyl analogue (35) showed each molecular pair to adopt a noncentrosymmetric "T-shaped" configuration with moderately close intermolecular contacts between the acceptor (C_4O_2) and donor (dialkylamino) groups of adjacent molecules.

However, not all squaraine dyes are SHG active; squaraine (37), which is the tetrahydroxy analogue of (36) forms heptameric rather than dimeric aggregates and no intermolecular charge-transfer occurs between the aggregates.[112]

34

(37)
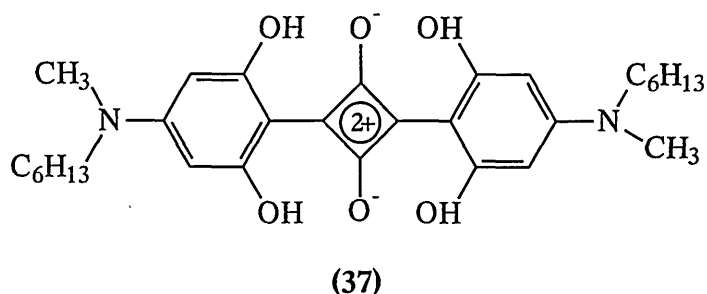
1.10 Surface Plasmon Resonance

Surface Plasmon Resonance (SPR) is an effective technique for the characterisation of thin organic overlays on metal films. Additionally SPR may be exploited for sensing applications, as surface plasmons are extremely sensitive to changes at the interface.

The experimental arrangement for the excitation of surface plasmons is known as the **Kretschmann configuration** and exploits evanescent electromagnetic waves (fig. 7).
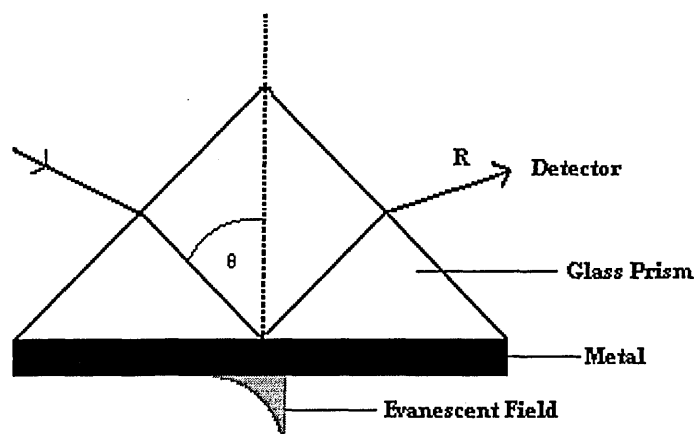
Figure 7 Kretschmann configuration for exciting surface plasmons.

Monochromatic (p-polarised light) at 632.8 nm enters the prism at a fixed angle of incidence and is refracted onto the base, and therefore onto the metal (silver or gold) film where it is reflected.

The resulting evanescent field penetrates to the opposite side of this film (i.e. the metal/air interface) if the metal is sufficiently thin. At the total internal reflection (TIR) condition, all of the light is absorbed by the atoms in the metal layer. If an LB film is

deposited onto the metal surface it affects the angle of the TIR, and subsequently if the LB substrate undergoes any change e.g. protonation, it also affects the TIR angle.

Changing the angle of incidence of the light alters the component of the wavevector parallel to the prism base. Surface plasmons are excited when this component matches the real part of the surface plasmon wavelength at (θ_0). This phenomenon (SPR) is detected by a pronounced reduction in the intensity of the reflected beam, **R**; an example of this is shown in figure 8.
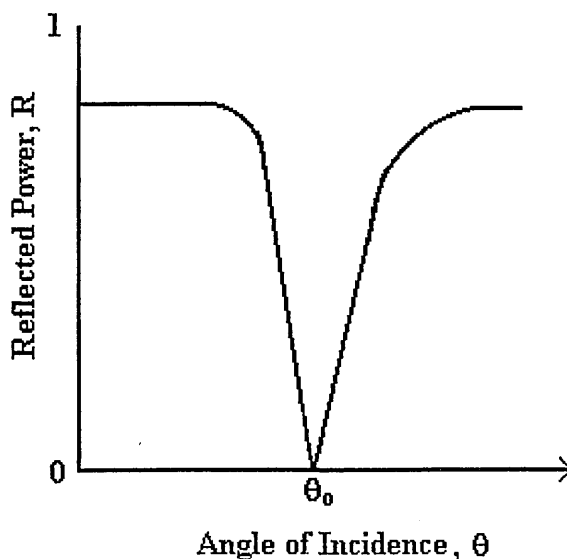
Figure 8: Typical reflectivity data for the glass Ag LB monolayer structure at 632.8 nm.

For sensing applications, changes in the optical properties of an "active layer" in response to external ambient conditions are detected.

1.11 Aims of the Present Work

This thesis reports the synthesis and characterisation of six types of solvatochromic system. The solvatochromic properties of each system have been investigated in a range of organic solvents, with measurement of their respective longest-wavelength absorption bands using UV/Visible spectroscopy.

The research centres mainly on the synthesis of solvatochromic phosphonio-betaine and related systems of which there are limited reports in the literature.

Type 1

The long chain analogues **(1)** of the already reported solvatochromic 4-N(*o*-triphenylphosphoniobenzylidene)-amino-2,6 disubstituted phenolate betaines[51] have been synthesised with the view to investigating any NLO properties by the LB film technique in collaboration with Professor Ashwell's group at Cranfield University.
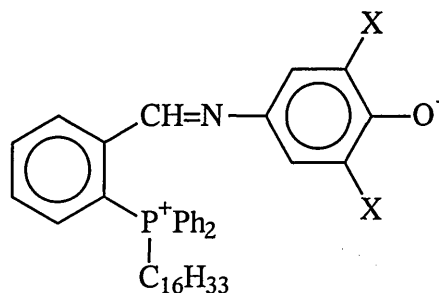
X= Cl, Br, Ph,

(1)

Type 2

The long chain analogues **(2)** of the already reported triphenylphosphonio imidazolide betaines[114] have been synthesised, again with a view to LB film formation and the investigation of any potential NLO properties.
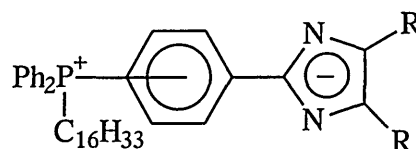
(2)

Type 3

The effects of annelation of a benzene ring on the betaine systems of types one and two, e.g. as in **(3)** has been investigated, and the effect of the overall increase in conjugation on the solvatochromism of the systems is reported.
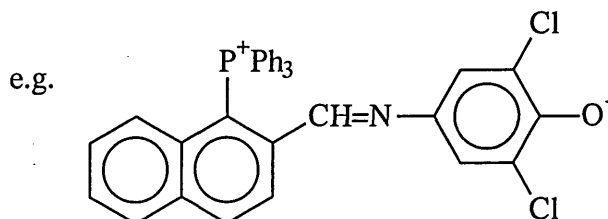
(3)

A related quinolinium system (4) has also been synthesised and characterised where the X group was varied. A comparison is made with the pyridinium system already reported in the literature.[115] These compounds have been studied at Cranfield University, and LB films have been formed and the compounds investigated for their sensor properties.

$$O^-$$
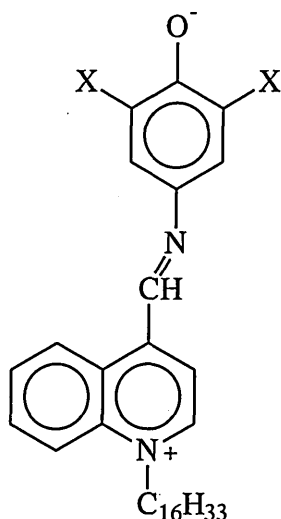
X = Cl, Br

(4)

Type 4

The positive phosphonium moiety in the iminophenolate betaines[51] has been replaced by the related arsonium and stibonium centres (5), using a novel synthetic approach. These are the first solvatochromic arsonium and stibonium betaine systems to be reported.

$$CH=N$$
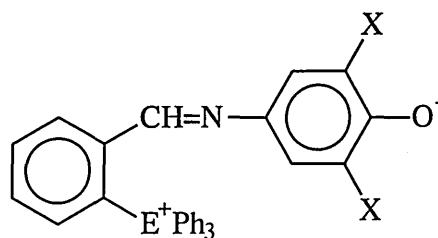
E = As, Sb; X = Cl, Br, Ph

(5)

Type 5

Triphenylphosphonium salts and related phosphine oxides having various donor groups **(6)** have been synthesised, and their solvatochromism is reported.

$$R-(CH=CH)_n-\langle\bigcirc\rangle-Y$$

$$Y = P^+Ph_3 \text{ or } Ph_2P=O$$

$$R = \text{ferrocenyl, 2-thienyl, } p\text{-Me}_2NC_6H_4$$

$$n = 1 \text{ or } 2$$
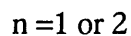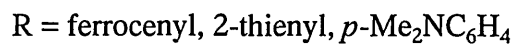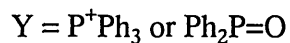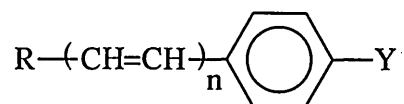
(6)

Type 6

Attempts to synthesise a range of bis and tris betaine systems e.g. **(7)** has been attempted, employing the pyridinium and quinolinium iminophenolate betaines as the chromophores.

e.g.
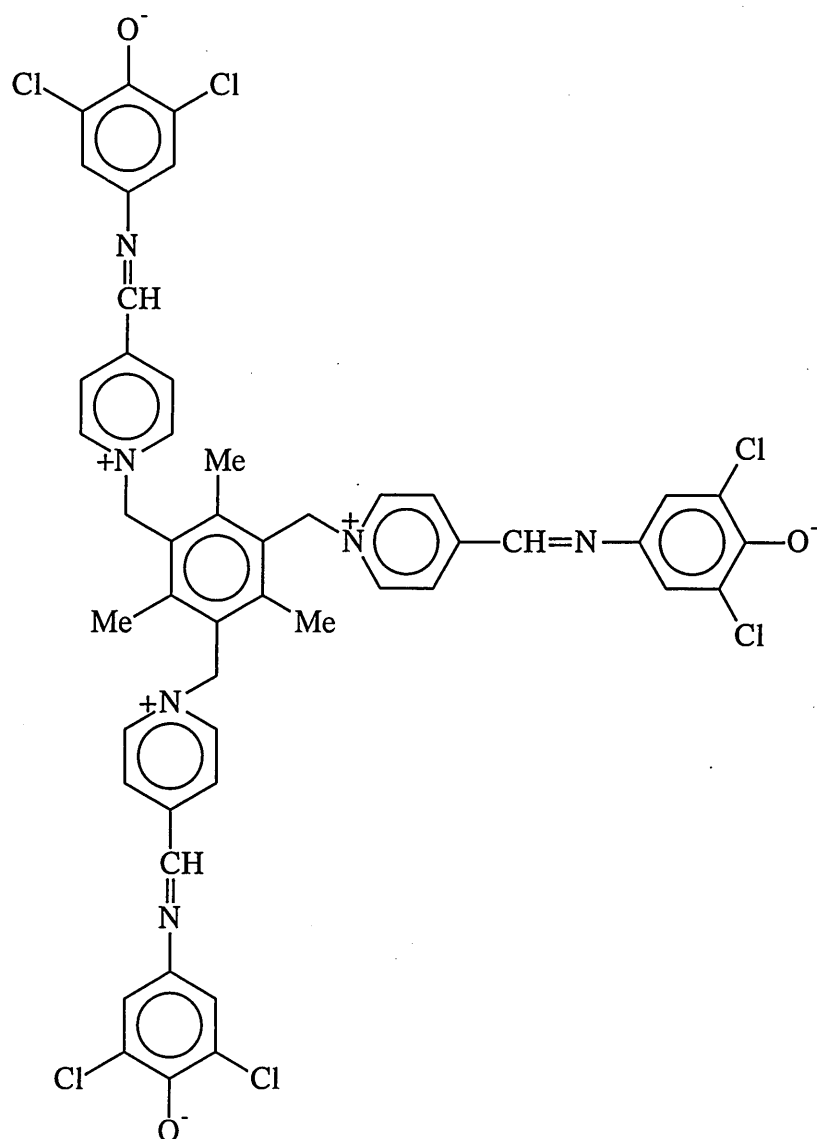
(7)

References

1. F. Szabadváry; *Geschichte der Analytischen Chemie*, V. Braunshweig and A. Kiado, Budapest, 1966, 38.

2. M. Bérthelot and L. Péan de Saint-Gilles, *Ann. Chim. et Phys.*, **65**(3), 1862, 385.

3. N. Menschutkin, *J. Phys. Chem.*, **1**, 1887, 611.

4. L. Claisen, *Liebigs Ann. Chem.*, **291**, 1896, 25.

5. W. Wislicenus, *Liebigs Ann. Chem.*, **291**, 1896, 147.

6. L. Knorr, *Liebigs Ann. Chem.*, **293**, 1896, 70.

7. A. Hantzch and O. W. Belfutze, *Ber. Dtsch. Chem. Ges.*, **29**, 1896, 2251.

8. H. Stobbe, *Liebigs Ann. Chem.,* **326**, 1903, 347.

9. A. Hantzch, *Ber. Dtsch. Chem. Ges.,* **55**, 1922, 953.

10. W. H. Keesom, *Physik. Z.,* **129**(22), 1921, 643.

11. R. L. Amey, *J. Phys. Chem.,* **72**, 1968, 3358.

12. H. H. Jaffé, *J. Chem. Educ.,* **40**, 1963, 649.

13. M. L. Huggins, *Angew. Chem.,* **83**, 1971, 163.

14. R. Paetzold, *Z. Chem.,* **15**, 1975, 377.

15. C. J. Bender, *Theoretical Chem. Soc. Rev.,* **15**, 1986, 475.

16. R. S. Mulliken and W. B. Person, *Molecular Complexes; A Lecture and Reprint Volume,* Wiley-Interscience, New York, 1969.

17. C. Reichardt, *Angew. Chem., Int. Ed. Engl.,* **4**, 1965, 29.

18. P. Jaques, *J. Phys. Chem.,* **90**, 1986, 5535.

19. C. Machado, M. de Graça Nascimento and M. C. Rezende, *J. Chem. Soc., Perkin Trans. 2,* 1994, 2539.

20. J. O. Morley, R. M. Morley, R. Docherty and M. H. Charlton, *J. Am. Chem. Soc.,* **119**(42), 1997, 10192.

21. L. G. S. Brooker, A. C. Craig, D. W. Heseltine, P. W. Jenkins and L. L. L. Lincoln, *J. Am. Chem. Soc.,* **80**, 1958, 3253.

22. L. G. S. Brooker, G. H. Keyes and D. W. Heseltine, *J. Am. Chem. Soc.,* **87**, 1965, 2443.

23. E. M. Kosower, *J. Am. Chem. Soc.,* **80**, 1958, 3253.

24. M. J. Kamlet and R. W. Taft, *J. Am. Chem. Soc.,* **98**, 1975, 2886.

25. M. J. Kamlet, J. L. Abboud and R. W. Taft, *J. Am. Chem. Soc.,* **99**, 1977, 6027.

26. S. Dähne, F. Schob, K.-D. Nolte and R. Radeglia, *Ukr. Khim. Zh., (Russ. Ed.),* **41**, 1975, 1170.

27. E. Buncel and S. J. Rajagopal, *J. Org. Chem.,* **54**, 1989, 798.

28. B. Freed, J. Biesecker and W. J. J. Middleton, *J. Fluorine Chem.,* **48**, 1990, 63.

29. K. Dimroth, C. Reichardt, T. Siepmann and F. Bohlmann, *Liebigs Ann. Chem.,* **661**, 1963, 1.

30. D. Walther, *J. Prakt. Chem.,* **316**, 1974, 604.

31. J.-E. Dubois, E. Goetz and A. Bienvenüe, *Spectrochim. Acta,* **20**, 1964, 1815.

32. I. A. Zhmyreva, V. V. Zelinskii, V. P. Kolobkov, N. D. Krasnitskaya, *Dokl. Acad. Nauk SSSR, Ser. Khim.,* **129**, 1959, 1089.

33. A. Jannowski, I. Turowska-Tyrk and P. K. Wrona, *J. Chem. Soc., Perkin Trans. 2,* 1985, 821.

34. C. Reichardt and E. Harbusch-Görnert, *Liebigs Ann. Chem.,* 1983, 721.

35. C. Reichardt, *Chem. Rev.,* **94**, 1994, 2319.

36. C. Reichardt and M. Eschner, *Liebigs Ann. Chem.,* 1991, 1003.

37. R. Gompper, V. Figala, R. Kellner, A. Lederle, S. Lensky, W. Lipp, *Lecture on the 11th International Colour Symposium,* Montreux, Switzerland, Sept 23-26, 1991.

38. P. Milart and K. Stadnicka, *Liebigs Ann./Recueil,* 1997, 2607.

39. K. Dimroth, G. Arnoldy, S. von Eichen and G. Schiffler, *Liebigs Ann. Chem.,* **604**, 1957, 221.

40. C. W. Bird, J. Partridge and D. Y. Wong, *J. Chem. Soc., Perkin Trans. 1,* 1972, 1020.

41. V. Snieckus and G. Kan, *J. Chem. Soc., Chem. Commun.,* 1970, 172.

42. R. A. Abramovitch and T. Takaya, *J. Org. Chem.,* 37, 1972, 2022.

43. A. R. Katritzky and P. Ballesteros, *J. Chem. Res.(S),* 1981, 172.

44. R. Carceller, J. L. Garcia-Navio, M. L. Izquierdo, J. Alvarez-Builla, M. Fajardo, P. Gomez-Sal and F. Gago, *Tetrahedron*, 50, 1994, 4995.

45. S. Arai, M. Yamazaki, K. Nagakura, M. Ishikawa and M. Hida, *J. Chem. Soc., Chem. Commun.,* 1983, 1037.

46. S. Arai, H. Arai, M. Hida and T. Yamagishi, *Heterocycles,* 38(11), 1994, 2449.

47. C. Reichardt, P. Milart and G. Schäefer, *Liebigs Ann. Chem.,* 1990, 441.

48. L. Silva, C. Machado and M. C. Rezende, *J. Chem. Soc., Perkin Trans. 2,* 1997, 1055.

49. C. Aliaga, J. S. Galdames and M. C.Rezende, *J. Chem. Soc., Perkin Trans. 2,* 1997, 1055.

50. J. Sworakowski, J. Lipinski, L. Ziólek, K. Palewska, S. Nešpurek, *J. Phys. Chem.,* **100**, 1996, 12288.

51. A. M. Hammam, N. M. Rageh and S. A. Ibrahim, *Dyes and Pigments,* 35(3), 1997, 289.

52. D. W. Allen and X. Li, *J. Chem. Soc., Perkin Trans. 2,* 1997, 1099.

53. C. Lambert, E. Schmälzlin, K. Meerholz, and C. Bräuchle, *Chem. Eur. J.,* 4(3), 1998, 513.

54. K. Chane-Ching, M. Lequan, R.-M. Lequan, C. Runser, M. Barzoukas and A. Fort, *J. Mater. Chem.,* 5(4), 1995, 649.

55. M. Lequan, R.-M. Lequan, K. Chane-Ching, P. Bassoul, G. Bravik, Y. Barrans and D. Chasseau, *J. Mater. Chem.,* 6(1), 1996, 5.

56. N. J. Long, *Angew. Chem. Int. Ed. Engl.,* 34, 1995, 21.

57. J. G. Dawber, J. Ward and R. A. Williams, *J. Chem. Soc., Faraday Trans. 1,* 84(3), 1988, 713.

58. C. Reichardt, G. Schäefer and P. Milart, *Collect. Czech. Chem. Commun.,* 55, 1990, 97.

59. M. B. Lay and C. J. Drumord, *J. Colloid Interface Sci.,* 128, 1989, 602.

60. S. Spange, D. Kentel, and F. Simon, *J. Chim. Phys.,* 89, 1992, 1615.

61. B. P. Johnson and B. Gabrielsen, *Anal. Lett.,* 19, 1986, 939.

62. S. J. Tavener, J. H. Clark, G. W. Gray, P. A. Heath and D. J. Macquarrie, *J. Chem. Soc., Chem. Commun.,* 1997, 1147.

63. J. J. Michels and J. G. Dorsey, *Langmuir,* 6, 1990, 414.

64. C. Hubert, D. Fichou, P. Valat, F. Garnier and B. Villeret, *Polymer,* 36(13), 1995, 2663.

65. Y. Sadaoka, M. Matsguchi, Y. Sakai and Y.-U. Murata, *Chem. Lett.,* 1992, 53.

66. D. Crowther and X. Lui, *J. Chem. Soc., Chem. Commun.,* 1995, 2245.

67. C. Reichardt, *Chem. Rev.,* 1992, 147.

68. A. Bayer and V. Villiger, *Ber. Dtsch. Chem. Gas.,* 35, 1902, 1189.

69. P. A. Franken and A. E. Hill, *Phys. Rev. Lett.,* 7, 1961, 118.

70. D. S. Chemla and J. Zyss, *Nonlinear Optical Properties of Organic Molecules and Crystals,* Academic Press, New York, 1987, Vol 1.

71. W. Liptay, *Angew. Chem. Int. Ed. Engl.,* 8, 1969, 177.

72. J. L. Oudar, *J. Chem. Phys.,* 67, 1977, 446.

73. B. F. Levine and C. G. Bethea, *J. Chem. Phys.,* 63, 1975, 2666.

74. A. Willets, J. E. Rice, D. M. Burland and D. P. Shelton, *J. Chem. Phys.,* 97, 1992, 7590.

75. K. Clays and A. Persoons, *Phys. Rev. Lett.,* 66, 1991, 2980.

76. T. Verbiest, M. Kauranen and A. Persoons, *J. Chem. Phys.,* 101, 1994, 1745.

77. M. C. Flipse, R. de Jonge, R. H. Woudenberg, A. W. Marsman, C. A. van Walree and L. W. Jenneskens, *Chem. Phys. Lett.,* 245, 1995, 297.

78. O. F. J. Noordman and N. F. van Hulst, *Chem. Phys. Lett.,* **253**, 1996, 145.

79. S. K. Kurtz and T. T. Perry, *J. Appl. Phys.,* **39**, 1968, 3798.

80. I. Langmuir, *J. Chem. Soc., Faraday Trans.,* 15, 1920, 62.

81. K. B. Blodgett, *J. Am. Chem. Soc.,* **57**, 1935, 1007.

82. M. Iwahashi, N. Maehara, Y. Kaneko, T. Seimiya, S. R. Middleton, N. R. Pallas and B. A. Pethica, *J. Chem. Soc., Faraday Trans.,* **81**, 1985, 973.

83. G. J. Ashwell, E. J. C. Dawney, A. P. Kuczynski and P. J. Martin, *Proc. SPIE. Phys. Concepts, Mater. Novel Optoelectron. Device Appl.,* 1990, 1361.

84. D. M. Burland, R. D. Miller and C. A. Walsh, *Chem. Rev.,* **94**, 1994, 31.

85. Y. M. Cai and A. K. Y. Jen, *Appl. Phys. Lett.,* **67**, 1995, 299.

86. D. J. Williams, *Angew. Chem. Int. Ed. Engl.,* **23**, 1984, 690.

87. M. Barzoukas, M. Blanchard-Desce, D. Josse, J.-M. Lehn and J. Zyss, *Chem. Phys.,* **133**, 1989, 323.

88. L.-T. Cheng, W. Tam, S. R. Marder, A. E. Stiegman, G. Rikken and C. W. Spangler, *J. Phys. Chem.,* **95**, 1991, 10643.

89. L.-T. Cheng, W. Tam, S. R. Marder, A. E. Stiegman, G. Rikken and C. W. Spangler, *J. Phys. Chem.,* **95**, 1991, 10631.

90. S. R. Marder, C. B. Gorman, B. G. Tiemann, and L.-T. Cheng, *J. Am. Chem. Soc.,* **115**, 1993, 3006.

91. G. Bornhill, J.-L. Brédas, L.-T. Cheng, S. R. Marder, F. Meyers, J. W. Perry and B. G. Tiemann, *J. Am. Chem. Soc.,* **116**, 1994, 2619.

92. M. Alheim, M. Barzoukas, P. V. Bedworth, M. Blanchard-Desce, A. Fort, Z. Y. Hu, S. R. Marder, J. W. Perry, C. Runser, M. Staehelin and B. Zysset, *Science*, **271**, 1996, 335.

93. V. P. Rao, A. K. Y. Jen, K. Y. Wong and K. J. Drost, *J. Chem. Soc., Chem. Commun.,* 1993, 1118.

94. V. P. Rao, A. K. Y. Jen and Y. Cai, *J. Chem. Soc., Chem Commun.,* 1996, 1237.

95. C. R. Moylan, R. D. Miller, R. D. Tweig, V. Y. Lee, I. H. McComb, S. Ermer, S. M. Lovejoy and D. S. Leung, *Proc. SPIE. Int. Soc. Opt. Eng.,* **2527**, 1995, 150.

96. C. R. Moylan, R. J. Tweig, V. Y. Lee, S. A. Swanson, K. M. Betterton and R. D. Miller, *J. Am. Chem. Soc.,* **115**, 1993, 12599.

97. T. Verbiest, D. M. Burland, M. C. Jurich, V. Y. Lee, R. D. Miller and W. Volksen, *Science,* **268**, 1995, 1604.

98. C. R. Moylan, S. Ermer, S. M. Lovejoy, I.-H. Heng McComb, D. S. Leung, R. Wortmann, P. Krdmer and R. J. Tweig, *J. Am. Chem. Soc.,* **118**, 1996, 12950.

99. B. L. Anderson, R. C. Hall, B. G. Higgins, G. A. Lindsay, P. Stroeve and S. T. Kowel, *Synth. Met.,* **28**, 1989, D683-D688.

100. L. M. Hayden, B. L. Anderson, J. Y. S. Lam, B. G. Higgins, P. Stroeve and S. T. Kowel, *Thin Solid Films*, **160**, 1988, 379.

101. R. C. Hall, G. A. Lindsay, B. L. Anderson, S. T. Kowel, B. G. Higgins and P. Stroeve, *Mater. Res. Soc. Symp. Proc.,* **109**, 1988, 351.

102. I. R. Girling, N. A. Cade, P. V. Kolinski, J. D. Earls, G. H. Cross and I. R. Peterson, *Thin Solid Films,* **132**, 1995, 101.

103. I. R. Girling, N. A. Cade, P. V. Kolinski, R. J. Jones, I. R. Peterson, M. M. Ahmad, D. B. Neal, M. C. Petty, G. C. Roberts and W. J. Feast, *J. Opt. Soc. Am. B,* **4**, 1987, 950.

104. G. J. Ashwell, R. C. Hargreaves, C. E. Baldwin, G. S. Bahra and C. R. Brown, *Nature,* **357**, 1992, 393.

105. G. J. Ashwell, T. Handa, G. Jefferies and D. Hamilton, *Colloids and Surfaces A: Physiochem. Eng. Aspects,* **102**, 1995, 133.

106. G. J. Ashwell, G. Jefferies, D. J. Hamilton and T. Handa, *Acta Physica Polonica A,* **88**(3), 1995, 483.

107. G. J. Ashwell, P. D. Jackson and W. A. Crossland, *Nature,* **368**, 1994, 438.

108. G. J. Ashwell, G, Jefferies, D. G. Hamilton, D. E. Lynch, M. P. S. Roberts, G. S. Bahra and C. R. Brown, *Nature,* **375**, 1995, 385.

109. G. J. Ashwell, *Adv. Mater.,* **8**(3), 1996, 248.

110. G. J. Ashwell, G. S. Bahra, C. R. Brown, D. G. Hamilton, C. H. L. Kennard and D. E. Lynch, *J. Mater. Chem.,* **6**(1), 1996, 23.

111. G. J. Ashwell and P. Leeson, *J. Opt. Soc. Am. B,* **15**(1), 1998, 484.

112. G. J. Ashwell, *J. Mater. Chem.,* **8**(2), 1998, 373.

113. G. J. Ashwell, T. Handa, P. Leeson, K. Skjonnemand, G. Jefferies and A. Green, *J. Mater. Chem.,* **8**(2), 1998, 337.

114. D. W. Allen, J. Hawkrigg, H. Adams, B. F. Taylor, D. E. Hibbs and M. B. Hursthouse, *J. Chem. Soc., Perkin Trans. 1,* 1998, 335.

115. G. J. Ashwell, K. Sjonnemand, M. P. S. Roberts, D. W. Allen and X. Li, *Colloids and Surfaces A: Physiochem. Eng. Aspects,* in press.

CHAPTER 2

The Synthesis and the Characterisation of Phosphonium and Quinolinium Betaines

2.0 Introduction

A novel series of triphenylphosphoniophenyl-imidazolide betaines of type **(1)** has recently been prepared which have shown to exhibit some degree of solvatochromism.[1] Consequently compounds of type **(2)** bearing a long alkyl chain are now of interest due to their possible nonlinear optical properties, (second harmonic generation) and the ability to form Langmuir Blodgett films as ordered self-assembled systems. They could also be incorporated into polymers, the long hydrocarbon chain facilitating solubility in hydrocarbon polymers, for example PMMA and polystyrene.
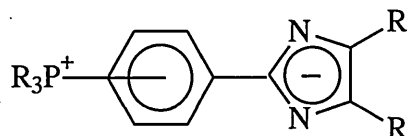
(1A) R=Ph

(1B) R=Bu
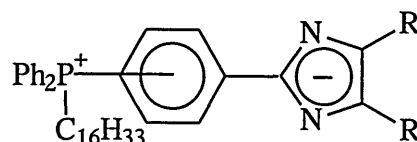
(2)

Additionally a new range of N-(*o*-phosphoniobenzylidene) aminophenolate betaines **(3)** has recently been prepared which were found to possess a fair degree of negative solvatochromism.[2] As with **(1)**, and **(2)** the long chain version of this family of betaines **(4)** is of interest for the study of possible nonlinear optical and other properties of value in the development of sensor systems.
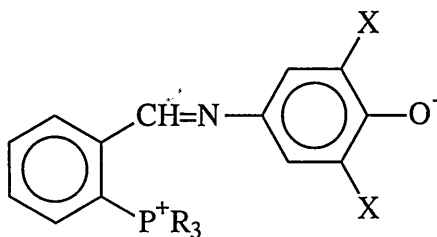
X = Cl, Br, Ph, Bu^t

(3A) X=Ph

(3B) X=Bu

X = Cl, Br, Ph,

(4)

47
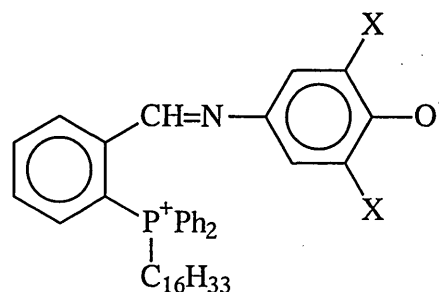
Systems (1) and (2) offer the possibility of short range charge-transfer from a charged aromatic electron-donor to a directly linked charged aromatic acceptor group, giving rise to a large difference between the dipole moments of the excited and ground state molecules.[1] In systems (3) and (4) the negative phenolate moiety is the electron-pair donor and the positive phosphonium centre is the electron-pair acceptor.

Apart from systems (1) and (3) very little has been published on solvatochromic phosphonium betaine systems. The azo phosphonium betaine dye (5) has been described along with its solvatochromic properties but this system was not found to be as solvatochromic as the related imino betaine (3).[2] The dipolar system (6) has been shown to exhibit a limited degree of solvatochromism,[3] and the phosphonium phenolates (7) have been characterised and reported to show an intense intramolecular charge-transfer absorption band at λ_{max} 480-500 nm in dichloromethane, but their solvatochromic properties do not seem to have been studied.[4]

R = Ph or Bu
X = Cl, F, Me

(5)

(6)

(7)

R = Me or Ph
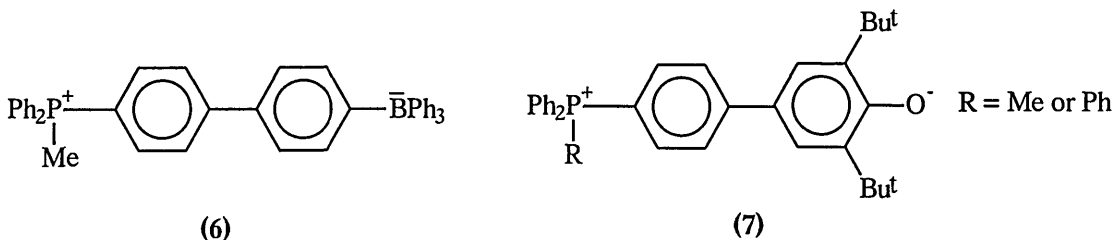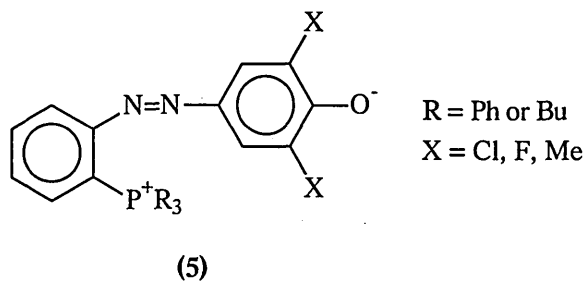
Recently Lambert et al, have synthesised and reported the nonlinear optical properties of three-dimensional phosphonium ion chromophores.[5] Comparison of the two three-dimensional dibutylaminoazobenzenephosphonium salts (9) and (10) against the one-dimensional system (8) showed that the NLO properties of the three-dimensional compounds behaved additively, whilst the first order hyperpolarisability (β) is greatly enhanced in (9) compared to (10).

48

Bu_2N—⟨⟩—$N=N$—⟨⟩—$P^+(Ph)_2Me$ I^- (8)

$[Bu_2N$—⟨⟩—$N=N$—⟨⟩—$]_nP^+Me_{4-n}$ I^- n = 3 (9) n = 4 (10)
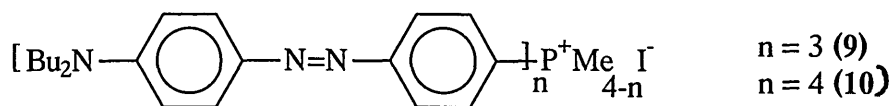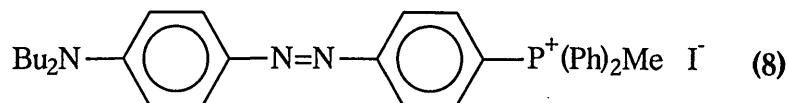
Mesomeric intramolecular charge-transfer in systems **(2)** and **(4)** is reduced compared to the pyridinium systems **(11)** and **(12)** due to the reluctance of phosphorus to become involved in d_π bonding.[6] However, these systems are still of interest as potential NLO systems as the π-electron system is perturbed by inductive and, or field effects, by the phosphonium centre. This has also been discussed for a range of organoammonium organoborate zwitterions **(13)**, in which the negative and positive centres are separated by a polarisable π system,[7] but themselves are incapable of conjugative interactions.

R—N^+⟨⟩— (benzimidazolide)

(11)

R—N^+⟨⟩—$CH=N$—⟨⟩—O^- (with X substituents)

(12)

Me_3N^+—⟨⟩—B^-Bu_3

(13)
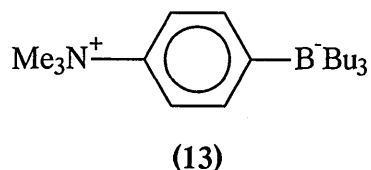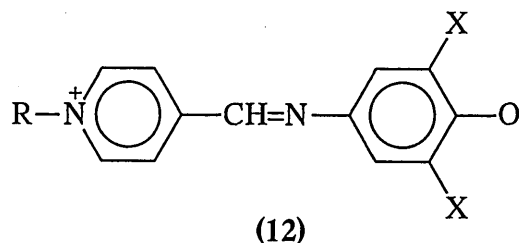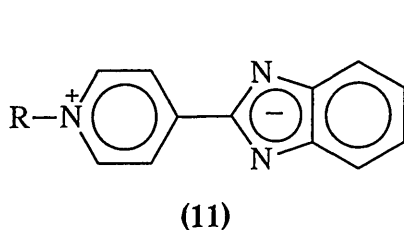
The first part of this chapter describes the synthesis and characterisation of the salts and betaines of type **(2)** and **(4)** with a long chain phosphonium group as the cationic centre.

The second part of the chapter describes the effects of annelation on the solvatochromic properties of systems **(1)** and **(3)**. This was of particular interest, as any potential NLO properties of the LB films of **(2)** and **(4)** could only be investigated (at Cranfield University), if the charge-transfer absorption band is appropriate with the wavelength of the laser used (1064 nm) (93985 cm^{-1}). Hence the emission line for SHG of an NLO material would be 532 nm (187970 cm^{-1}), and it is required that the

compounds have an absorption band which just about overlaps with 532 nm, (i.e. low absorption), but the main absorption maxima should be as far away from this emission line as possible. Annelation would be expected to move the wavelength of the charge-transfer absorption band to a more useful area, (i.e. to longer wavelength) due to an increase in overall conjugation. In consequence, compounds of type (14) and (15) have been synthesised and characterised, and the effects of annelation on their absorption maxima are reported.

(14)   (15)
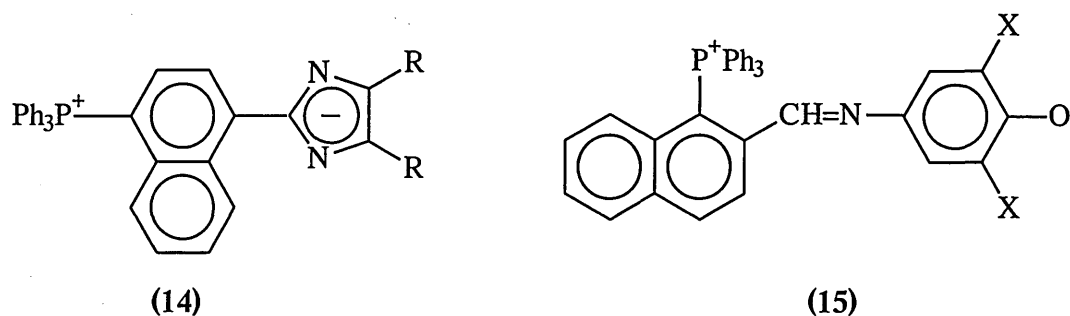
An LB film of the pyridinium betaine (16) has previously been prepared and its properties as a sensor system studied.[8] However, at Cranfield an expensive Nd:YAG laser was used to test for sensing applications instead of an inexpensive laser diode, which would have been of greater applicability. For the latter source, the betaine would have to absorb at a higher operating wavelength, which may be achievable by modifying the heterocyclic acceptor and or the π- electron bridge of the betaine. Hence it was considered that the related quinolinium system (17) would be ideal, in that it should be strongly absorbing yet essentially transparent at any likely emission wavelength. In this chapter the synthesis and characterisation of quinolinium betaines of type (17) is reported, together with an investigation of their sensor properties.

$$\text{X} \quad \overset{\displaystyle O^-}{\bigcirc} \quad \text{X}$$

$$\underset{\text{N}}{\parallel}$$

$$\text{CH}$$

$$\underset{\overset{|}{\text{C}_{16}\text{H}_{33}}}{\text{N}+}$$
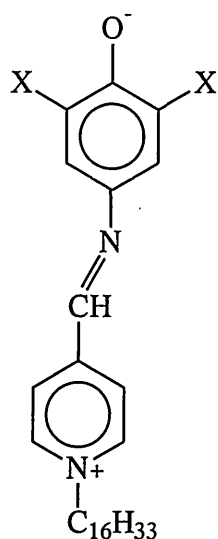
X = Cl, Br, Bu^t

(16)
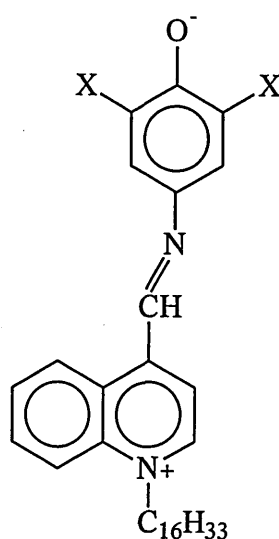
X = Cl, Br

(17)

2.1 Long chain phosphoniophenyl imidazolide betaines

2.1.1 Synthesis of the imidazoles.

The imidazoles **(18)** and **(19)** were prepared according to the general procedure (scheme 1).[9] 2-Bromo and 4-bromobenzaldehyde, respectively, were allowed to react with benzil or 9,10-phenanthraquinone in refluxing glacial acetic acid with nine mole equivalents of ammonium acetate. The mechanism of the reaction is shown in scheme 2.
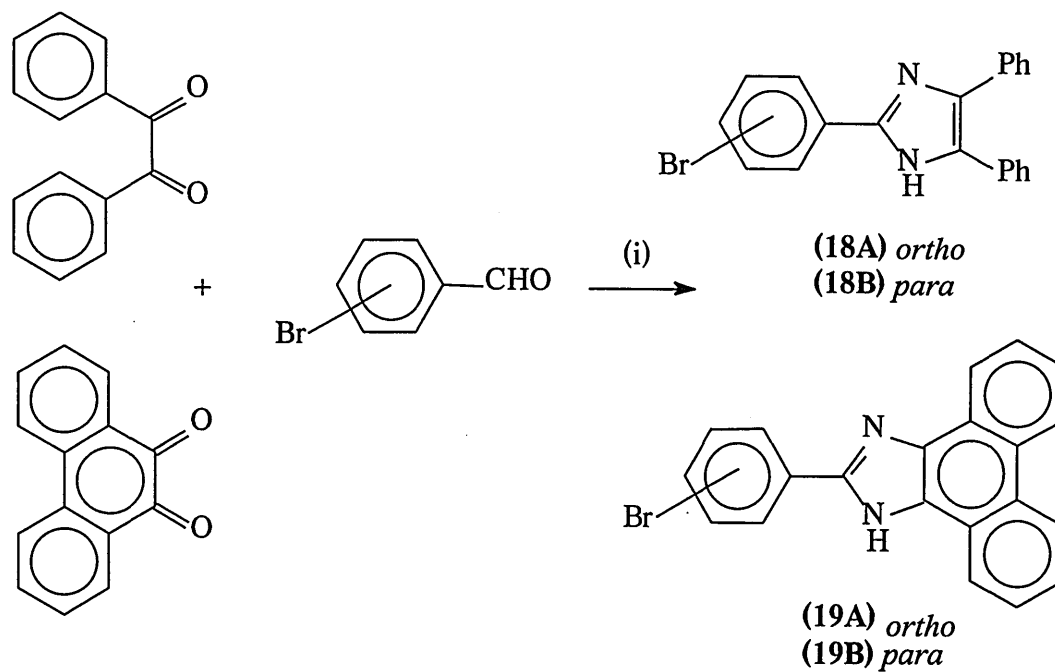
(i) ammonium acetate, glacial acetic acid, reflux, 5hrs

Scheme 1

The synthesis is the condensation of the 1,2 dicarbonyl compound (benzil or 9,10-phenanthraquinone) with ammonium acetate and an aldehyde (2- or 4-bromobenzaldehyde). A reasonable rationalisation is a cyclocondensation type process to give **(20)** followed by irreversible tautomerism **(21)**.[10]

R$_1$ ... O ... + ... O ... H ... R$_2$ ... $\overset{+}{N}H_4\overset{-}{O}Ac$ ... R$_1$ ... NH ... NH ... H ... R$_2$ ... H$^+$

(20)

tautomerism

(21)

E.g. R$_1$ = Ph

R$_2$ = (benzene ring)—Br

−NH$_3$
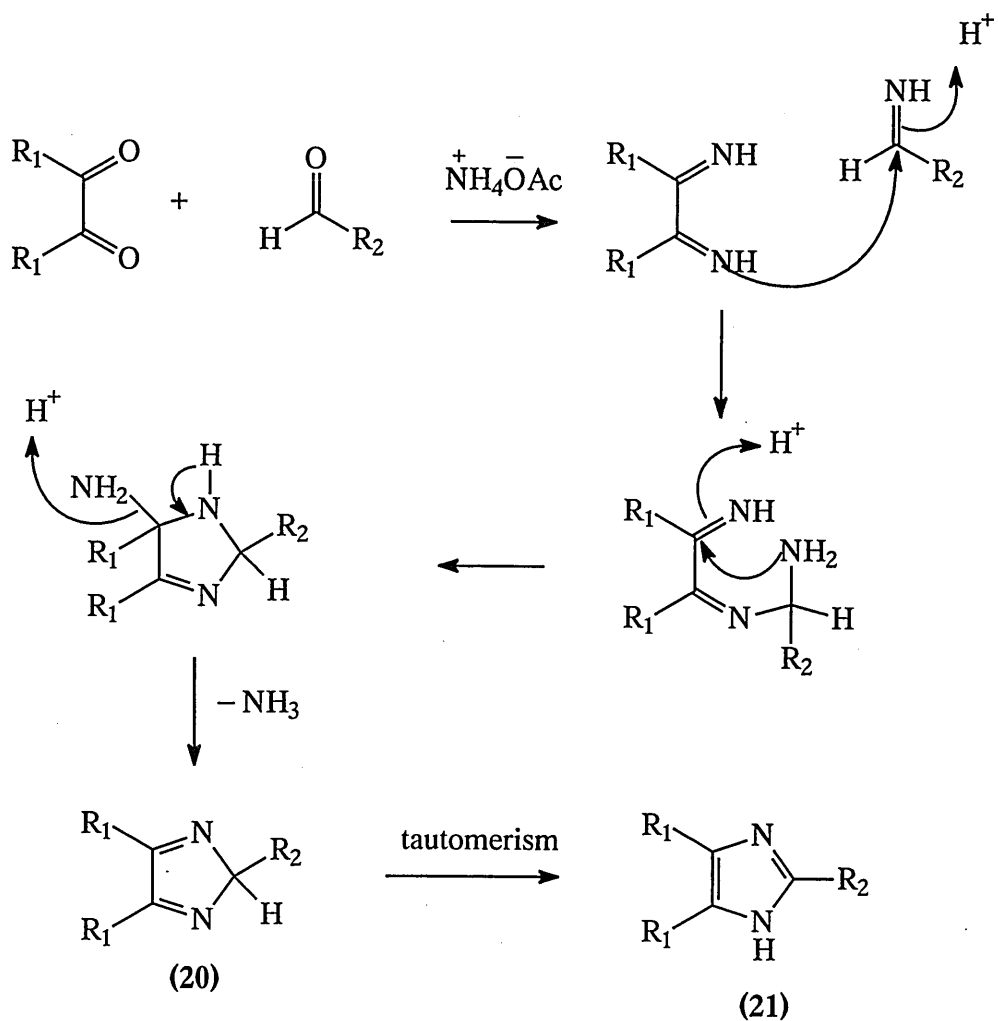
H$^+$
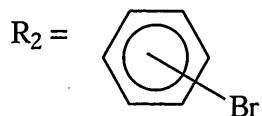
Scheme 2

2.1.2 Synthesis of N-hexadecyldiphenylphosphine.

The synthesis of the phosphine **(22)** was first attempted by a Grignard reaction (scheme 3), in dry ether and subsequently in dry THF. The Grignard reaction did not proceed, even using the preformed Grignard reagent $BrMg(CH_2)_2MgBr$ to help initiate the reaction. It is thought that, possibly, the long hydrocarbon chain of 1-iodohexadecane coats the surface of the magnesium metal, hindering the reaction.

$$C_{16}H_{33}I \xrightarrow{\text{(i)}} C_{16}H_{33}MgI \xrightarrow{\text{(ii)}} C_{16}H_{33}PPh_2$$

$$\textbf{(22)}$$
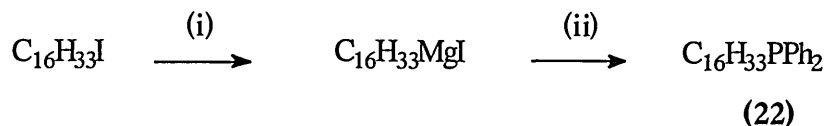
(i) Mg, diethyl ether (dry) or THF (dry), I_2

(ii) $ClPPh_2$, diethyl ether (dry), or THF (dry)

Scheme 3

The phosphine **(22)** was successfully synthesised by the formation of lithium diphenylphosphide, followed by its reaction with 1-iodohexadecane (scheme 4). The crude product was recrystallised from methanol to remove a polar impurity and the oxide of **(22)**. As the phosphine was found to be stable in air, purification by column chromatography (using dichloromethane as the eluting solvent) greatly improved the yield.

$$ClPPh_2 \xrightarrow{\text{(i)}} Ph_2PLi \xrightarrow{\text{(ii)}} C_{16}H_{33}PPh_2$$

$$\textbf{(22)}$$
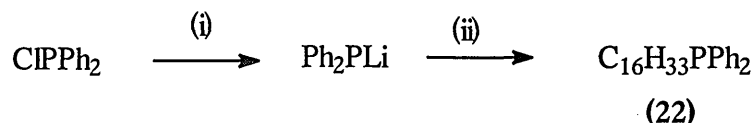
(i) 2Li, THF (dry)

(ii) $C_{16}H_{33}I$, THF (dry)

Scheme 4

2.1.3 Synthesis of the long chain phosphonium salts.

Trivalent phosphorus compounds such as triphenylphosphine do not undergo direct nucleophilic substitution with aryl halides as they do with alkyl halides via an S_N2 mechanism, and the use of a transition metal catalyst needs to be used. Tertiary phosphines react readily with most aryl halides to form phosphonium salts at high temperature (150-200 °C) usually in the absence of a solvent (melt reaction),[11] although these reactions have also been conducted in refluxing benzonitrile (191 °C)[12] and ethylene glycol (196-198 °C).[13] These reactions are carried out in the presence of a metal salt catalyst e.g. $Co(II)Br_2$, $Ni(II)Br_2$, and $Cu(II)Br_2$.

The imidazoles **(18)** and **(19)** were treated with a slight excess of the phosphine **(22)** and half a mole equivalent of nickel (II) bromide (as the catalyst) in refluxing benzonitrile for between four to five hours under nitrogen (scheme 5). Upon cooling, the solutions were poured into aqueous potassium bromide solution and extracted with dichloromethane. In the synthesis of conventional arylphosphonium salts, once the

54

dichloromethane is evaporated, the benzonitrile solution is usually poured into diethyl ether, causing the salt to precipitate out, commonly as an oil. Subsequent trituration with fresh diethyl ether removes benzonitrile and other impurities, leaving the salt as a solid. However, due to the presence of the long chain, the salts **(23)** and **(24)** were found to be *soluble* in diethyl ether. Precipitation of the salts did not occur from petrol either, so they were successfully isolated from the benzonitrile solution (and the non-polar impurities) as pale yellow solids by column chromatography, using a mixture of dichloromethane and methanol as the eluting solvents.

R = Ph **(23A)** *ortho*, **(23B)** *para*

R = *o*-phenanthra. **(24A)** *ortho*, **(24B)** *para*
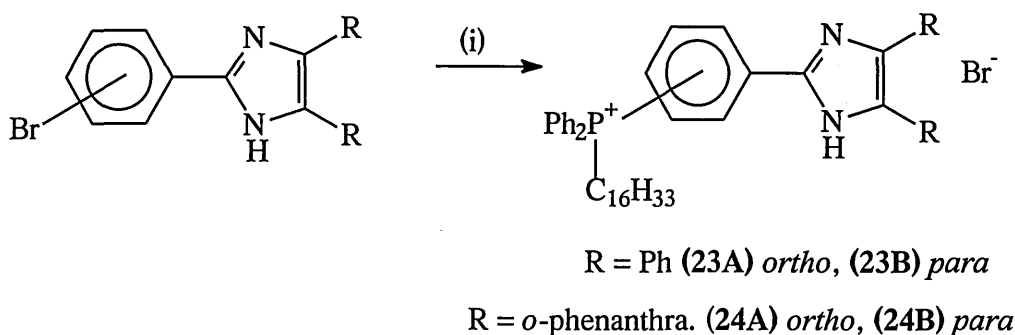
(i) $C_{16}H_{33}PPh_2$, $NiBr_2$, PhCN, reflux, 5hrs, N_2

Scheme 5

In the above reaction, it is likely that the nickel (II) bromide is reduced in the presence of the tertiary phosphine and the aryl halide to the nickel (I) oxidation state. The nickel (I) species is thought to be the active catalyst, which undergoes oxidative insertion into the carbon-halogen bond forming the arylnickel (III) intermediate **(25)**, (scheme 6). Reductive elimination then follows with the formation of the carbon-phosphorus bond and regeneration of the nickel (I) catalyst.[12]

Scheme 6

55
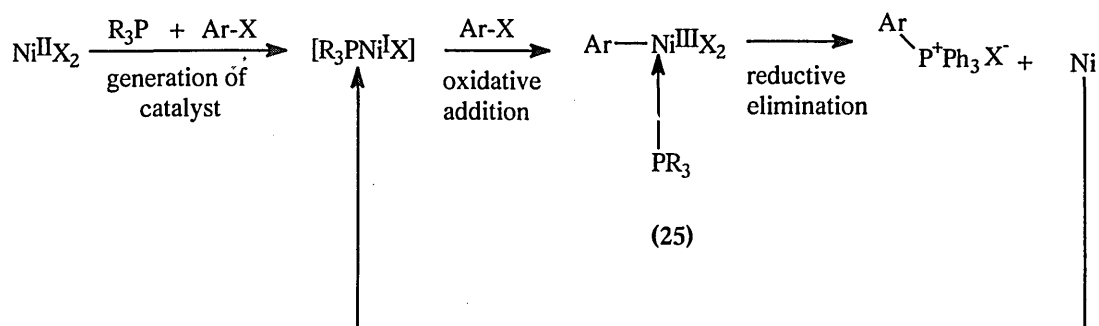
2.1.4 Synthesis of the long chain phosphonium betaines.

The phosphonium salts (23) and (24) were converted to the related betaines by stirring for an hour at room temperature with an excess of potassium carbonate in acetonitrile (scheme 7). Both betaines (26) and (27) were obtained as bright fluorescent yellow solids. In earlier work, the related triphenyl phosphonium salts of type (1) had been converted to the betaines by treating with one mole of aqueous sodium hydroxide in ethanol.[1] Both procedures are equivalent.

(23, 24)

(i)

R=Ph (26A) *ortho*, (26B) *para*

R = *o*-phenanthra. (27A) *ortho*, (27B) *para*
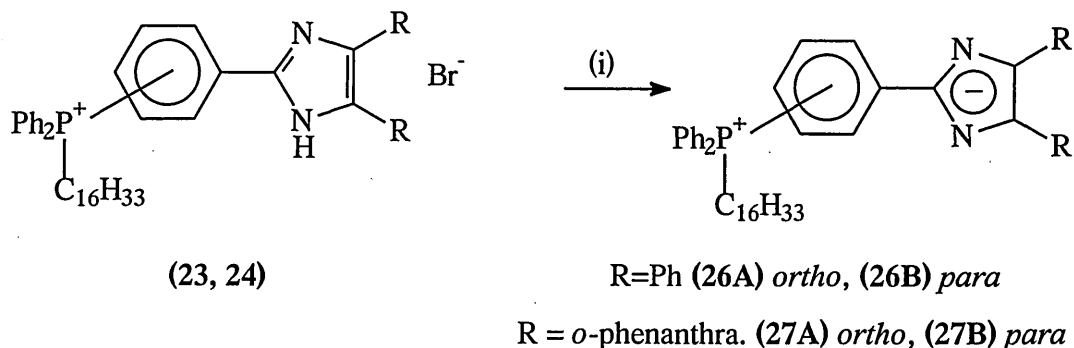
(i) K_2CO_3, MeCN, r.t., 1hr

Scheme 7

2.1.5 Characterisation of the long chain salts and betaines.

The phosphorus NMR spectra of all four salts and their respective betaines consisted of a single resonance (table 1). In the case of the long chain *ortho* phosphonio-phenyl systems, there is a significant difference in chemical shift between the salt and the respective betaine (3.50-3.75 ppm), suggesting that the betaines possess a different electronic structure to that of the salts. In the case of the related *para* isomers there is only very little difference in the chemical shift (*ca*. 0.2-0.6 ppm).

Salt	Chemical shift (ppm)	Betaine	Chemical shift (ppm)
23A	26.33	26A	22.84
23B	22.75	26B	22.12
24A	27.37	27A	23.63
24B	22.70	27B	22.49

Table 1 ^{31}P NMR data for betaines (26) and (27) and the parent phosphonium salts (23) and (24).

Previous phosphorus NMR studies on triphenylphosphoniobenzimidazolide compounds[14] and those of type (1)[(1)] have shown that the *ortho* betaines have a considerably lower chemical shift than that of the parent salt. This suggests that there is an interaction between the positive phosphonium centre and the negative imidazolide centre, thus tending towards a phosphorane species (fig.1).
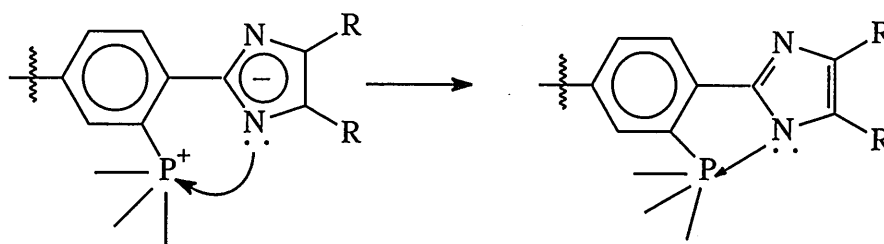
Figure 1

The proton NMR spectra of all the salts and betaines showed the presence of the long aliphatic chain between *ca.* 0.8-3.4 ppm. Conversion to the betaine was confirmed by the disappearance of the NH signal (singlet), and additionally the betaines gave a negative halide test on treatment with nitric acid-silver nitrate.

Under FABMS conditions, all salts gave a characteristic molecular cation, and the betaines showed the required (molecular ion + 1). Both salts and betaines could not be characterised by electron impact mass spectrometry as no molecular ion was observed.

Microanalysis results for the salt (23B) correlate well with the theoretical data, and suggest that betaine (26B) is mono-hydrated.

2.1.6 Solvatochromism studies.

The UV/Visible absorption spectra were measured on a UNICAM UV$_2$-100 spectrophotometer, with a matched pair of quartz cells of 1 cm thickness. The absorption spectra of each solution was obtained in the range 200 – 850 nm, using one cell containing pure solvent as the reference. The solvents used were all analytical reagent grade (Aldrich), and the measurements were taken at room temperature and pressure. The concentrations of the solutions used were *ca.* 1 x 10^{-4} mol l^{-1}.

Due to the presence of the long chain, the salts (23) and (24), and betaines (26) and (27) were soluble in toluene, which was not the case for system (1).

A slight shift in wavelength was observed in each of the solvents for the salts (23) and (24) (table 2). The long chain betaines (26) and (27) showed the characteristic

57

intramolecular charge-transfer (CT) absorption band at a very similar wavelength to that of the betaines of type (1A) (tables 3 and 4).[1] All the betaines showed negative solvatochromism (a hypsochromic shift), the absorption maximum moving to longer wavelength in non-polar solvents. The absorption maximum of the betaines occurred at a significantly longer wavelength than that of the parent salts.

The betaine systems did not show a very large solvatochromic range, but as with (1A), it was seen that the betaines with the phosphonium centre in the *para* position to the negative imidazole centre were more solvatochromic than the *ortho* analogues. For example (27A) (*ortho* analogue) undergoes a hypsochromic shift of 30 nm (15873 cm^{-1}) from toluene to acetonitrile, compared to (27B) (*para* analogue) which undergoes a larger hypsochromic shift of 44 nm (21588 cm^{-1}) from toluene to acetonitrile. This may be due to the *ortho* analogues tending towards a phosphorane species (as discussed above), so there will be less intramolecular charge-transfer throughout the system. All the betaine systems appear to be effectively protonated back to the salt in methanol.

Solvent	λ_{max} nm (23A)	λ_{max} nm (23B)	λ_{max} nm (24A)	λ_{max} nm (24B)
Methanol	362	360	368	390
Acetonitrile	362	374	370	376
Acetone	364	378	372	380
Dichloromethane	366	378	372	392
Tetrahydrofuran	368	380	374	400
Toluene	370	382	374	402

Table 2. Absorption maxima (λ_{max} nm) of salts (23) & (24) in various solvents.

Solvent	λ_{max} nm (26A)	ν_{max} x10^{-3} cm^{-1} (26A)	λ_{max} nm (26B)	ν_{max} x10^{-3} cm^{-1} (26B)
Methanol	(362)*	(27.62)	(360)*	(27.78)
Acetonitrile	426	23.47	432	23.15
Acetone	430	23.26	450	22.22
Dichloromethane	434	23.04	446	22.42
Tetrahydrofuran	446	22.42	464	21.55
Toluene	452	22.12	468	21.37
$\Delta_{Toluene-MeCN}$	26	-1.35	36	-1.78

$\Delta\nu_{max} = \nu_{nonpolar} - \nu_{polar}$

* = salt

Table 3   Absorption maxima (λ_{max} nm) of betaine (26) in various solvents.

Solvent	λ_{max} nm (27A)	ν_{max} x10^{-3} cm^{-1} (27A)	λ_{max} nm (27B)	ν_{max} x10^{-3} cm^{-1} (27B)
Methanol	(368)*	(27.17)	(390)*	(25.64)
Acetonitrile	420	23.80	430	23.26
Acetone	432	23.15	446	22.42
Dichloromethane	434	23.04	448	22.32
Tetrahydrofuran	446	22.42	470	21.28
Toluene	450	22.22	474	21.09
$\Delta_{Toluene-MeCN}$	30	-1.58	44	-2.17

$\Delta\nu_{max} = \nu_{nonpolar} - \nu_{polar}$

* = salt

Table 4   Absorption maxima (λ_{max} nm) of betaine (27) in various solvents.

The molar transition energies E_T (Kcal mol^{-1}) have been calculated for the betaines (26) and (27), indicating the interaction of the betaine molecules with the solvent systems. They were calculated from equation (1) in chapter 1.

	E_T values (Kcal mol^{-1})			
Solvent	**(26A)**	**(26B)**	**(27A)**	**(27B)**
Methanol	(78.98)*	(79.42)*	(77.69)*	(73.31)*
Acetonitrile	67.12	66.18	68.07	66.49
Acetone	66.49	63.53	66.18	64.70
Dichloromethane	65.88	64.11	65.88	63.82
Tetrahydrofuran	64.11	61.62	64.11	60.83
Toluene	63.25	61.09	63.54	60.31
ΔE_T	-3.87	-5.09	-4.53	-6.18

* = salt

$\Delta E_T = E_{T\,nonpolar} - E_{T\,polar}$

Table 5   The molar transition energies E_T (Kcal mol^{-1}) of betaines (26) and (27) in various solvents.

Looking at table 5, the E_T values of (26) and (27) are lower than that of the $E_T = $ (Z) values obtained by Kosower[15] for acetonitrile, (table 6), but for the other solvents the values are very similar. Comparing to the $E_T(30)$ values for Reichardt's betaine dye[16] (table 6) the values are significantly higher for all solvents.

Thus, e.g., for (26A), an E_T value of 67.12 Kcal mol^{-1} in acetonitrile means that a transition energy of 67.12 Kcal is required to bring one mole of (26A) dissolved in acetonitrile from the electronic ground state (28A) to the first excited state (28B).

(28A) ↔ (28B)
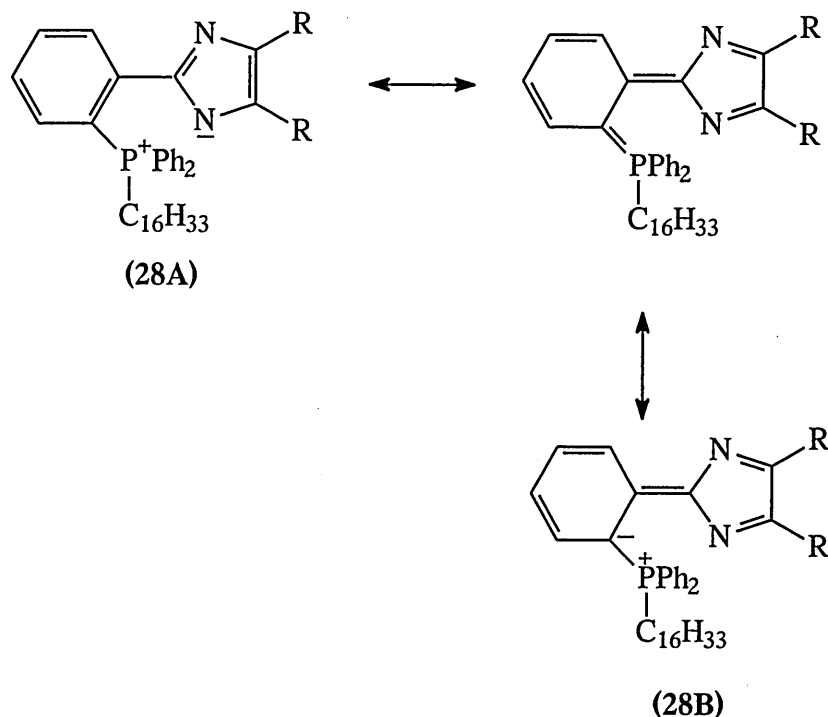
This means that the ground state of each of the betaines **(26)** and **(27)** is less stable in acetonitrile compared to Kosower's 1-ethyl-4-methoxycarbonylpyridinium iodide, but, the ground state of **(26)** and **(27)** is more stable in acetonitrile compared to Reichardt's betaine dye.[16]

A stronger stabilising effect of the solvent on the ground state, as compared with the excited state, will lead to a higher transition energy (E_T). Hence, for **(26)** and **(27)** the polar ground state is more stable in the polar solvents than in the non polar solvents, compared to the less polar excited state.

The empirical parameters of solvent polarity $E_T(30)$ and the normalised empirical solvent polarity parameters[34] E_T^N are shown in table 6 as well as Kosower's $E_T = (Z)$ values.[15] These $E_T(30)$ values have been derived from Reichardt's betaine dye as discussed in chapter 1.

61

Solvent	$E_T = Z$ (Kcal mol^{-1})	$E_T(30)$ (Kcal mol^{-1})	E_T^N
Methanol	83.6	55.4	0.762
Ethanol	79.6	51.9	0.654
Acetonitrile	71.3	45.6	0.460
Acetone	65.5	42.2	0.355
Benzonitrile	65.0	41.5	0.333
Dichloromethane	64.7	40.7	0.309
Ethyl acetate	59.4	38.1	0.228
Tetrahydrofuran	58.8	37.4	0.207
Toluene	—	33.9	0.099

Table 6 Empirical scales of solvent polarity.

Figure 2 shows a plot of wavenumber v of the intramolecular absorption band for the betaines against the normalised solvent polarity parameter E_T^N. The similarity of all the plots indicates that all are showing similar behaviour in each solvent with respect to the solvation of the ground and excited state.
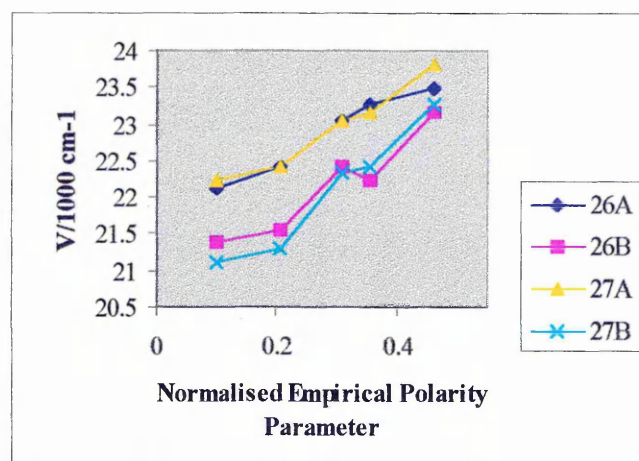
Figure 2 Plot of wavenumber of longest visible absorption band of the betaines (26) and (27) against the normalised polarity parameter.

2.1.7 Isotherm Data.

The formation of monolayer LB films of the two *para* long chain betaines **(26B)** and **(27B)** was studied at Cranfield University.

The betaine dye **(26B)** was spread from dilute chloroform (Analar) solution (0.096 gL^{-1}) on to the pure water subphase of the LB trough (Nima Technology, model 622), at 23 °C. The dye was then compressed at 50 $\text{mm}^2 \text{ s}^{-1}$ (equivalent to a surface area loss of 0.1 % s^{-1}). The pressure-area (π-A) isotherm (fig. 3) shows collapse at 42 mNm^{-1}.
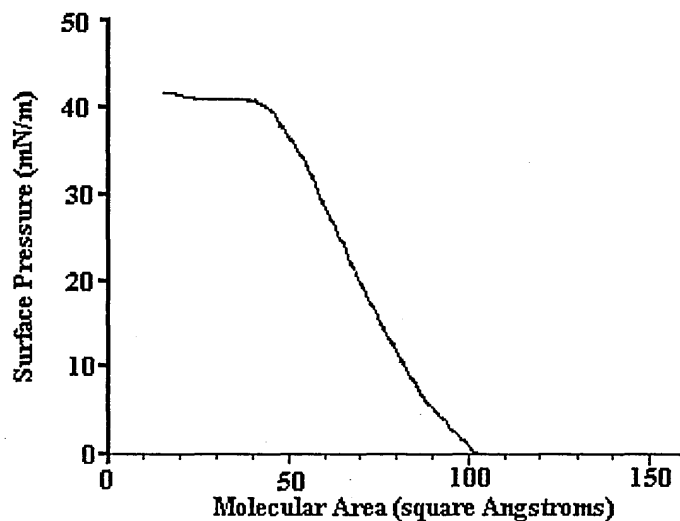
Figure 3   Surface pressure versus area isotherm of betaine **(26B)**.

As with **(26B)** the betaine dye **(27B)** was spread from dilute chloroform (Analar) solution (0.101 g L^{-1}) at 23 °C and then compressed at 50 $\text{mm}^2 \text{ s}^{-1}$. The pressure-area ($\pi$-A) isotherm (fig. 4) shows collapse at 49 mNm^{-1}.
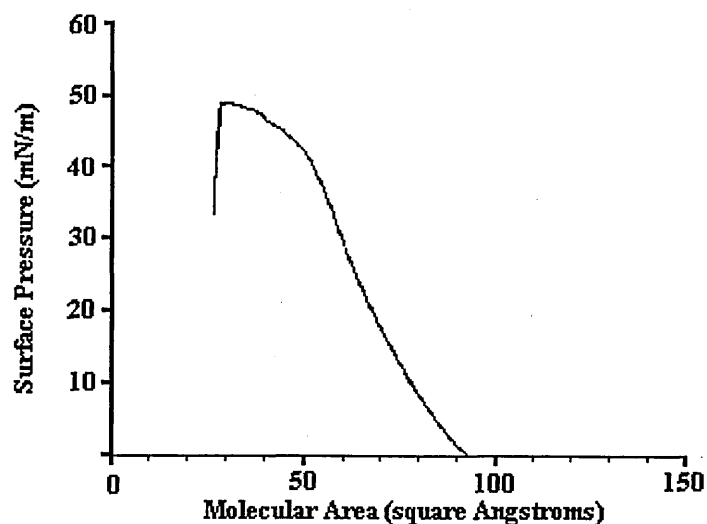
Figure 4 Surface pressure versus area isotherm of betaine (**27B**).

There are no obvious phase changes in any of the isotherms which suggests no major re-orientations of the molecules. A comparison between the isotherms of (**26B**) and (**27B**) can be made, and shows that (**26B**) with the phenyl groups has a wider profile at a low pressure (i.e. take off at 102 Å^2) and is more compressible due to the flexible bonding to the phenyl groups. Betaine (**27B**) has a more rigid head group which occupies a smaller molecular area at low pressures. This rigid group seems to make the monolayer less compressible which is evident in the steeper isotherm.

2.2 Long chain phosphonium benzylidene iminophenolate betaines

2.2.1 Synthesis of the imines.

The iminophenol intermediates **(29-32)** were synthesised by the reaction of 2-bromobenzaldehyde and the appropriate 3,5-disubstituted aminophenol in refluxing ethanol (scheme 8).[2]
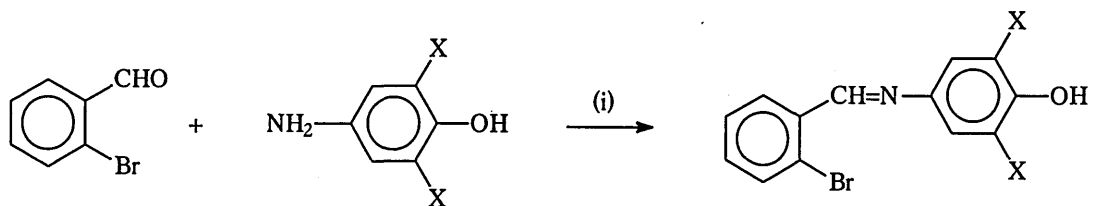
(29) X=Cl, **(30)** X=Br, **(31)** X=Ph, **(32)** X= Bu^t

(i) EtOH, reflux, 2-3hrs, N_2

Scheme 8

The reaction is an addition-elimination reaction, (scheme 9), where the amine nucleophile attacks the carbonyl group to form the intermediate aminal, and the stable imine is subsequently formed through loss of water.
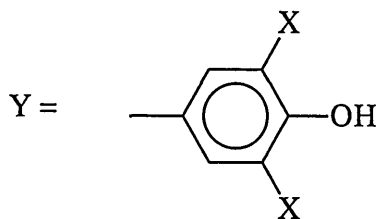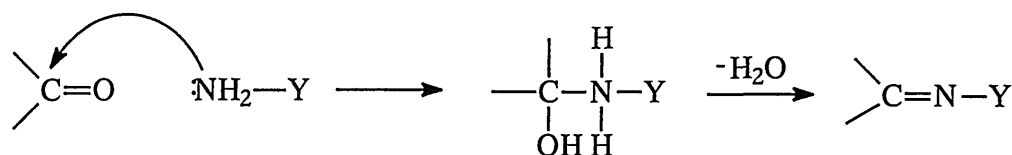
X = Cl, Br, Ph

Scheme 9

The 4-amino-2,6-dichlorophenol and the -dibromophenol were available commercially but the amino-diphenylphenol and -di-t-butylphenol had to be synthesised, (schemes 10 and 11) respectively.[17, 18]
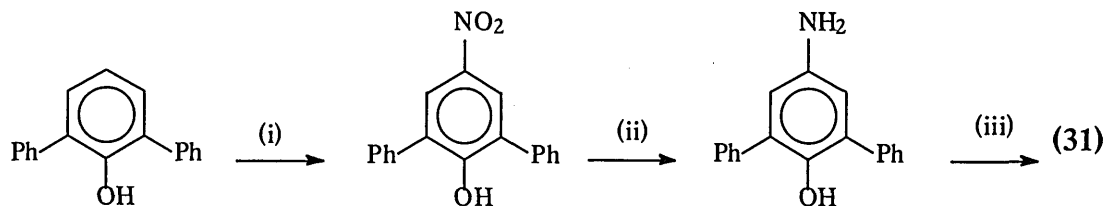
(i) 50:50 HNO$_3$(70 %):H$_2$O, r.t., stir overnight

(ii) NaOH(aq), reflux, Na$_2$S$_2$O$_4$

(iii) 2-Bromobenzaldehyde, EtOH, reflux, 3hrs, N$_2$

Scheme 10
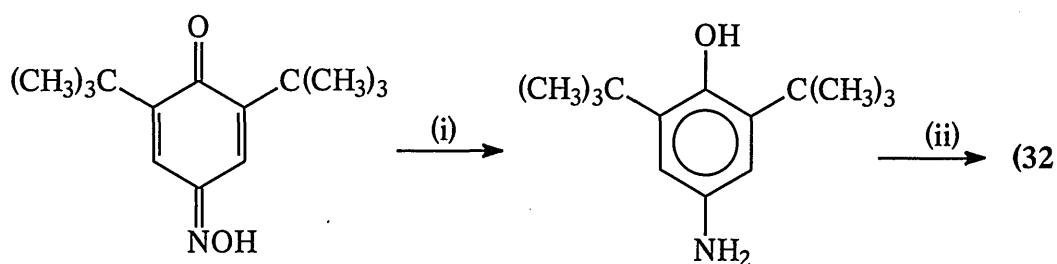
(i) THF, NaOH (aq), 45 °C, Na$_2$S$_2$O$_4$

(ii) 2-Bromobenzaldehyde, EtOH, reflux, 2hrs, N$_2$

Scheme 11

2.2.2 <u>Synthesis of the long chain phosphonium salts.</u>

The phosphonium salts were prepared under mild conditions in refluxing ethanol (b.p. 80 °C) (instead of benzonitrile) from the related imine and **(22)** in the presence of nickel (II) bromide as the catalyst, (scheme 12).

(22)   **(33)** X=Cl, **(34)** X=Br, **(35)** X=Ph, **(36)** X=Bu^t
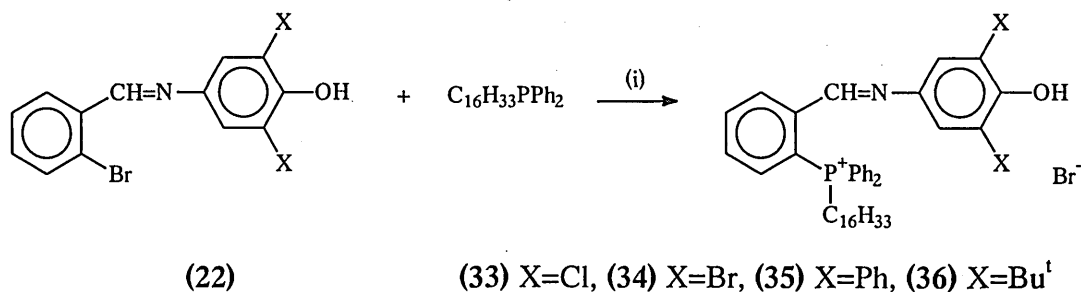
(i) EtOH, NiBr$_2$, reflux, 5-8hrs, N$_2$

Scheme 12

66

These reactions make use of the well established *kinetic template effect* in which there is a metal ion-promoted replacement of the halogen *ortho* to a suitable donor group (e.g. nitrogen atom).[19-24] It aids the catalytic role of the metal ion in promoting the substitution reaction, and allows the reaction to be conducted at a much lower temperature (refluxing ethanol) rather than at the usual temperature at 200 °C.

The *ortho* phosphonium imidazole salts (**23A** and **24A**) could have also been prepared in ethanol, as there is also a suitable donor group *ortho* to the halogen to be replaced by the phosphine. The synthesis of the above Schiffs base salts (**33-36**) cannot be carried out in benzonitrile as, at the high temperature, the phosphine acts as a nucleophile and attacks the imine carbon instead of replacing the *ortho* halogen. Consequently the respective *para* salts of this Schiffs base series cannot be synthesised by this method as the *para* iminophenol precursors will not act as a kinetic template and so the reaction will not take place in ethanol.

Initial studies of the kinetic template effect in phosphonium salt synthesis centred on a series of Schiffs bases of type (**37**),[19] and further studies were carried out on a series of azo dyes of type (**38**).[19, 20]
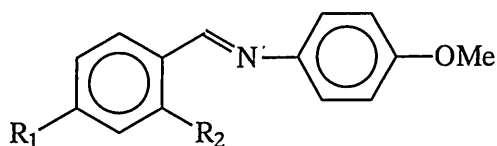
(37)

R_1 =H, R_2 =Br

R_1 =H, R_2 =Cl
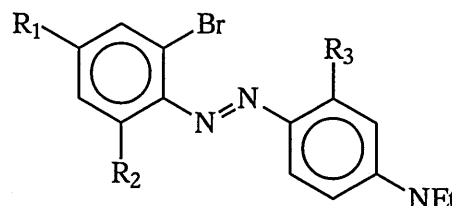
(38)

R_1 =Br, R_2 =Me

R_3 =NHCOMe

The formation of the above compounds (**37**) and (**38**) has much in common with the related reactions, carried out by Price *et al*, of *o*-bromodiarylazo compounds (**38**) with triethylphosphite (and diethylphosphite) in refluxing ethanol catalysed by copper (II) acetate, leading to the formation of *o*-diethylphosphonatodiarylazo compounds (**39**) in good yield.[25, 26] However, these phosphonation reactions were only catalysed by copper (II) acetate and not by nickel (II) bromide.

It was seen that these reactions proceeded at a faster rate if R_2 was not hydrogen,

and if R_3 was NHCOMe or any other coordinating group. If R_1 was bromine, it was not converted to the phosphonate ester, as it is *para* to the donor atom.
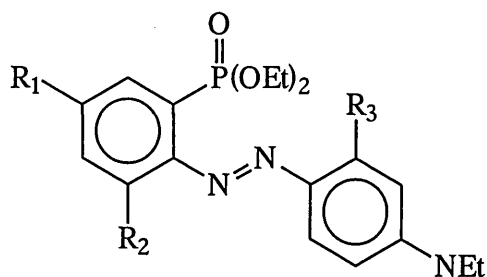
(39)

The mechanism of these reactions has been studied and has been found to be rather complex.[27] It has also been shown that phosphonate esters are formed in the reactions of the *o*-bromodiaryl azo dyestuffs with diethylphosphite in the presence of copper (I) iodide and sodium acetate in ethanol.[26]

For the reactions of the bromo Schiffs bases and dyestuffs with triphenyl- or tributyl- phosphine catalysed by nickel (II) bromide in ethanol, it was seen that, unlike in the reactions of Price *et al,* if R_3 is NHCOMe the formation of the *o*-phosphonium salt is slower than if R_3 is hydrogen. Additionally if R_2 is hydrogen the reaction rate was faster rather than slower.[20]

The critical nature of the donor atom and its position with respect to the *ortho* halogen for the promotion of a template-assisted replacement reaction has been studied. Unlike the Schiffs base **(40)**, the Schiffs bases **(41)** and **(42)** do not undergo conversion to the related phosphonium salts because neither is able to be involved in the correct mode of metal coordination, (i.e. formation of a five membered ring which involves the *ortho*-halogen and the nitrogen atom).[21]
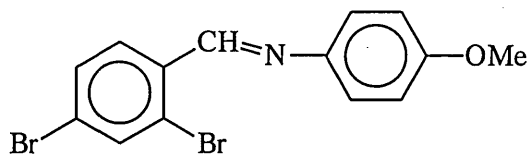
(40)
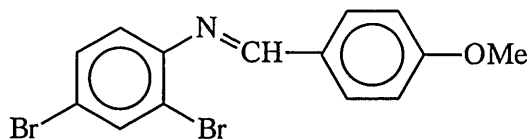
(41)
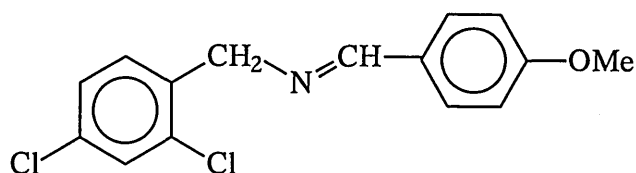
(42)

The related oximes and semicarbazones are similarly unreactive, and replacement of the nitrogen by either oxygen, (as an ether) or sulphur does not aid formation of the phosphonium salts. It appears that these metal-ion promoted substitution reactions require a very specific template of type **(43)**, where Z = CH or N and R is a non sterically crowded alkyl or aryl.
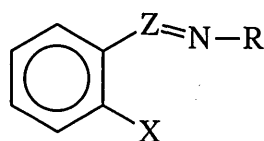
(43)

It is likely that these reactions involve electron-transfer catalysis[28] in which the metal salt (e.g. nickel (II) halide) is initially reduced to a lower oxidation state (e.g. Ni^I species) in the presence of the phosphine and the o-halogenoaryl template, and the nickel (I) species is the active catalyst.

This phosphine nickel (I) species undergoes a coordination template-assisted oxidative insertion into the carbon-halogen bond to form the intermediate **(44)**. Reductive elimination then follows with the formation of the carbon-phosphorus bond, and the regeneration of the nickel (I) catalyst (scheme 13).
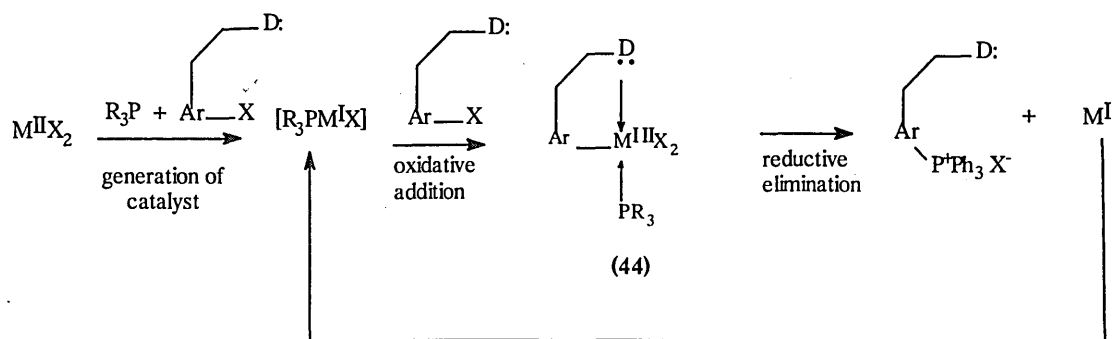
Scheme 13

For the range of Schiffs bases and azo dyes studied, it was found that iodine was

69

easier to replace than bromine, which was easier to replace than chlorine. The related *o*-fluoro Schiffs bases and azo dyes could not be converted to the related phosphonium salts, presumably due to the greater strength of the carbon-fluorine bond.

The reactions of the azo dyestuffs were catalysed by both nickel (II) bromide and copper (II) acetate (slower), but the Schiffs base reactions were only catalysed by nickel (II) bromide. The reactions did not occur in the absence of a transition metal catalyst, and the reaction rate was found to increase with increasing concentration of catalyst. The optimum conditions were found to be arylhalide (1 mol), tertiary phosphine (3 mol), and $NiBr_2$ (0.2 mol).[24]

In the present study the long chain phosphonium salts were isolated usually in a pure state by column chromatography. If not completely pure, they were then converted to the related perchlorate salt by treatment with lithium perchlorate in methanol. The salts were formed in good yield as yellow-beige solids, and all gave a positive halide test on treatment with nitric acid and silver nitrate.

2.2.3 Synthesis of the long chain phosphonium betaines.

The betaines were obtained from the related salts by stirring with a large excess of potassium carbonate in acetonitrile at room temperature (X = Cl, Br). For X = Ph and Bu^t, the betaine was formed by shaking the salt in dichloromethane with aqueous sodium hydroxide (scheme 14). This is because for systems (47 and 48) where (X=Ph and Bu^t), it was found that, using the potassium carbonate/acetonitrile system, the colour of the betaine faded in the solvent overtime, whereas under the latter conditions, conversion to the betaine was carried out in a much shorter time. The betaines were obtained as deep red (X=Cl, Br) or deep purple solids (X=Ph and Bu^t). Where X = Bu^t, (48) the isolated betaine was very crude and many peaks were observed in the phosphorus NMR spectrum. It did not prove possible to purify this compound, and no further studies were carried out on it. All the betaines (45-47) gave a negative halide test on treatment with nitric acid and silver nitrate.

$$\text{(33-36)} \qquad\qquad \text{(45) X=Cl, (46) X=Br, (47) X=Ph, (48) X=Bu}^t$$
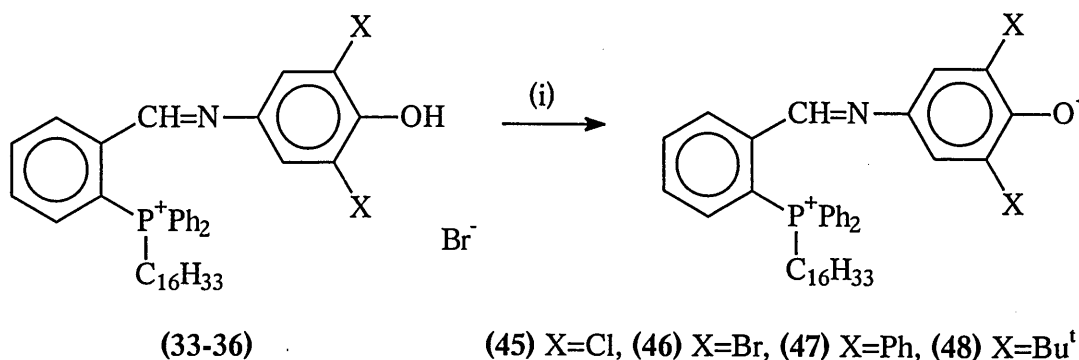
(i) K_2CO_3, MeCN, r.t. 1hr, or NaOH (aq), CH_2Cl_2

Scheme 14

2.2.4 Characterisation of the starting materials, salts and betaines.

All the iminophenols (29-32) (X=Cl, Br, Ph, Bu^t) showed a characteristic molecular ion by electron impact mass spectrometry. In the proton NMR spectrum (CDCl$_3$) the imino proton (CH=N) appeared as a singlet at around 8.8 ppm and the phenolic -OH group was observed at *ca.* 5.9 ppm as a broad singlet for (X=Cl, Br). The corresponding OH signals for (X=Ph) and (X=Bu^t) were seen further upfield at 5.5 ppm and at 5.2 ppm, respectively, due to the shielding effects of the phenyl and butyl groups.

The long chain phosphonium salts and betaines (4) were characterised by ^{31}P NMR and ^{1}H NMR spectroscopy. Accurate FAB mass spectrometry gave the required molecular cation for the salts and the (molecular cation + 1) for the betaines.

^{31}P NMR showed a single sharp resonance signal for each salt and betaine (table 7). The signal for each of the betaines is moved upfield by *ca.* 0.3-1.4 ppm from the parent salt, and there was a greater shift in the signal for (X=Ph) and (X=Bu^t) compared to (X=Cl) and (X=Br). The phosphorus nucleus has become shielded on going from the salt to the betaine, and more so for (47) and (48).

71

Salt	^{31}P NMR signal (ppm)	Betaine	^{31}P NMR signal (ppm)
(33)	27.41	(45)	26.7
(34)	27.03	(46)	26.72
(35)	27.67	(47)	26.28
(36)	27.48	(48) (crude)	26.15 (main)

Table 7 ^{31}P NMR signals for salts (33-36) and betaines (45-48).

The ^{1}H NMR spectra of both salts and betaines showed signals due to the long aliphatic chain between 0.8 and 3.5 ppm. For salt (36) and betaine (48), the signal due to the tertiary butyl group was masked by the long chain protons. Significant differences were seen in the electronic environment on conversion to the betaines. In the salts, the protons meta to the phenol group appeared as a sharp singlet at *ca.* 6.3-6.6 ppm, and on conversion to the betaines the singlet moved downfield slightly, (table 8).

For the parent salts of system (3A), conversion to the betaines resulted in the shift of this singlet to around 7.0-8.8 ppm, now as part of the aromatic multiplet.[2] For the long chain betaines (4) this was not the case, and the singlet could easily be discerned as a separate entity.

On conversion to the betaines (4) the CH=N proton moved upfield by *ca.* 0.3-0.7 ppm, (table 8). For system (3A) and the parent salts, these CH=N protons were not easily observed as they were hidden by the aromatic multiplet. This was not the case for the betaines and salts of type (4) and also for (3B) and its respective salts, where these protons were seen separately from the aromatic multiplet.

Compound	aromatic protons meta to -OH/O⁻ (ppm)	CH=N proton ppm
Salt (33) (X=Cl)	6.4	8.66
(34) (X=Br)	6.64	8.89
(35) (X=Ph)	6.32	8.71
(36) (X=Bu^t)	6.30	8.46
Betaine (45) (X=Cl)	6.47	8.24
(46) (X=Br)	6.71	8.19
(47) (X=Ph)	6.65	8.37
(48) (X=Bu^t)	-	—

Table 8 CH=N and aromatic proton shifts for salts (33-36) and betaines (45-48).

The phenolic OH could be observed only in the salts (X=Ph) and (X=Bu^t), at 5.5 ppm and 5.2 ppm, respectively.

2.2.5 <u>Solvatochromism studies of the long chain phosphonium betaines.</u>

As with (3A) and (3B) the long chain phosphonium betaine dyes exhibited negative solvatochromism in solution, (at ca. 1 x 10^{-4} mol l^{-1}), the position of the visible absorption band moving towards a longer wavelength as the solvent polarity decreased, (tables 9, 10 and 11). The betaines were soluble in the less polar solvents due to the presence of the long alkyl chain, enabling the observation of a wider solvatochromic range than was possible for (3A) and (3B).

The long chain betaines absorbed at a slightly shorter wavelength than the triphenyl analogues. For X = Cl, and Br, the difference was, on average, 10 nm in each solvent, and for X= Ph the difference was about 20 nm.

Betaine (45) exhibited a hypsochromic shift of 122 nm (49337 cm^{-1}) from tetrahydrofuran to methanol compared to (46), which exhibited a hypsochromic shift of 120 nm (48309 cm^{-1}). Surprisingly the absorption maxima of both these betaines shifted to a shorter wavelength in toluene. A comparison cannot be made against (3A) (X=Cl) and (X=Br) as they were not soluble in toluene. A possible explanation for this observation is that the long chain betaines were either forming micelles in the non-polar solvent, in which the polar head groups are clustered in the interior of the micelle (fig. 5), or are showing reverse solvatochromism.

73
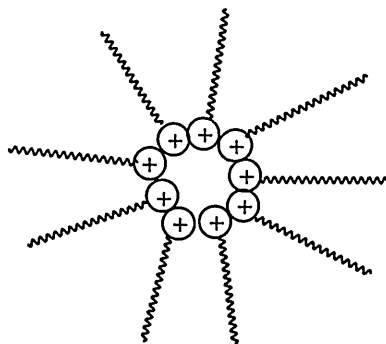
Figure 5

In methanol, betaine **(47)** appeared to exist essentially as the salt; the betaine exhibited a hypsochromic shift of 106 nm (28799 cm^{-1}) from toluene to acetonitrile. In contrast to **(45)** and **(46)**, the absorption wavelength maximum increased in toluene.

The observation of negative solvatochromism reflects the stabilisation in the more polar solvents of the ground state dipolar betaine form **(49A)** relative to the less polar excited-state forms **(49B)** and **(49C)**, (quinoidal structures), in which the ylidic form **(49C)** would be expected to be dominant in view of the minimal d-orbital involvement in the bonding in formally pentacovalent but four coordinate phosphorus compounds.[6]

(49A) ↔ (49B)

(49C)
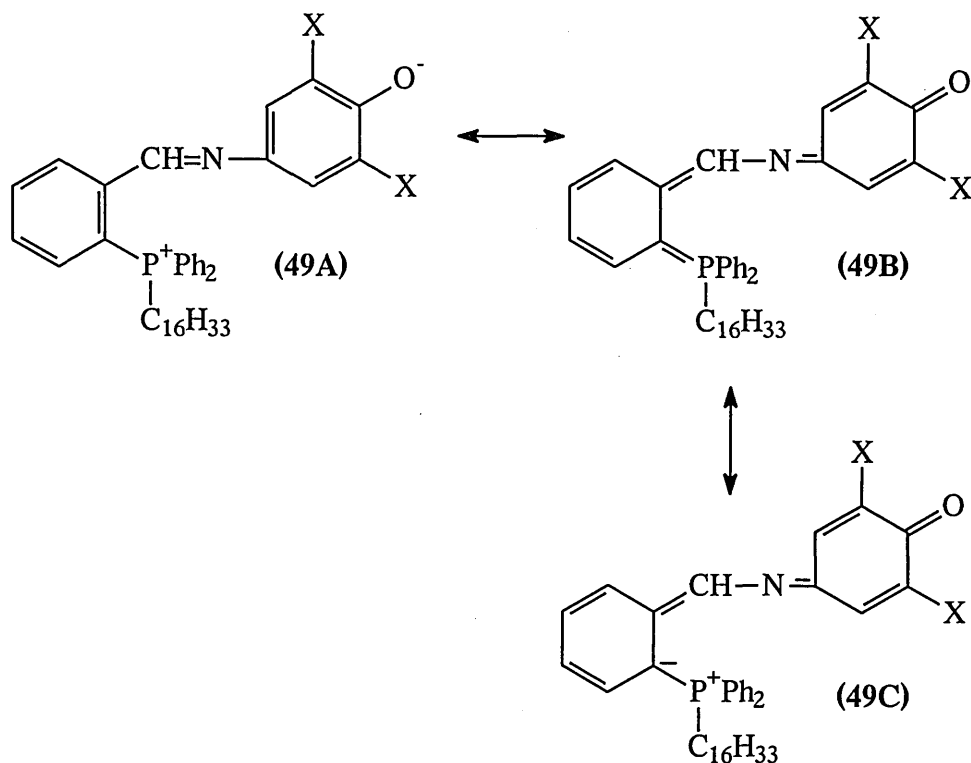
It has been noted with (3A) that the phenyl substituents at the phosphorus clearly shift the absorption maximum to a longer wavelength in each solvent compared to (3B) which has butyl groups at the phosphorus, although the effect is not large.[2] The phenyl substituents increase the wavelength on average by about 30 nm. The absorption maxima of the long chain phosphonium betaines are somewhere in between those of (3A) and (3B).

As with (3), there is a significant effect if phenyl is the group surrounding the oxygen atom bearing the negative charge, and this less polar substituent moves the absorption maximum towards longer wavelength by about 60 nm.

In methanol (a polar HBD solvent), betaines (45 and 46) showed a CT absorption band that was very much different from that of the salt. However, the related benzimidazolide betaines (26) and (27) were effectively protonated back to the salt in methanol, and did not show a CT absorption band due to the betaine. This is probably because the long chain imidazolide betaines (26 and 27) are more basic than the long chain iminophenol betaines (45 and 46), so they are more easily protonated back to the salt in methanol.
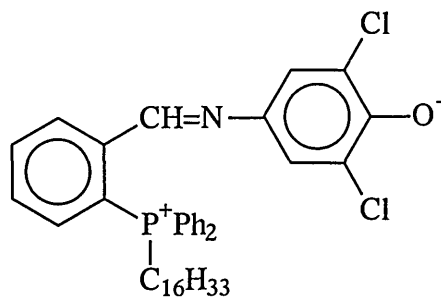
(45)   (3A)
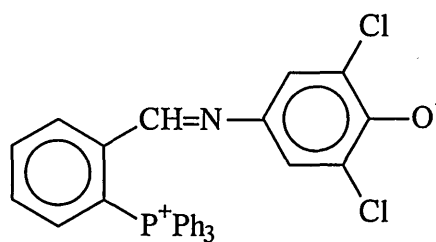
Solvent	Colour	Wavelength λ_{max} nm (45)	Wavelength λ_{max} nm (3A) (X=Cl)	v_{max} x10^3 (cm^{-1}) (45)
Methanol	yellow	440	446	22.73
Acetonitrile	red	494	504	20.24
Acetone	"	524	536	19.08
Dichloromethane	"	520	532	19.23
Ethyl acetate	red-purple	560	564	17.86
Tetrahydrofuran	"	562	578	17.79
Toluene	"	536	insoluble	18.66
$\Delta_{THF-MeOH}$		122	132	-4.94

$\Delta v_{max} = v_{nonpolar} - v_{polar}$

Table 9
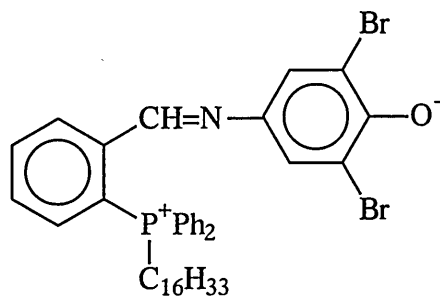
(46)   (3A)
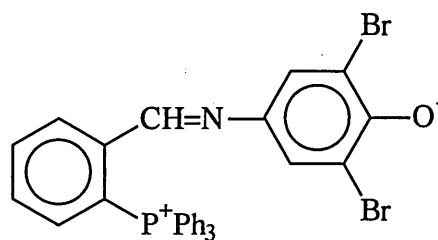
Solvent	Colour	Wavelength λ_{max} nm (46)	Wavelength λ_{max} nm (3A) (X=Br)	$v_{max} \times 10^3$ (cm^{-1}) (46)
Methanol	yellow	442	454	22.62
Acetonitrile	red-orange	494	496	20.24
Acetone	red	520	534	19.23
Dichloromethane	"	520	532	19.23
Ethyl acetate	red-purple	558	insol	17.92
Tetrahydrofuran	"	562	insol	17.79
Toluene	"	530	insol	18.87
$\Delta_{THF-MeOH}$		120	78	-4.83

$\Delta v_{max} = v_{nonpolar} - v_{polar}$

Table 10
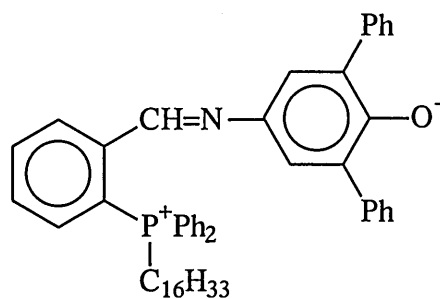
(47)   (3A)
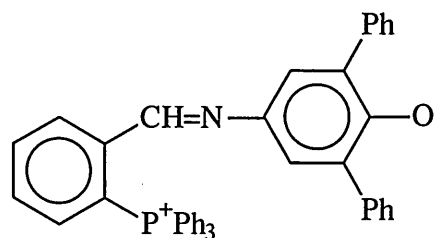
Solvent	Colour	Wavelength λ_{max} nm (47)	Wavelength λ_{max} nm (3A) (X=Ph)	$v_{max} \times 10^3$ (cm^{-1}) (47)
Methanol	yellow	370	498	27.0
Acetonitrile	purple	556	562	17.98
Acetone	blue	588	604	17.92
Dichloromethane	purple	578	596	17.30
Ethyl acetate	turquoise	624	642	16.02
Tetrahydrofuran	"	626	648	15.97
Toluene	"	662	insoluble	15.11
$\Delta_{Toluene - MeCN}$		106	150	-2.87

$\Delta v_{max} = v_{nonpolar} - v_{polar}$

Table 11

The plot of wavenumber v of the intramolecular absorption band for (45), (46), and (47) against the normalised solvent polarity parameter E_T^N (fig. 6) reveals a very similar trend for the long chain betaines (45) and (46). However, betaine (47) is solvated differently in toluene (and methanol).
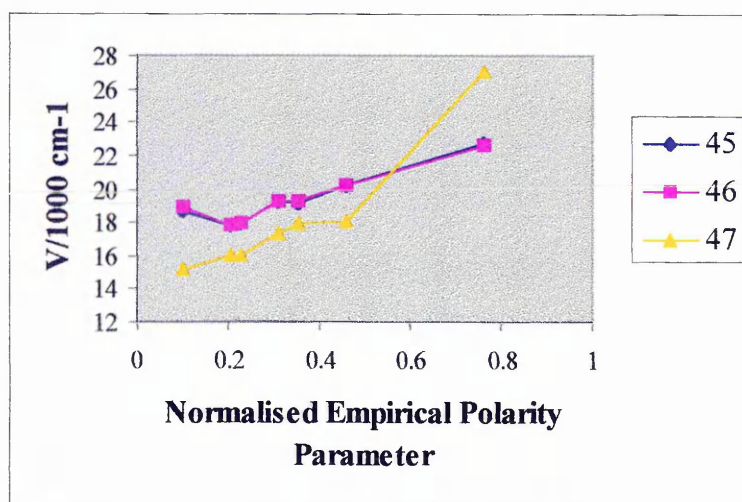
Figure 5 Plot of wavenumber of longest wavelength visible absorption band of betaines **(45-47)** against the normalised polarity parameter.

The molar transition energies E_T (Kcal mol^{-1}) have been calculated for betaines **(45-47)** and are a measure of the interaction of the betaine molecules with the solvent systems (table 12). The values indicate that the ground state of the betaines is less stable in all the solvents compared to Kosower's polarity indicator salt,[15] but more stable than Reichardt's betaine dye.[16]

	E_T values (Kcal mol^{-1})		
Solvent	**(45)**	**(46)**	**(47)**
Methanol	64.97	64.69	-
Acetonitrile	57.88	57.88	51.42
Acetone	54.56	54.98	48.62
Dichloromethane	54.98	54.98	49.46
Ethyl acetate	51.06	51.24	45.82
Tetrahydrofuran	50.87	51.24	45.67
Toluene	53.34	52.93	43.19
ΔE_T	-14.1	-13.45	-8.23

$\Delta E_T = E_{T\ nonpolar} - E_{T\ polar}$

Table 12 The molar transition energies E_T (Kcal mol^{-1}) of betaines **(45-47)** in various solvents.

2.2.6 Micelle formation studies.

Some preliminary studies were carried out on betaine **(46)** dissolved in toluene and THF, respectively, to see whether micelles were forming in solution at a certain concentration which might shift the absorption maxima to a different wavelength. In THF, and more so in the non-polar solvent toluene, the polar part of the molecule should be directed inwards and the non-polar tails should face the non-polar medium. It has been reported for long chain phosphonium salts that the critical micelle concentration (CMC) is observed at around 2.5×10^{-5} mol l^{-1} in non-aqueous solvents,[29] and therefore a range of standards were prepared for betaine **(46)** in the concentration range *ca.* 10^{-7} mol l^{-1} to 10^{-3} mol l^{-1}.

For THF solutions, concentrations lower than 1.6×10^{-5} mol l^{-1} could not be used, as they were too weakly absorbing and no absorption maximum was observed; in toluene, the betaine did not show an absorbance for concentrations of less than 1.1×10^{-5} mol l^{-1}. For the range of standards used the λ_{max} was constant (in THF $\lambda_{max} = 562$ nm); however in toluene, apart from the main charge-transfer absorption band ($\lambda_{max} = 530$ nm), a small shoulder was observed (596 nm) for all the concentrations studied. This band could reflect the formation of micelles. If so, the CMC is less than 1.1×10^{-5} mol l^{-1}, otherwise the shoulder at 596 nm could be the true charge-transfer absorption band, and a splitting of bands is observed, which has been reported in the literature on several occasions for the merocyanine type dyes in non polar solvents.[30]

The intensity of the band at 596 nm decreased linearly compared to the band at 530 nm as the concentration of the betaine increased, (fig. 7). The betaine also obeyed the Beer Lambert law in both THF, (fig. 8) and toluene (absorbances at both 530 nm and 596 nm), (fig. 9 and 10, respectively).

80
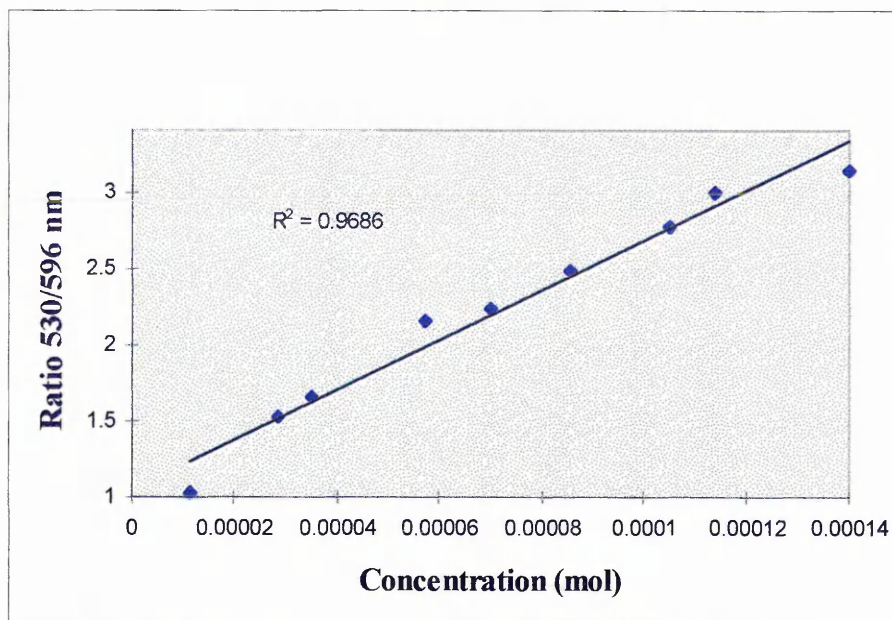
Figure 7 Ratio of absorbance of 530 nm/596 nm for betaine **(46)** in toluene.
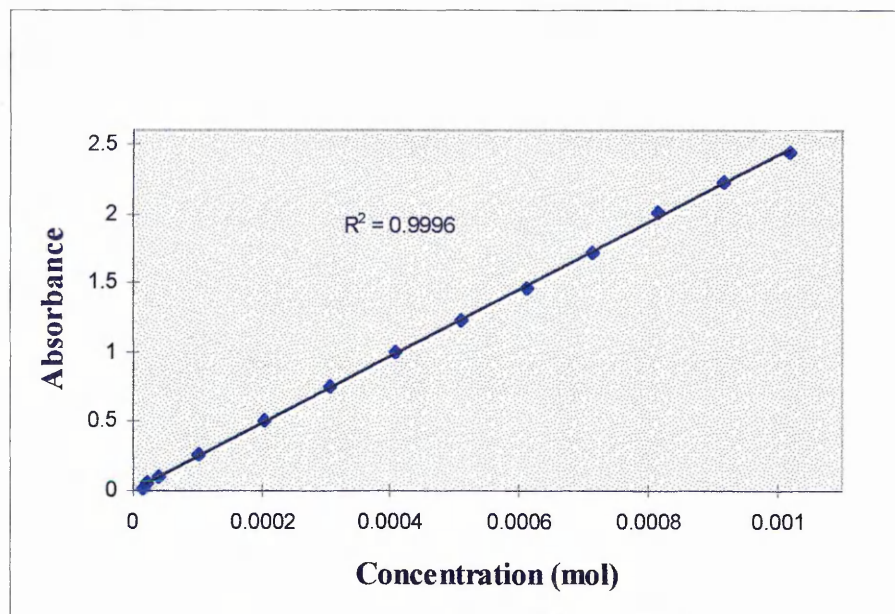
Figure 8 Beer Lambert plot for betaine **(46)** in THF.
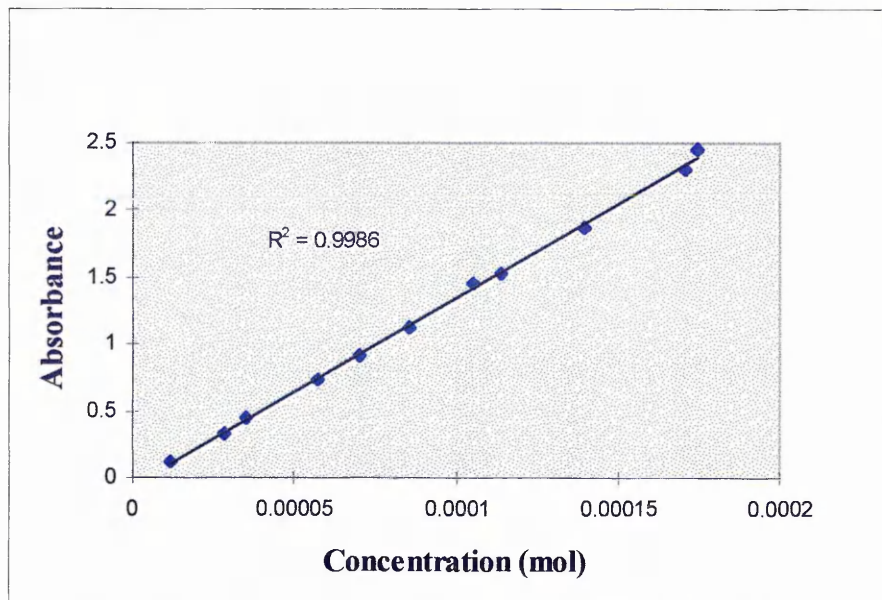
Figure 9 Beer Lambert Plot for betaine **(46)** in toluene λ_{max} 530 nm.
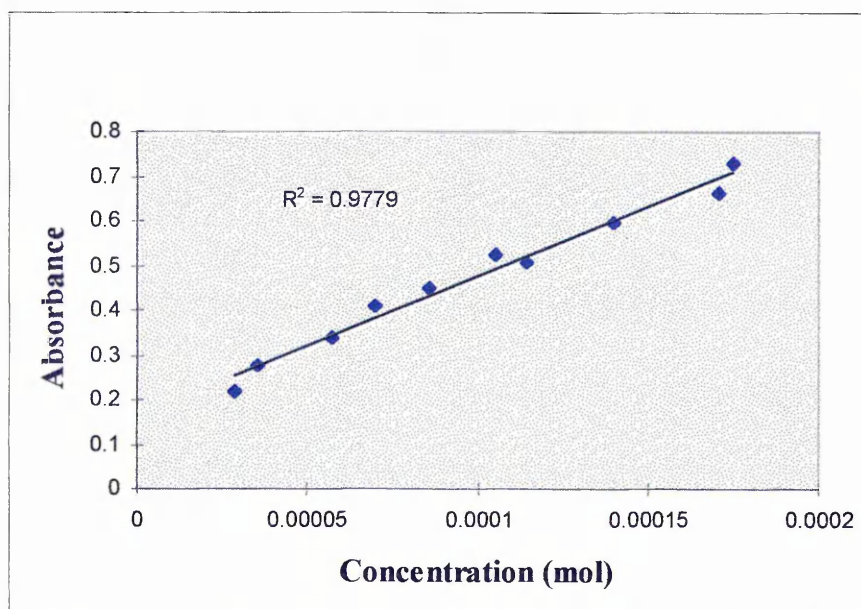
Figure 10 Beer Lambert Plot for betaine **(46)** in toluene λ_{max} 596 nm.

Concentration studies were also carried out in the polar solvent acetonitrile to see whether a CMC could be observed. In this solvent, the non-polar part of the molecule would be expected to direct inwards and the polar part to face the polar medium. Again concentrations lower than 1.4×10^{-5} mol. l^{-1} could not be studied and no change in wavelength with concentration was observed. Betaine **(46)**, whose charge-transfer band was observed at 494 nm in this solvent also obeyed the Beer-Lambert law, (fig. 11).
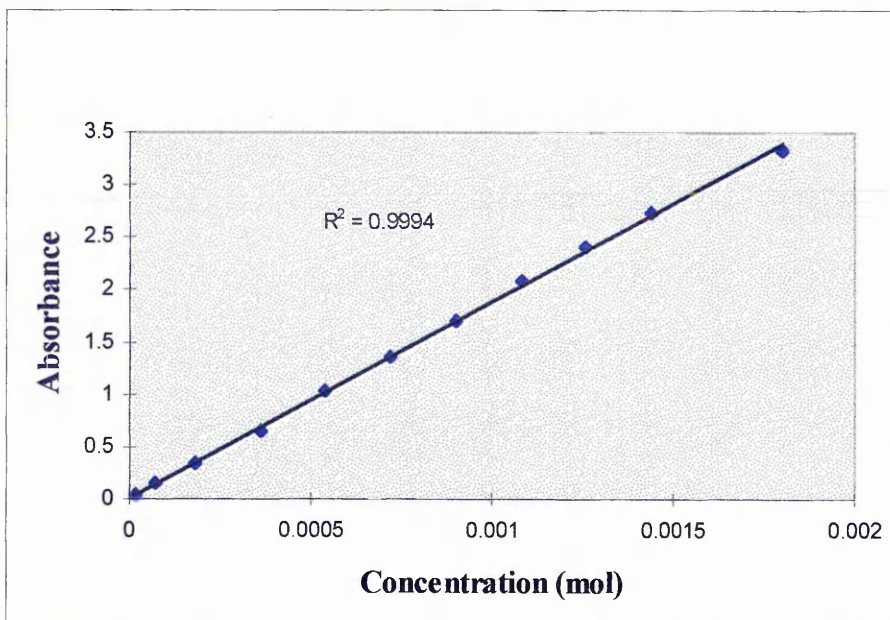
Figure 11 Beer Lambert Plot for betaine **(46)** in acetonitrile.

2.3.7 Isotherm Data.

As with the long chain benzimidazolide betaines **(26B)** and **(27B)** the formation of a monolayer LB film of **(45)** has been studied at Cranfield University. The pressure-area (π-A) isotherm (fig. 12) shows collapse of the betaine **(45)** at 38 mNm^{-1}. The film was spread from 0.101 gL^{-1} of the betaine in dilute chloroform (Analar) solution and compressed at 50 mm^2 s^{-1}. There are no obvious phase changes in the isotherm, suggesting no major re-orientations of the molecules.
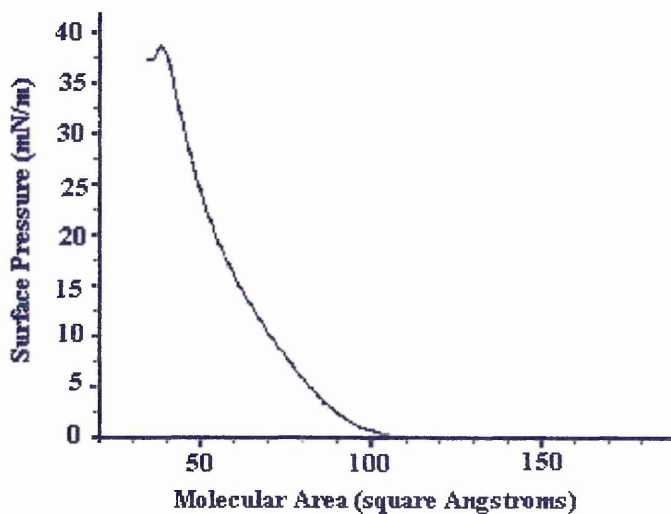
Figure 12 Surface pressure versus area isotherm of betaine **(45)**.

2.3 Effects of annelation on the absorption properties of 4-(N-hexadecylpyridinium-4-ylmethylideneamino)-2,6-dihalophenolate systems

2.3.1 Synthesis of the quinoline imines.

The iminoquinoline intermediates (50 and 51) were synthesised by the reaction of quinoline-4-carboxaldehyde and the appropriate 3,5-disubstituted aminophenol in refluxing ethanol (scheme 15). Unlike in the synthesis of the pyridine aminophenol intermediates,[8] the products crystallised out of the refluxing ethanol immediately. There was no need for recrystallisation, as the solutions were only cooled slightly before crystallisation and filtration, and the solids washed with ethanol to produce pure beige-green solids in good yield, similar in appearance to the related pyridine imines.

X = Cl (50)
X = Br (51)
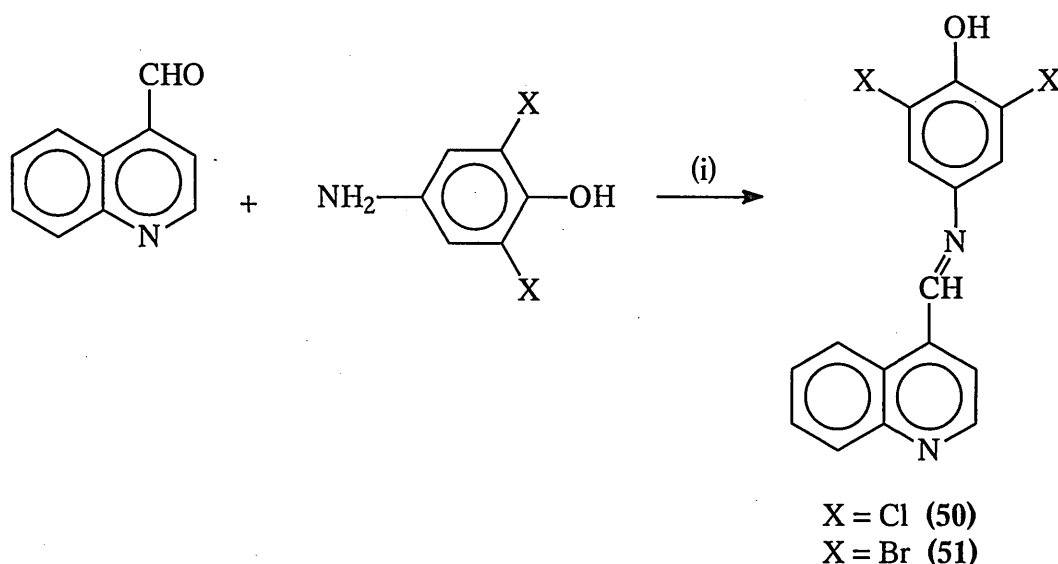
(i) EtOH, reflux, 3hrs, N_2

Scheme 15

2.3.2 Synthesis of the betaines

The respective pyridinium salts of betaine (16) were obtained by treating the pyridine imine with a slight excess of iodohexadecane in refluxing acetonitrile for five hours.[8] However the related quinolinium salts could not be obtained in this manner, due to the insolubility of the quinoline imines (50) and (51). The quinoline imines were found to be insoluble in all common laboratory solvents apart from TFA and DMF, and they were also slightly soluble in DMSO. Even so the reaction was attempted in acetonitrile

84

(for X = Cl), with one mole equivalent of 1-iodohexadecane in the hope that the imine would slowly go into solution on formation of the salt. However, only the starting materials were recovered after five hours of reflux.

The reaction was repeated in the slightly higher boiling point solvent propionitrile (b.p. 97 °C), but again no reaction occurred due to the insolubility of the imine. The reaction was conducted in refluxing DMF, but the temperature (b.p. 153 °C) was too harsh and many products were obtained (including only a trace amount of a possible salt, observed by tlc).

In DMF (at 80 °C), a trace amount of salt was obtained after column chromatography (<0.01 g) even though the reaction was carried out on a fairly large scale. A silver nitrate test carried out on the blue-black solid gave a strong indication that the related betaine had been isolated, as no precipitate formed on addition of silver nitrate to the solid in ethanol-nitric acid solution, confirming the absence of the halide anion. The formation of the betaine rather than the salt is probably due to the basic nature of the DMF. Attempts at improving the yield of the betaine were attempted by using two mole equivalents of 1-iodohexadecane and stirring the reaction mixture for three days, but once more only a small amount of the betaine was isolated.

Another route to the quinolinium salt (53) which would overcome solubility problems was to N-alkylate quinoline-4-carboxaldehyde with 1-iodohexadecane in acetonitrile (scheme 16), and then to treat this salt (52) with the appropriate 3,5 disubstituted aminophenol. After twenty four hours reflux many salt like products were observed by tlc of the crude reaction mixture, so this approach was not investigated any further.

(52)

(53)
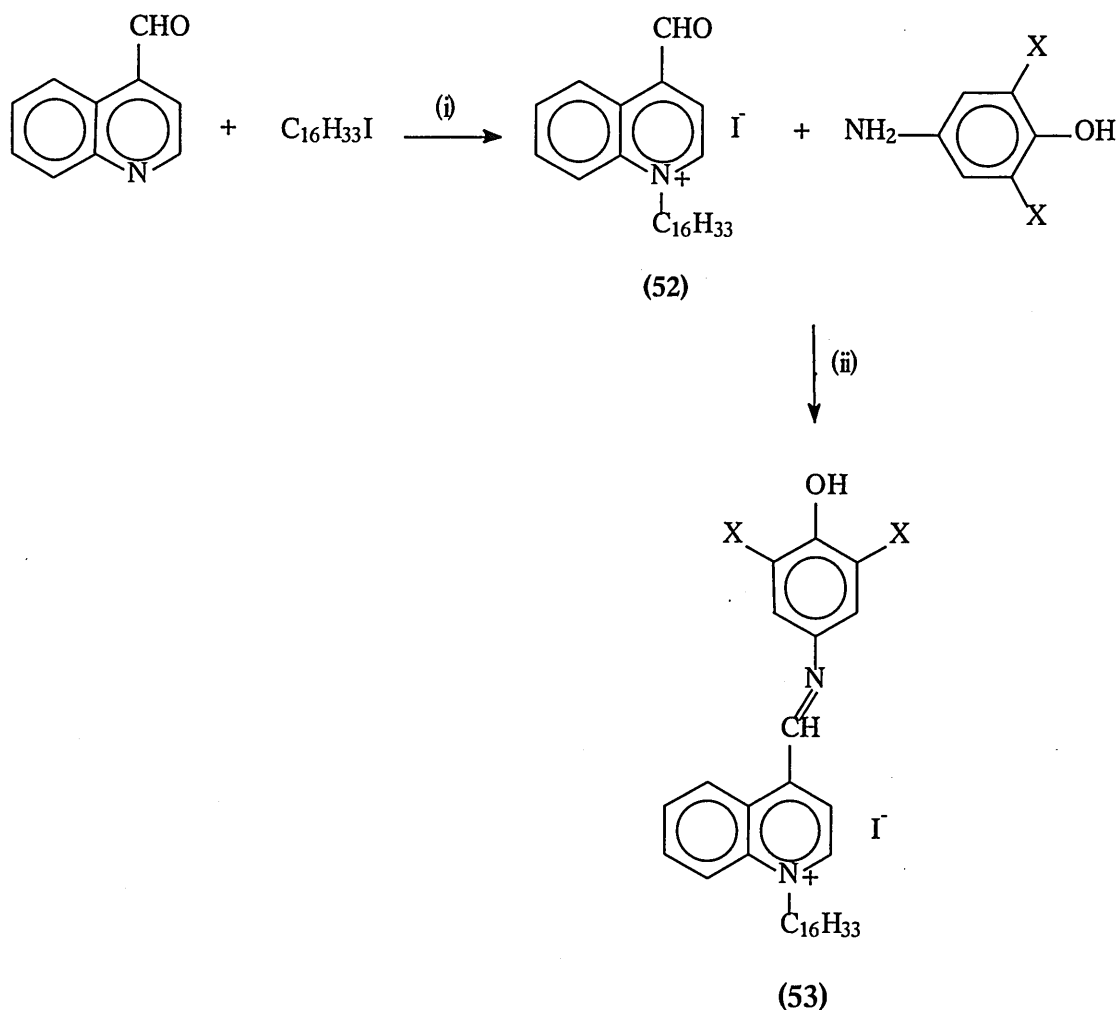
(i) and (ii) MeCN, reflux, N_2

Scheme 16

After unsuccessful attempts at synthesising the salt in DMSO at 80 °C, probably due to the effect of the iodide ion in promoting the reverse reaction, the betaines **(54)** and **(55)** were obtained both in a 6 % yield by using one mole equivalent of silver-*p*-toluene sulphonate to every mole of 1-iodohexadecane to aid salt formation by removing the iodide counter-ion as AgI, which was insoluble in the reaction mixture (scheme 17). This formed almost immediately but the reaction mixture was left for three days. Both betaines were obtained as blue-black solids; however, the yields were surprisingly very low.

$$(50) \text{ or } (51) \quad + \quad C_{16}H_{33}I \quad \xrightarrow{(i)}$$

X = Cl (54)
X = Br (55)
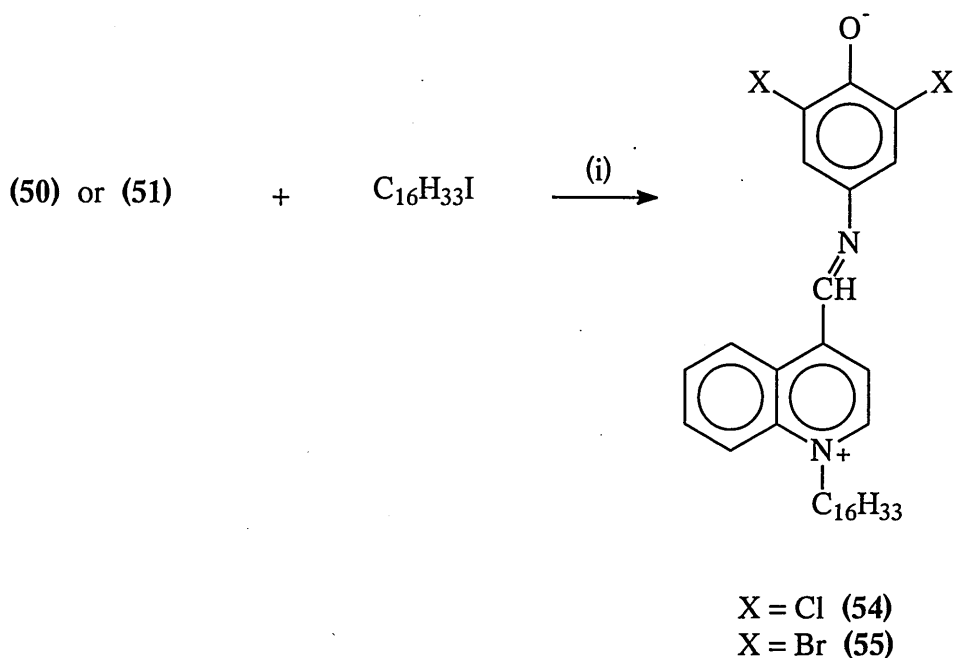
Scheme 17

(i) silver-*p*-toluene sulphonate, DMF, 80-100 °C, 3-4 days, N_2

2.3.3 <u>Characterisation of the quinolinium systems.</u>

Due to the high degree of insolubility of the quinolinium imines **(50)** and **(51)**, the only reasonable proton NMR spectra obtained were in TFA. The CH=N signal of both betaines was shifted further downfield than would usually be expected, at 10.65-10.71 ppm. In DMSO, this signal was observed at 9.41 ppm.

For both betaines **(54)** and **(55)** the signal due to the long aliphatic chain was observed between *ca.* 0.8-4.8 ppm, and the CH=N proton as a singlet at *ca.* 8.5-8.7 ppm.

Both betaines gave the required (molecular ion + 1) by FAB mass spectrometry, and in addition gave negative halide tests on treatment with nitric acid-silver nitrate.

2.3.4 <u>Solvatochromism studies.</u>

Solvatochromism studies were caried out on betaines **(54)** and **(55)** at concentrations of *ca.* 1×10^{-4} mol l^{-1}). The absorption maximum of the CT absorption band of the betaines **(54)** (X = Cl) and **(55)** (X= Br) are very similar (tables 13 and 14). Both quinolinium betaines, exhibited a reasonable degree of negative solvatochromism similar to the related pyridinium systems.[8] Betaine **(55)** (X=Br), was far less soluble in the solvents than **(54)** (X=Cl), and was only completely soluble in dichloromethane whereas betaine **(54)** was completely soluble in all the solvents tested.

It is seen that the absorption maxima of the quinolinium betaines has been shifted dramatically compared to the pyridinium betaines of type **(16)**. For both **(54)** and **(55)**, the intramolecular CT absorption maxima has been shifted to a longer wavelength, by on average, 90 nm, in all the solvents compared to **(16)**, apart from in methanol where the wavelength was only increased by 66-68 nm. For **(54)**, the intramolecular CT absorption band undergoes a hypsochromic shift of 170 nm (38843 cm^{-1}) from toluene to methanol. By comparison, for the pyridinium betaine **(16)** (X=Cl), the absorption maximum undergoes a shift of 132 nm (39478 cm^{-1}) from THF to methanol. Similarly for **(54)** over the same solvent range the shift is 152 nm (35582 cm^{-1}). Betaine **(54)** has a greater solvatochromic range of 20 nm compared to that of **(16)** (X=Cl).

The intramolecular absorption band of **(55)** undergoes a hypsochromic shift of 146 nm (34036 cm^{-1}) from THF to methanol compared to 122 nm (36800 cm^{-1}) for **(16)** (X=Br), the difference being 24 nm.

In the UV/Visible spectrum, it was noticed that the longest wavelength absorption bands of betaines **(54)** and **(55)** were accompanied by the appearance of shoulders, and the splitting of bands. Both **(54)** and **(55)** showed a slight shoulder in dichloromethane, and two intramolecular CT absorption bands in THF. Betaine **(54)**, which was the more soluble of the two betaines, showed two bands in ethyl acetate and three in toluene.

The appearance of split bands has been reported in the literature,[30] and has also been observed in the case of the pyridinium betaines **(16)**.[31] For betaine **(16)**, only the longest wavelength absorption band was reported. Recent studies at Cranfield University on betaine **(54)** in chloroform have shown that with increase in concentration of the betaine in solution, the longest wavelength absorption band at *ca.* 740 nm decreases in intensity, whilst the absorption band at *ca.* 610 nm increases (fig. 13).
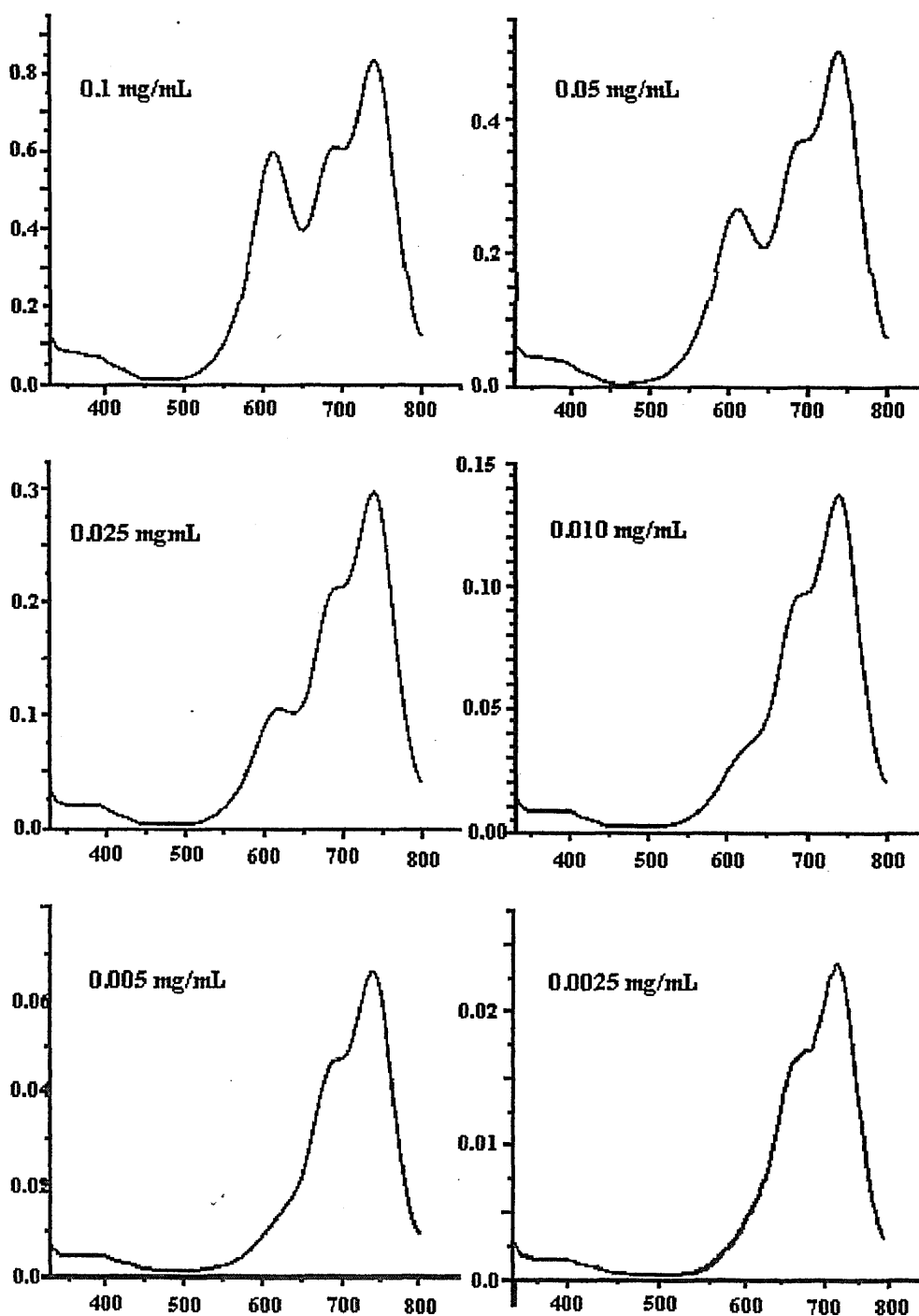
Figure 13 Non-protonated solutions of betaine (54) at various concentrations.

It is thought that the absorption band at *ca.* 610 nm is due to the formation of aggregates in more concentrated solutions, and is the *intermolecular* charge-transfer absorption band), whilst the band at *ca.* 740 nm is the *intramolecular* charge-transfer

absorption band. Using the Bernesi-Hildebrand equation, the aggregates have been shown to be dimers. In the present study all the bands have been reported, but only the longest wavelength absorption band is considered as the true solvatochromic band.

This range of betaines shows a larger solvatochromic range compared to the phosphoniophenyl-imidazolide betaines (1A) and the phosphonioiminophenolate betaines (45-47), as the internal charge-transfer between the dipolar ground state (56A) and the more non polar excited state (56B) would be expected to be more significant than in systems (1A) and (45-47) because of the inability of the phosphonium centre to aid delocalisation of the negative charge.

(56A)   (56B)
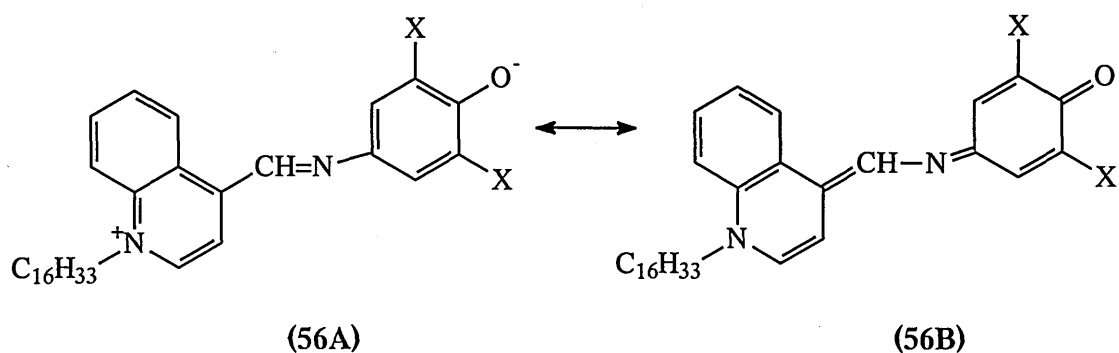
A comparison of the solvatochromism data for (54) and (16) (X = Cl)

(54)   (16)

90
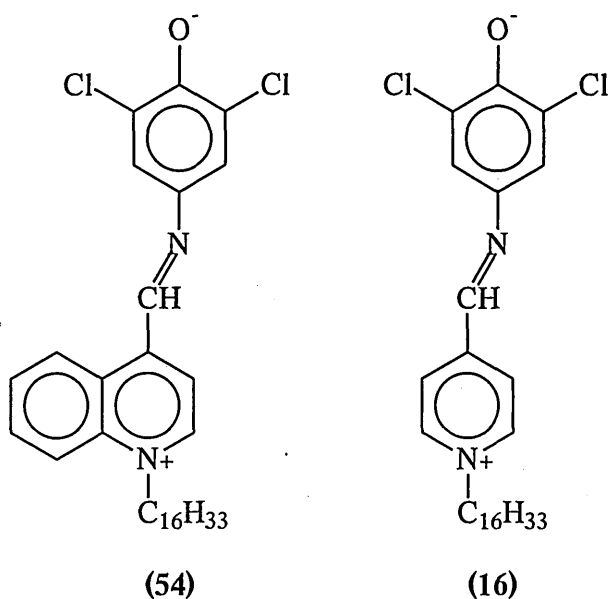
Solvent	Colour	Wavelength λ_{max} nm (54)	ν_{max} x10^3cm^{-1} (54)	Wavelength λ_{max} nm (16) (X=Cl)	ν_{max} x10^3cm^{-1} (16) (X=Cl)
Methanol	blue	582	17.18	516	19.38
Acetonitrile	blue - turquoise	668	14.97	578	17.30
Acetone	turquoise	696	14.37	606	16.50
Dichloromethane	turquoise	730	13.70	646	15.48
Tetrahydrofuran	green - turquoise	(680) 734	13.62	648	15.43
Ethyl acetate	green - turquoise	(684) 736	13.59	-	-
Toluene*	green - turquoise	(642) (688) 752	13.30	-	-
$\Delta_{Toluene - MeOH}$		170	-3.88	132	-3.95

$\Delta\nu_{max} = \nu_{nonpolar} - \nu_{polar}$

* low solubility

Table 13

A comparison of the solvatochromism data for (55) and (16) (X=Br)

(55) (16)
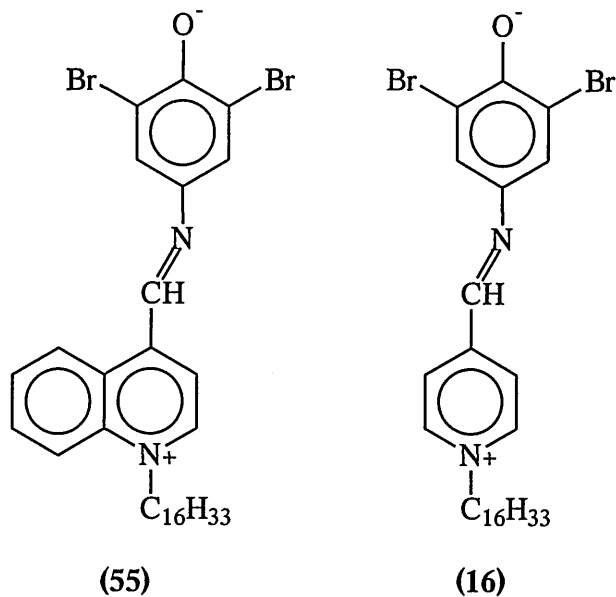
Solvent	Colour	Wavelength λ_{max} nm (55)	ν_{max} x10^{3}cm^{-1} (55)	Wavelength λ_{max} nm (16) (X=Br)	ν_{max} x10^{3}cm^{-1} (16) (X=Br)
Methanol	blue	586	17.06	518	19.3
Acetonitrile	blue - turquoise	666	15.01	576	17.36
Acetone	turquoise	690	14.49	602	16.61
Benzonitrile	turquoise	706	14.16	-	-
Dichloromethane	turquoise	728	13.74	632	15.82
Tetrahydrofuran	turquoise	(686) 732	13.66	640	15.63
Ethyl acetate	turquoise	(690) 734	13.62	-	-
$\Delta_{EA - MeOH}$	-	148	-3.44	122	-3.67

$\Delta\nu_{max} = \nu_{nonpolar} - \nu_{polar}$

Table 14

Table 15 shows the molecular transition energies E_T (Kcal mol^{-1}) of the two quinolinium betaines (54) and (55). It is apparent that the ground-state is far less stable in all the solvents compared to Kosower's polarity indicator.[15] Additionally the ground-state of (54) and (55) is slightly less stable in the polar solvents, but slightly more stable in the non-polar solvents, (THF, ethyl acetate and toluene), compared to Reichardt's betaine dye.[16]

Solvent	E_T values (Kcal mol^{-1})	
	(54)	(55)
Methanol	49.13	48.79
Acetonitrile	42.80	42.93
Acetone	41.08	41.44
Benzonitrile	-	40.50
Dichloromethane	39.17	39.27
Tetrahydrofuran	38.95	39.06
Ethyl acetate	38.85	38.95
Toluene	38.00	-
ΔE_T	-11.13	-9.84

$\Delta E_T = E_{Tnonpolar} - E_{Tpolar}$

Table 15 The molar transition energies E_T (Kcal mol^{-1}) of betaines (54) and (55) in various solvents.

Figure 14 shows the plot of wavenumber ν of the longest intramolecular CT absorption band of the quinolinium betaines (54) and (55) compared to those of the pyridinium betaines of type (16) against the normalised solvent polarity parameter E_T^N.
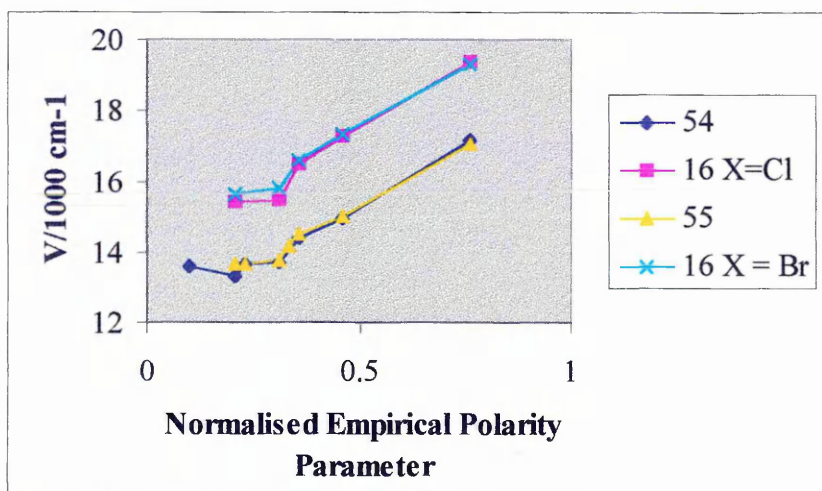
Figure 14 Plot of longest wavenumber visible absorption band for betaines **(54)**, **(55)**, and **(16)** against the normalised empirical polarity parameter.

The graphs show a positive slope (indicating negative solvatochromism). All the plots show similar solvatochromic behaviour in solvents of different polarity implying that all the betaines are similarly solvated in all the solvents used.

2.3.5 Isotherm Data.

A report from Karl Skjonnemand at Cranfield University.

A monolayer LB film of betaine **(54)** was obtained by spreading **(54)** from dilute chloroform (Analar) solution (0.1 gL^{-1}) onto the pure water subphase of the LB trough (Nima Technology, model 622), at 23°C and then compressed at 50 mm^2s^{-1} (equivalent to surface area loss of 0.1 % s^{-1}).

The isotherm of the monolayer LB film of betaine **(54)** is shown in figure 15, and shows collapse at 42 mNm^{-1}, and the profile is very similar to that of the pyridinium analogue **(16)** (X=Cl).[8]

94
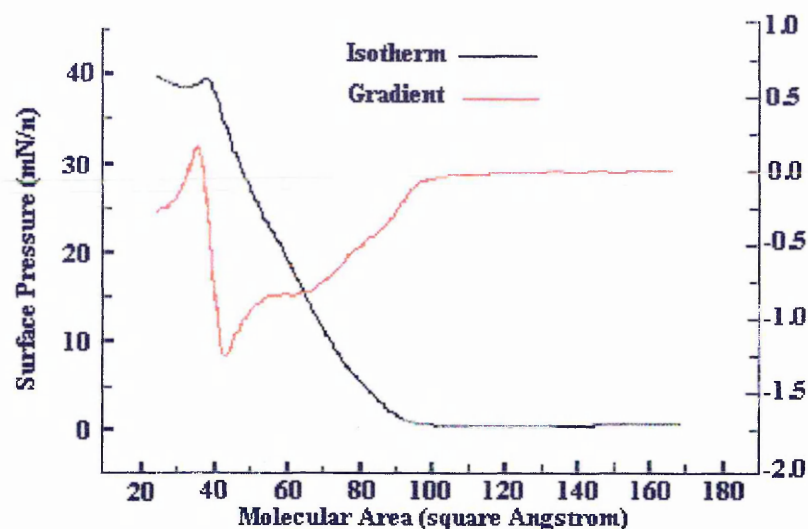
Figure 15 Surface pressure versus area isotherm of betaine **(54)**.

Figure 16 shows the spectra of an LB film of this betaine dye before (a) and after (b) exposure to hydrogen chloride vapour. Betaine **(54)** has an intramolecular charge transfer axis and is SHG active whereas the protonated form shows no SHG. The UV/Visible spectra shows that the LB film has a maximum absorption at $\lambda_{max} \approx 575$ nm. After exposure to hydrogen chloride vapour it has a maximum absorption at $\lambda_{max} \approx 410$ nm, undergoing a hypsochromic shift of *ca.* 165 nm due to its protonation.
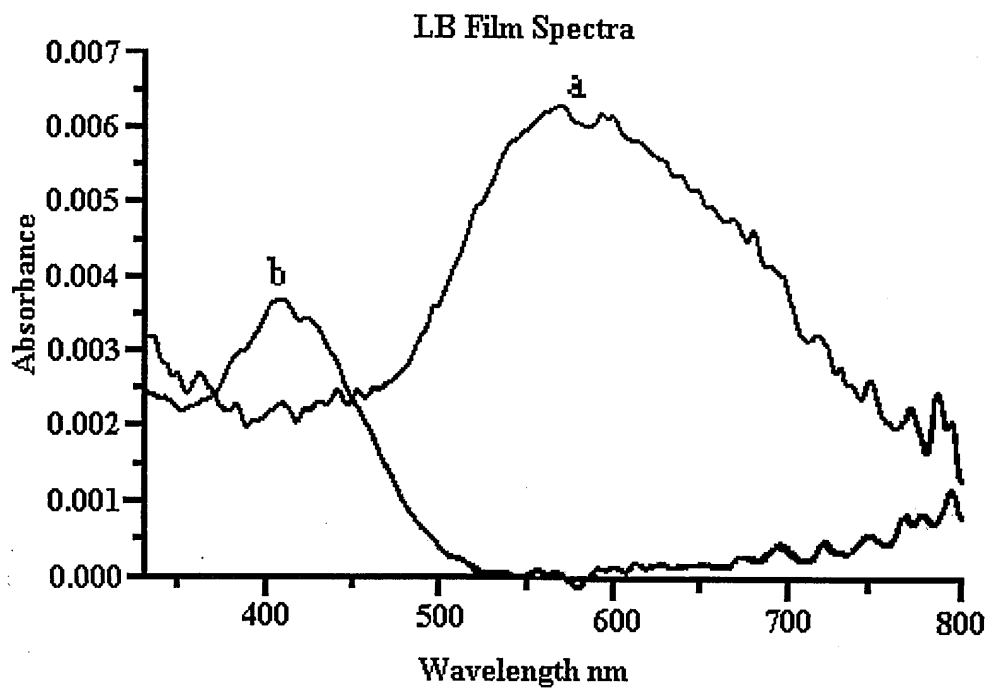
LB Film Spectra

Figure 16 UV/Visible spectra of a LB film of **(54)** before **(a)** and after **(b)** exposure to HCl.

Surface plasmon resonance (SPR) studies are presently being carried out on films of betaine **(54)**. The films will be exposed to ammonia and hydrogen chloride gas, monitoring the changes in the SPR at a fixed angle of incidence, to test for potential sensor applications. Similar studies will be conducted on betaine **(55)**.

2.4 Effects of annelation on N-[-(o-Triphenylphosphoniobenzylidene]-4-amino-2,6-dichlorophenolate

2.4.1 Synthesis of 2-bromonaphthaldehyde.

Unlike 2-bromobenzaldehyde, 2-bromonaphthaldehyde **(57)** was not available commercially, so the synthesis of **(57)** was initially attempted from the one step reaction of 1-bromo-2-methylnaphthalene with four mole equivalents of cerium (IV) ammonium nitrate (CAN) in 50 % acetic acid (scheme 18).[32]

(57)
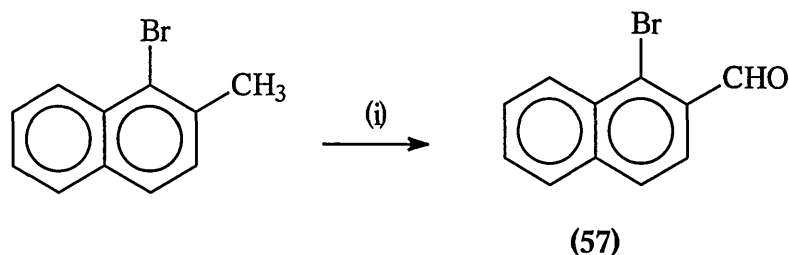
(i) CAN, 50 % acetic acid, 85 °C, 2hrs

Scheme 18

Although this reaction works well for naphthalenes with a substituent in the 4-position, it has been reported that for naphthalenes with a substituent in the 2- position the naphthaldehyde is formed in very low yield.[32]

This was seen for the above reaction, and a large amount of unreacted 1-bromo-2-methylnapthalene was indicated by GCMS, together with the products **(58)** and possibly **(59)**, with a trace amount of the aldehyde **(57)**. Another four unidentified products were observed.
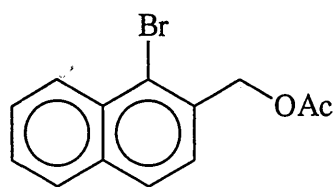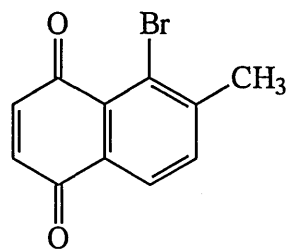
(58)   **(59)**

The synthesis was therefore carried out in three steps (scheme 19)[33] and the naphthaldehyde was obtained as a cream solid, but in a poor yield. In the first step, side chain bromination occurs using NBS as the brominating agent, and the halomethyl intermediate **(60)** is subjected to the *Sommelet reaction*.[33] This procedure involves an

97

initial reaction between the halomethyl compound **(60)** and hexamethylenetetramine (hexamine) and the hydrolysis of the resulting quaternary hexamine salt **(61)** with hot aqueous acid.
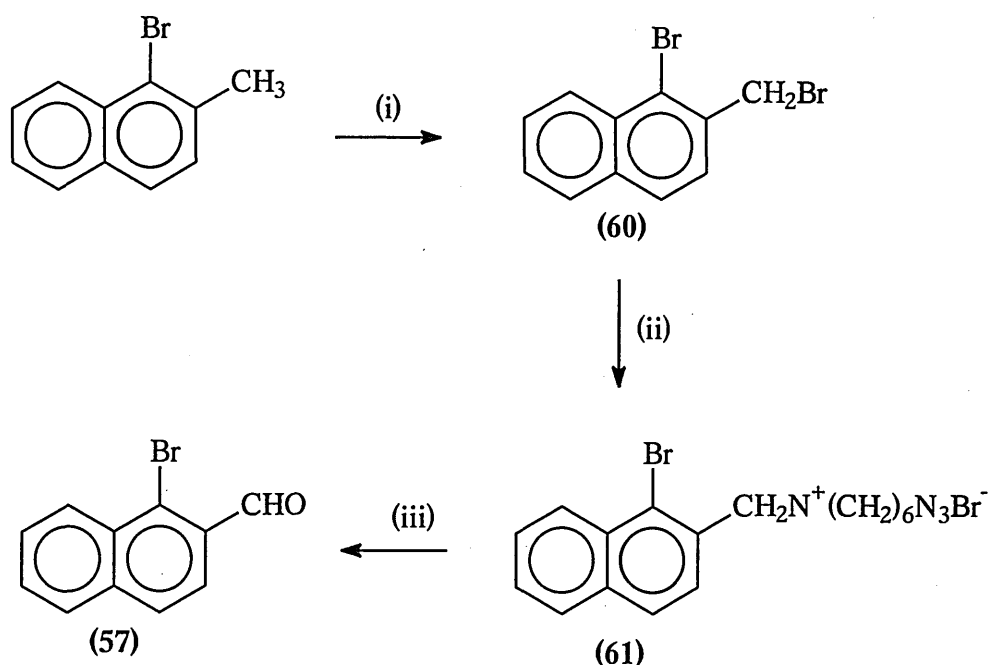
(i) NBS, CCl_4, benzoyl peroxide, reflux, 16hrs

(ii) CH_2Cl_2, hexamine, reflux, 1hr

(iii) 50 % glacial acetic acid, reflux, 2hrs, conc. HCl, reflux, 5 min

Scheme 19

The mechanism of the reaction is uncertain (scheme 20) but hydrolysis of the salt may yield the primary amine **(62)**, formaldehyde and ammonia. A hydride ion transfer then probably occurs between the naphthylamine **(62)** and the protonated aldimine **(63)** derived from formaldehyde and ammonia. Hydrolysis of the resulting aromatic aldimine **(64)** then yields the required naphthaldehyde **(57)**.
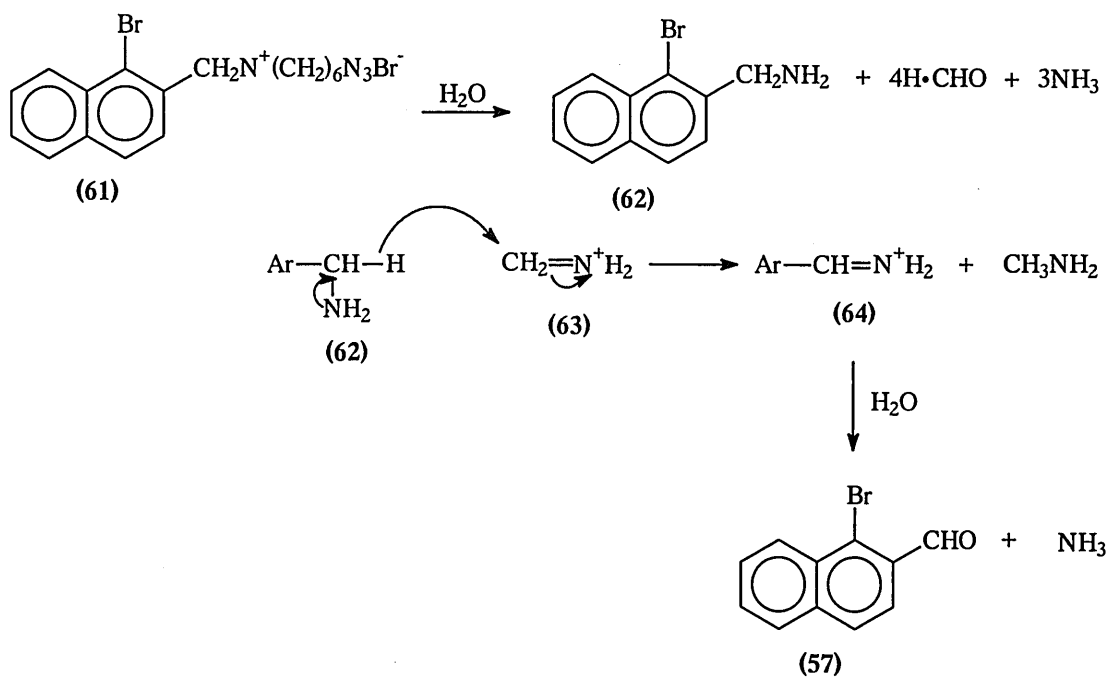
Scheme 20

The naphthyl imine (65) was synthesised in a reasonably good yield as with the phenol imines, by heating (57) with 4-amino-2,6-dichlorophenol under reflux in ethanol (scheme 21).

2.4.2 Synthesis of the salt.

The phosphonium salt (66) was formed under the usual conditions (scheme 21), making use of the kinetic template effect.[19] The salt was obtained in a very low yield (12 %) compared to 60-80 % achieved with the respective salts of the phenyl derivatives (3A). Additionally, on trituration of the salt (66) with ether, the salt was found to be slightly soluble due to the extension of the aromatic system, making the salt less polar. Salt (66) was obtained as a rusty-orange solid which gave a positive halide test with nitric acid-silver nitrate.

2.4.3 Synthesis of the betaine.

The betaine was obtained as a purple solid on treating the salt with aqueous sodium hydroxide in dichloromethane (scheme 21). The solid gave a negative halide test on treatment with nitric acid-silver nitrate. In comparison the respective triphenylphosphonio phenyl betaine (3A) (X=Cl) was obtained as a red solid.

(57)   +   NH$_2$—⬡—OH (with Cl, Cl substituents)   →(i)   (65) [naphthalene with Br, CH=N—aryl with Cl, Cl, OH]

(ii) ↓

(67) [naphthalene with P$^+$Ph$_3$, CH=N—aryl with Cl, Cl, O$^-$]   ←(iii)   (66) [naphthalene with P$^+$Ph$_3$, CH=N—aryl with Cl, Cl, OH, Br$^-$]
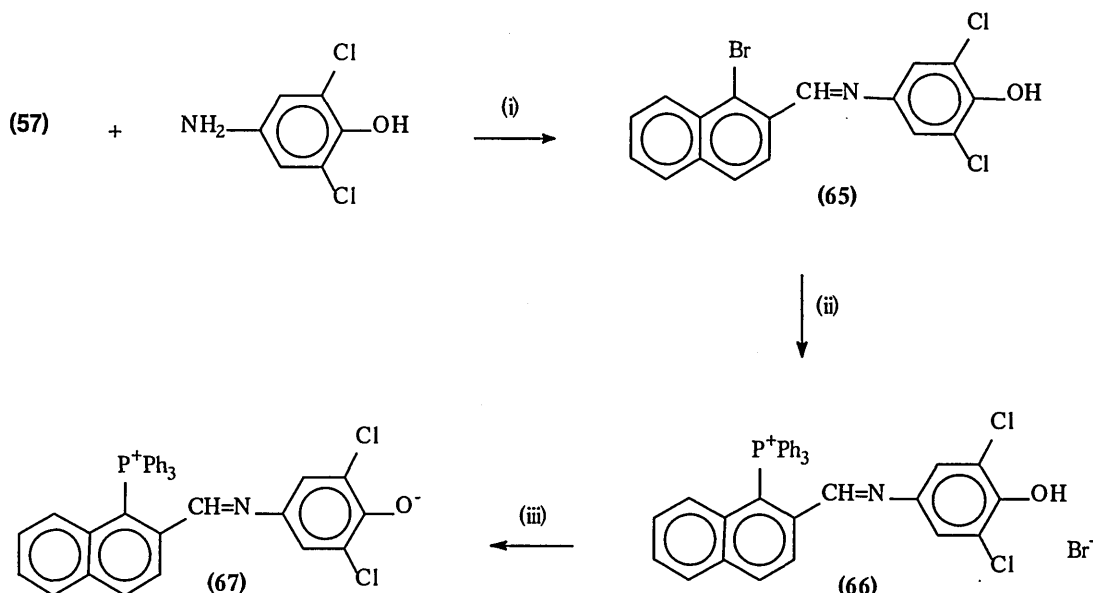
(i) EtOH, reflux, 3hrs, N$_2$

(ii) Ph$_3$P, NiBr$_2$, EtOH, reflux, 8hrs, N$_2$

(iii) NaOH(aq), CH$_2$Cl$_2$

Scheme 21

2.4.4 Characterisation of the naphthyl system.

The imine (65) gave the characteristic molecular ion by mass spectrometry (EI), and the CH=N proton was observed at 9.22 ppm as a singlet in the proton NMR. The phosphorus NMR spectrum showed the phosphorus nucleus to have become shielded slightly on going from the salt (66) to the betaine (67) by 0.22 ppm.

Another point to be noted is that the ^{31}P signal of the naphthyl-phosphonio salt (66) and betaine (67) occured at *ca.* 9 ppm upfield (at *ca.* 18 ppm) than expected. Usually, the phosphorus resonance for tetra-aryl phosphonium salts appear further downfield; the signals for the triphenyl (3A) and the long chain (33-36) phenyl-phosphonium salts appear at *ca.* 27 ppm, and the related betaines at *ca.* 26 ppm. Hence, the phosphorus nucleus of the naphthyl-phosphonio salt (66) and the respective betaine (67) are greatly shielded in comparison.

In the ^{1}H NMR spectrum, on conversion to the betaine, the CH=N signal moved upfield. In the salt (66) the CH=N singlet was observed as a separate entity at 8.52 ppm, but for the betaine (67), it was hidden by the aromatic multiplet.

For the phenyl betaine (3A) (X=Cl), the singlet due to the aromatic protons meta to the phenol group moved upfield into the aromatic multiplet, (compared to the parent

100

salt); this was not the case for the naphthyl betaine **(67)**, and the related signal moving slightly downfield.

Both salt **(66)** and betaine **(67)** gave the required molecular cation and (molecular ion + 1), respectively, under FABMS conditions, and the betaine **(67)** gave a negative halide test.

2.4.5 Solvatochromism studies.

The salt **(66)** and the betaine **(67)** were studied by UV/Visible spectroscopy in a variety of solvents at approximately 1×10^{-4} mol l^{-1} (tables 16 and 17), and the betaine showed negative solvatochromism as expected.

In each of the solvents, the salt also showed an intramolecular CT absorption band for the betaine in addition to an absorption band for the salt (except in benzonitrile), indicating that the betaine was in equilibrium with the salt in solution. No comparison can be made with the phenyl salts of type **(3A)**, as UV/Visible absorption studies were only carried out on the betaines.[2]

At the dilution studied, the absorption spectra of the betaine showed a complete absence of the salt in solution, and shows the effects of extension of the aromatic system from phenyl to naphthyl, resulting in a shift of the wavelength of the CT absorption band by 58-82 nm depending on the solvent (but not including methanol). The shift in wavelength of the absorption maxima from the phenyl to the naphthyl betaine is more evident in the lower polarity solvents, for example in acetonitrile, where the shift is 58 nm and in ethyl acetate 82 nm.

The betaine underwent a hypsochromic shift of 168 nm (53622 cm^{-1}) from THF to methanol) compared to the hypsochromic shift of 132 nm (51205 cm^{-1}) for the phenyl derivative **(3A)** (X=Cl). It is seen that the naphthyl system is slightly more solvatochromic than the phenyl system in that the solvatochromic range has increased by 36 nm (from THF to methanol).

Solvatochromism data for salt (66)
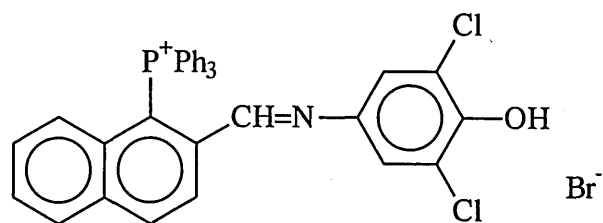
(66)

Solvent	Colour	Wavelength λ_{max} nm
Methanol	gold	368 (482)*
Acetonitrile	pink-purple	358 (560)*
Benzonitrile	pale purple	564
Acetone	blue-grey	356 (594)*
Dichloromethane	blue-grey	364 (590)*
Tetrahydrofuran	pale turquoise	352 (646)*
Ethyl acetate	pale turquoise	352 (650)*

* = betaine

Table 16

102

(67)   (3A)
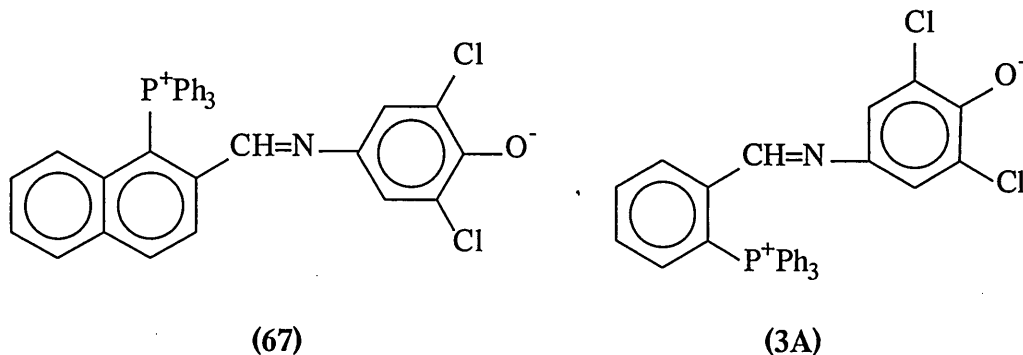
Solvent	Colour	Wavelength λ_{max} nm (67)	ν_{max} $\times 10^3 cm^{-1}$ (67)	Wavelength λ_{max} nm (3A) (X=Cl)	ν_{max} $\times 10^3 cm^{-1}$ (3A) (X=Cl)
Methanol	red	482	20.75	446	22.42
Acetonitrile	deep purple	562	17.79	504	19.84
Benzonitrile	deep purple	574	17.42	-	-
Acetone	deep blue	596	16.78	536	18.66
Dichloromethane	deep blue	590	16.94	532	18.80
Ethyl acetate	turquoise	646	15.48	564	17.73
Tetrahydrofuran	turquoise	650	15.38	578	17.30
$\Delta_{THF - MeOH}$		168	-5.37	132	-5.12

$\Delta\nu_{max} = \nu_{nonpolar} - \nu_{polar}$

Table 17

Table 18 shows the molar transition energies E_T (Kcal mol^{-1}) of the phosphonio-naphthyl betaine (67) and the phosphonio-phenyl betaine (3A) (X=Cl). Betaine (67) has a ground-state which is less stable than the related phosphonio-phenyl system (3A) (X=Cl) in both polar and non-polar solvents.

Solvent	E_T values (67)	E_T values[31] (3A) (X=Cl)
Methanol	59.31	64.1
Acetonitrile	50.87	56.7
Benzonitrile	49.81	-
Acetone	47.97	53.3
Dichloromethane	48.46	53.7
Ethyl acetate	44.81	50.7
THF	43.99	49.5
ΔE_T	-15.32	-14.60

$\Delta E_T = E_{Tnonpolar} - E_{Tpolar}$

Table 18   The molar transition energies E_T (Kcal mol^{-1}) of betaine **(67)** and **(3A)** in various solvents.

Figure 17 shows a plot of wavenumber of longest wavelength visible absorption band of the phosphonium phenolate betaine dyes **(67)** and **(3A)** (X=Cl) against the normalised polarity parameter E_T^N. The graph shows a very similar trend for both betaines, which are solvated in an identical manner with respect to the solvated ground and excited-state structures.
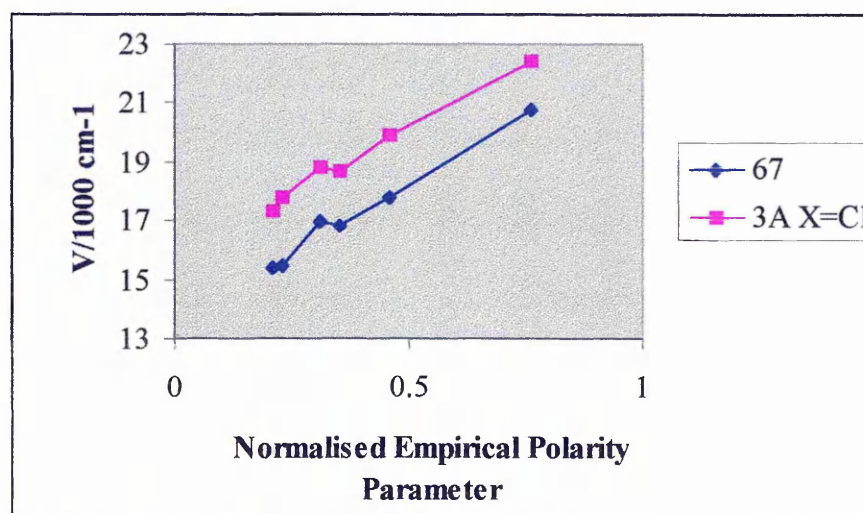
Figure 17   Plot of longest wavenumber visible absorption band of betaine **(67)** and **(3A)** against the normalised polarity parameter.

104

2.5 Effects of annelation on phosphonio-imidazolide betaine systems

2.5.1 Synthesis of 4-bromonaphthaldehyde.

4-Bromonaphthaldehyde (68) was not available commercially and so was synthesised as in scheme 22 and obtained in a fairly good yield as a white solid.[32] The imidazoles (69) and (70) were formed by the published general procedure[9] in good yields, (schemes 22 and 23).

2.5.2 Synthesis of the salts.

The salts (71) and (72) were obtained by the reactions of the imidazoles (69) and (70) with triphenylphosphine in benzonitrile with nickel (II) bromide as the catalyst (scheme 22 and 23). They were obtained as bright yellow solids in reasonable yields, and gave a positive halide test with silver nitrate-nitric acid.

2.5.3 Synthesis of the betaines.

After treating the salts with aqueous sodium hydroxide and extraction into dichloromethane, the phosphonionaphthyl betaines (73) and (74) were obtained as bright red and bright orange solids, respectively, both giving negative halide tests. In comparison, the respective phosphoniophenyl betaines of type (1A) were obtained as orange solids.[1]
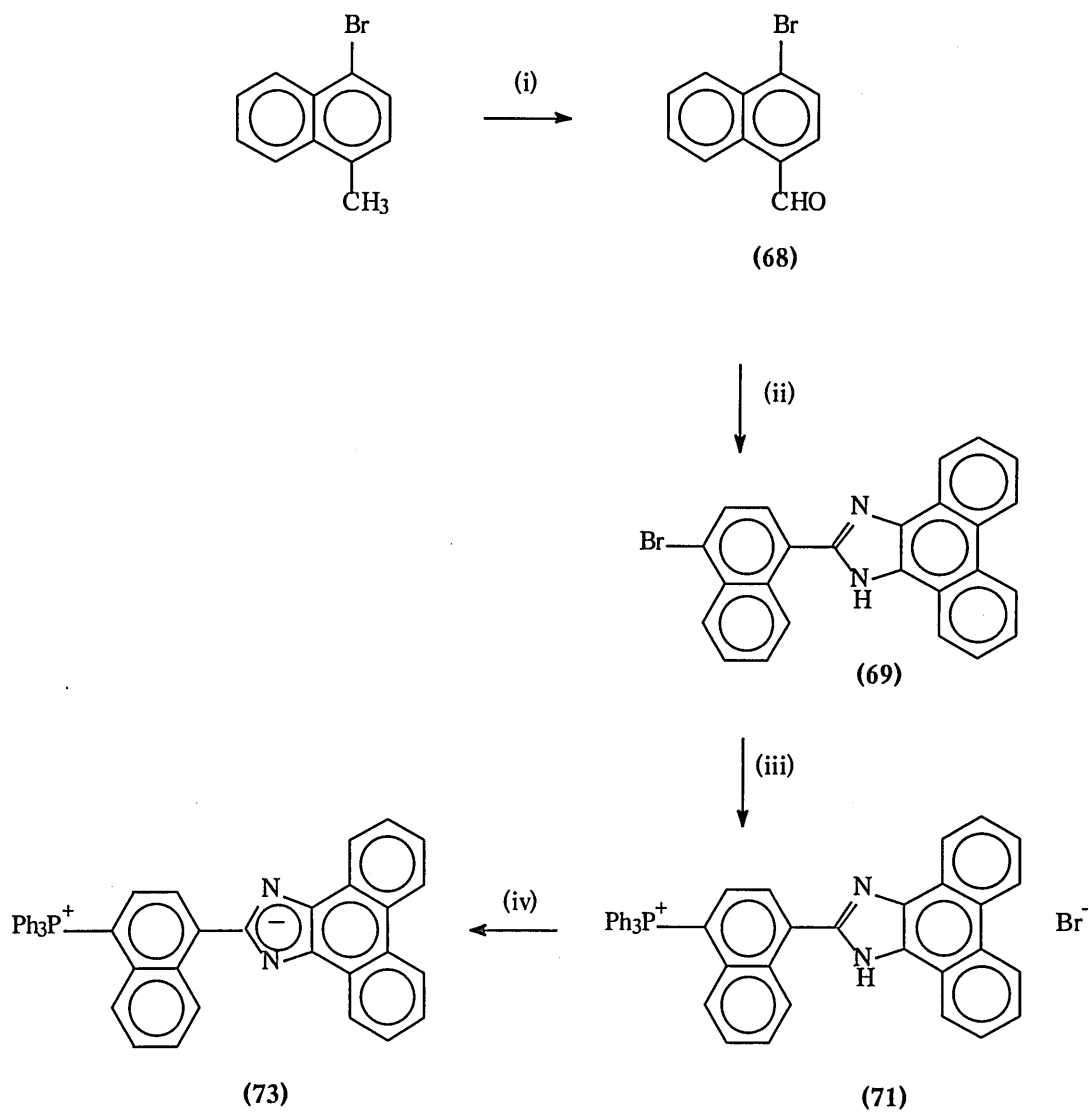
(i) CAN, 50 % acetic acid, 85 °C, 2hrs

(ii) phenanthraquinone, ammonium acetate, glacial acetic acid, reflux, 6hrs

(iii) Ph_3P, $NiBr_2$, PhCN, reflux, 5hrs, N_2

(iv) NaOH (aq), CH_2Cl_2 shake

Scheme 22

106

(i) ammonium acetate, glacial acetic acid, reflux, 6hrs

(ii) Ph_3P, $NiBr_2$, PhCN, reflux, 4hrs, N_2

(iii) NaOH (aq), CH_2Cl_2 shake

Scheme 23

2.5.4 Characterisation of the salts and betaines.
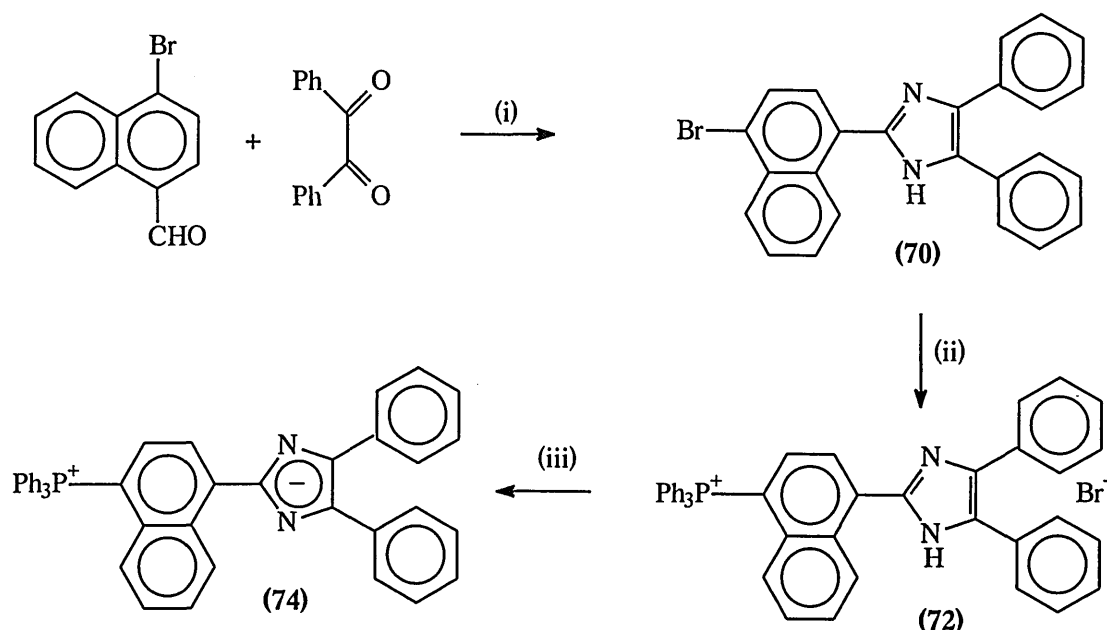
Both salts **(71)** and **(72)** and betaines **(73)** and **(74)** gave single sharp resonances in the phosphorus NMR spectra. In each case, the phosphorus nucleus was shielded slightly by 0.39-0.64 ppm on going from the salt to the betaine. As seen earlier, such a small shift was also observed with the *para* analogues of the systems of type **(1A)**.

The proton NMR spectra of salts **(71)** and **(72)** showed a singlet for the NH proton, which disappeared on conversion to the betaines **(73)** and .**(74)**. The salts and betaines gave a characteristic molecular cation and (molecular ion + 1), respectively, by FAB mass spectrometry.

The betaines also gave a negative halide test compared to the positive halide test given by the salts.

2.5.5 Solvatochromism studies.

UV/Visible absorption spectra of the salts **(71)** and **(72)**, (tables 19 and 21) together with the respective betaines **(73)** and **(74)**, (tables 20 and 22) were recorded (at *ca.* 1 x 10^{-4} mol l^{-1}). As with the phosphoniophenyl derivatives, the related salts were seen to be slightly solvatochromic. The shift in wavelength was seen to be 34 nm (20561 cm^{-1}) for the naphthyl salt **(71)** compared to 10 nm (6410 cm^{-1}) for the respective

107

phosphoniophenyl salt of type (1A) on going from methanol to tetrahydrofuran. The absorbance band of the salt shifted about 18-26 nm in wavelength from the phenyl to the naphthyl system in each of the solvents used. In the case of the phosphoniophenyl salts, the presence of the betaine in solution was not observed, unlike with the naphthyl salt (66), for which dissociation to the betaine was very evident.

For betaines (73) and (74), negative solvatochromism was observed. The intramolecular CT absorption bands were seen to have moved to a longer wavelength by between 48-62 nm for (73) and 58-76 nm for (74) depending on the solvent. In methanol, the betaines reverted back to the salt, which was also observed in the systems of type (1A). [1]

The shift in wavelength on going from the phosphoniophenyl- to the phosphonio-naphthyl imidazolide betaines was more noticeable in the lower polarity solvents, as with betaine (67). Thus for (73) the increase in wavelength in tetrahydrofuran is 62 nm and in acetonitrile 48 nm compared with (1A), and for (74) 76 nm in tetrahydrofuran, whereas in acetonitrile it was 58 nm compared with (1A).

The phosphoniophenyl betaines of type (1A) were fluorescent yellow in each solvent, but the related naphthyl betaines (73) and (74) were orange in acetonitrile, red in acetone and dichloromethane, and purple in tetrahydrofuran.

Betaine (73) exhibited a hypsochromic shift of only 54 nm (21068 cm^{-1}) (on going from THF to acetonitrile) but the phosphoniophenyl betaine (1A) showed an even smaller hypsochromic shift of 40 nm (19617 cm^{-1}). Similarly for betaine (74), a hypsochromic shift of 52 nm (19429 cm^{-1}) was observed compared to 34 nm (16739 cm^{-1}) for (1A).

The naphthylphosphonio imidazolide systems are seen to be slightly more solvatochromic than the phenyl phosphonio imidazolide systems, but far less so than the naphthyl-phosphoniophenolate betaines discussed beforehand. The solvatochromic range is increased on annelation by 14 nm for (73) and 18 nm for (74). Even so, the wavelength range in which the betaines absorb is still not ideal for a study to be made at Cranfield University of any nonlinear optical properties the systems might possess.
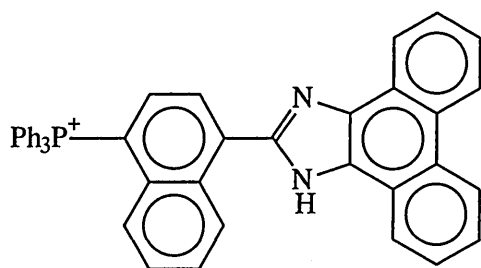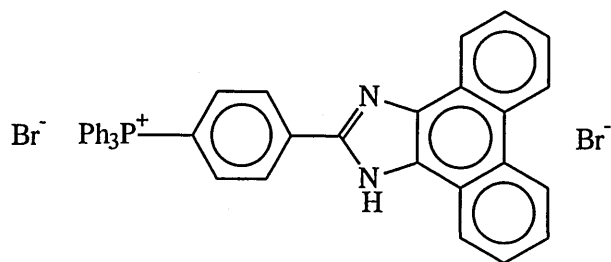
(71)   salt of (1A)

Solvent	Colour	Wavelength λ_{max} nm (71)	Wavelength λ_{max} nm (1A)
Methanol	fluorescent yellow	390	390
Acetonitrile	"	394	376
Acetone	"	402	380
Dichloromethane	"	418	392
Tetrahydrofuran	"	424	400

Table 19

A comparison of the solvatochromism data of (73) and (1A)

(73)   (1A)
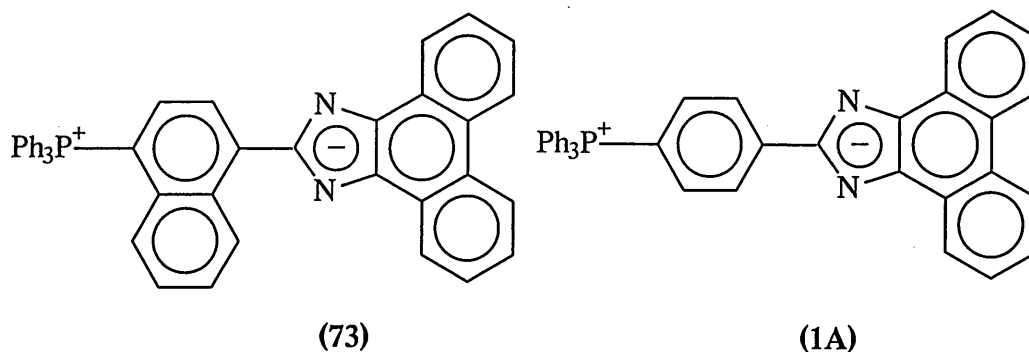
Solvent	Colour	Wavelength λ_{max} nm (73)	ν_{max} $\times 10^3 cm^{-1}$ (73)	Wavelength λ_{max} nm (1A)	ν_{max} $\times 10^3 cm^{-1}$ (1A)
Methanol	fluorescent yellow	(390)*	(26.54)*	-	-
Acetonitrile	pale orange	480	20.83	432	23.15
Acetone	red	504	19.84	446	22.42
Dichloromethane	orange	500	20.00	446	22.42
Tetrahydrofuran	red	534	18.73	472	21.19
$\Delta_{THF - MeCN}$		54	-2.1	40	-1.96

* = salt

$\Delta\nu_{max} = \nu_{nonpolar} - \nu_{polar}$

Table 20

110

A comparison of the solvatochromism data for salt (72) and the related salt of (1A)

(72)

salt of (1A)
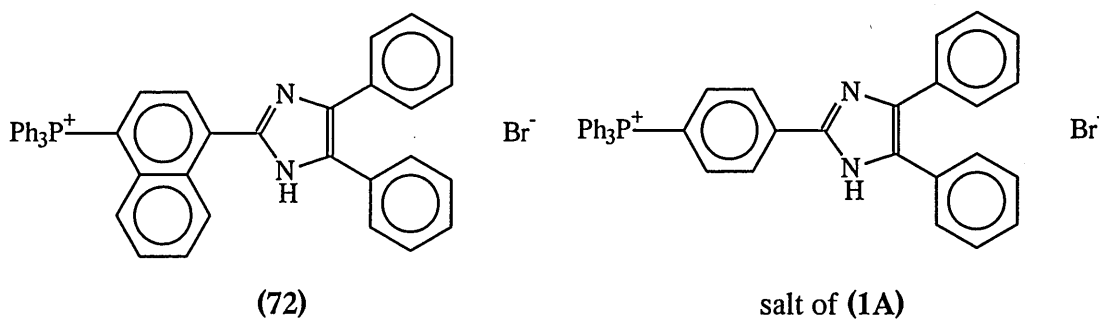
Solvent	Colour	Wavelength λ_{max} nm (72)	wavelength λ_{max} nm (1A)
Methanol	fluorescent yellow	382	362
Dichloromethane	"	406	378

Table 21

A comparison of solvatochromism data for (74) and (1A)
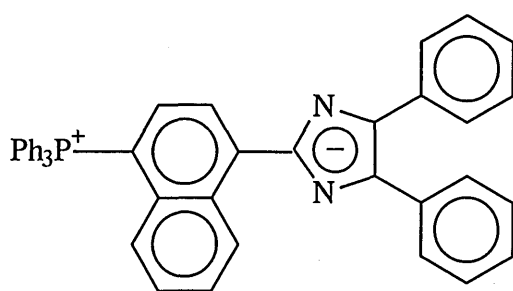
(74)   (1A)
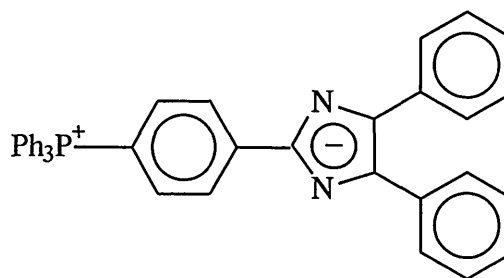
Solvent	Colour	Wavelength λ_{max} nm (74)	ν_{max} $x10^3cm^{-1}$ (74)	Wavelength λ_{max} nm (1A)	ν_{max} $x10^3cm^{-1}$ (1A)
Methanol	fluorescent yellow	(382)*	(26.17)*	(358)*	(27.93)*
Acetonitrile	orange	492	20.33	434	23.04
Acetone	red	516	19.38	452	22.12
Dichloromethane	red	506	19.76	448	22.32
Tetrahydrofuran	red - purple	544	18.38	468	21.37
$\Delta_{THF-MeCN}$		52	-1.95	34	-1.67

* = salt

$\Delta\nu_{max} = \nu_{nonpolar} - \nu_{polar}$

Table 22

Table 23 shows the E_T values (Kcal mol^{-1}) for betaines (73) and (74). They show a very similar trend, and have a much lower stabilisation of the ground-state compared to Kosower's polarity indicator,[15] and a much larger ground-state stabilisation than Reichardt's dye.[16]

112

| Solvent	E_T values (Kcal mol^{-1})	
	(73)	(74)
Methanol	-	-
Acetonitrile	59.56	58.11
Acetone	51.37	55.41
Dichloromethane	57.18	56.50
Tetrahydrofuran	53.54	52.56
ΔE_T	-6.02	-5.55

$\Delta E_T = E_{Tnonpolar} - E_{Tpolar}$

Table 23   The molar transition energies E_T (Kcal mol^{-1}) of betaines **(73)** and **(74)** in various solvents.

Figure 18 shows a plot of the longest wavenumber visible absorption band of the phosphonio-naphthyl imidazolides **(73)** and **(74)** and phosphonio-phenyl imidazolide betaines **(1A)** against the normalised polarity parameter E_T^N. The similarity of the plots indicates that all are showing similar behaviour with respect to the solvation of ground and excited state structures.
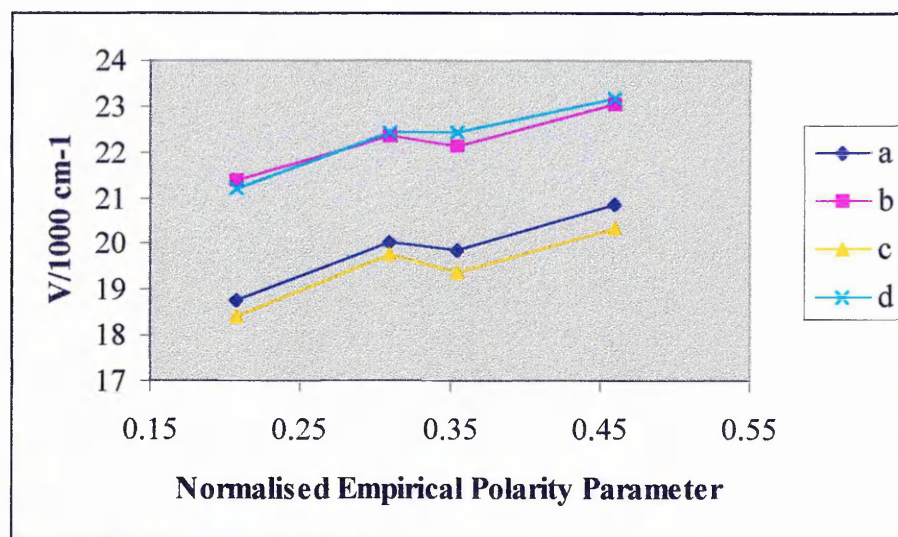

a = **(73)**, b = **(1A)** R = Ph, c = **(74)**, d = **(1A)** R = o-phenanthro

Figure 18   Plot of longest wavelength visible absorption band against the normalised empirical polarity parameter.

2.6 Future Developments

It would be of interest to make the long chain version of the phosphonio-naphthyliminodichlorophenolate betaine (67) as the charge-transfer absorption band occurs in the region of the emission wavelength of an inexpensive laser diode. Such a long chain betaine (75) could then be assembled as an LB film and its NLO (SHG) properties tested, as well as those for sensor applications, for the detection of electrophilic species.
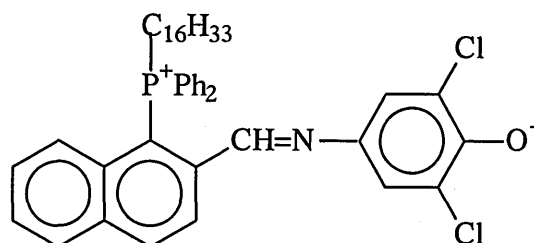
(75)

It would also be of interest to study the NLO properties of the above compound where phenyl groups are *ortho* to the negative oxygen as this has already been seen to shift the CT absorption maxima to a longer wavelength by 60 nm.[2]

It would also be advantageous to make the betaines (76) and (77) as further annelation forming the anthracene systems would shift the charge-transfer absorption band to an even longer wavelength. Systems having anthracene units at both ends of the molecule could also be made.

R = Ph or $C_{16}H_{33}$

(76)

(77)

R = Ph or $C_{16}H_{33}$
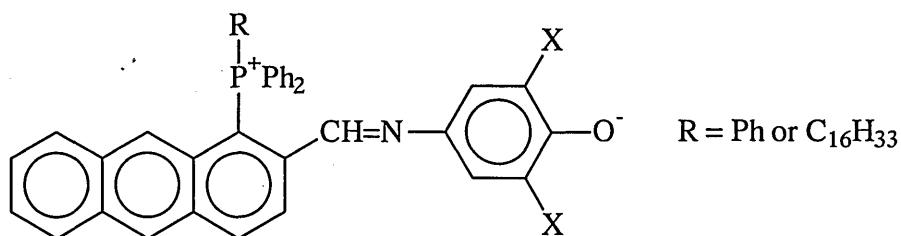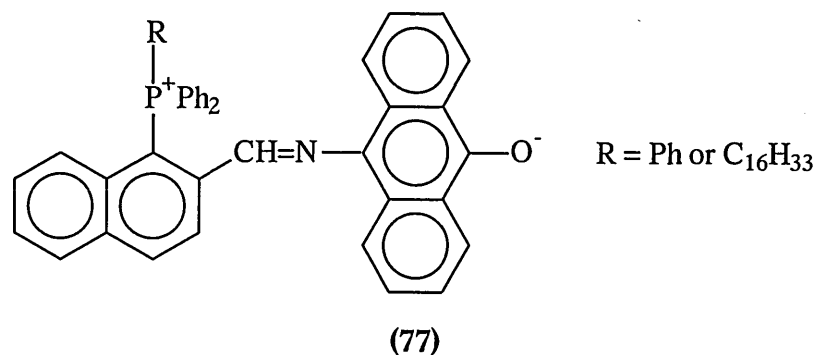
Similarly the effect of further annelation on the imidazolide betaines should also be explored as in e.g. (78) and (79), to see the effect of annelation upon the shift in wavelength of the charge-transfer absorption band.

(78)

(79)
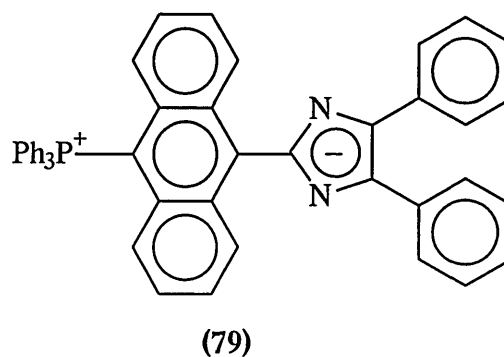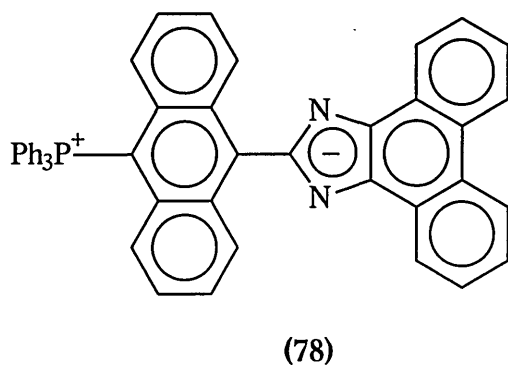
The presence of anthracene units could also confer on these systems some interesting fluorescence properties, which may differ substantially between salt and betaine or betaine and complexed betaine, and therefore provide an alternative means of sensing.

2.7 Experimental

Analysis

^{1}H NMR spectra were obtained using a Brüker 250 AC spectrometer at 250 MHz. ^{1}H NMR data are given on the δ scale (ppm) using tetramethylsilane as the internal reference. Abbreviations for the form of the signal are: s = singlet, ss = singlet-singlet, d = doublet, dd = doublet-doublet, t = triplet, m = multiplet, and br = broad. Coupling constants J are given in Hz. ^{31}P NMR and ^{13}C NMR were also obtained using a Brüker 250 AC spectrometer at 250 MHz.

Mass spectra (EI and FAB) and high resolution mass spectra (EI) were obtained on a VG Micromass 7070F. For the FAB technique, the compounds were dissolved in *p*-nitrobenzylalcohol (*p*-NBA) or glycerol. High resolution mass spectra (FAB) were obtained at the EPSRC Mass Spectrometry Service, University of Wales, Swansea and on a Prospec Magnetic Sector Mass Spectrometer, (Micromass, Manchester, UK) at the University of Sheffield.

GC-MS was carried out on a Hewlett Packard 5890 GC, attached to a VG Trio-1 spectrometer.

Thin layer chromatography (TLC) was performed on silica gel 60F254 plates (2 mm thickness), and flash chromatography was carried out with BDH flash silica gel (particle size 40-63 μm).

Microanalytical Data were obtained by Medac Ltd (Brunel Science Centre).

Solvents

Dry tetrahydrofuran (THF) was obtained by distillation from potassium metal. Dry diethyl ether was obtained by distillation from sodium metal, and then storing over sodium wire.

DMF was distilled under nitrogen, and then stored over molecular sieve.

Conditions

All reactions requiring an inert atmosphere were performed under nitrogen, using either a nitrogen balloon or a nitrogen cylinder.

116

(22) N-Hexadecyldiphenylphosphine

$$C_{16}H_{33}PPh_2$$
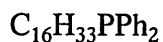
Small strips of lithium metal (0.252 g, 36 mmol) were stirred in dry THF (10 ml) at room temperature. Chlorodiphenylphosphine (4.0 g, 18 mmol) in THF (20 ml) was added dropwise and within half an hour of stirring the solution turned deep red in colour.

1-Iodohexadecane (6.34 g, 18 mmol) in dry THF (30 ml) was added dropwise and the mixture turned pale yellow. An exothermic reaction was observed and the solution was stirred at room temperature for one hour, and heated under reflux for a further hour. The mixture was hydrolysed with a 10 % solution of aqueous ammonium chloride (30 ml). The organic layer was dried (MgSO$_4$), and the solvent evaporated in vacuo to leave a cream waxy solid. Recrystallisation from methanol several times afforded a white waxy solid Yield 5.42 g, 37 %. Alternatively column chromatography gave a yield of *ca.* 80 %.

mp 43-45 °C

^{31}P NMR (CDCl$_3$): -16.38 ppm.

^{1}H NMR (CDCl$_3$): δ 0.91(t, 3H, CH$_3$), 1.26-2.05(m, 30H, aliphatic), 7.32-7.47(m, 10H, aromatic).

MS (EI) Exact mass calculated for C$_{28}$H$_{43}$P: 410.30941 Found: 410.31024 (2.0 ppm).

(18A) 2-(2-Bromophenyl)-4,5-diphenyl imidazole
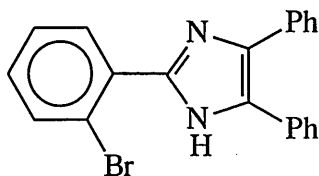
Benzil (3.41 g, 16.22 mmol) was heated under reflux with 2-bromobenzaldehyde (3 g, 16.21 mmol) and ammonium acetate (11.25 g, 146 mol) in glacial acetic acid (70 ml) for six hours. The reaction mixture was cooled and poured into iced water and neutralised with ammonia. The cream solid was filtered and recrystallised from

acetonitrile to afford a white solid which was dried under vacuum over water. Yield 4.36 g, 73 %.

mp 251-252 °C (lit. mp>250 °C)[1]

MS (EI) 373.8 and 375.7 (M$^+$) base peak.

(18B) 2-(4-Bromophenyl)-4,5-diphenyl imidazole
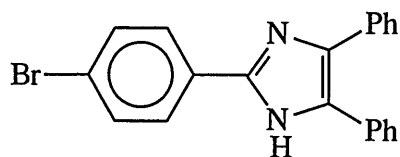
(18B) was synthesised as with (18A) using 4-bromobenzaldehyde resulting in a white-cream solid after triturating in ether.Yield 5 g, 83 %.

mp 267-270 °C (lit. mp 268-271 °C)[1]

MS (EI) 373.8 and 375.8 (M$^+$) base peak.

(19A) 2-(2-Bromophenyl)-1H-phenanthro[9,10-d]imidazole
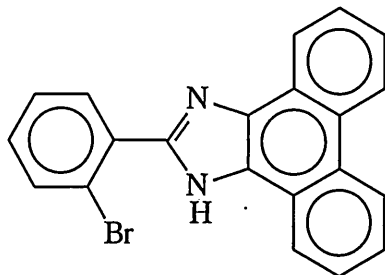
9,10-Phenanthraquinone (3.5 g, 16.83 mmol) and 2-bromobenzaldehyde (3.4 g, 18.4 mmol) were allowed to react with ammonium acetate (11.5 g, 150 mmol) in glacial acetic acid (70 ml) under reflux for six hours. On cooling, the reaction mixture was poured into iced water and neutralised with ammonia. The cream solid was filtered and recrystallised from ethanol and water to afford a cream solid. Yield 4.2 g, 70 %.

mp 235-237 °C (lit. mp 235-237 °C)[1]

^{1}H NMR (CDCl$_3$): δ 7.8-9.5(m, 12H, aromatic),12.9(s, 1H, NH).

MS (EI) 371.9 and 373.8 (M$^+$) (base peaks).

(19B) 2-(4-Bromophenyl)-1H-phenanthro[9,10-*d*]imidazole
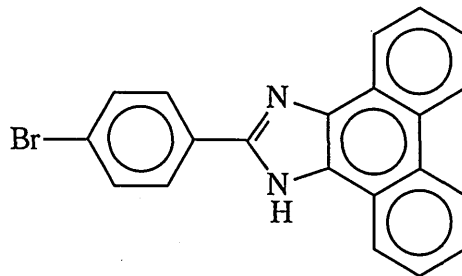
The imidazole **(19B)** was synthesised in the same manner as **(19A)** using 4-bromobenzaldehyde to afford a cream-white solid. Yield 4.5 g, 75 %.

mp 273-276 °C (lit. mp 274-276 °C)[1]

^{1}H NMR (CDCl$_3$): δ 7.9-9.3(m, 12H, aromatic),13.1(s, 1H, NH).

MS (EI) 371.9 and 373.9 (M$^+$) (base peaks).

(23A)2-(2-N-Hexadecyldiphenylphosphoniophenyl)-4,5-diphenylimidazole bromide
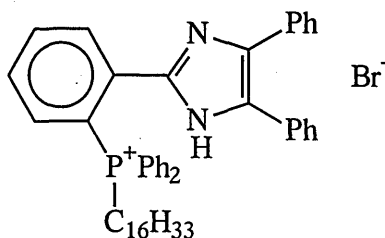
The imidazole **(18A)** (1.98 g, 5.28x10^{-3} mol) was heated under reflux with phosphine **(22)** (2.17 g, 5.28 x10^{-3} mol) and NiBr$_2$ (0.58 g, 2.64 x10^{-3} mol) in benzonitrile (30 ml) for four hours under nitrogen. After cooling, the bottle green reaction mixture was poured into aqueous KBr solution (100 ml, 10 % w/v) and extracted with dichloromethane (3 x 30 ml) and washed with aqueous KBr (10 % w/v). The combined organic extracts were dried (MgSO$_4$), and the solvent evaporated in vacuo. The salt was isolated pure from the remaining benzonitrile mixture by column chromatography, (eluting solvents 100 % CH$_2$Cl$_2$; 20:80 MeOH:CH$_2$Cl$_2$) to afford a pale yellow solid. Yield 2.29 g, 56 %.

mp 89-92 °C

^{31}P NMR (CDCl$_3$): 26.33 ppm.

^{1}H NMR (CDCl$_3$): δ 0.8-0.9(t, 3H, CH$_3$ aliphatic), 1.0-2.0(m, 28H, aliphatic), 3.1-3.3(t, 2H, CH$_2$ aliphatic), 6.8-8.0(m, 20H, aromatic), 8.9(t, 4H, aromatic), 13.6(s, 1H, NH).

119

MS (FAB) Exact mass calculated for (M$^+$ cation) C$_{49}$H$_{58}$N$_2$P:705.43376 Found:705.43279 (1.3 ppm).

(26A) 2-(4-N-Hexadecyldiphenylphosphoniophenyl)-4,5-diphenylimidazolide

The salt (23A) (1g, 1.27 x10^{-3} mol) was stirred at room temperature with an excess of anhydrous potassium carbonate (0.02 mol) for one hour in acetonitrile, where the pale yellow solution turned bright yellow immediately. The solution was filtered and the solvent evaporated in vacuo to leave a bright yellow solid. Yield 0.7g, 78 %.
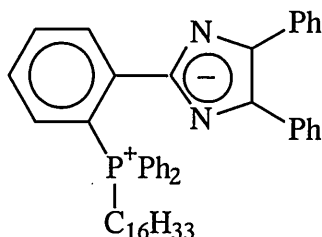
mp 58-60 °C

^{31}P NMR (CDCl$_3$): 22.84 ppm.

^{1}H NMR (CDCl$_3$): δ 0.8-2.0(m, 31H, aliphatic), 3.1-3.3(t, 2H, CH$_2$ aliphatic), 6.5-7.8(m, 20H, aromatic), 8.8(t, 4H, aromatic).

MS (FAB) Exact mass calculated for (M$^+$ 1) C$_{49}$H$_{58}$N$_2$P:705.43376 Found:705.43970 (-8.4 ppm).

(23B) 2-(4-N-Hexadecyldiphenylphosphoniophenyl)-4,5-diphenylimidazole bromide
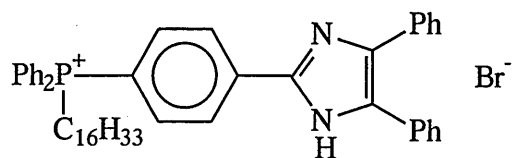
Imidazole (18B) (2.28 g, 0.006 mol) was heated under reflux with phosphine (22) (2.5 g, 0.006 mol) in benzonitrile (40 ml) for four hours under nitrogen. After cooling the bottle green reaction mixture was poured into aqueous KBr solution (300 ml, 10 % w/v) and extracted with dichloromethane (3 x 50 ml), and washed with aqueous KBr (10 % w/v). The combined organic extracts were dried (MgSO$_4$), filtered, and the solvent evaporated in vacuo. The salt was isolated from the remaining benzonitrile mixture by column chromatography, (eluting solvents, 100% CH$_2$Cl$_2$; 5:95 MeOH:CH$_2$Cl$_2$; 10:90 MeOH:CH$_2$Cl$_2$). A pale yellow solid was obtained, yield 2.3 g, 49 %.

120

mp 100-103 °C

^{31}P NMR (CDCl$_3$): 22.75 ppm.

^{1}H NMR (CDCl$_3$): δ 0.8-1.0(t, 3H, CH$_3$), 1.2-2.3(m, 28H, aliphatic), 3.0-3.3(t, 2H, CH$_2$ aliphatic), 3.1-3.3(t, 2H, CH$_2$ aliphatic), 7.0-8.0(m, 20H, aromatic), 9.0(t, 4H, aromatic), 13.0(s, 1H, NH).

MS (FAB) Exact mass calculated for (M$^+$ cation) C$_{49}$H$_{58}$N$_2$P:705.43376 Found: 705.43672 (-4.2 ppm).

Anal. Cald. for C$_{49}$H$_{58}$N$_2$PBr: C,74.90; H,7.44; N,3.56. Anal. found: C,73.88; H,7.48; N, 3.41.

(26B) 2-(4-N-Hexadecyldiphenylphosphoniophenyl)-4,5-diphenylimidazolide
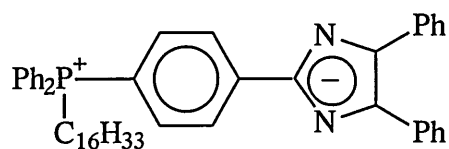
<u>Sodium Hydroxide Method.</u>

The salt (23B) (0.5 g, 0.06 x10^{-3} mol) was stirred with 1M NaOH (1.5 ml, 15 mmol) in ethanol (10 ml) for thirty minutes at room temperature, where a bright yellow solution formed immediately. The reaction mixture was poured into water (75 ml) and extracted with dichloromethane (3 x 50 ml). The organic layer was dried (MgSO$_4$) and evaporated in vacuo. A bright yellow solid was obtained. Yield 0.4 g, 95 %.

mp 73-75 °C

^{31}P NMR (CDCl$_3$): 22.12 ppm.

^{1}H NMR (CDCl$_3$): δ 0.8-1.0(t, 3H, CH$_3$), 1.1-1.8(m, 28H, aliphatic), 2.8-2.9(t, 2H, CH$_2$ aliphatic), 7.0-7.9(m, 20H, aromatic), 8.6(t, 4H, aromatic).

MS (FAB) Exact mass calculated for (M$^+$ 1) C$_{49}$H$_{58}$N$_2$P:705.43376 Found:705.43375 (0.0 ppm).

Anal. Cald. for C$_{49}$H$_{57}$N$_2$P.H$_2$O: C,79.42; H,8.30; N,3.78. Anal. found: C,79.66; H,7.97; N, 3.89.

121

The salt (23B) (0.5 g, 0.06 x10^{-3} mol) was stirred with K_2CO_3 (1.3 g, 9 x 10^{-3} mol) in dry acetonitrile (10 ml) at room temperature for one hour. The reaction mixture was filtered, and the solvent evaporated in vacuo to leave a bright yellow solid. Yield, 0.41 g, 98%.

Anal. Cald. for $C_{49}H_{57}N_2P.H_2O$: C,79.42; H,8.30; N,3.78. Anal. found: C,80.41; H,8.02; N, 3.82.

(24A) 2-(2-N-Hexadecyldiphenylphosphoniophenyl)-1H-phenanthro[9,10-d]imidazole bromide
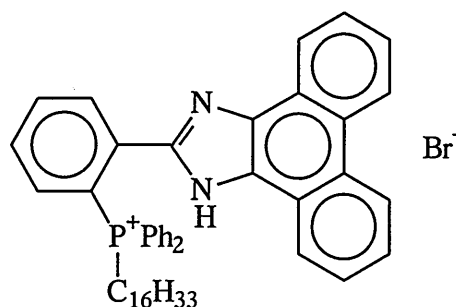
Analogous to the procedure for salts (23), the imidazole (19A) (0.7 g, 1.88 x 10^{-3} mol) was heated under reflux with phosphine (22) (0.77 g, 1.88 x 10^{-3} mol) and $NiBr_2$ (0.94 x 10^{-3} mol) for eight hours under nitrogen. A beige solid was isolated after column chromatography. Yield 0.87 g, 59 %.

mp 90-92 °C

^{31}P NMR ($CDCl_3$): 27.37 ppm.

^1H NMR ($CDCl_3$): δ 0.8-2.0(m, 31H, aliphatic), 3.4(t, 2H, CH_2), 7.0-9.4(m, 22H, aromatic), 14.4(s, 1H, NH).

MS (FAB) Exact mass calculated for (M^+ cation) $C_{49}H_{56}N_2P$:703.41811 Found:703.41796 (0.2 ppm).

(27A) 2-(2-N-Hexadecyldiphenylphosphoniophenyl)-1H-phenanthro[9,10-*d*]imidazolide
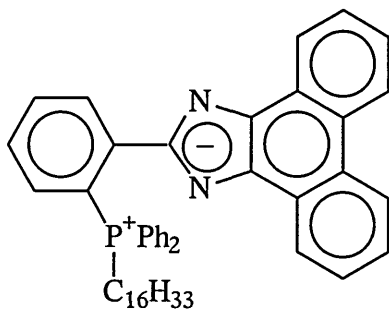
The salt **(24A)** was converted to the betaine using potassium carbonate, analogous to the procedure for betaines **(26)**. A bright yellow solid was obtained. Yield 0.21 g, 73 %.

mp 60-63 °C

^{31}P NMR (CDCl$_3$): 23.63 ppm.

^{1}H NMR (CDCl$_3$): δ 0.7-1.8(m, 31H, aliphatic), 3.4(t, 2H, CH$_2$), 6.8-7.0(m, 16H, aromatic), 8.0(d, 1H, aromatic), 8.6(d, 1H, aromatic), 9.0(m, 4H, aromatic).

MS (FAB) Exact mass calculated for (M$^+$ 1) C$_{49}$H$_{56}$N$_2$P:703.41811 Found:703.41732 (1.1 ppm).

(24B) 2-(4-N-Hexadecyldiphenylphosphoniophenyl)-1H-phenanthro[9,10-*d*]imidazole bromide
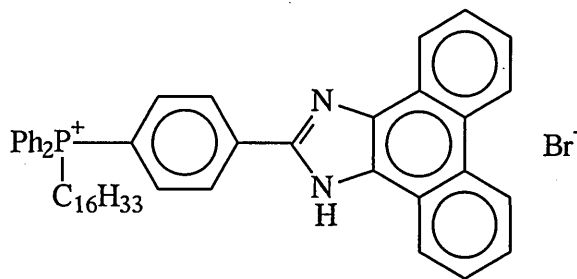
Analogous to the procedure for salts **(26)**, imidazole **(19B)** (2.1 g, 5.6 mmol) was heated under reflux with phosphine **(22)** (2.28 g, 5.6 mmol) and NiBr$_2$ (0.61 g, 2.8 mmol) in benzonitrile (50 ml) for four hours under nitrogen. After purification by column chromatography a beige solid was afforded. Yield 2.53g, 58 %.

mp 72-74 °C

^{31}P NMR (CDCl$_3$): 22.70ppm

^{1}H NMR (CDCl$_3$): δ 0.8-2.1(m, 31H, aliphatic), 3.5(t, 2H, CH$_2$), 7.0-8.7(m, 14H, aromatic), 9.3-9.4(m, 8H, aromatic). 14.4(s,1H, NH).

123

MS (FAB) Exact mass calculated for (M$^+$ cation) $C_{49}H_{56}N_2P$: 703.41811 Found: 703.41912 (-1.4 ppm).

(27B) 2-(4-N-Hexadecyldiphenylphosphoniophenyl)-1H-phenanthro[9,10-d]imidazolide
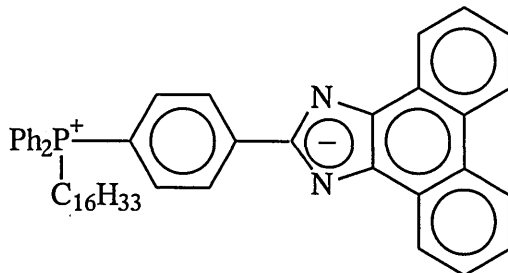
Analogous to the procedure for betaine (26) (potassium carbonate method), a bright yellow solid was obtained. Yield 2.03 g, 99 %.

mp 57-59 °C

^{31}P NMR (CDCl$_3$): 22.49ppm.

^{1}H NMR (CDCl$_3$): δ 0.8-1.0(t, 3H, aliphatic), 1.1-1.8(m, 28H, aliphatic), 2.8(t, 2H, aliphatic), 7.8-8.0(m, 17H, aromatic), 8.7(d, 1H, aromatic), 9.0(m, 4H, aromatic).

MS (FAB) Exact mass calculated for (M$^+$ cation) $C_{49}H_{56}N_2P$:703.41811 Found:703.41925 (-1.6 ppm).

(29) 4-N(o-Bromobenzylidene)amino-2,6-dichlorophenol
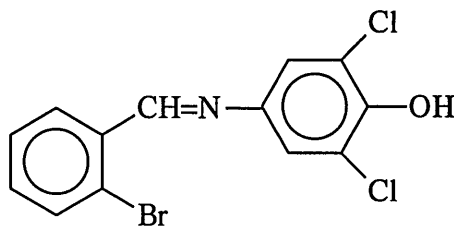
2-Bromobenzaldehyde (1.11 g, 6 mmol) and 4-amino-2,6-dichlorophenol (1.06 g, 6 mmol) were heated under reflux in ethanol (20 ml) for two hours under nitrogen. Recrystallisation of the crude solid gave the product as a pale brown solid. Yield 1.4 g, 74 %.

mp 155 – 157 °C (lit. 155-156 °C)[2]

^{1}H NMR (CDCl$_3$): δ 5.90(s, 1H, OH), 7.2 (m, 4H), 7.7(d, 1H), 8.2(d, 1H), 8.9(s, 1H, CH=N).

MS (EI) (M$^+$) 345 and 347 (100 and 48 %).

(30) 4-N(o-Bromobenzylidene)amino-2,6-dibromophenol

Analogous to the procedure described for compound (29) 2-bromobenzaldehyde (1.11 g, 6 mmol) was heated under reflux in ethanol (20 ml) with 4-amino-2,6-dibromophenol (1.6 g. 6 mmol) for two hours under nitrogen. After recrystallisation (30) was isolated as a brown solid. Yield 1.99 g, 76 %.

mp 117 – 118 °C (lit. 116-118 °C)[2]

^{1}H NMR (CDCl$_3$): δ 6.0(s, 1H, OH), 7.3(m, 4H), 7.7(d, 1H), 8.2(d, 1H), 8.8(s,1H, CH=N).

MS (EI) (M$^+$) 433 and 435 (99 and 95 %).

4-Nitro-2,6-diphenylphenol
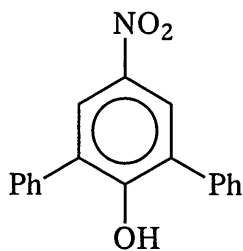
This synthesis was carried out according to the procedure described in the literature.[18] 2,6-diphenylphenol (2.5 g, 10.15 mmol) was added slowly to a well-stirred mixture containing nitric acid (70 %,7.5 ml) and distilled water (7.5 ml) at room temperature. The suspension became yellow after a few minutes and orange when left to stir overnight. The crude product was filtered off, and washed with distilled water. The solid was dissolved in hot water, treated with a small amount of charcoal and filtered. Recrystallisation gave pale orange - yellow crystals.

4-Amino-2,6-diphenylphenol
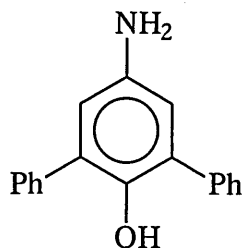
4-Nitro-2,6-diphenylphenol (1.5 g, 5 mmol) was dissolved in boiling aqueous sodium hydroxide solution (5 % w/v, 62 ml). The deep red solution was stirred and sodium hydrosulfite added in small portions until the colour changed to pale yellow. After a small excess of the sodium hydrosulfite was added, the solution was refluxed for a further fifteen minutes. The hot mixture was adjusted to pH5 with glacial acetic acid, whereupon a precipitate formed. The solution was cooled and the solid filtered and washed with ice-cold water to give a tan coloured solid. This was used for the next stage of the reaction almost immediately.

(31) 4-N(o-Bromobenzylidene)amino-2,6-diphenylphenol

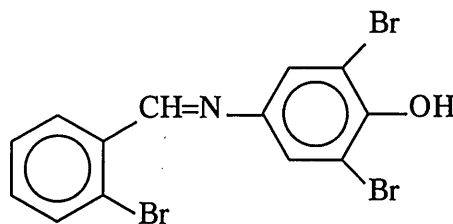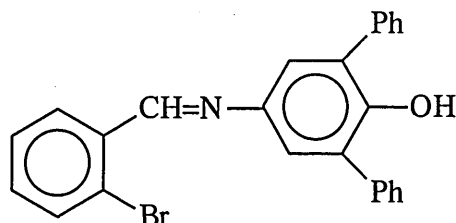Analogous to the procedure described for **(29)** 2-bromobenzaldehyde (0.93 g, 5 mmol) and 4-amino-2,6-diphenylphenol (1.3 g, 5 mmol) were heated under reflux in ethanol (20 ml) under nitrogen for three hours. After cooling, a small amount of diethyl ether and ethanol were added to the mixture, whereupon a white solid precipitated out, which was filtered and washed with a small amount of cold ethanol. Yield 1.32 g, 62 %.

mp 123-126 °C (lit. 124-126 °C)[2]

^{1}H NMR (CDCl$_3$): δ 5.5(s,1H, OH), 6.5 - 8.0(m, 15H, aromatic), 8.2(d, 1H), 8.9(s, 1H, CH=N).

MS (EI) (M$^+$) 427 and 429 (base peaks).

4-Amino-2,6-*tert*-butylphenol

$$OH$$

(CH₃)₃C ... C(CH₃)₃ with NH₂

Structure: 4-amino-2,6-di-tert-butylphenol showing OH at top, (CH$_3$)$_3$C and C(CH$_3$)$_3$ substituents, and NH$_2$ at bottom.
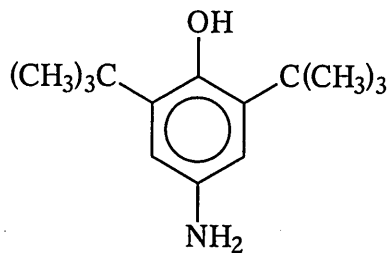
The synthesis was carried out according to the procedure described in the literature.[17]

2,6-Di-*t*-butyl-*p*-benzoquinine-4-oxime (5.0 g, 21.2 mmol) was dissolved in THF (50 ml). Sodium hydroxide (1.27 g, 31.4 mmol) in water (50 ml) was added to the THF solution with stirring (efficiently). The mixture was heated to 45 °C and sodiun hydrosulfite (5.5 g, 31.8 mmol) was added to the solution slowly. After completion of the addition, the mixture was stirred for another hour, during which time its colour changed from deep red to pale yellow -colourless. The mixture was poured into a large volume of water, and the precipitate formed was filtered and washed with water to afford a white-yellow product. This was used quickly without purification in the following step.

(32) 4-N(*o*-Bromobenzylidene)amino-2,6-di-*tert*-butylphenol

Structure: 4-N(o-bromobenzylidene)amino-2,6-di-tert-butylphenol showing CH=N linkage, Br on one ring, Bu^t substituents and OH on the other ring.
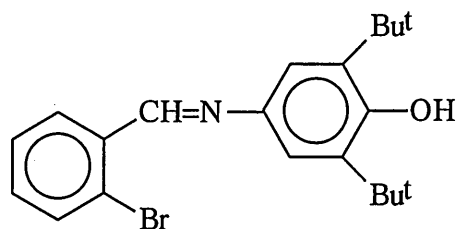
Analogous to the procedure given for (29), 2-bromobenzaldehyde (3.92 g, 21.2 mmol) was heated under reflux in ethanol (20 ml) with 4-amino-2,6-di-*tert*-butylphenol under nitrogen for two hours. After cooling the orange solid was filtered and recrystallised from acetonitrile. Yield 3.3 g, 48 %.

mp 108-110 °C (lit. 109-110 °C)[2]

^{1}H NMR (CDCl₃): δ 1.29(s, 18H), 5.2(s, 1H, OH), 7.1(s, 2H), 7.4(m, 2H), 7.6(d, 1H), 8.2(d, 1H), 8.9(s, 1H, CH=N).

MS (EI) (M⁺) 386.9 and 388.9 (base peaks).

(33) 4-N[-(*o*-Diphenyl-hexadecylphosphoniobenzylidene)-amino]-2,6-dichlorophenol bromide
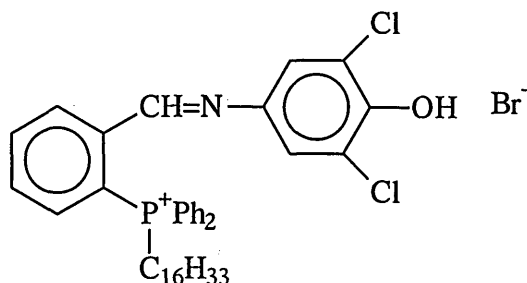
(29) (0.9 g, 2.6 mmol) was heated under reflux with the long chain phosphine **(22)** (1.61 g, 3.9 mmol) and nickel (II) bromide (0.17 g, 1.3 mmol) in ethanol (27 ml) for eight hours under nitrogen. After cooling the reaction mixture was poured into aqueous potassium bromide (200 ml, 10% w/v) and extracted with dichloromethane (3 x 50 ml). The combined organic layers were washed with aqueous potassium bromide and dried (MgSO$_4$). After evaporation of the solvent the oily solid was purified by chromatography, triturated with petrol, and the solid recrystallised from petrol/dichloromethane to afford an orange solid. Yield 0.66 g, 34 %.

mp > 300 °C (decomp.)

^{31}P NMR (CDCl$_3$): 27.41 ppm.

^{1}H NMR (CDCl$_3$): δ 0.85(t, 3H, CH$_3$), 0.87-1.45(m, 28H, aliphatic), 3.3(t, 2H, CH$_2$), 6.40(s, 2H, aromatic), 7.35-8.32(m, 14H, aromatic), 8.66(s, 1H, CH=N).

MS (FAB) Exact mass calculated for (M$^+$ cation) C$_{41}$H$_{51}$NOPCl$_2$: 674.3085 Found: 674.3105 (-2.9ppm).

(45) 4-N[-(*o*-Diphenyl-hexadecylphosphoniobenzylidene)-amino]-2,6-dichlorophenolate
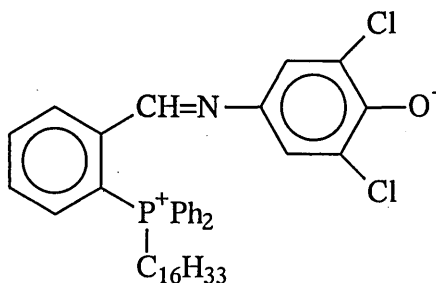
The perchlorate salt was stirred with anhydrous potassium carbonate for an hour in acetonitrile, the solution was filtered and the potassium carbonate washed with

acetonitrile. The solvent was evaporated in vacuo and the betaine was obtained as a dark red solid. Yield 93 %.

mp >153 °C (decomp.)

^{31}P NMR (CDCl$_3$): 26.70 ppm.

^{1}H NMR (CDCl$_3$): δ 0.85(t, 3H, CH$_3$), 1.10-1.56(m, 28H, aliphatic), 3.11(t, 2H, CH$_2$), 6.47(s, 2H, aromatic), 7.4 - 7.89(m, 14H, aromatic), 8.24(s, 1H, CH=N).

MS (FAB) Exact mass calculated for (M$^+$ + 1) C$_{41}$H$_{50}$NOPCl$_2$: 674.3085 Found: 674.3093 (-1.1 ppm).

(34) 4-N[-(o-Diphenyl-hexadecylphosphoniobenzylidene)-amino]-2,6-dibromophenol bromide
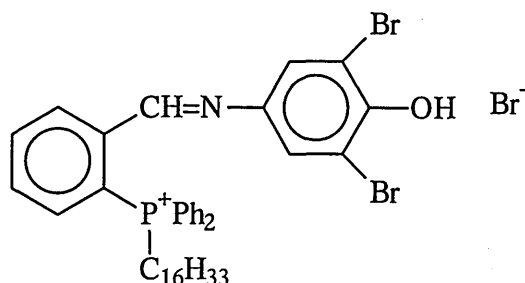
Analogous to **(33)**, **(30)** (1.45 g, 3.3 mmol) was heated under reflux in ethanol (37 ml) with the long chain phosphine **(22)** (2.03 g, 4.95 mmol) and nickel (II) bromide (0.2 g, 1.65 mmol) for six to eight hours under nitrogen. After aqueous work up of the reaction mixture and trituration with petrol, and subsequent recrystallisation from dichloromethane/petrol an orange solid was obtained. Yield 1.43 g, 51 %.

mp 422 °C (by DSC).

^{31}P NMR (CDCl$_3$): 27.03 ppm.

^{1}H NMR (CDCl$_3$): δ 0.85(t, 3H, CH$_3$), 0.88-1.56(m, 28H, aliphatic), 3.20(t, 2H, CH$_2$), 6.64(s, 2H, aromatic), 7.47-7.93(m, 14H, aromatic), 8.39(s, 1H, CH=N).

MS (FAB) Exact mass calculated for (M$^+$ cation) C$_{41}$H$_{51}$NOPBr$_2$: 762.2075 Found: 762.2094 (-2.5 ppm).

(46) 4-N[-(o-Diphenyl-hexadecylphosphoniobenzylidene)-amino]-2,6-dibromophenolate
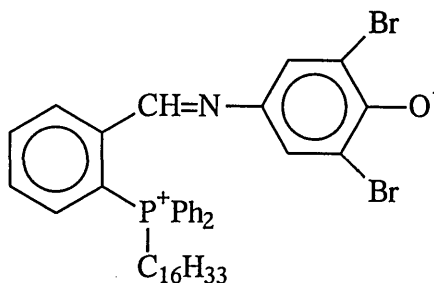
Analogous to (45) the perchlorate salt was converted to the betaine, which was obtained as a dark red solid. Yield 96 %.

mp > 150 °C (decomp.)

^{31}P NMR (CDCl$_3$); 26.72 ppm.

^{1}H NMR (CDCl$_3$): δ 0.85(t, 3H, CH$_3$), 0.87-1.55(m, 28H, aliphatic), 3.10(t, 2H, CH$_2$), 6.71(s, 1H, aromatic), 7.4 - 8.1(m, 14H, aromatic), 8.19(s, 1H, CH=N).

MS (FAB) Exact mass calculated for (M$^+$ + 1) C$_{41}$H$_{50}$NOPBr$_2$: 762.2075 Found: 762.2091 (-2.1ppm).

(35) 4-N[-(o-Diphenyl-hexadecylphosphoniobenzylidene)-amino]-2,6-diphenylphenol bromide
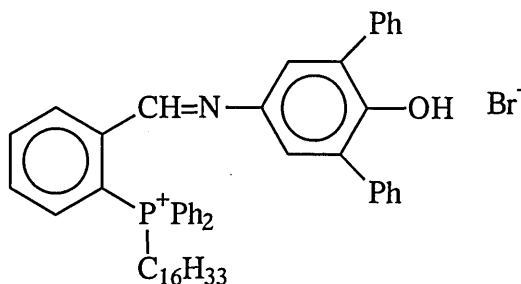
(31) (1.71 g, 4 mmol) was heated under reflux with the long chain phosphine (22) (2.45 g, 6 mmol) and nickel (II) bromide (0.26 g, 2 mmol) in ethanol (40 ml) for eight hours under nitrogen. Aqueous work up was carried out analogous to (33), however, purification on a silica column was not employed. The brown sticky solid was triturated several times with fresh petrol and recrystallised from dichloromethane/petrol to afford a brown – orange powder. Yield 2.26 g, 68 %.

mp 455-456 °C

^{31}P NMR (CDCl$_3$): 27.67 ppm.

^{1}H NMR (CDCl$_3$): δ 0.81(t, 3H, CH$_3$), 0.83 - 1.57(m, 28H, aliphatic), 5.5(bs, 1H, OH), 6.32(s, 2H, aromatic), 7.30 - 8.34(m, 24H, aromatic), 8.71(s, 1H, CH=N).

MS (FAB) Exact mass calculated for (M$^+$ cation) C$_{53}$H$_{61}$NOP: 758.4491 Found: 758.4485 (0.8 ppm).

(47) 4-N[-(*o*-Diphenyl-hexadecylphosphoniobenzylidene)-amino]-2,6-diphenylphenolate
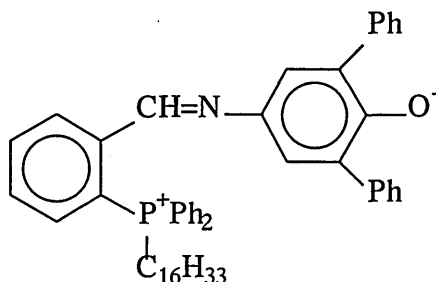
The perchlorate salt was shaken with aqueous sodium hydroxide and dichloromethane, and then the organic layer was washed with water. The organic layer was dried (MgSO$_4$), and the solvent removed in vacuo. The betaine was triturated with petrol to afford a purple solid. Yield 85 %.

mp > 130 °C (decomp.)

^{31}P NMR (CDCl$_3$): 26.28 ppm.

^{1}H NMR (CDCl$_3$): δ 0.85(t, 3H, CH$_3$), 0.88 - 1.59(m, 28H, aliphatic), 3.15(t, 2H, CH$_2$), 6.65(s, 2H, aromatic), 7.29-7.78(m, 24H, aliphatic), 8.37(s, 1H, CH=N).

MS (FAB) Exact mass calculated for (M$^+$) C$_{53}$H$_{60}$NOP: 757.4413 Found: 757.4381 (4.2 ppm).

(36) 4-N[-(*o*-Diphenyl-hexadecylphosphoniobenzylidene)-amino]-2,6-di-*tert*-butylphenol bromide
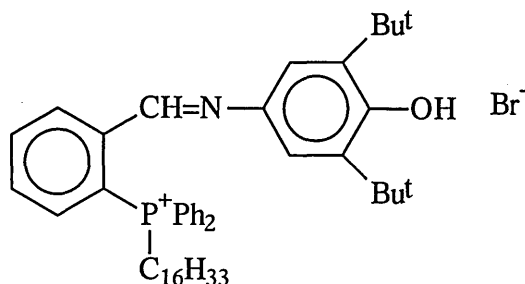
(32) (0.53 g, 1.4 mmol) was heated under reflux with the long chain phosphine (22) (0.86 g, 2.1 mmol) and nickel (II) bromide (0.09 g, 0.7 mmol) in ethanol (10 ml) for eight hours. Analogous to (33) aqueous work up was carried out, and the crude salt was triturated with petrol, and recrystallised from dichloromethane/petrol to afford a pale yellow solid. Yield 0.56 g, 51 %.

mp >130 °C (decomp.)

^{31}P NMR (CDCl$_3$): 27.48 ppm

^{1}H NMR (CDCl$_3$): δ 0.86(t, 3H, CH$_3$ of long chain), 0.88-1.58(m, 46H, long chain and *t*-butyl), 3.23(t, 2H, CH$_2$, aliphatic), 5.3(s, 1H, OH), 6.3(s, 2H, aromatic), 7.35-8.10(m, 14H, aromatic), 8.46(s, 1H, CH=N).

MS(FAB) Exact mass calculated for (M$^+$ cation) C$_{49}$H$_{69}$NOP: 718.5117. Found 718.5102 (2.1 ppm).

(48) 4-N[-(*o*-Diphenyl-hexadecylphosphoniobenzylidene)-amino]-2,6-di-*tert*-butylphenolate
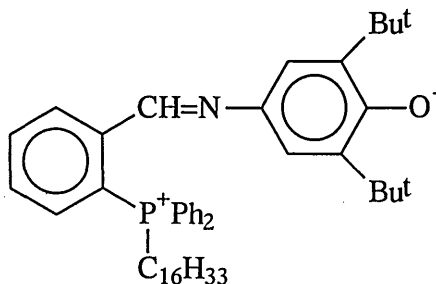
Analogous to (45) the betaine was obtained as a very crude purple solid. Yield 80 %.

^{31}P NMR (CDCl$_3$): 19.86, 26.15 (main) 32.38, 34.50, 39.28 ppm

(55) N-(4-Quinolinylmethylidene)-4-amino-2,6-dichlorophenol
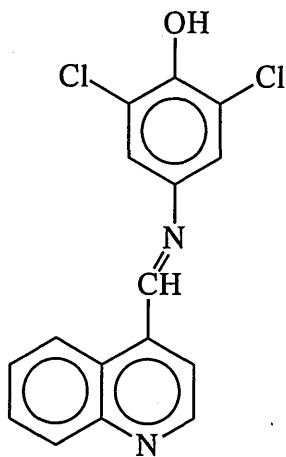
4-amino-2,6-dichlorophenol (1.43 g, 8 mmol) and quiniline-4-carboxaldehyde (1.26g, 8 mmol) were heated under reflux in ethanol (20 ml) under nitrogen for three hours. The reaction mixture was cooled and filtered, washing with ethanol to afford a yellow-green solid. Yield 2.42 g, 95 %.

mp 261-263 °C

^{1}H NMR (DMSO): δ 7.62-9.41(m, 8H, aromatic), 9.41 (s, 1H, CH=N).

^{1}H NMR (TFA) δ 7.32(s, 2H, aromatic), 8.04-8.40(m, 4H, aromatic), 9.08-9.22(dd, 2H, aromatic), 10.65(s, 1H, CH=N), 11.2(br s, TFA).

UV/VIS (in TFA) 334 nm.

MS (EI) Exact mass calculated for (M$^+$) $C_{16}H_{10}N_2{}^{35}Cl_2O$: 316.01703 Found: 316.01639 (2.0 ppm).

(54) 4-(N-Hexadecylquinolinium-4-ylmethylideneamino)-2,6-dichlorophenolate

$$O^-$$

(structure of 4-(N-Hexadecylquinolinium-4-ylmethylideneamino)-2,6-dichlorophenolate with Cl, Cl on phenolate ring, N=CH imine linkage to quinolinium bearing $C_{16}H_{33}$ on N^+)

The imine (50) (1 g, 3.2 mmol) was stirred with 1-iodohexadecane (1.13 g, 3.2 mmol) and silver-*p*-toluene sulphonate (0.89 g, 3.2 mmol) in dry DMF (30 ml) at 80-100 °C for three days under nitrogen. The reaction mixture was kept in the dark throughout. After cooling the insoluble solid (AgI) was filtered off, and the filtrate was poured into water (containing a small amount of KI) and extracted with dichloromethane (4 x 100 ml). The combined organic layers were washed with water, dried (MgSO₄) and the solvent evaporated in vacuo to leave a green-black solid (crude yield 0.26 g). The betaine was purified by column chromatography (eluting solvent 5:95 MeOH:CH₂Cl₂, then 100% MeOH) to afford a blue-black solid. Yield 0.1g, 6 %.

Phase change 100-110 °C, mp 114-120 °C (decomp.)

^{1}H NMR (CDCl₃): δ 0.87-0.89(t, 3H, CH₃), 1.24-1.67(br m, 24H, aliphatic), 1.89(m, 2H, CH₂), 3.65(m, 2H, CH₂), 4.92(t, 2H, CH₂), 7.12(s, 2H, aromatic), 7.53-8.10(m, 4H, aromatic), 8.74(s, 1H, CH=N), 8.92(d, 2H, aromatic).

MS (FAB) Exact mass calculated for $(M+1)^+$ $C_{32}H_{43}N_2OCl_2$: 541.275245 Found: 541.273823 (2.6 ppm).

(51) N-(4-Quinolinylmethylidene)-4-amino-2,6-dibromophenol
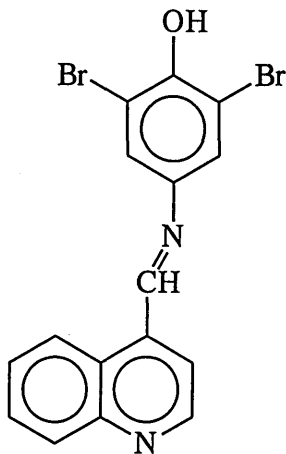
4-Amino-2,6-dibromophenol (2.67 g, 0.01 mol) and quiniline-4-carboxaldehyde (1.62 g, 0.01 mol) were heated under reflux in ethanol (30 ml) for three hours under nitrogen. After cooling slightly the insoluble solid was filtered, washed with ethanol, and then diethyl ether. A yellow-green solid was obtained. Yield 3.80 g, 83 %.

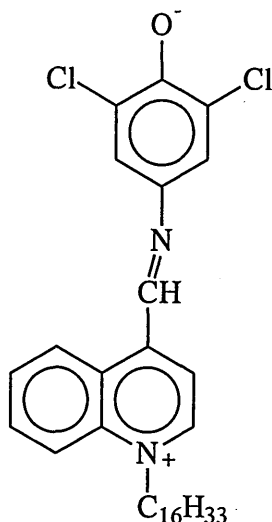mp 248-249 °C

^{1}H NMR (DMSO): δ 7.62-9.10 (m, 8H, aromatic), 9.41 (s, 1H, CH=N).

^{1}H NMR (TFA) δ 7.56(s, 2H, aromatic), 8.11-8.46(m, 4H, aromatic) 9.17-9.28(dd, 2H, aromatic), 10.71(s, 1H, CH=N), 11.1(br s, TFA).

MS (EI) Exact mass calculated for (M$^+$) $C_{16}H_{10}N_2O^{79}Br^{81}Br$: 405.91394 Found: 405.91487 (-2.3 ppm).

(55) 4-(N-Hexadecylquinilinium-4-ylmethylideneamino)-2,6-dibromophenolate
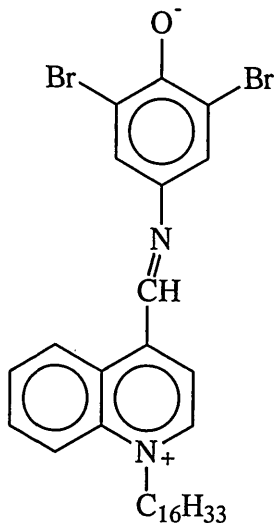
Analogous to the procedure for **(54)**, the imine **(51)** (2 g, 4.9 mmol) was stirred with 1-iodohexadecane (1.73 g, 4.9 mmol) and silver-p-toluene sulphonate (1.37 g, 4.9 mmol) in dry DMF (50 ml) at 80-100 °C for four days, (in the dark). After column chromatography a blue-black solid was obtained. Yield 0.17 g, 6 %.

mp 158-160 °C

^{1}H NMR (CDCl$_3$): δ 0.85-0.87(t, 3H, CH$_3$), 1.13-1.24(br m, 24H, aliphatic), 1.98-2.3(m, 2H, CH$_2$), 3.60(m, 2H, CH$_2$), 4.77(t, 2H, CH$_2$), 7.34(s, 2H, aromatic), 7.34-7.97(m, 4H, aromatic), 8.56(s, 1H, CH=N), 8.82(d, 2H, aromatic).

MS (FAB) Exact mass calculated for $(M+1)^+$ C$_{32}$H$_{43}$N$_2$OBr$_2$: 632.179991 Found: 632.179589 (0.6 ppm).

(60) 1-Bromo-2-bromomethylnaphthalene
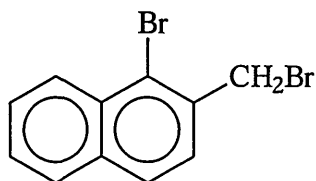
1 Bromo-2-methylnaphthalene (15 g, 0.068 mol) was dissolved in tetrachloromethane (48 ml) with stirring. N-bromosuccinimide (recryst. from water) was added slowly, and a crystal of benzoyl peroxide was added. The mixture was heated under reflux for sixteen hours under nitrogen. Once cooled, the succinimide was filtered off and the filtrate was evaporated in vacuo. The crude solid (7.42 g, 36 %) was used for the next stage without purification.

(61) (1-Bromo-2-naphthylmethyl)hexamethylenetetramine bromide

$$\text{Br}$$

$$CH_2N^+(CH_2)_6N_3 \quad Br^-$$
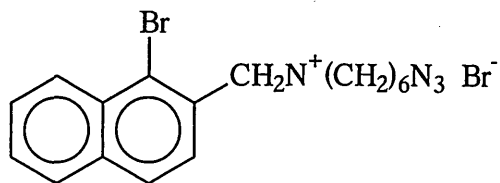
(60) (7.42 g, 0.025 mol) was dissolved in dichloromethane (20 ml) and added dropwise to hexamethylenetetramine (3.50 g, 0.025 mol) in dichloromethane (20 ml). The reaction mixture was heated under reflux for one hour, whereupon a white-cream solid precipitated out. The mixture was cooled, and the solid filtered under suction and washed with petrol. Yield 5.44 g, 56 %.

mp 166-170 °C

MS (FAB) (M^+ cation) 358.7 and 360.7 (base peaks).

(57) 1-Bromo-2-naphthaldehyde

$$\text{Br}$$

$$CHO$$
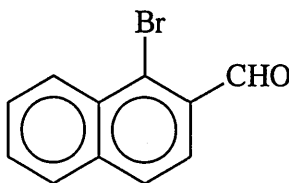
The quaternary hexamine salt (61) (5 g, 0.013 mol) was heated under reflux for two hours with 50 % glacial acetic acid (25 ml). Conc. HCl (10 ml) was then added whereupon the clear pink solution turned milky, and then clear again. After five minutes the solution was cooled, poured into water, and exracted with diethyl ether (3 x 50 ml). The combined ether layers were washed with water and dried ($MgSO_4$). The solvent was evaporated in vacuo to afford a cream solid, which was recrystallised from petrol, and dried under vacuum over petrol. Yield 0.73 g, 24 %.

mp 118-119 °C

^{1}H NMR ($CDCl_3$): δ 7.27-8.51(m, 6H, aromatic), 10.65(s, 1H, CHO).

MS (EI) Exact mass calculated for (M^+) $C_{11}H_7O^{79}Br$: 233.96803 Found: 233.96793 (0.4 ppm).

(65) N(1-Bromo-2-naphthymethylidene)-4-amino-2,6-dichlorophenol
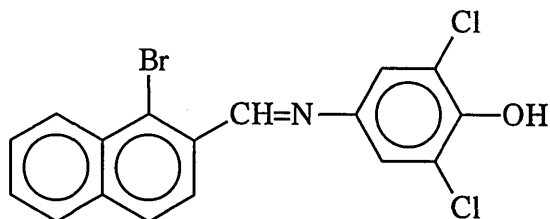
The aldehyde (57) (0.66 g, 2.8 mmol) and 4-amino-2,6-dichlorophenol (0.499 g, 2.8 mmol) were allowed to react under refluxing ethanol (20 ml) for three hours under nitrogen. The ethanol was evaporated in vacuo and the imine purified by reprecipitating the crude solid with petrol from a mixture of dichloromethane and acetone, to afford a beige solid. Yield 0.7 g, 64 %.

mp 205-208 °C

^{1}H NMR ((CD$_3$)$_2$CO): δ 7.46(s, 2H, aromatic), 7.68-8.45(m, 6H, aromatic), 9.22(s, 1H, CH=N).

MS (EI) Exact mass calculated for (M$^+$) C$_{17}$H$_{10}$NO^{35}Cl^{79}Br: 394.92932 Found 394.92815 (3.0 ppm).

(66)N-(1-Triphenylphosphonio-2-naphthylmethylidene)-4-amino-2,6-dichlorophenol bromide
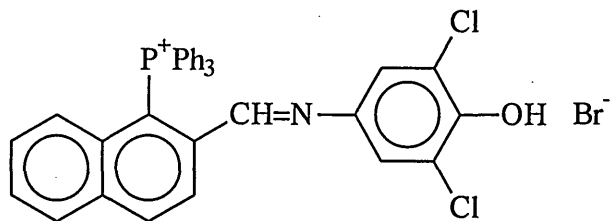
The imine (65) (0.5 g, 1.27 mmol) was heated under reflux in ethanol (12ml) with triphenylphosphine (0.5 g, 1.9 mmol) and NiBr$_2$ (0.14 g, 0.64 mmol) under nitrogen for eight hours. The cooled reaction mixture was poured into aqueous KBr (10 % w/v) and extracted with dichloromethane (3 x 30 ml). The combined organic layers were washed with aqueous KBr (10 % w/v), dried (MgSO$_4$), and the solvent evaporated in vacuo to afford a dark orange solid. The solid was triturated with diethyl ether to remove non-polar impurities. Yield 0.1 g, 12 %.

Phase change 100-120 °C, mp 130-132 °C

^{31}P NMR (CDCl$_3$): 18.15 ppm.

^{1}H NMR (CDCl$_3$): δ 6.44(s, 2H, aromatic), 7.17-8.31(m, 22H, aromatic), 8.52(s, 1H, CH=N).

MS (FAB) Exact mass calculated for (M$^+$ cation) C$_{35}$H$_{25}$PNOCl$_2$^{35}: 576.105084 Found: 576.101906 (5.5 ppm).

(67) N-(1-Triphenylphosphonio-2-naphthylmethylidene)-4-amino-2,6-dichlorophenolate
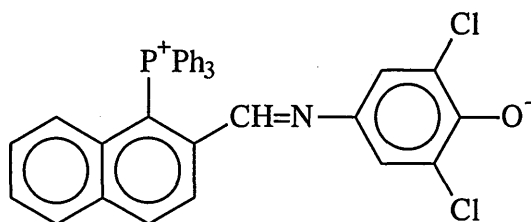
The salt **(66)** was shaken with aqueous sodium hydroxide and dichloromethane to afford a dark red-purple solid. (No yield was recorded as the reaction was carried out on a very small scale).

Phase change 190 °C, mp 205-207 °C

^{31}P NMR (CDCl$_3$): 18.03 ppm.

^{1}H NMR (CDCl$_3$): δ 6.16(s, 2H, aromatic), 7.05-8.3(m, 22H, aromatic and CH=N).

MS (FAB) Exact mass calculated for (M+1)$^+$ C$_{35}$H$_{25}$PNO^{35}Cl$_2$: 576.105084 Found: 576.102032 (5.3 ppm).

(68) 1-Bromo-4-naphthaldehyde
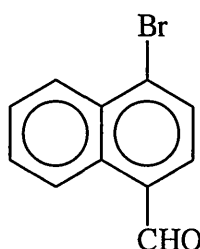
CAN (13.12 g, 0.024 mol) in 50 % acetic acid (200 ml) was added to 1-bromo-4-methyl naphthalene (1.33 g, 6 mmol) in 50 % acetic acid (150 ml) and stirred for two hours at 85 °C. The cooled reaction mixture was poured into water and extracted with dichloromethane (3 x 100 ml) and the combined extracts were washed twice with water (2 x 500 ml). The organic layer was dried (MgSO$_4$) and the solvent was evaporated in

vacuo to leave a brown sticky solid. The aldehyde was isolated pure by column chromatography (eluting solvent 70:30 CH_2Cl_2: Petrol) and was obtained as a white solid. Yield 0.79 g, 56 %.

mp 83-85 °C

^{1}H NMR ($CDCl_3$): δ 7.5-8.39(m, 4H, aromatic), 9.31(d, 1H, aromatic), 9.28(d, 1H, aromatic), 10.37(s, 1H, CHO).

MS (EI) Exact mass calculated for (M^+) $C_{11}H_{20}{}^{79}Br$: 233.96803 Found: 233.96702 (4.3 ppm).

(69) 2-(1-Bromo-4-naphthyl)-1H-phenanthro[9,10-*d*]imidazole
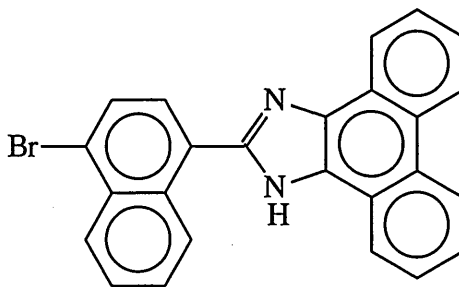
Aldehyde **(68)** (0.28 g, 1.2 mmol) was allowed to react for six hours with 9,10-phenanthraquinone (0.25 g, 1.2 mmol) and ammonium acetate (0.83 g, 10.8 mmol) in refluxing glacial acetic acid (14 ml). The cooled reaction mixture was poured into water (150 ml) where upon a beige solid precipitated out, then ammonia was added to the mixture until just basic. The solid was filtered and washed with plenty of water, and dried under suction. **(69)** was purified by washing with cold petrol to afford a cream-beige solid which was dried under vacuum over toluene. Yield 0.48 g, 94%.

mp > 165 °C

^{1}H NMR ($CDCl_3$): δ 6.68-8.69(m, 14H), 13.0(s, 1H, NH).

MS (EI) Exact mass calculated for (M^+) $C_{25}H_{15}N_2{}^{81}Br$: 424.03983 Found: 424.03784 (4.7 ppm).

(71) 2-(1-Triphenylphosphonio-4-naphthyl)-1H-phenanthro[9,10-*d*]-imidazole bromide
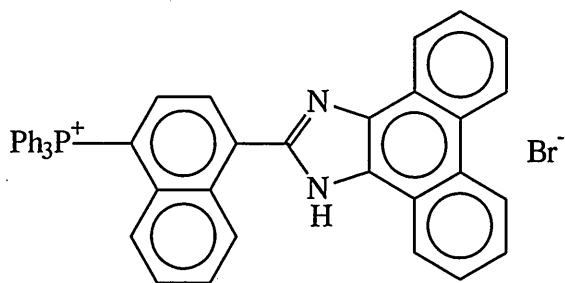
The imidazole **(69)** (0.35 g, 0.83 mmol) was heated under reflux with triphenylphosphine (0.33 g, 0.83 mmol) and $NiBr_2$ (0.09 g, 0.415 mmol) in benzonitrile (10 ml) for five hours under nitrogen. The cooled reaction mixture was poured into aqueous KBr (10 % w/v) and extracted with dichloromethane (3 x 30 ml). The combined organic extracts were washed with KBr (10 % w/v) and dried ($MgSO_4$). The dichloromethane was evaporated in vacuo to leave the benzonitrile solution, which was poured into diethyl ether to precipitate the salt. The salt was triturated several times in fresh portions of diethyl ether and filtered, and was further purified by column chromatography (eluting solvent 5:95 MeOH:CH_2Cl_2, and then 100 % MeOH to remove traces of starting material which could not be removed by trituration with diethyl ether. A bright yellow solid was obtained which was dried under vacuum over ethanol. Yield 0.26 g, 46 %.

mp > 200 °C (decomp.)

^{31}P NMR ($CDCl_3$): 22.09 ppm.

^{1}H NMR ($CDCl_3$): δ 7.26-8.96(m, 25H), 9.36-9.39(d, 2H), 9.66-9.69(d, 2H), 14.34(s, 1H, NH).

MS (FAB) Exact mass calculated for (M^+ cation) $C_{43}H_{30}N_2P$: 605.214663 Found: 605.216593 (-3.2 ppm).

(73) 2-(1-Triphenylphosphonio-4-naphthyl)-1H-phenanthro[9,10-d]-imidazolide
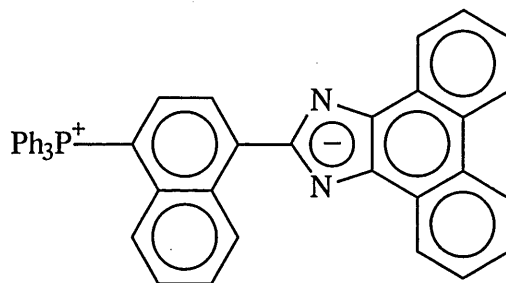
The salt (71) (0.13 g, 0.2 mmol) was shaken with aqueous sodium hydroxide and dichloromethane. The organic layer was dried (MgSO$_4$) and the solvent evaporated in vacuo. The bright red solid was triturated in ether, filtered and dried under vacuum over ethanol. Yield 0.1 g, 83 %.

mp > 180 °C (decomp.)

^{31}P NMR (CDCl$_3$): 21.70 ppm.

^{1}H NMR (CDCl$_3$): δ 7.21-7.84(m, 25H), 8.67-8.71(d, 2H), 8.85-8.88(d, 2H).

MS (FAB) Exact mass calculated for (M+1)$^+$ C$_{43}$H$_{30}$N$_2$P: 605.214663 Found: 605.217591 (-4.8 ppm).

(70) 2-(1-Bromo-4-naphthyl)-4,5-diphenylimidazole
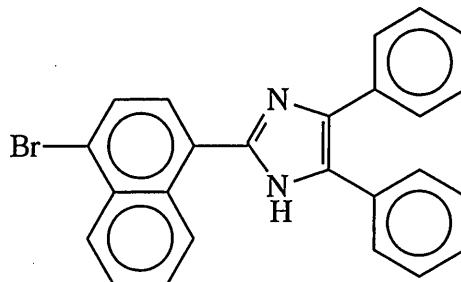
Aldehyde (68) (0.1 g, 0.43 mmol) was heated under reflux with benzil (0.09 g, 0.43 mmol) and ammonium acetate (0.3 g, 3.9 mmol) in glacial acetic acid (5 ml) for six hours. The cooled reaction mixture was poured into water (80 ml) where a cream solid precipitated out. The mixture was made just alkali with ammonia and the solid filtered washing with lots of water. The solid was recrystallised from dichloromethane to give a cream solid. Yield 0.12 g, 67 %.

mp 261-264 °C

^{1}H NMR ((CD$_3$)$_2$CO): δ 7.25-7.75(m, 10H), 8.29-8.33(d, 2H), 9.45-9.49(d, 2H), 11.91(s, 1H, NH).

MS (EI) Exact mass calculated for (M$^+$) C$_{25}$H$_{17}$N$_2$^{79}Br: 424.05750 Found: 424.05541 (4.9 ppm).

142

(73) 2-(1-Triphenylphosphonio-4-naphthyl)-4,5-diphenylimidazole bromide
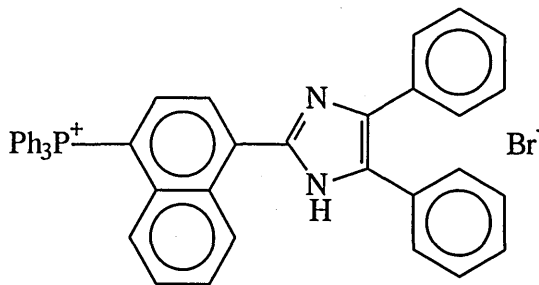
Analogous to the procedure for **(71)** imidazole **(70)** (0.155 g, 0.37 mmol) was heated under reflux with triphenylphosphine (0.146 g, 0.56 mmol) and $NiBr_2$ (0.040 g, 0.19 mmol) in benzonitrile (4 ml) for four hours under nitrogen. A bright yellow solid was obtained after trituration in diethyl ether, which was dried under vacuum over ethanol. Yield 0.063 g, 25 %.

mp > 195 °C

^{31}P NMR (CDCl$_3$): 22.14 ppm

^{1}H NMR (CDCl$_3$): δ 7.24-8.59(m, 31H), 13.1(s, 1H, NH).

MS (FAB) Exact mass calculated for (M$^+$ cation) C$_{43}$H$_{32}$N$_2$P: 607.230313 Found: 607.231308 (-1.6 ppm).

(74) 4-(1-Triphenylphosphonio-4-naphthyl)-4,5-diphenylimidazolide
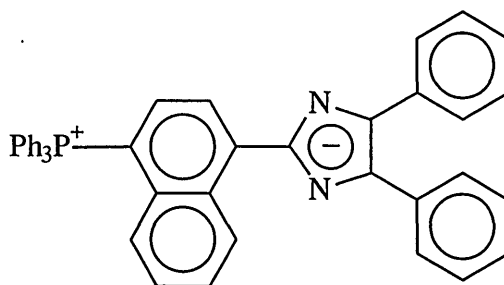
Analogous to the procedure for **(73)**, a bright orange solid was obtained. Yield 0.024 g, 86 %.

mp > 285 °C (decomp.)

^{31}P NMR (CDCl$_3$): 21.5 ppm.

^{1}H NMR (CDCl$_3$): δ 7.25-7.86(m, 31H).

MS (FAB) Exact mass calculated for (M+1)$^+$ C$_{43}$H$_{32}$N$_2$P: 607.230313 Found: 607.230149 (0.3 ppm).

143

References

1. D. W. Allen, J. Hawkrigg, H. Adams, B. F. Taylor, D. E. Hibbs and M. B. Hursthouse, *J. Chem. Soc., Perkin Trans. 1*, 1998, 335.

2 D. W. Allen and X. Li, *J. Chem. Soc., Perkin Trans. 2*, 1997, 1099.

3. K. C. Ching, M. Lequan, R.-M. Lequan, A. Grisard and D. Markouitsi, *J. Chem. Soc., Faraday Trans.*, 87, 1991, 2225.

4. C. Combellas, H. Marzouk, C. Suba and A. Thiebault, *Synthesis*, 1993, 788.

5. C. Lambert, E. Schmälzlin, K. Meerholz and C. Bräuchle, *Chem. Eur. Journal*, 4(3), 1998, 512.

6. D. G. Gilheany, *Chem. Rev.*, 94, 1994, 1339.

7. C. Lambert, S. Stadler, G. Bournhill and C. Bräuchle, *Angew. Chem., Int. Ed. Engl.*, 35, 1996, 644.

8. G. J. Ashwell, K Sjonnemand, M. P. S. Roberts, D. W. Allen and X. Li, Colloids and Surfaces A: Physicochem. Eng. Aspects, in press.

9. E. Alcade, J. Denares, J. Frigola, J. Ruis and C. Mirauitlles, *J. Chem. Soc., Chem. Commn.*, 1989, 1086.

10. D. T. Davies, *Aromatic Heterocyclic Chemistry*, Oxford Science Publications, Chapter 3, 1991.

11. Y. Hirusawa, M. Oku and R. Yamamoto, *Bull. Chem. Soc. Japan*, 30, 1957, 667.

12. (a) L. Horner, G. Mummenthey, H. Moser and P. Beck, *Chem. Ber.*, 99, 1966, 2782.

    (b) L. Horner and U. M. Duda, *Tetrahedron Letters*, 1970, 5177.

13. Industrial Patent: 128: 48368q *Preparation of Tetraarylphosphonium Halides*, Harada, Katsumasa, Kasiwagi, Koichi, Suginose, Ryoji, Doi, Takashi, (Ube Industries, Japan), 1997.

14. D. W. Allen and P. Benke, *J. Chem. Soc., Perkin Trans. 1*, 1995, 2789.

15. E. M. Kosower, J. Am. Chem. Soc., 80, 1958, 3253.

16. (a) C. Reichardt, *Solvent and Solvent Effects in Organic Chemistry*, 2nd Revised and Enlarged Edition, Weinheim, 1988. (b) C. Reichardt, Chem. Rev., 94, 1994, 2319.

17. M. Kjaer and J. Ulstrup, *J. Am. Chem. Soc.*, 109, 1987, 1934.

18. M. A. Kessler and O. S. Wolfbeis, *Synthesis*, 1988, 635.

19. D. W. Allen, I. W. Nowell and L. A. March, *Tetrahedron Letters*, 23(51), 1982, 5479.

20. D. W. Allen, I. W. Nowell and L. A. March, *J. Chem. Soc., Perkin Trans. 1*, 1984, 2523.

21. D. W. Allen, P. E. Cropper and P. G. Smithhurst, *J. Chem. Soc., Perkin Trans. 1*, 1986, 1989.

22. D. W. Allen, P. E. Cropper and I. W. Nowell, *Polyhedron*, 8(8), 1989, 1039.

23. D. W. Allen and P. E. Cropper, *Polyhedron*, 9(1), 1990, 129.

24. D. W. Allen and P. E. Cropper, *Journal of Organometallic Chemistry*, **435**, 1992, 203.

25. N. Hall and R. Price, *J. Chem. Soc., Perkin Trans. 1*. 1979, 2634.

26. N. Hall and R. Price, *J. Chem. Soc., Perkin Trans. 1*, 1979, 2873.

27. J. A. Connor, D. Dubowski, A. C. Jones and R. Price, *J. Chem. Soc., Perkin Trans. 1*, 1982, 1143.

28. M. Chanon and M. L. Tobe, *Angew. Chem., Int. Ed. Engl.*, **21**, 1982, 1.

29. Escoula, N. Hajjaji, I. Rico and A. Lattes, *J. Chem. Soc., Chem. Commun.*, 1984, 1233.

30. (a) Machado, M. de G. Nascimento and M. C. Rezende, *J. Chem. Soc., Perkin Trans. 2*, 1994, 2539.

    (b) J. Catalán, E. Mena, W. Meutermans and J. Elguero, *J. Phys. Chem.*, **96**, 1992, 3615.

    (c) V. Luzhkov and A. Warshel, *J. Am. Chem. Soc.*, **113**, 1991, 4491.

    (d) I. Gruda and F. Bolduc, *J. Org. Chem.*, **49**(18), 1984, 3300.

31. X. Li, *New Solvatochromic and Halochromic Phosphonium Betaine Dyes*, A thesis submitted in partial fulfilment of requirements of Sheffield Hallam University for the degree of Master of Philosophy, March 1997.

32. L. K. Sydnes, I. C. Burkow and S. H. Hansen, *Tetrahedron*, 41(23), 5703, 1985.

33. B. S. Furniss, A. J. Hannaford, P. W. G. Smith and A. R. Tatchell, *Vogels Textbook of Practical Organic Chemistry*, 5th Ed., Longman Scientific and Technical, 1989, 1003.

CHAPTER 3

The Synthesis of Solvatochromic

Aryl-arsonium and –stibonium

Iminophenolate Betaines

3.0 Introduction

This chapter describes the novel copper (I) catalysed template synthesis of a series of aryl-arsonium and -stibonium salts **(1)** and their respective betaines **(2)**. Their solvatochromic properties are reported, and compared with the corresponding triphenylphosphonium analogues.[1] It is thought that these are the first solvatochromic arsonium and stibonium betaine systems to be reported in the literature.

$$E = Sb \text{ or } As$$
$$X = Cl, Br, Ph$$
$$Z^- = I^- \text{ or } CuI_2^-$$

(1)   **(2)**
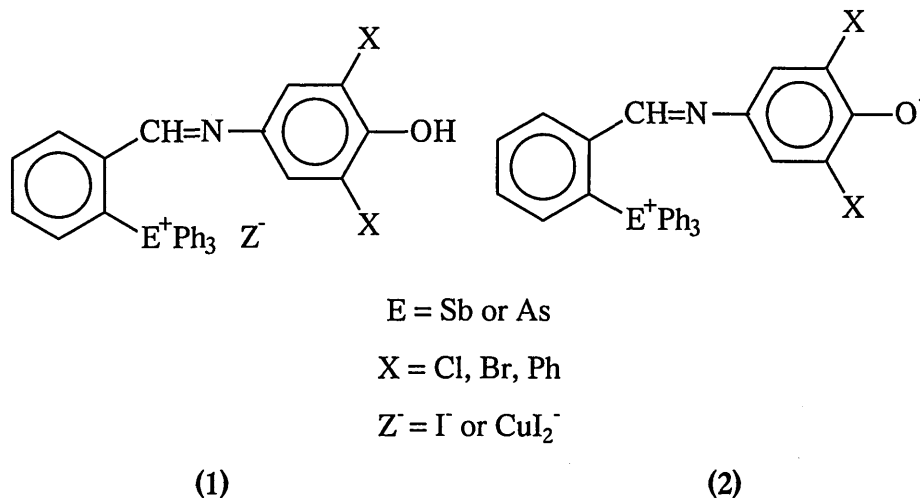
Additionally, the salts **(3)** and **(4)** were synthesised by the reaction of the corresponding aryl halide with triphenyl-stibine and -arsine or tri-*p*-tolyl-stibine and -arsine, although there was no possibility of a related betaine, unlike salts **(1)**. The nature of the anion Z^- for salts **(1-4)** will be discussed later.

$$X = H$$
$$Ar = Ph, p\text{-tolyl}$$
$$E = As, Sb$$

(3)

$$Ar = Ph, p\text{-tolyl}$$
$$E = Sb$$

(4)
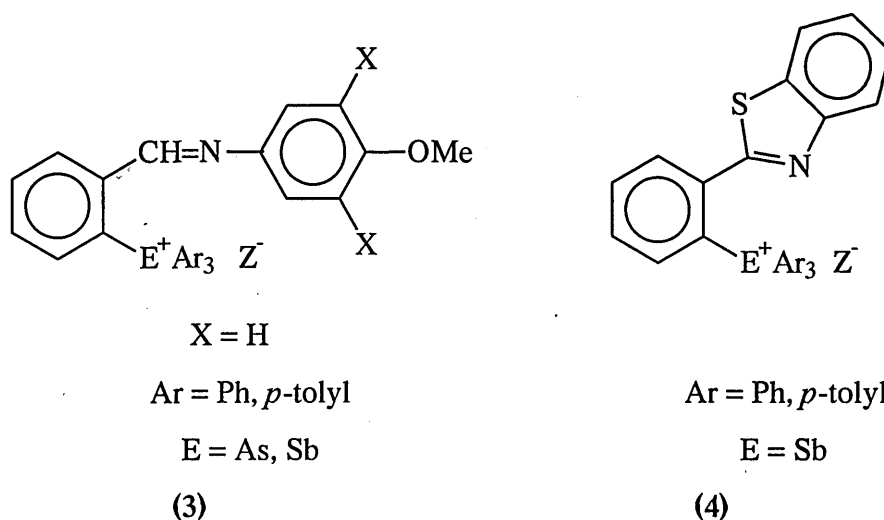
Methods for the synthesis of aryl-arsonium and -stibonium salts from the reaction of aryl halides with tertiary arsines or stibines are rather limited. The usual conditions require the reactants to be heated together at >200 °C in the presence of aluminium chloride,[2] and this method has only been used to prepare simple tetra-arylarsonium and −stibonium salts, lacking other functional groups. As discussed in chapter 2, it has been shown that tertiary phosphines react with aryl halides bearing appropriate donor atoms in the *ortho* position to the halogen in the presence of catalytic quantities of nickel (II) or copper (II) compounds under mild conditions in refluxing ethanol.[3-5] However triaryl-arsonium and −stibonium salts are not formed by the reaction of triphenylarsine or triphenylantimony with aryl halides under the same conditions.[3]

As triarylarsines and -stibines co-ordinate readily to copper (I) halides to form complexes which are labile in solution,[6-8] the reactions of template aryl halides in the presence of copper (I) iodide in acetonitrile were investigated, and the corresponding stibonium and arsonium salts were formed in reasonable yield.

Attempts to prepare the related phosphonium salts using one mole equivalent of copper (I) iodide as the catalyst in acetonitrile were unsuccessful. Clearly the group 15 ligand must influence the crucial stages of the reaction for which the mechanism is uncertain. However, it is likely that a similar mechanism to the nickel (II) catalysed template phosphonium salt formation reaction applies in this case, perhaps involving a copper (I)-copper (III) redox cycle, in which the triaryl-stibine and −arsine ligands are able to stabilise the intermediate organometallic species more effectively than the related triarylphosphines. Salt-formation was not observed in the related reactions of the template aryl halides with triphenylbismuth using copper (I) iodide as the catalyst in acetonitrile. Arsonium, stibonium, and bismuthonium salts were not formed when these reactions were conducted in ethanol using a nickel (II) catalyst.

The reactions of triphenylstibine with the non-template aryl halides *p*-bromoanisole and *p*-bromotoluene were investigated using copper (I) iodide as the catalyst, but no salt was formed, using acetonitrile or benzonitrile as the solvent. Nickel (II) bromide was also employed as the catalyst in both solvents, but with no success. This indicates that the synthesis of the above aryl-stibonium and -arsonium salts (1, 3 and 4) using copper (I) iodide as the catalyst proceeds via a kinetic template effect involving a suitable donor atom in the *ortho* position to the halogen replaced.

3.1 Synthesis of the aryl halides.

The imine intermediates (5) were prepared as previously described in chapter 2.[1] The aryl halide (6) was provided by Prof. D.W. Allen.

3.2 Synthesis of the salts.

The reaction of the template aryl halides with triphenyl- or tri-*p*-tolyl-arsine, or triphenyl- or tri-*p*-tolyl-stibine and copper (I) iodide in refluxing acetonitrile (scheme 1) gave the corresponding salts in a reasonable yield. The triarylstibonium salts were obtained in a higher yield compared to the triarylarsonium salts, which required a longer reaction time. The triarylstibonium and –arsonium salts were obtained as yellow-pale orange solids.

(5)

X = Cl, Br, Ph; Y = OH, Me;

(1)

X = Cl, Br, Ph; E = Sb, As;

Y = OH; Ar = Ph, *p*-tolyl

(3)

X = H; E = Sb, As;

Y = OMe; Ar = Ph, *p*-tolyl

or

(6)

(4)

E = Sb, Ar = Ph, *p*-tolyl
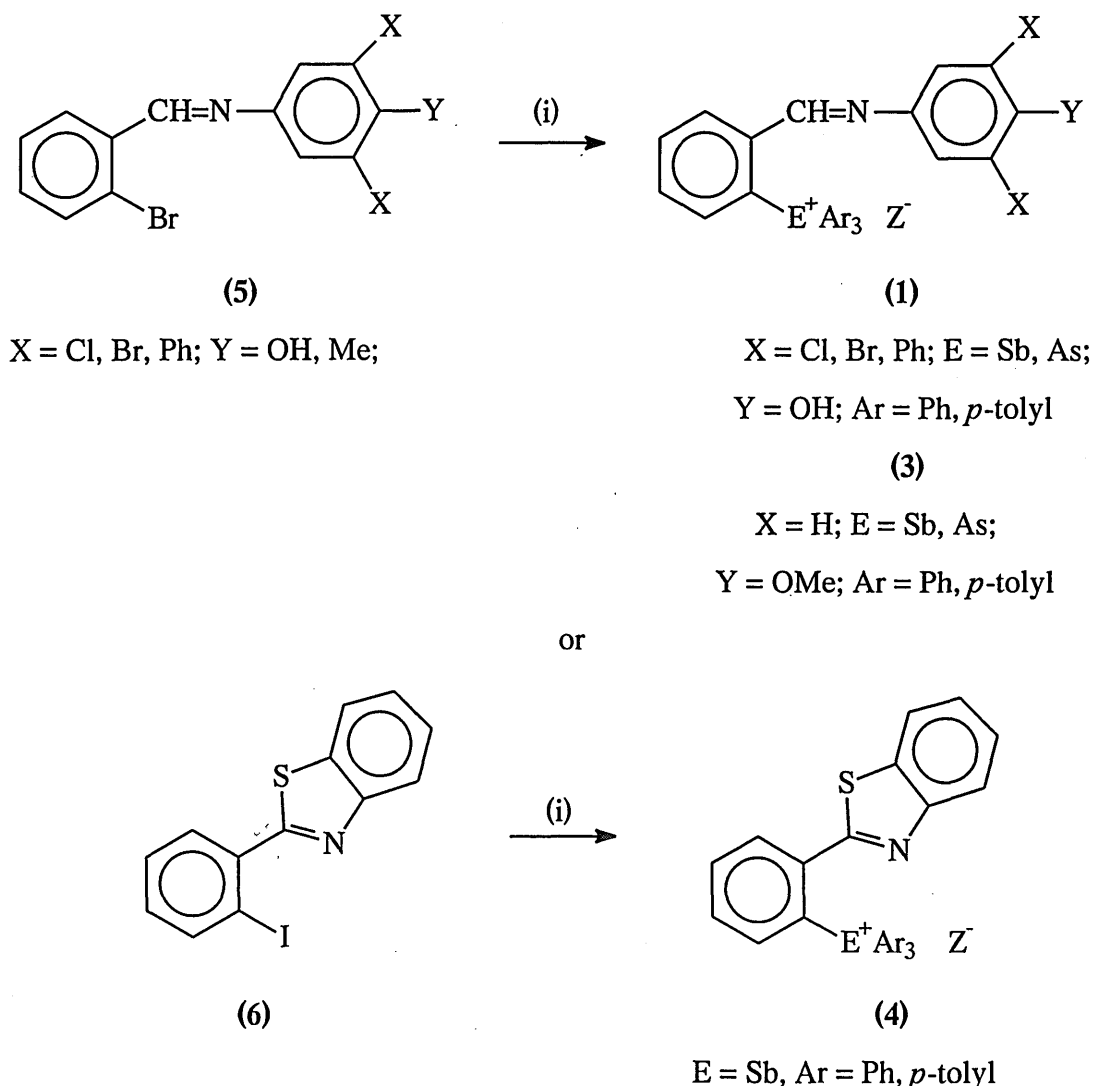
(i) Ph_3As, tri-*p*-tolylarsine, Ph_3Sb, tri-*p*-tolylstibine, CuI, MeCN, reflux, N_2

Scheme 1

149

3.3 Synthesis of the betaines.

Unlike the triphenylphosphonium analogues,[1] and the long chain phosphonium analogues discussed in chapter 2, only a small amount of the betaine (2) was obtained by the treatment of the salts (1) (E = As, Sb) with an excess of potassium carbonate in acetonitrile or dichloromethane at room temperature, and mostly salt (1) was recovered (except E = Sb; X = Cl, Br where 100 % conversion to the betaine was observed). However, the betaines (2) (E = As, Sb; X = Cl, Br) were obtained in good yield as orange-red solids and (E = As, Sb; X = Ph) were obtained as purple solids, by treatment of the corresponding salts with aqueous sodium hydroxide followed by solvent extraction into dichloromethane (scheme 2).

$$E = Sb, As; X = Cl, Br, Ph$$
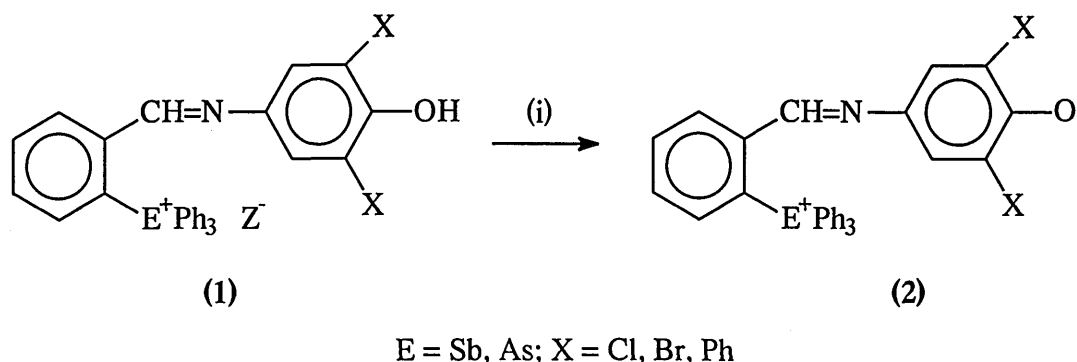
(i) NaOH (aq), CH_2Cl_2 or K_2CO_3, MeCN

Scheme 2

3.4 Characterisation of the salts and betaines.

The salts and betaines gave characteristic ^1H NMR spectra. As with the phosphonium analogues (1) (E = Ph)[1] the CH=N proton became shielded on going from the salt (1) (E = As or Sb) to the betaine (2) (E = As or Sb). In table 1 it is seen that the CH=N proton of the stibonium betaines was shielded slightly more (0.67-0.90 ppm) than that of the arsonium betaines (0.43-0.63 ppm) compared to the parent salts (1). Unlike the phosphonium analogues the CH=N proton of the arsonium and stibonium analogues was not hidden by the aromatic proton envelope in the spectra of the betaines and the salts.

The CH=N proton becomes less shielded on going from the phosphonium salts and betaines to the stibonium salts and betaines.

150

'onium centre	X = Cl	X = Br	X = Ph
*(1) E = P [1]	8.50	Hidden in aromatic envelope (7.0-8.7)	8.70
(2) E = P [1]	Hidden in aromatic envelope (7.0-8.8)	Hidden in aromatic envelope (7.0-8.6)	Hidden in aromatic envelope (7.0-8.5)
(1) E = As	8.70	8.79	8.69
(2) E = As	8.12	8.16	8.26
(1) E = Sb	9.41	9.41	9.36
(2) E = Sb	8.51	8.74	8.64

* perchlorate salt

Table 1: CH=N proton shifts (ppm) for salts (1) and betaines (2) in CDCl₃.

Under FAB MS conditions the arsonium and stibonium salts (1) (3) and (4) gave characteristic molecular cations and the betaines (2) gave characteristic (molecular ions + 1). All accurate mass measurements were within a ± 10 ppm limit.

In the synthesis of the salts, even though bromine was being replaced by the arsonium or stibonium moiety, it was presumed that the anion present would be iodide, due to the use of copper (I) iodide as the catalyst, and the use of aqueous potassium iodide in the workup procedure. However, although the crystal structure of salt (3) (E = As; Ar = Ph) showed the anion to be iodide, the full crystal structure of (1), (E = Sb; X = Br; Ar = Ph) showed the anion to be di-iodocuprate (CuI₂⁻). The crystal structures are presented and discussed further in section 3.5.

The nature of the anion in the salts (1), (3) and (4) was also confirmed by negative ion mass spectrometry. The salts (1) gave a molecular ion at m/z 317 for the di-iodocuprate anion and a peak at m/z 127 for iodide anion in EI mode. It is unknown whether the mass at m/z 127 is due to fragmentation of the di-iodocuprate anion or whether the salts contain the iodide anion as well as the di-iodocuprate anion. Salts (3) and (4) also gave molecular anions at m/z 127 and m/z 317 as with salts (1) but only under FAB conditions. For all the salts, m/z 127 had a higher abundance (100 %) compared to m/z 317 (ca. 10-20 %).

The presence of copper in the salts was also confirmed by ICP analysis (table 2), and the experimental values correlate well with the theoretical values for salts (3) and (4) assuming the anion is 100 % CuI_2^-. For salts (1) the results are not so good and are lower than the expected value (apart from [E = As, X = Cl]); this may be because there is a mixture of anions present (I$^-$ and CuI_2^-).

	Experimental (% Cu)	Theoretical (% Cu)
(1) E = Sb X = Cl	5.7	6.79
(1) E = Sb X = Br	4.0	6.20
(1) E = Sb X = Ph	4.5	6.24
(1) E = As X = Cl	8.7	7.15
(1) E = As X = Br	3.2	6.50
(1) E = As X = Ph	5.6	6.54
(3) E = Sb Ar = Ph	7.0	7.22
(3) E = Sb Ar = p-tolyl	6.9	6.89
(3) E = As Ar = Ph	_*	_*
(4) E = Sb Ar = Ph	7.8	7.32
(4) E = Sb Ar = p-tolyl	6.4	6.98

* no sample available for analysis

Table 2 Percentage copper content in the arsonium and stibonium salts.

3.5 Structural studies.

A full X-ray structure has been made of the arsonium salt (3) (E = As; Ar = Ph, X = H). The observed structure is shown in figure 1 and the selected bond lengths and angles are shown in table 3. A significant point of interest is the distance between the imino nitrogen and the arsonium centre. The arsenic-nitrogen distance is 2.77 Å, lying well within the sum of the van der Waal's radii (3.40 Å),[9] this leading to distortion of the bond angles at the arsenic from an idealised tetrahedral angle towards a five coordinate arrangement consistent with an intramolecular coordinative interaction from nitrogen to arsenic to form a five membered ring.

152

Although there does not appear to be any structural data in the literature for comparison with the substituted *o*-phenylarsonium salt, a similar intramolecular coordinative interaction (albeit forming a four membered ring) has been observed in triphenylarsonium(phenylsulphonyl)methylide **(7)** and triphenylarsonium 4,4-dimethyl-2,6-dioxocyclohexylylide **(8)**.[10]
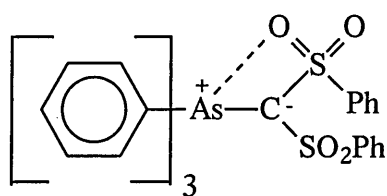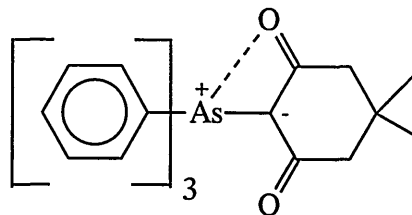
(7)   **(8)**

For both **(7)** and **(8)** the arsenic-oxygen distance was 2.881 Å, significantly less than the sum of the van der Waal's radii (3.4 Å).

Figure 1   Crystal structure for the arsonium salt **(3)** (E = As; X = H).

	Bond Angles (degrees)
C1-As-C7	103.7(3)
C1-As-C13	105.2(3)
C1-As-C19	107.1(3)
C7-As-C13	118.0(2)

C7-As-C19	113.1(3)
C13-As-C19	108.7(3)
C19-C24-C25	123.7(6)
N1-C25-C24	119.6(6)
	Bond Lengths (Å)
As-N1	2.77
As-C1	1.924(7)
As-C7	1.902(6)
As-C13	1.925(7)
As-C19	1.925(6)
C25-N1	1.276(7)

Table 3 Selected bond lengths and bond angles for the arsonium salt (3).
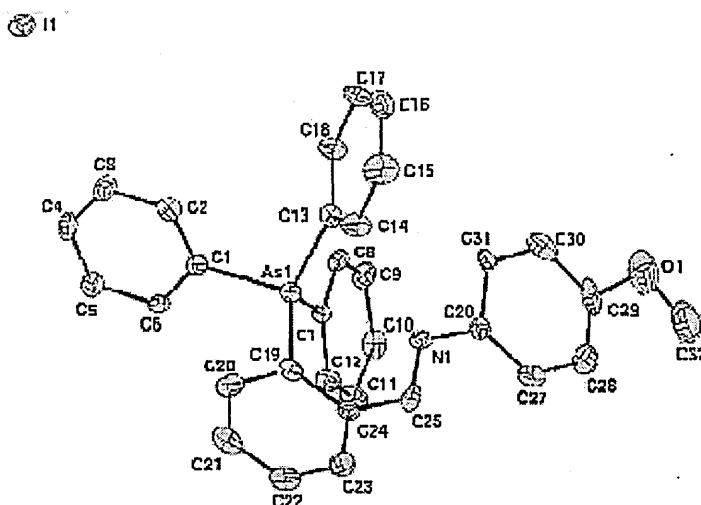
A full synchotron structural study of the stibonium salt (1) (E = Sb; X = Br) was carried out as the crystals were too small for the usual rotating anode X-ray source, and insufficient intensity was produced to give a fully refineable structure. Data were collected upon a crystal of dimensions 200x20x20 µm, using station 9.8 of the Daresbury Synchotron Radiation Source (SRS).[11] The structure of the stibonium salt cation is shown in figure 2 and the selected bond angles and bond lengths are given in table 4. As with the arsonium salt previously discussed, the 'onium centre is shown to have a strong interaction with the imino nitrogen, and the antimony–nitrogen distance is 2.65 Å, slightly shorter than the arsenic-nitrogen distance (2.77 Å), and lying well within the sum of·the van der Waals radii (3.75 Å).[9] Consequently there is distortion of the bond angles at antimony from the idealised tetrahedral angle towards a five-coordinate arrangement, consistent with an intramolecular coordinative interaction from nitrogen to antimony to form a five membered ring.

A search in the literature shows no comparable intramolecularly coordinated five coordinate stibonium salts; however the structures of Me_4Sb^+ I^- [12] and Ph_4Sb^+ Cl^- [13] also show considerable distortion from idealised tetrahedral geometry as a result of the approach of the anion to the 'onium centre. It appears that the coordination sphere of the

stibonium ion is susceptible to distortion, which may allow weak interactions at a fifth coordination site. However in these cases the antimony-halide bond length is relatively long.

As with the arsonium salt (3) there does not appear to be any structural data for comparison for the interaction between antimony and nitrogen. However, the analogous stibonium counterparts of ylides (7) and (8)[10] have been reported and shown to have a similarly short antimony-oxygen distance of 2.844 Å for (7), and 2.835 Å for (8), again significantly less than that of the sum of the van der Waal's radii (3.6 Å).

An important point to note is that the antimony-oxygen distance is shorter than the arsenic-oxygen distance in these compounds, despite the greater atomic radius of antimony, indicating a much stronger interaction for the stibonium ylides compared to the arsonium ylides. This effect is also seen for the arsonium (3) and stibonium salt (1) where the antimony-nitrogen distance is shorter than the arsenic-nitrogen distance. A comparison of the interaction of the arsonium and stibonium centres with the imino nitrogen cannot be compared to the phosphonium centre with the imino nitrogen as crystal structures of the analogous phosphonium salts have not been obtained to date.

The structure co-crystallises with a 50 % occupied CH_2Cl_2 and the presence of a di-iodocuprate (I) anion is also observed (fig. 3) which interacts with a second di-iodocuprate anion via a short copper-copper interaction (2.73 Å) to give a dinuclear anion. The selected bond lengths and angles are shown in table 5.

Since the early 1980's there have been many reports in the literature concerning $[Cu_2I_4]^{2-}$ anions with varying cations, such as $[N(C_4H_9)_4]_2$ $[Cu_2I_4]^{(14)}$ and $[As(C_6H_5)_4]_2$ $[Cu_2I_4]$.[15] In the bis-tetrabutylammonium compound the $(Cu_2I_4)^{2-}$ dimer is centrosymmetric and planar, in which the copper (I) has approximately trigonal planar coordination; however in the bis-tetraphenylarsonium compound, the dimer was neither centrosymmetric nor planar.

Comparing the above bis-arsonium salt anion[15] with the anion of the stibonium salt (1) (E = Sb; X = Br, Z = CuI_2^-), the copper-copper distance is 2.66 Å compared to the slightly longer 2.73 Å for (1); the corresponding distance in $[N(C_4H_9)_4]_2$ $[Cu_2I_4]^{(14)}$ is 2.73 Å.

The only related stibonium salt involving a dimeric copper-containing anion is that of $[Sb(C_6H_5)_4]_2$ $[Cu_2Cl_6]$;[16] however the copper-copper separation in this copper

(II) structure is much greater (3.39 Å) than that in the di-iodocuprate (I) counter ion of the stibonium salt (1).

In the above and related salts,[14,15] if iodine is replaced by chlorine or bromine, the anion tends to be the linear monomeric $[CuX_2]^-$. The coordination number of copper in halogenocuprate (I) anions is found to vary immensely,[17,18] as is also found for the coordination number of silver in related halogenoargenate (I) anions.[17] The structure of the polyhalocuprate anions $[Cu_mX_n]^{(n-m)-}$ is strongly dependent on the nature of the cation, and the coordination number of copper ranges from two as already observed for the discrete linear anion $[MX_2]^-$ to as high as thirty six for the polyanion $[C_{36}I_{56}]^{20}$.[19] Previous structural studies on dihalocuprates (I)[14,20,21] $[CuX_2]^-$ and related anions[22-24] appear to indicate that the tendency of the anion to catenation increases in the order of $X = Cl = Br < I < CN$, and that the formation of discrete anions rather than polymeric anions in the solid state is favoured by the presence of large cations with low well screened charge.

Although monomeric $[CuI_2]^-$ has been shown to exist in solution[25-27] there does not yet appear to be any conclusive evidence for the existence of a discrete monomeric $[CuI_2]^-$ ion in the solid state.
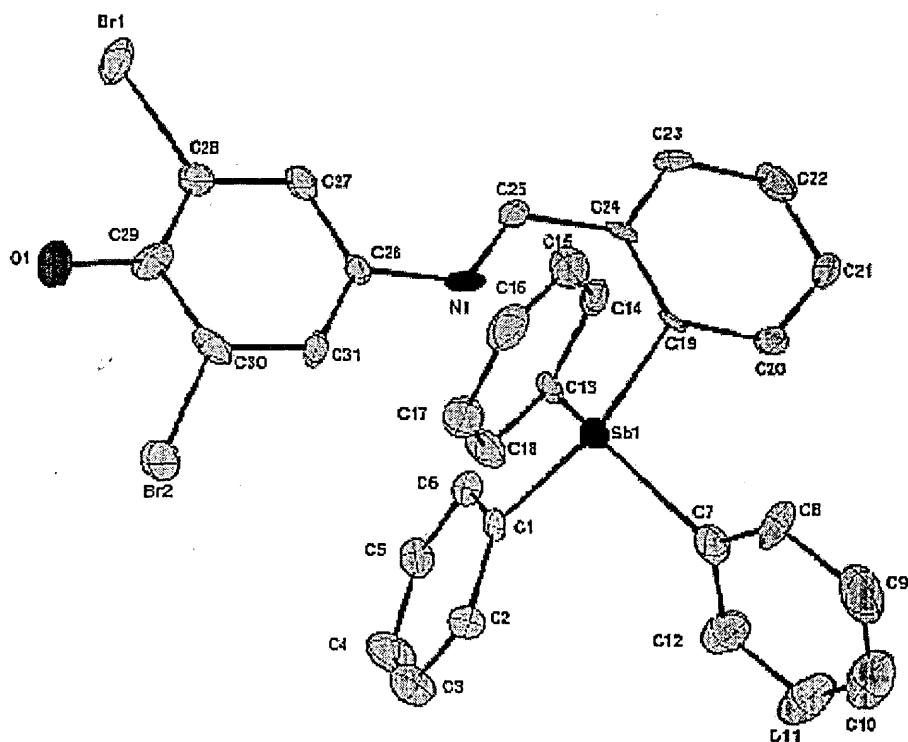
Figure 2 Crystal structure for salt (1) (E = Sb; X = Br) cation.

156

	Bond Angles (degrees)
C1-Sb-C7	106.7(7)
C1-Sb-C13	119.2(6)
C1-Sb-C19	113.6(6)
C7-Sb-C13	102.0(7)
C7-Sb-C19	101.4(6)
C13-Sb-C19	115.9(6)
C19-C24-C25	121.2(14)
N1-C25-C24	118.9(13)
N1-Sb-C1	83.9(7)
	Bond Lengths (Å)
Sb-N1	2.65(4)
Sb-C1	2.09(2)
Sb-C7	2.13(2)
Sb-C13	2.13(2)
Sb-C19	2.114(14)
C25-N1	1.28(2)

Table 4 Selected bond angles and bond lengths for the stibonium salt cation (**1**).
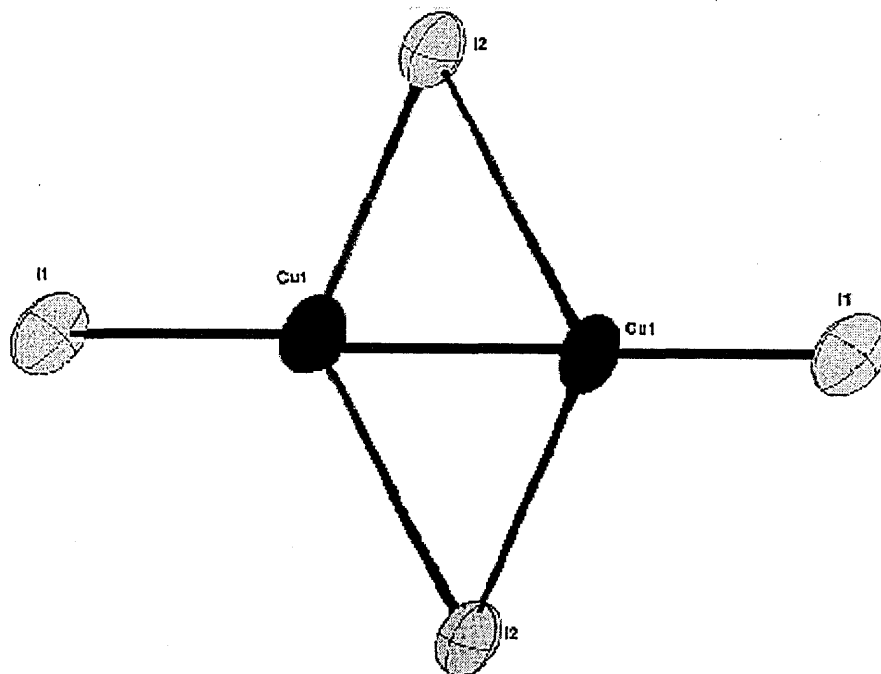
Figure 3 Crystal structure for salt (1) (E = Sb, X = Br) anion.

	Bond Lengths (Å)
Cu1-I1	2.508(2)
Cu1-I2	2.576(2)
Cu-Cu	2.732(4)

Table 5 Selected bond lengths for the stibonium salt (1) (E = Sb; X = Br) anion.

3.6 Solvatochromism studies.

The UV/Visible absorption spectra were recorded on a UNICAM UV_2-100 spectrophotometer, using a pair of matched 1 cm quartz cells. The spectra were recorded at room temperature and pressure using spectroscopic grade solvents (Aldrich) at concentrations of *ca.* 1×10^{-4} mol l^{-1}.

The solvatochromic behaviour of the arsonium and stibonium betaines (2) (E = Sb, As; X = Cl, Br, Ph) is almost identical to that of the related phosphonium betaines (E = P; X = Cl, Br, Ph). Negative solvatochromism is observed, in which the wavelength (λ_{max}) of the charge-transfer band of the betaines occurs at approximately the same wavelength as for the related phosphonium betaines. Negative solvatochromism reflects the stabilisation in the more polar solvents of the ground state

158

dipolar betaine form (9A) relative to the less polar excited state (9B). Furthermore this shows that the positive arsonium and stibonium centres are as efficient electron acceptors as the positive phosphonium centre in the related betaines. This again suggests that d-orbital involvement of the group 15 heteroatom is minimal, as one would have expected that it would have diminished from phosphorus (3d) to arsenic (4d) to antimony (5d), as the size and energy of the d orbitals increases. The UV/Visible absorption data of the salts is shown in table 6, and that of the betaines in table 7.

(9A)

(9B)
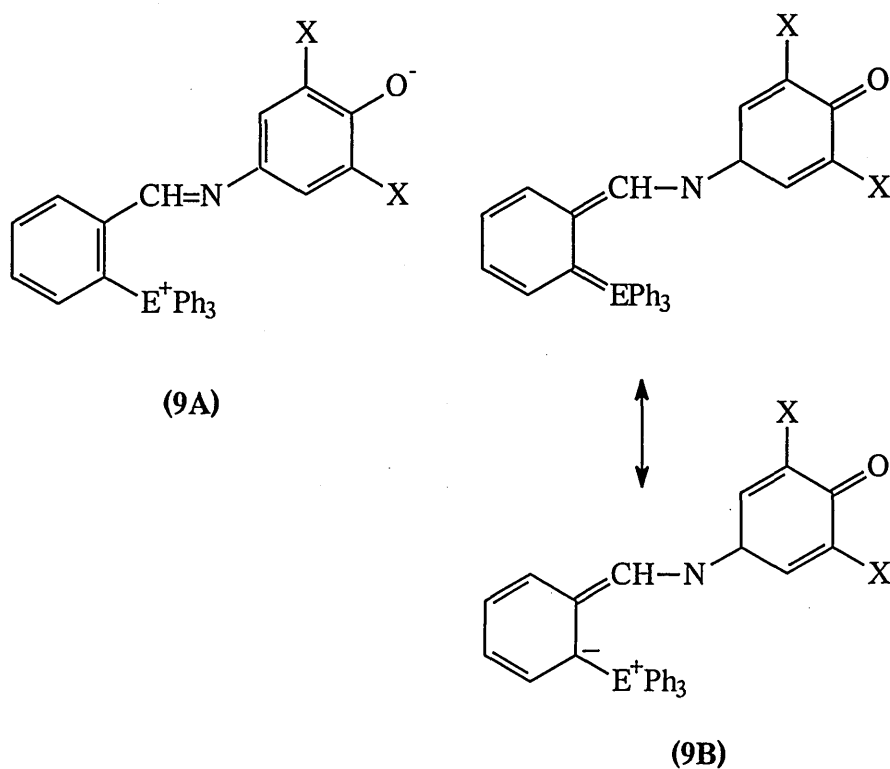
E = As or Sb

	λ_{max}/nm		λ_{max}/nm		λ_{max}/nm	
	X = Cl		X = Br		X = Ph	
Solvent	E = Sb	E = As	E = Sb	E = As	E = Sb	E = As
Methanol	360	360	354	354	376	370
Acetonitrile	348	350	348	350	370	366
Acetone	350	354	352	354	370	370
Dichloromethane	358	356	354	356	380	376
Tetrahydrofuran	294 / 364	294 / 366	294 / 364	294 / 364	294 / 370	294 / 368
Ethyl acetate	354	342	348	352	370	368

Table 6   Long-wavelength UV/Visible absorption maxima of the arsonium and stibonium-iminophenolate salts (1).

|	λ_{max}/nm		λ_{max}/nm		λ_{max}/nm	
	X = Cl		X = Br		X = Ph	
Solvent	E = Sb	E = As	E = Sb	E = As	E = Sb	E = As
Methanol	452	440	452	442	370[#]	370[#]
Acetonitrile	508	494	506	498	556	552
Acetone	538	524	534	524	590	586
Dichloromethane	536	520	534	522	578	576
Tetrahydrofuran	576	562	572	564	624	620
Ethyl acetate	570	558	566	558	620	618
Δ (THF-MeOH)	124	122	120	122	68*	68*

* = Δ (THF-MeCN)   # = salt

Table 7   Long-wavelength UV/Visible absorption maxima of the arsonium and stibonium-iminophenolate betaine dyes (2).

It is seen that the arsonium betaines absorb at a slightly shorter wavelength compared to the stibonium betaines (and the related phosphonium betaines). For both the arsonium and stibonium betaines (X = Ph), the spectra of the related salt was observed in methanol. This behaviour was not seen for the phosphonium betaine (X = Ph) and a charge-transfer band at 498 nm was observed.[1] Additionally for (X = Ph) the phosphonium betaine absorbed at a slightly longer wavelength than the arsonium and stibonium analogues in all of the solvents.

3.7 Future Developments

As mentioned earlier the copper (I) catalysed template reaction of triphenylbismuth with an aryl halide does not form the expected tetraarylbismuthonium salt (9). This is probably because the triarylbismuth ligand is not able to stabilise the intermediate organometallic species effectively as with the related phosphine, arsine, and stibine.

It would be interesting to investigate different catalysts (such as cobalt (II)) and different solvents in the synthesis of triarylbismuthonium salts, and to investigate any solvatochromism that the related betaines (10) might possess, comparing the electron accepting ability of the positive bismuthonium centre compared to those of the other group 15 elements.

(9)   (10)
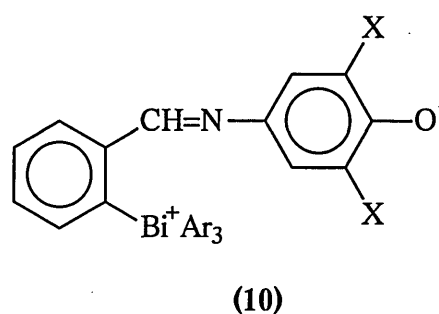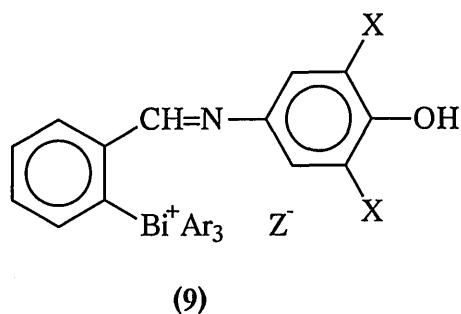
Furthermore it would be of interest to see any interaction between the imino nitrogen and the 'onium centre and compare the interaction, if any, with the arsonium and stibonium centres.

3.8 Experimental

^{1}H NMR spectra were recorded using a Brüker 250 AC FT NMR spectrometer. Low resolution mass spectra, and related FABMS determinations (in a *p*-nitrobenzylalcohol matrix) were recorded using a VG Micromass 7070F instrument. High resolution accurate FABMS determinations were recorded at the EPSRC National Mass Spectrometry Service Centre, University of Wales Swansea, and at the Mass Spectrometry Unit at the University of Sheffield. Negative mode EI and FAB mass spectra were also recorded at the Mass Spectrometry Unit at the University of Sheffield, and ICP analysis was carried out on a Spectroflame instrument.

3.8.1 Preparation of the imine intermediates.

(5) 4-N(*o*-bromobenzylidene)amino-2,6-dichlorophenol; –2,6-dibromophenol and -2,6-diphenylphenol were prepared as previously described.[1]

(6) 2-(2-Iodophenyl)benzothiazole
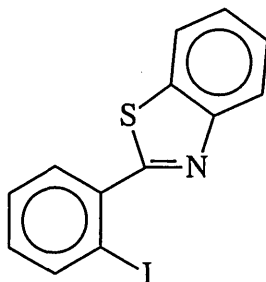
This was provided by Prof. D. W. Allen

3.8.2 General procedure for the synthesis of the arsonium and stibonium salts.

The appropriate halogenoaryl halide (5) or (6) was allowed to react with the triarylarsine or –stibine (1.1 mol equiv) in refluxing acetonitrile, in the presence of copper (I) iodide (1 mol equiv). The mixture was heated under reflux for between six and twenty four hours under nitrogen in the case of the reactions with the triarylstibines and between twenty four and forty eight hours under nitrogen for the reactions with the triarylarsines.

After cooling the reaction mixture was poured into aqueous potassium iodide solution (10 % w/v) and extracted three times with dichloromethane. The dried (MgSO$_4$) organic extract was evaporated in vacuo, and the oily residue triturated several times with fresh portions of diethyl ether to give the salts as yellow solids. If

162

purification of the salts was required, the salt was dissolved in the minimum cold dichloromethane and reprecipitated slowly with diethyl ether.

3.8.3 General procedure for the synthesis of arsonium and stibonium betaines.

For conversion to the related betaines the salts were dissolved in dichloromethane, and the solution shaken with dilute aqueous sodium hydroxide solution. After drying $(MgSO_4)$ the organic layer was evaporated and trituration with diethyl ether gave the related betaine dye.

**(1) 4-N[-(2-Triphenylstiboniobenzylidene)-amino]-2,6-dichlorophenol di-
    iodocuprate**
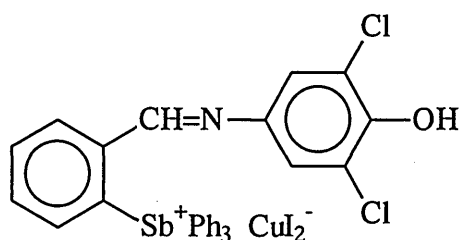
This was obtained as a pale orange solid. Yield 80 %.

mp *ca.* 121-124 °C

^{1}H NMR (CDCl$_3$): δ 6.5(s, 2H, aromatic), 7.23-7.70(m, 17H, aromatic), 8.00(t, 2H, aromatic), 9.41(s, 1H, CH=N).

MS (FAB): Exact mass calculated for M$^+$ cation $C_{31}H_{23}NSbCl_2O$: 616.019494 Found: 616.020261 (-1.2 ppm).

(2) 4-N[(2-Triphenylstibonio)benzylidene]-4-amino-2,6-dichlorophenolate

This was obtained as a dark orange-red solid. Yield 94 %.

Phase change 210 °C, mp 215 °C

^{1}H NMR (CDCl$_3$): δ 6.5(s, 2H, aromatic), 7.09(d, 1H), 7.43-7.58(m, 16H, aromatic), 7.81(d, 1H), 7.94(d, 1H), 8.51 (s, 1H, CH=N).

163

MS (FAB): Exact mass calculated for (M^++ 1) $C_{31}H_{23}NSbCl_2O$: 616.019494 Found: 616.019614 (-0.2 ppm).

(1) 4-N[-(2-Triphenylstiboniobenzylidene)-amino]-2,6-dibromophenol di- iodocuprate
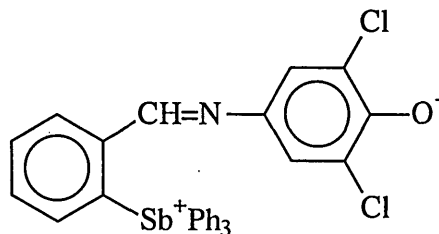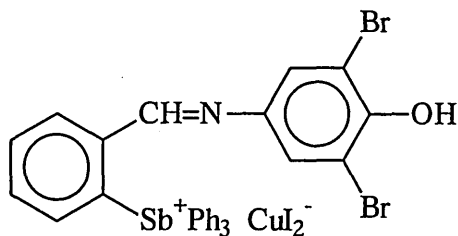

This was obtained as a pale orange solid. Yield 70 %.

mp *ca.* 121-124 °C

^{1}H NMR (CDCl$_3$): δ 6.72(s, 2H, aromatic), 7.26-7.75(m, 16H, aromatic), 8.02(t, 2H, aromatic), 8.70(d, 1H), 9.41(s, 1H, CH=N).

MS (FAB): Exact mass calculated for M^+ cation $C_{31}H_{23}NSbBr_2O$: 703.918460 Found: 703.918504 (-0.1 ppm).

(2) 4-N[(2-Triphenylstibonio)benzylidene]-4-amino-2,6-dibromophenolate

This was obtained as a dark red solid. Yield 96 %.

Phase change 165 °C, mp *ca.* 177-178 °C

^{1}H NMR (CDCl$_3$): δ 6.76(s, 2H, aromatic), 7.11-7.14 (d, 1H), 7.26-7.76(m, 16H, aromatic), 7.76-7.82(t, 1H, aromatic), 7.93-7.96(d, 1H), 8.74(s, 1H, CH=N).

MS (FAB): Exact mass calculated for (M^++1) $C_{31}H_{23}NSbBr_2O$: 703.918460 Found: 703.920763 (-3.3 ppm).

(1) 4-N[-(2-Triphenylstiboniobenzylidene)-amino]-2,6-diphenylphenol di-iodocuprate
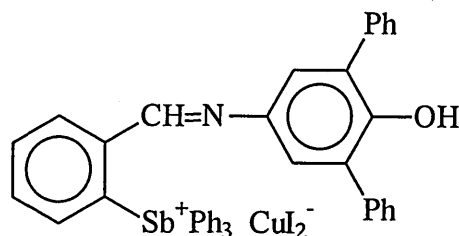
This was obtained as a pale yellow solid. Yield 67 %.

mp 128-129 °C

^{1}H NMR (CDCl$_3$): δ 6.56(s, 2H, aromatic), 7.23-7.72(m, 26H, aromatic), 8.09-8.03(t, 2H, aromatic), 8.59(d, 1H, aromatic), 9.36(s, 1H, CH=N).

MS (FAB): Exact mass calculated for M$^+$ cation C$_{43}$H$_{33}$NSbO: 700.160039 Found: 700.160044 (0.00 ppm).

(2) 4-N[(2-Triphenylstibonio)benzylidene]-4-amino-2,6-diphenylphenolate
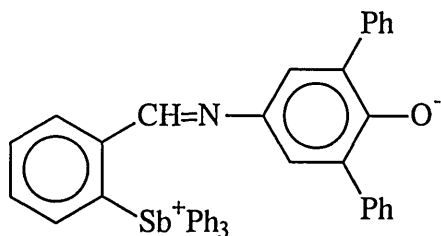
This was obtained as a dark purple solid. Yield 91 %.

Phase change 83 °C, mp *ca.* 110 °C

^{1}H NMR (CDCl$_3$): δ 6.22(s, 2H, aromatic), 6.39-8.07(m, 29H, aromatic), 8.64(s, 1H, CH=N).

MS (FAB): Exact mass calculated for (M$^+$+1) C$_{31}$H$_{23}$NSbO: 700.160039 Found: 700.165527 (-7.8 ppm).

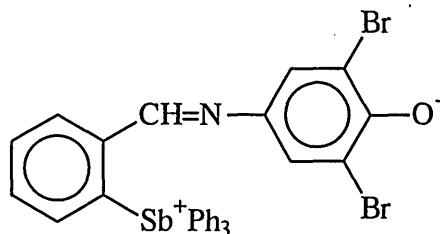## (1) 4-N[-(2-Triphenylarsoniobenzylidene)-amino]-2,6-dichlorophenol di-iodocuprate
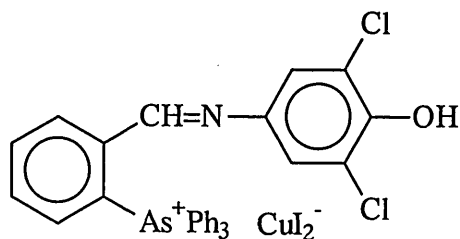
This was obtained as a pale orange solid. Yield 48 %.

mp *ca.* 128-130 °C

^{1}H NMR (CDCl$_3$): δ 6.13(s, 2H, aromatic), 7.27-7.71(m, 16H, aromatic), 7.81(t, 2H, aromatic), 8.52(d, 1H, aromatic), 8.70(s, 1H, CH=N).

MS (FAB): Exact mass calculated for M$^+$ cation C$_{31}$H$_{23}$NAsCl$_2$O: 570.037266 Found: 570.038449 (-2.1 ppm).

(2) 4-N[(2-Triphenylarsonio)benzylidene]-4-amino-2,6-dichlorophenolate
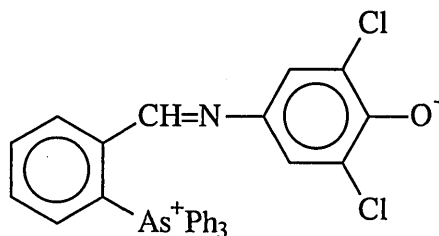
This was obtained as a red solid. Yield 97 %.

Phase change 115 °C, mp 125 °C

^{1}H NMR (CDCl$_3$): δ 6.15(s, 2H, aromatic), 7.27-7.86(m, 19H, aromatic), 8.12(s, 1H, CH=N).

MS (FAB): Exact mass calculated for (M$^+$+1) C$_{31}$H$_{23}$NAsCl$_2$O: 570.037266 Found: 570.039011 (-3.1 ppm).

(1) 4-N[-(2-Triphenylarsoniobenzylidene)-amino]-2,6-dibromophenol di-iodocuprate
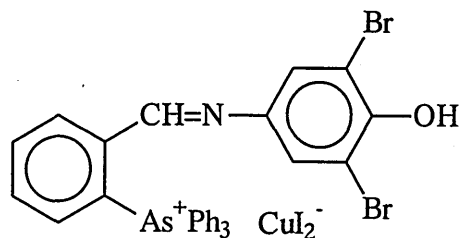
This was obtained as a pale orange solid. Yield 53 %.

mp *ca.* 127-130 °C

^{1}H NMR (CDCl$_3$): δ 6.31(s, 2H, aromatic), 7.26-7.80(m, 16H, aromatic), 8.09(t, 2H, aromatic), 8.51(d, 1H, aromatic), 8.79(s, 1H, CH=N).

MS (FAB): Exact mass calculated for M$^+$ cation C$_{31}$H$_{23}$NAsBr$_2$O: 657.936232 Found: 657.936556 (-0.5 ppm).

(2) 4-N[(2-Triphenylarsonio)benzylidene]-4-amino-2,6-dibromophenolate
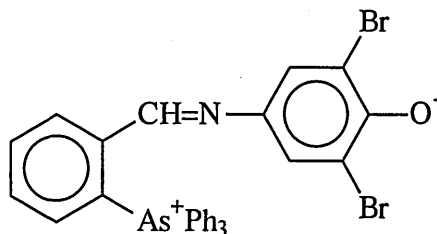
This was obtained as a red solid. Yield 90 %.

mp >150 °C (decomp.)

^{1}H NMR (CDCl$_3$): δ 6.39(s, 2H, aromatic), 7.12-7.90(m, 19H, aromatic), 8.16(s, 1H, CH=N).

MS (FAB): Exact mass calculated for (M$^+$+1) C$_{31}$H$_{23}$NAsBr$_2$O: 657.936232 Found: 657.937760 (-2.3 ppm).

(1) 4-N[-(2-Triphenylarsoniobenzylidene)-amino]-2,6-diphenylphenol di-iodocuprate
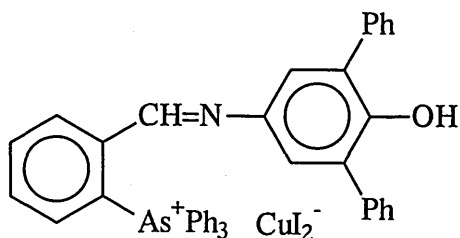
This was obtained as a beige-yellow solid. Yield 37 %.

Phase change 110 °C, mp *ca.* 127 °C

^{1}H NMR (CDCl$_3$): δ 6.11(s, 2H, aromatic), 7.26-7.77(m, 26H, aromatic), 8.10(t, 2H, aromatic), 8.35(d, 1H, aromatic), 8.69(s, 1H, CH=N).

MS (FAB): Exact mass calculated for M$^+$ cation C$_{43}$H$_{33}$NAsO: 654.177810 Found: 654.178826 (-1.6 ppm).

(2) 4-N[(2-Triphenylarsonio)benzylidene]-4-amino-2,6-diphenylphenolate
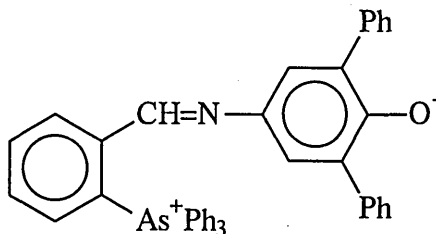
This was obtained as a dark purple solid. Yield 89 %.

Phase change 125 °C, mp 150-152 °C

^{1}H NMR (CDCl$_3$): δ 6.35(s, 2H, aromatic), 7.06-7.83(m, 29H, aromatic), 8.26(s, 1H, CH=N).

MS (FAB): Exact mass calculated for (M$^+$+1) C$_{43}$H$_{33}$NAsO: 654.177810 Found: 654.173591 (6.4 ppm).

(3) N-(2-Triphenylarsoniobenzylidene)amino-4-methoxybenzene iodide

CH=N—〈 〉—OMe

As⁺Ph₃ I⁻

As^+Ph_3 I^-
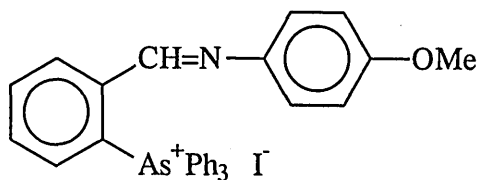
This was obtained as yellow crystals. Yield 11 % (after recrystallisation from CH_2Cl_2 – diethyl ether).

mp 186 °C

^{1}H NMR ($CDCl_3$): δ 3.7(s, 3H, OCH_3), 7.55 and 6.20(ss,4H, aromatic), 7.8-7.2(m, 17H, aromatic), 8.1(m, 1H, aromatic), 8.4(d, 1H, aromatic), 8.7(s, 1H, CH=N).

MS (FAB): Exact mass calculated for M^+ cation $C_{32}H_{27}NAsO$: 516.130860 Found: 516.130334 (1.0 ppm).

(3) N-(2-Triphenylstiboniobenzylidene)amino-4-methoxybenzene di-iodocuprate

CH=N—〈 〉—OMe

Sb^+Ph_3 CuI_2^-
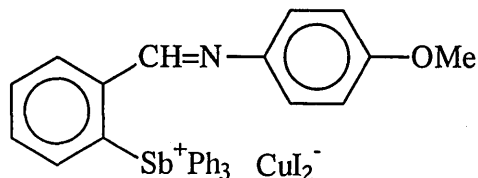
This was obtained as yellow crystals. Yield 77 %.

mp > 95 °C (decomp.)

^{1}H NMR ($CDCl_3$): δ 3.60(s, 3H, OCH_3), 6.70 and 6.55(ss, 4H, aromatic), 8.30-6.90(m, 18H, aromatic), 8.65(d, 1H, aromatic), 9.45(s, 1H, CH=N).

MS (FAB): Exact mass calculated for M^+ cation $C_{32}H_{27}NSbO$: 562.113088 Found: 562.114831 (-3.1 ppm).

(3) N-[2-Tris-(4-methylphenyl)stibonio]benzylidene-1-amino-4-methoxybenzene di-iodocuprate

CH=N—〈 〉—OMe

$Sb^+(PhCH_3)_3$ CuI_2^-
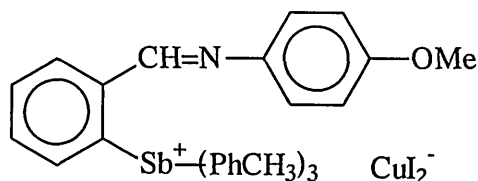
This was obtained as yellow crystals. Yield 88 %.

mp >110 °C (decomp.)

^{1}H NMR (CDCl$_3$): δ 2.40(s, 9H, CH$_3$), 3.70(s, 3H, OCH$_3$), 6.75 and 6.60(ss, 4H, aromatic), 8.20-6.90(m, 15H, aromatic), 8.65(d, 1H, aromatic), 9.40(s, 1H, CH=N).

MS (FAB): Exact mass calculated for M$^+$ cation C$_{35}$H$_{33}$NSbO: 604.160039 Found: 604.161605 (-2.6 ppm).

(4) 2-[2-(Triphenylstibonio)phenyl]benzothiazole di-iodocuprate
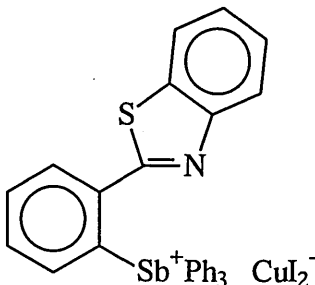
This was obtained as a beige solid. Yield 100 %.

mp 138-140 °C

MS (FAB): Exact mass calculated for M$^+$ cation C$_{31}$H$_{23}$NSSb: 562.058945 Found: 562.060441 (-2.7 ppm).

(4) 2-{2-[Tris(4-methylphenyl)stibonio]phenyl}benzothiazole di-iodocuprate
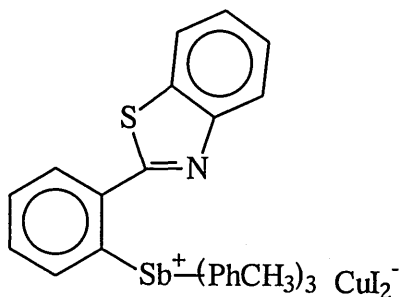
This was obtained as a beige solid. Yield 86 %.

mp >105 °C (decomp.)

^{1}H NMR (CDCl$_3$): δ 2.4(s, 9H, CH$_3$), 8.50-6.70(m, 20H, aromatic).

MS (FAB): Exact mass calculated for M$^+$ cation C$_{34}$H$_{29}$NSSb: 604.105896 Found: 604.107879 (-3.3 ppm).

References

1. D. W. Allen and X. Li, *J. Chem. Soc., Perkin Trans. 2,* 1997, 1099.

2. J. Chatt and F. G. Mann, *J. Chem. Soc.,* 1940, 1192.

3. D. W. Allen, P. E. Cropper, P. G. Smithhurst, P. R. Ashton and B. F. Taylor, *J. Chem. Soc., Perkin Trans. 1,* 1986, 1989.

4. D. W. Allen, I. W. Nowell, L. A. March and B. F. Taylor, *J. Chem. Soc., Perkin Trans. 1,* 1984, 2523.

5. D. W. Allen and P. E. Cropper, *Polyhedron,* **9,** 1990, 129.

6. N. R. Champness and W. Levason, *Coord. Chem. Rev.,* **133,** 1994, 115.

7. G. A. Bowmaker, R. D. Hart, E. N. de Silva, B. W. Skelton and A. H. White, *Aust. J. Chem.,* **50,** 1997, 553.

8. G. A. Bowmaker, R. D. Hart and A. H. White, *Aust. J. Chem.,* **50,** 1997, 567.

9. A. Bondi, *J. Phys. Chem.,* **68,** 1964, 441.

10. G. Ferguson, C. Glidewell, I. Gosney, D, Lloyd, S. Metcalfe and H. Lumbroso, *J. Chem. Soc., Perkin Trans. 2,* 1988, 1829.

11. R. J. Cernik, W. Clegg, C. R. A. Catlow, G. Bushnell-Wye, J. V. Flaherty, G. N. Greaves, I. D. Burrows, D. J. Taylor, S. J. Teat and M. Hamichi, *J. Synchotron Rad.,* **4,** 1997, 279.

12. B. Milewski-Malurla and H. Schmidbaur, *Z. Naturforsch, Teil B*, **37,** 1982, 1393.

13. M. Hall, D. B. Sowerby, *J. Chem. Soc., Dalton Trans.,* **6,** 1983, 1095.

14. M. Asplund, S. Jagner and M. Nilsson, *Acta Chem. Scand.,* **A36,** 1982, 751.

15. M. Asplund and S. Jagner, *Acta Chem. Scand.,* **A38,** 1984, 279.

16. A. Bencini, D. Gatteschi and C. Zanchini, *Inorg. Chem.,* **24,** 1985, 704.

17. S. Jagner and G. Helgesson, *Advances in Inorganic Chemistry,* **37,** 1991, 1.

18. L. Subramanian and R. Hoffmann, *Inorg. Chem.,* **31,** 1992, 1021.

19. H. Hartl and J. Fuchs, *Angew. Chem. Int. Ed. Engl.,* **25**(6), 1986, 569.

20. M. Asplund, S. Jagner, M. Nilsson, *Acta Chem. Scand.,* **A37,** 1983, 57.

21. M. Asplund and S. Jagner, *Acta Chem. Scand.,* **A38,** 1984, 135.

22. M. Asplund, S. Jagner and M. Nilsson *Acta Chem. Scand.,* **A37,** 1983, 165.

23. M. Asplund, S. Jagner and M. Nilsson *Acta Chem. Scand.,* **A38,** 1984, 57.

24. M. Asplund and S. Jagner, *Acta Chem. Scand.,* **A38,** 1984, 129.

25. D. N. Walters and B. J. Basak, *Chem. Soc., A,* 1971, 2733.

26. S. Ahrland, P. Bläuenstein, B. Tagesson and D. Tuhtar, *Acta Chem. Scand.,* **A34,** 1980, 265.

27. S. Ahrland, K. Nilsson and B. Tagesson, *Acta Chem. Scand.,* **A37,** 1983, 193.

CHAPTER 4

The Synthesis and the

Characterisation of Push-Pull

Triphenylphosphonium Salt Systems

and their Respective Phosphine

Oxides

4.0 Introduction

This chapter describes the synthesis of four new dipolar push-pull triphenylphosphonium salts **(1-4)** based on the very much discussed 4-dimethylamino-4'-nitrostilbene (DANS) **(5)**[1,2] which has been extensively studied by the *EFISH* technique and exhibits a hyperpolarisability of $(\beta_\mu (0) = 70 \times 10^{-30}$ esu). In DANS the dimethylamino electron-donor group is linked via an extended π-electron bridge to the nitro electron-acceptor group. It was thought that the nitro group could be replaced by the positive triphenylphosphonium group, which could act as the electron acceptor. Additionally in systems **(1)** and **(2)** the dimethylamino donor group has been replaced with the electron rich ferrocene and thiophene systems, respectively. A preliminary study into the effect of increasing the conjugation length has also been carried out for system **(3)**.

(1)   **(2)**

n = 1 **(3)**   n = 2 **(4)**

(5)
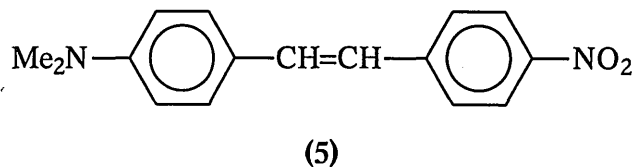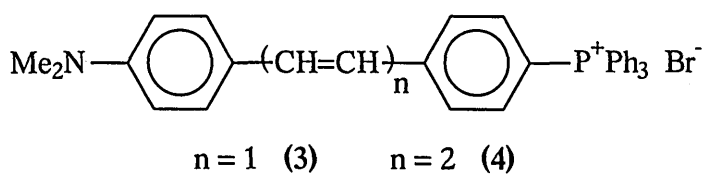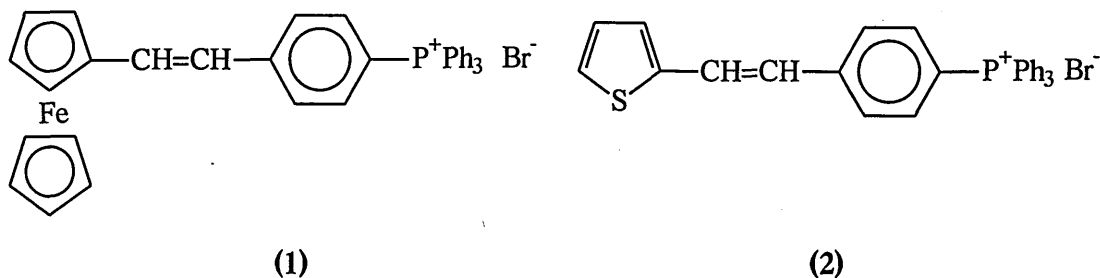
Subsequently the four phosphine oxides **(6-9)** have been synthesised by the alkaline hydrolysis of the corresponding phosphonium salts **(1-4)**. It has already been shown that the P=O moiety has the ability to be a good electron-acceptor, whereby the strong polarisation of the P=O bond induces an electronic deficiency at the phosphorus atom, this then having the ability to withdraw an electron from a donor group in an internal charge-transfer process.[3] The neutral phosphorus compound **(8)** and the

174

analogous compounds **(10)** and **(11)** have already been reported and discussed in the literature;[3,4] however the synthesis of **(8)** from the triphenylphosphonium salt **(3)** has not previously been reported.

$$\text{Fe-ferrocenyl}-CH=CH-\langle\text{C}_6\text{H}_4\rangle-PPh_2=O$$

(6)

$$\text{thienyl}-CH=CH-\langle\text{C}_6\text{H}_4\rangle-PPh_2=O$$

(7)

$$Me_2N-\langle\text{C}_6\text{H}_4\rangle-(CH=CH)_n-\langle\text{C}_6\text{H}_4\rangle-PPh_2=O$$
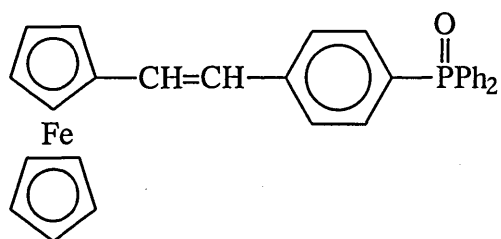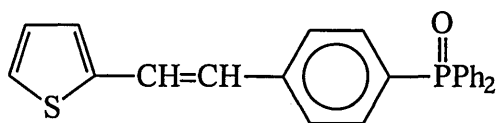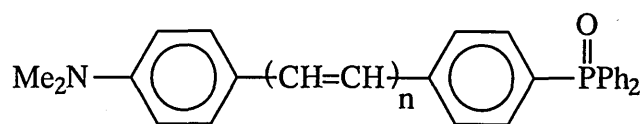
n = 1 **(8)**   n = 2 **(9)**

The phosphine oxide PONA **(10)** has shown a high quadratic polarisability (β_μ (0) = 45 x 10^{-30} esu) (EFISH method); its efficiency is somewhere in between those of the cyano and nitro analogues.[3] However it was shown that this polar molecule exhibited very weak non-linear optical properties due to the molecules being centrosymmetric in the crystalline state. By exchanging the azo linkage for a *trans* stilbene unit (PONS-E) **(8)**, the crystals were found to align in acentric space groups. This was also achieved by introducing a methyl substituent on one of the phenyl groups of **(10)**, to form (2'MPONA) **(11)**. Unfortunately **(8)** and **(11)**[4] exhibited very weak non-linear optical properties due to alignment, of the molecules in a head-to-tail arrangement, and therefore these systems were not able to generate strong second harmonic radiation.

$$Me_2N-\langle\text{C}_6\text{H}_3(R_1)\rangle-N=N-\langle\text{C}_6\text{H}_4\rangle-PPh_2=O$$
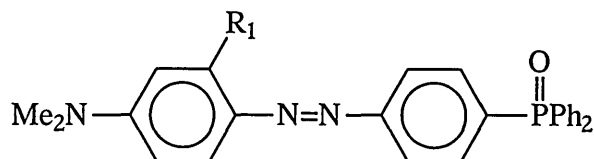
R_1 = H **(10)** R_1 = Me **(11)**

PONA **(10)** has also been incorporated into polymers (co-polymethylmethacrylate and polyurethanes) as pendant groups,[5] and the NLO active chromophore has been incorporated at different concentrations. Orientation of the chromophores was accomplished by corona poling and the second harmonic generation was measured; however this value was found to decrease for over 45 % functionalisation of the polymethylmethacrylate polymer. The polyurethanes containing PONA as the chromophore were found to exhibit larger second harmonic coefficients.

Additionally these polymers exhibited unusually high glass transition temperatures (120-185 °C), due to the presence of the bulky phosphine oxide moieties and the dipolar interactions between strongly polarised P=O bonds (P=O----P=O), giving rigidity to the network.

Whereas the understanding of the non-linear optical properties of organic and inorganic materials has developed over the years, the related study of organometallic compounds and the understanding of their non-linear optical behaviour has not developed at the same rate. However, in the last ten years, reports of organometallic compounds with second order nonlinear optical properties have significantly increased in number. Traditionally, inorganic solids such as $LiNbO_3$ and KH_2PO_4 have been nonlinear optical materials of the greatest interest,[6,7] but publications over the last few decades have suggested that molecule-based macroscopic π-electron assemblies possess many superior nonlinear optical characteristics.

Organometallic complexes possessing NLO properties represent a very interesting and potentially useful category of compounds which bridge the well known areas of organic and inorganic NLO substances. They are worthwhile studying due to their low energy, (but sometimes intense), electronic transitions.

Enhanced optical nonlinearities could be observed by the coordination of a ligand containing highly polarisable π-electrons to a metallic centre possessing weakly bound valence electrons. These systems can possess metal $\rightarrow$ ligand or ligand $\rightarrow$ metal charge-transfer bands in the visible region of the spectrum. However, although these optical absorption bands are associated with a large second-order activity, they can also lead to transparency problems.

Redox changes are also possible for systems which are largely associated with the metal centre. This centre can either be electron-rich or –poor, depending on the oxidation-state of the metal and the ligand environment. These redox changes can

possibly lead to larger hyperpolarizabilities than those in conventional organic systems, with the metal centre being either the donor or the acceptor.

Another advantage of organometallic systems is the larger range of non-aromatic ligands that can be attached to the metallic centre, and therefore β can be more easily optimised. Furthermore, these metal centres can increase the solubility of the material in common organic solvents and so processability will be easier.

The great structural and electronic diversities available in metal-organic environments could produce new parameters not available in the traditional π-organic structures, and therefore compounds of this type are worthy of study.

Since its discovery over four decades ago, ferrocene is the most widely studied metallocene in the area of nonlinear optics. It was found to be a versatile building block, and, on the basis of both theory and experimental data, ferrocene systems have been found to possess large hyperpolarisabilities. They are also good candidates for NLO systems as they possess excellent thermal and photochemical stability and show low sensitivity to di-oxygen and water.

In the metal cyclopentadienyl systems, iron has also been replaced by ruthenium, which is a less electron rich metal, and therefore a less effective donor.[8] However compounds of this type have only crystallised out in a centrosymmetric orientation.

In 1987, Green *et al* were the first to report the great potential of ferrocene in the field of second order nonlinear optics.[9] As well as being fairly solvatochromic, the *cis* isomer of compound (12) (Y = NO$_2$), (R$_1$ = H) also exhibited a high value of β. In this compound the electron rich ferrocene is the electron donor, and the nitro group is the electron acceptor. In contrast the *trans* isomer showed no SHG signal, as the compound crystallised out into a centrosymmetric space group. The powder SHG signal of the *cis*-isomer was sixty two times greater than that of the urea reference sample.

R_1

$CH=CH$—Y

Fe
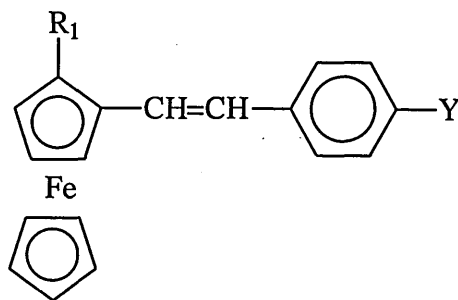
$R_1 = H$ or Me

(12)

The large hyperpolarisability of **(12)** is due to its charge-transfer ability and the delocalisation of electrons throughout the molecule via π-electron conjugation (fig. 1). For **(12)**, where Y = CN and CHO (R_1 = H) (*E*-isomer), the powder SHG signals were only between 0.95 and 0.72 times greater than that of the urea reference standard.[10]

$CH=CH$—

Fe

$CH-CH$=

Fe^+
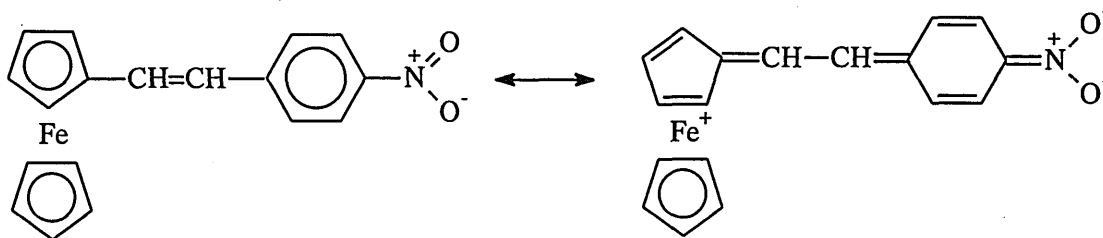
Figure 1

Asymmetry and optical activity were introduced into the molecules by substituting the cyclopentadienyl ring, which contains the acceptor moiety with an additional methyl group (R_1 = Me), leading to a more desirable alignment of the molecular dipole in the crystal lattice.[10]

Where Y = -C=CH-CH=C(NO_2)O the SHG signal was found to be over 500 times greater for (R_1 = Me) compared to (R_1 = H) (*E*-isomer).[10] It is interesting to note that when Y = NO_2 and R_1 = Me (*E* isomer), the powder SHG signal was eight times greater than that of the urea reference sample; however when R_1 = H (*E* isomer), the compound was SHG inactive as discussed earlier.

A series of organometallic salts containing the ferrocenyl moiety has also been reported in the literature.[11] Compound **(13)** (X^- = I) has been synthesised and has a powder SHG of approximately 220 times that of urea. It was found that the magnitude of the powder SHG signal was sensitive to the nature of the counter-ion. With bromide

as the counter-ion, the powder SHG signal decreased to 170 times that of urea, whereas with chloride as the counter-ion, no SHG signal was observed, probably due to the material being centrosymmetric in the crystalline state. This was also observed by Meredith *and coworkers*[12] who synthesised a range of dialkylaminostilbene salts, and in changing the counterion a change in the SHG was observed.

$$X^- = I^-, Br^-, NO_3^-, BF_4^-, B(C_6H_5)_4^-, (p)\text{-}CH_3\text{-}C_6H_4SO_3^-, PF_6^-, Cl^-, CF_3SO_3^-$$
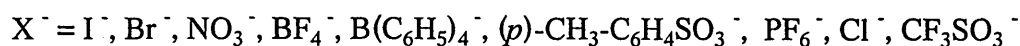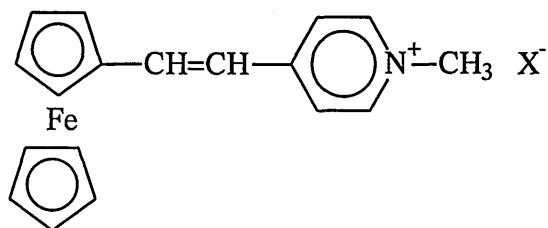
(in decreasing SHG values)

(13)

Theoretical[13] and experimental[14] comparisons have been made between the ferrocenyl compound **(14)** and the dimethylamino derivatives **(15)**. Electronic absorption data[14] of both **(14)** and **(15)** have showed **(15)** to have a slightly larger shift (bathochromic) in absorption in going from DMF to diethyl ether. However **(14)** (Y = CN and F) showed a negligible hypsochromic shift in these solvents.

$$Y = F, Cl, Br, CN, NO_2$$
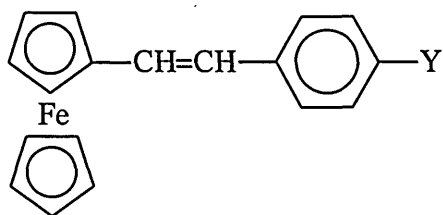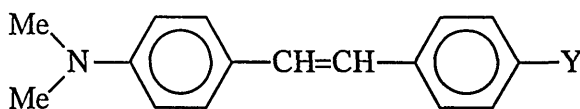
(14)   **(15)**
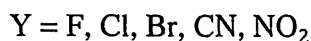
A single crystal X-ray study was undertaken on the ferrocenyl derivative **(16)**, as it seemed to be potentially the best from the electronic absorption data, and in view of its D-π-A nature. Unfortunately no SHG experiments could be conducted due to its centrosymmetric packing, (DAAD rather than DADA stacking).[14]

179
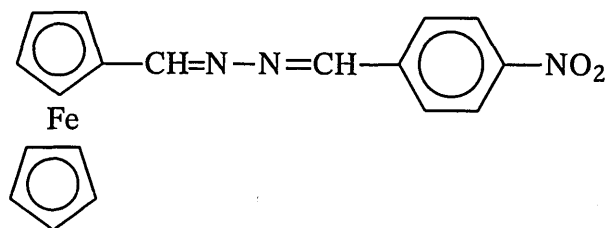
(16)

Investigations have been carried out on the solvatochromism of compounds **(17)** and **(18)**[15] For compound **(17)**, if the acceptor group (R_3) is NO_2, the degree of solvatochromism increased if R_1 is another electron donating group such as methoxy, but if R_2 is methoxy or alkoxy, hardly any solvatochromism was observed.

Unexpectedly high solvatochromism was observed if R_2 is hydroxy; this is thought to be due to formation of hydrogen bridges, enhancing the electron-accepting power of the nitro group which compensates for the electron donating effect of the hydroxy group.
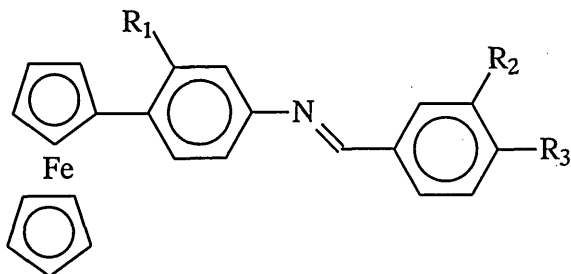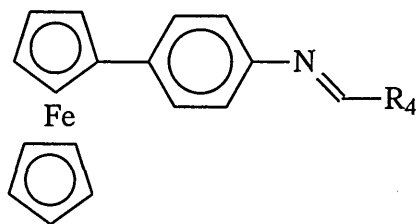
(17)   **(18)**

For **(18)** $(R_4 = Ph)$, strong solvatochromic effects were observed if the benzene ring (R_4) was replaced by a furan or thiophene ring, as a result of their lower aromatic character and higher polarisability compared to benzene. The system was also found to be strongly solvatochromic if R_4 was ferrocene.

The ferrocenyl moiety has also been incorporated into polymers. The first SHG active organometallic polymer was synthesised by Wright et al,[16] where the ferrocene NLO phores were attached as a pendant group to a poly(methyl methacrylate) copolymer, displaying a SHG efficiency of ca. four times that of the quartz reference standard.

Ferrocene moieties have also been incorporated into polymers as part of the backbone.[17,18] The main chain polymer **(19)** displayed SHG activity after corona poling at 150 °C. However, decomposition of the NLO-phores during the poling process was

observed resulting in a colour change from purple to red, and consequently gave an underestimation of its true orientational stability.

$$-[CONH(CH_2)_6NHCO]-OCH_2-\underset{Fe}{\overset{\text{(ferrocenyl)}}{}}\underset{CN}{\overset{H}{=}}CO_2(CH_2)_2O-]$$
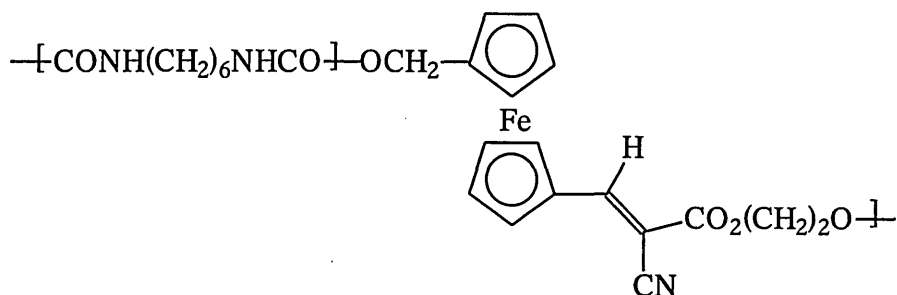
(19)

There are limited reports on the electron-donating ability of thiophene compared to that of ferrocene, although the thiophene moiety has been extensively used as a spacer between donor and acceptor groups of NLO active materials.[19-21]

For example the push-pull systems **(20)**, containing the negatively charged dicyanomethanide as the donor group, and the positively charged N-alkylpyridinium moiety as the acceptor group, have been synthesised.[19] The acceptor and donor groups were spaced by thiophene based moieties containing one or two heterocyclic rings, and sometimes an ethylene bridge was employed in addition to the heterocyclic spacer.
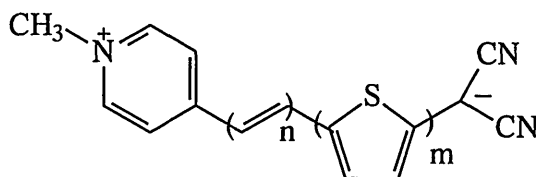
(20a) n= 0, m = 1

(20b) n = 0, m = 2

(20c) n = 1, m = 1
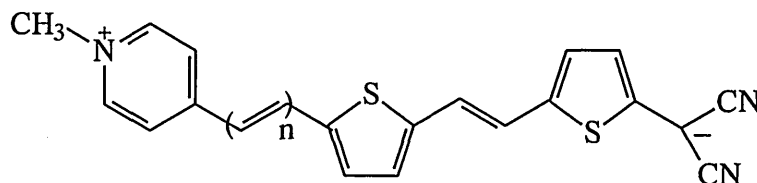
(20d) n = 0

(20e) n = 1

181

Greater negative solvatochromism was observed with increase in conjugation and length of the spacer, e.g. both (20d) and (20e) exhibited a hypsochromic shift of *ca.* 70 nm whereas (20a) and (20c) only exhibited a shift of 22 nm and 30 nm respectively from methanol to acetone.

Effenberger *et al*[20] and Dubois *et al*[21] have also employed thiophene as a spacer in systems, this time employing a nitro group as the electron-acceptor and a dimethylamino group as the electron-donor. Effenberger showed system (21) to be positively solvatochromic (λ_{max} 466 nm in n-hexane and 597 nm in formamide/water), and Dubois' range of compounds with symmetrical spacers (22) have undergone preliminary NLO investigations by Hyper-Raleigh Scattering. It was seen that the ethene spacer (X = CH=CH) had a hyperpolarisability ten times that of the sulphide spacer   (X = S), and this was explained as a consequence of the complete conjugation throughout the molecule.

(21)

X = N, S, SiMe$_2$, CMe$_2$, and CH=CH

(22)
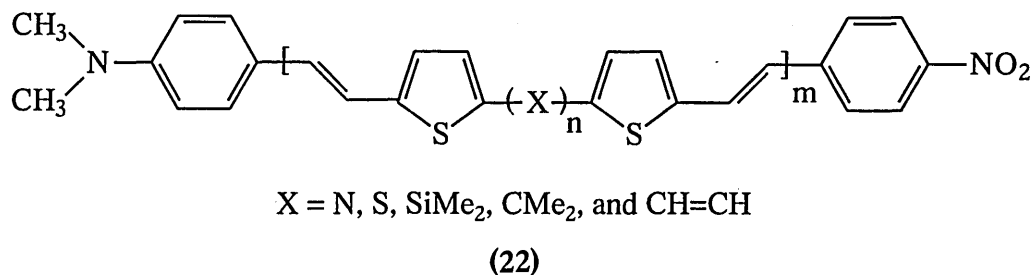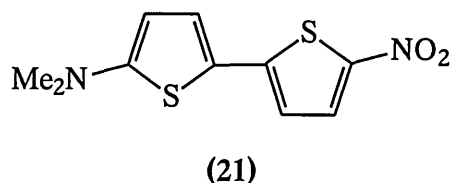
Thiophene has also been used as an efficient conjugating moiety in NLO pendant chromophores in polymers.[22,23] The use of polymers results in thermally stable and processable NLO polymeric materials.

Little is known about the relative strengths of heterocyclic donors compared to heterocyclic acceptors, as quantitative ranking is not available on the same scale as for π-deficient systems nor on a similar one having carbonium ions instead of carbanions as a reference.[24]

One of the first reports of thiophene being used as an electron donor was by Pagani *and co-workers.*[24] They studied the effects on the solvatochromism of various compounds using the already studied π-deficient heterocycles[25-27] as the acceptor group

(pyridine, pyrazine, pyridazine and pyrimidine), and pyrrole, indole and thiophene as the donor group.

Comparisons of the solvatochromism of (23) and (24) showed that (23) exhibited negative solvatochromism, with shifts of -2 nm (Z=N) and -6 nm (Z=CH$_3$N$^+$) observed between the solvents methanol and dichloromethane, and water and methanol respectively. On the other hand, (24) (Z=N) exhibited positive solvatochromism of 6 nm between methanol and water, whereas (24) (Z=CH$_3$N$^+$) exhibited a negative solvatochromism of 22 nm in the same solvents.

It is already known that pyrrole is more π-excessive than thiophene[29-31] and this is reflected in the greater solvatochromism of (24) compared to (23). The positive charge in the N-alkyl triflates increases the electron withdrawal of the pyridine ring, and thus favouring the push-pull characteristics of the systems.

$$Z = N \text{ or } Z = CH_3N^+ \ CFSO_3^-$$
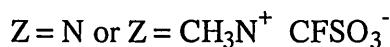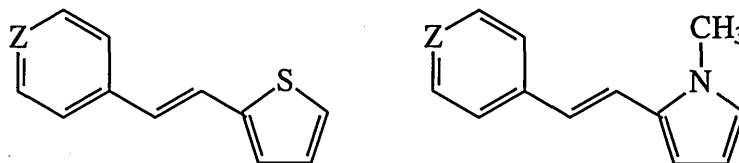
(23)   (24)

The overall results of the investigation showed there was a strong charge-transfer interaction between the donor and acceptor heterocycles. Compound (23) (Z=N) has been reported to have a β_μ value of 33×10^{-30} esu compared to a value of 28×10^{-30} esu for p-nitroaniline.

4.1 Synthesis of the stilbene precursors.

The dimethylaminostilbenes (26) and (27) were synthesised as in scheme 1 by the initial reaction of 4-bromobenzyl bromide with triphenylphosphine in acetonitrile to form the phosphonium salt (25), which undergoes a *Wittig Reaction* with 4-dimethylaminobenzaldehyde or 4-dimethylaminocinnamaldehyde to form the stilbenes.

$$BrCH_2 \longrightarrow \langle\text{ring}\rangle \longrightarrow Br \quad \xrightarrow{(i)} \quad Ph_3P^+CH_2 \longrightarrow \langle\text{ring}\rangle \longrightarrow Br \quad Br^-$$

(25)

$$\downarrow (ii)$$

$$\underset{Me}{\overset{Me}{>}}N \longrightarrow \langle\text{ring}\rangle \longrightarrow (CH=CH)_n \longrightarrow \langle\text{ring}\rangle \longrightarrow Br$$

cis-trans isomers

(26) n = 1

(27) n = 2
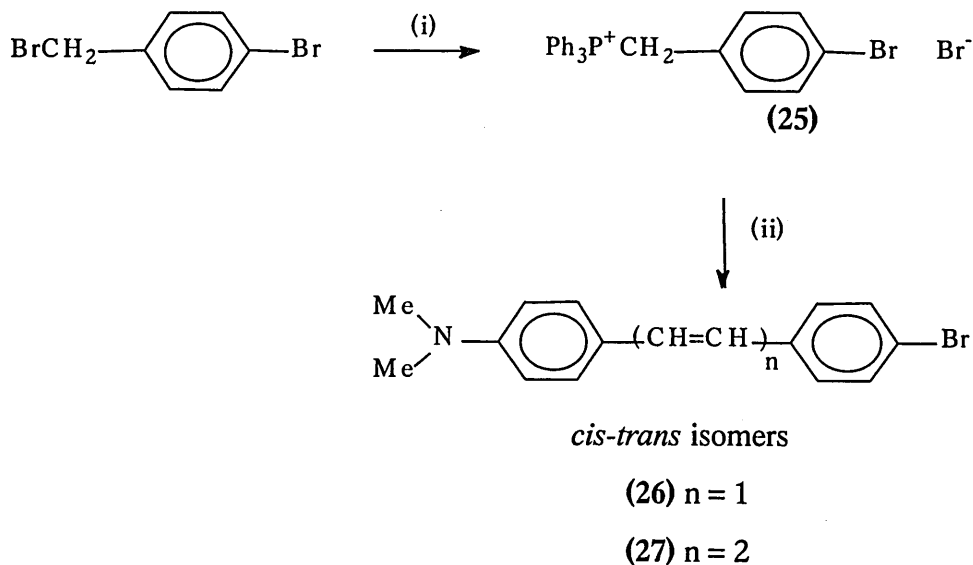
(i) Ph_3P, CH_3CN, reflux, 1-2hrs

(ii)   4-Dimethylaminobenzaldehyde or 4-dimethylaminocinnamaldehyde, $KOBu^t$,
       THF, r.t., overnight

Scheme 1

The ferrocene system **(30)** was produced by the quaternisation of (dimethylaminomethyl)ferrocene with iodomethane followed by the reaction of this salt **(27)** with triphenyl phosphine to form the phosphonium salt **(29)**, (scheme 2). Both these reactions were carried out in acetonitrile. The salt **(29)** underwent a *Wittig Reaction* with 4-bromobenzaldehyde to form the stilbene **(30)**.
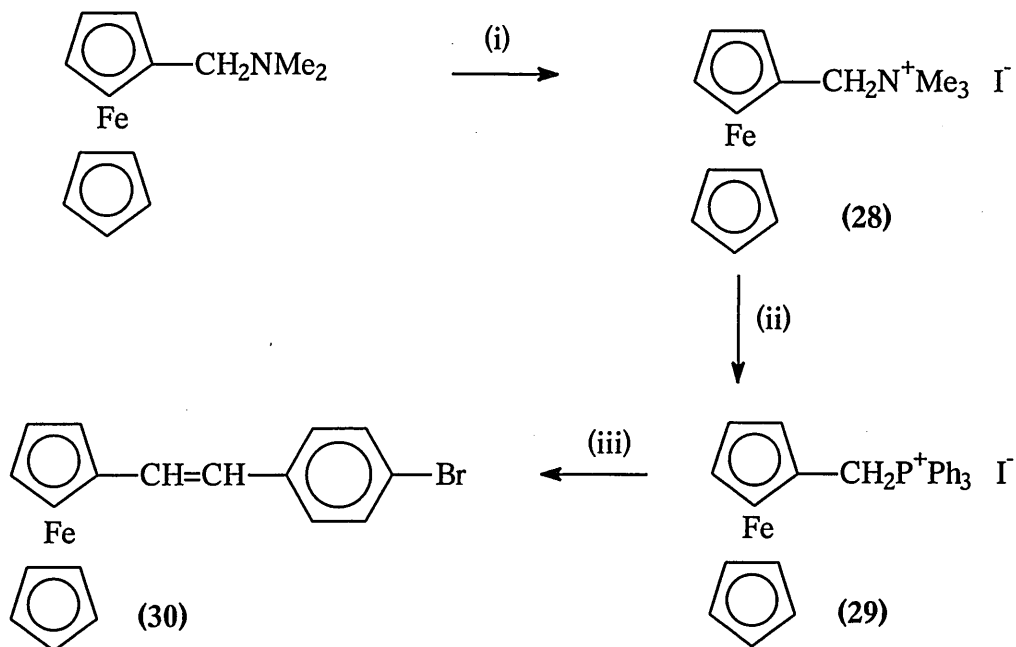
(i)   MeI, CH$_3$CN, r.t.

(ii)   Ph$_3$P, CH$_3$CN, reflux

(iii)   4-Bromobenzaldehyde, KOBu^t, dry THF, r.t., overnight

Scheme 2

It was initially presumed that the thiophene system (35) could be synthesised in a similar manner to the ferrocene precursor (30). However, treatment of the trimethylammonium salt (31) with triphenyl phosphine did not form the phosphonium salt (32), and salt (31) was recovered unchanged (scheme 3). The reaction was repeated with two mole equivalents of triphenylphosphine in acetonitrile, in methanol and in benzonitrile, but no phosphonium salt was formed.

(31)

(32)
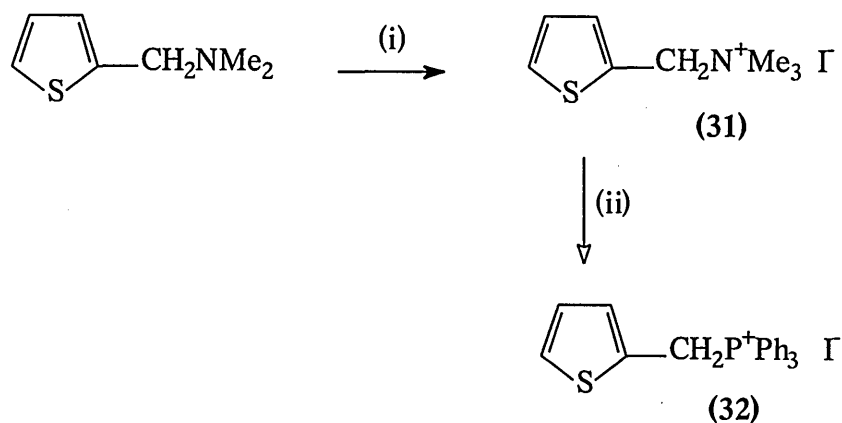
(i)   MeI, CH_3CN, r.t.

(ii) Ph_3P, CH_3CN, reflux

Scheme 3

The thienylstilbene **(35)** was prepared by brominating 2-methylthiophene with NBS and quaternising **(33)** with triphenylphosphine to form the phosphonium salt **(34)**, (scheme 4). The phosphonium salt **(34)** then underwent a *Wittig Reaction* with 4-bromobenzaldehyde to form the stilbene **(35)**. The mechanism of the *Wittig Reaction* is shown in scheme 5.

(35)   **(34)**
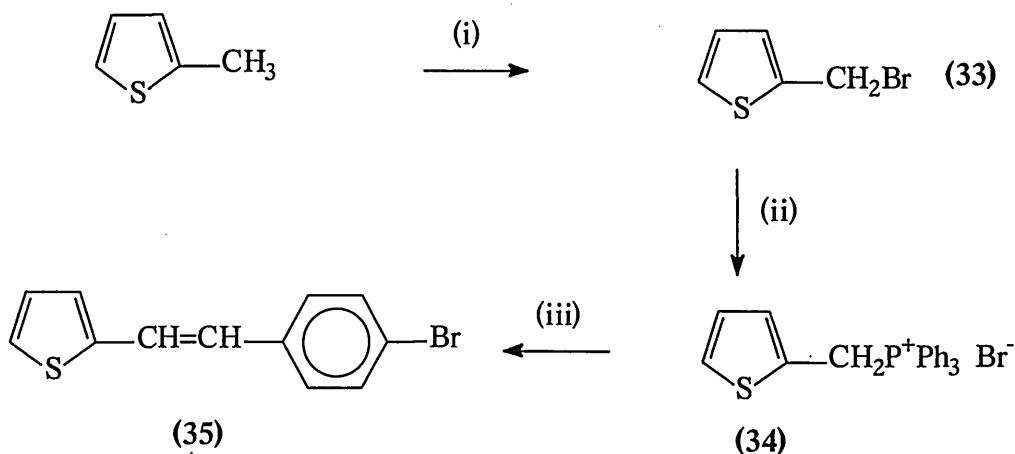
(i)   NBS, chloroform, reflux

(ii) Ph_3P, CH_3CN, reflux

(iii)   4-Bromobenzaldehyde, $KOBu^t$, dry THF, r.t., overnight

Scheme 4

The first step is nucleophilic attack on the aldehyde (4-bromobenzaldehyde, 4-dimethylaminobenzaldehyde or 4-dimethylaminocinnamaldehyde) by the ylide

186

carbanion to form the betaine intermediate **(A)**. This species then collapses to form the alkene **(26, 27, 30, 35)** and triphenylphosphine oxide.
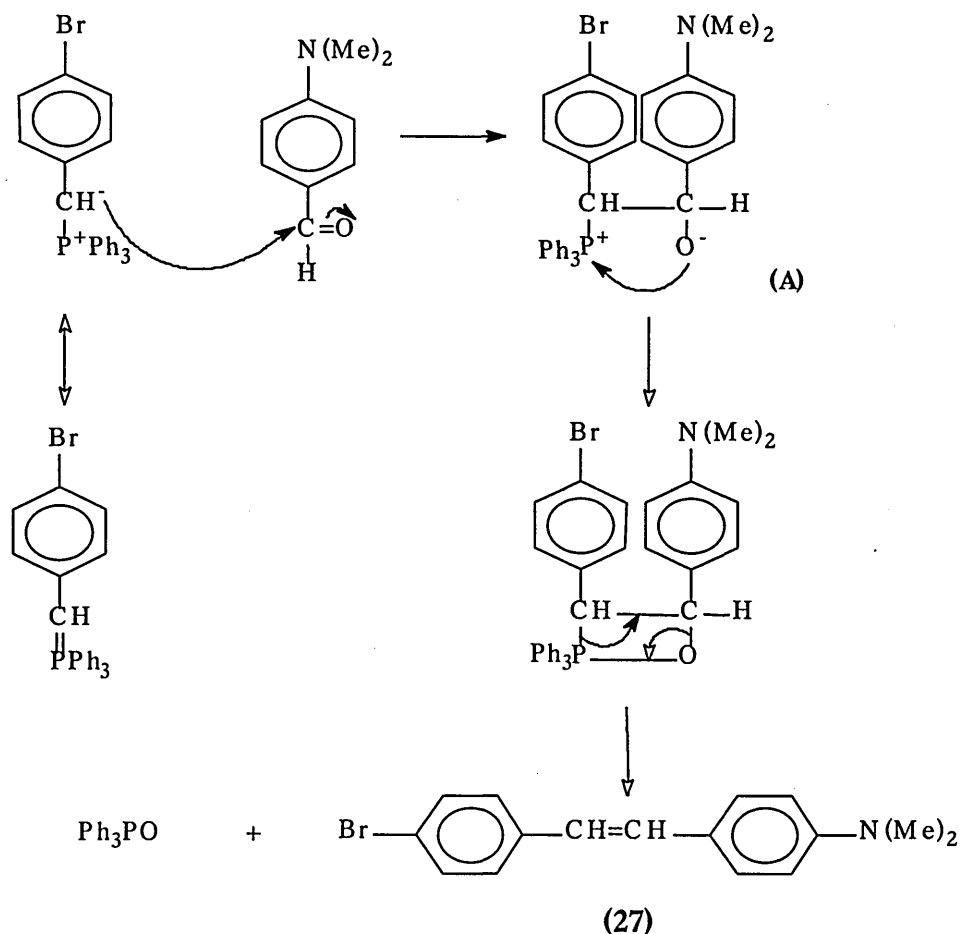
Scheme 5   Mechanism of Wittig Reaction.

4.2 Synthesis of the phosphonium salts.

The respective phosphonium salts **(1-4)** were synthesised by the Horner reaction[32] by treating the bromoarylalkenes **(26, 27, 30, 35)** with triphenylphosphine and nickel (II) bromide under reflux in benzonitrile, (scheme 6). The phosphonium salt solutions were poured into water and extracted several times with dichloromethane, prior to isolation and purification either by trituration with dry diethyl ether or column chromatography.
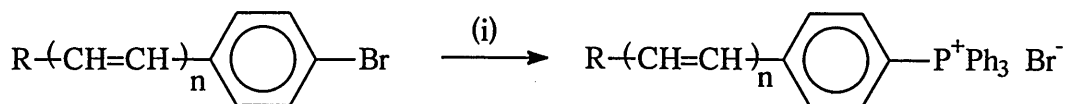
(30) R = ferrocenyl	(1) R = ferrocenyl
(35) R = 2-thienyl	(2) R = 2-thienyl
(26) R = p-Me$_2$NC$_6$H$_4$(n = 1)	(3) R = p-Me$_2$NC$_6$H$_4$(n = 1)
(27) R = p-Me$_2$NC$_6$H$_4$(n = 2)	(4) R = p-Me$_2$NC$_6$H$_4$(n = 2)

(i)   Ph$_3$P, NiBr$_2$, PhCN, reflux, N$_2$, *ca.* 4hrs

Scheme 6

The dimethylaminostilbene phosphonium salt (3) was obtained as an orange solid, and the related dienylphosphonium salt (4) was obtained as a bright red crystalline solid. The ferrocenyl phosphonium salt (1) was isolated as a purple solid, as were the other ferrocenyl phosphonium compounds described in the literature.[9,10,11,14,15] The thiophene salt (2) was a very pale yellow solid.

4.3 Synthesis of the phosphine oxides.

The phosphine oxides (6-9) were obtained by the hydrolysis of the phosphonium salts (1-4) in refluxing aqueous ethanol with an excess of aqueous sodium hydroxide, (scheme 7). Once cooled, the reaction mixture was poured into water and extracted several times with dichloromethane, and removal of the solvent left the impure phosphine oxides.
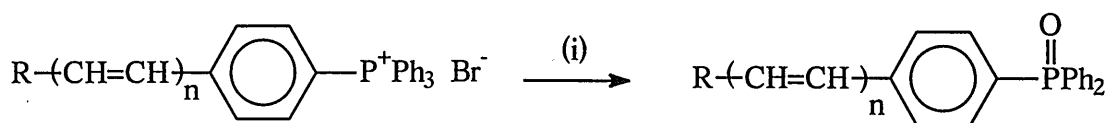
(i)   NaOH (aq), EtOH (aq), reflux, 1-2 hrs

(1) R = ferrocenyl	(6) R = ferrocenyl
(2) R = 2-thienyl	(7) R = 2-thienyl
(3) R = p-Me$_2$NC$_6$H$_4$(n = 1)	(8) R = p-Me$_2$NC$_6$H$_4$(n = 1)
(4) R = p-Me$_2$NC$_6$H$_4$(n = 2)	(9) R = p-Me$_2$NC$_6$H$_4$(n = 2)

Scheme 7

188

In comparison PONS-E (8), already reported in the literature, was synthesised as shown in scheme 8.[4] The synthon bromide was prepared in a similar manner to that of (26) prepared for the reaction with triphenylphosphine to form the salt (3). The crude phosphine was prepared by treating the aryl lithium reagent derived from the synthon bromide with chlorodiphenylphosphine, and then oxidising this phosphine to the phosphine oxide with hydrogen peroxide. The *cis-trans* isomeric mixture was converted to the *trans*-isomer only, by heating under reflux in toluene with a crystal of iodine.

Br—⟨O⟩—CH$_2$P$^+$Ph$_3$ Br$^-$ $\xrightarrow{\text{(i)}}$ Br—⟨O⟩—CH=CH—⟨O⟩—NMe$_2$

$\downarrow$ (ii)

$$Ph_2\overset{\overset{\textstyle O}{\|}}{P}\text{—⟨O⟩—CH=CH—⟨O⟩—}NMe_2$$

(cis and trans)

$\downarrow$ (iii)

$$Ph_2\overset{\overset{\textstyle O}{\|}}{P}\text{—⟨O⟩—CH=CH—⟨O⟩—}NMe_2$$

(trans)

(8)
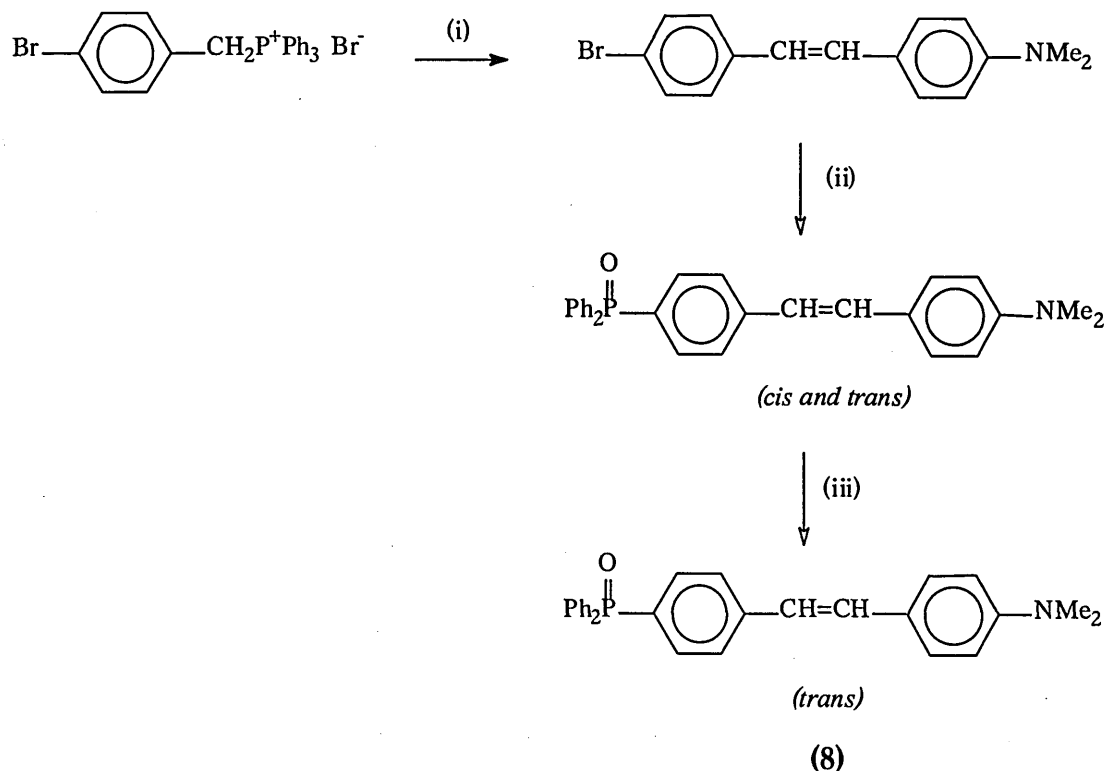
(i)   Li$^+$EtO$^-$, 4-dimethylaminobenzaldehyde

(ii)   BuLi, -60°C, THF then Ph$_2$PCl then H$_2$O$_2$

(iii) Toluene, I$_2$, reflux, 1hr.

Scheme 8

The mechanism (as well as the kinetics) of the alkaline hydrolysis of phosphonium salts has been greatly studied[33-39] and involves four steps to give a phosphine oxide and a hydrocarbon, (scheme 9).

The first step is the reversible addition of the hydroxide ion to the phosphorus atom of the quaternary phosphonium salt. Step (2) involves the fast reversible formation of the conjugate base of the intermediate, where the phosphorus atom is pentacovalent. The formation of the phosphine oxide and the carbanion are seen in the rate determining

189

step (3). Finally step (4) involves the fast protonation of the carbanion to the appropriate hydrocarbon by (the solvent) water.

$$R_4P^+ \quad + \quad OH^- \quad \overset{rapid}{\rightleftharpoons} \quad R_4P.OH \qquad (1)$$

$$R_4P.OH \quad + \quad OH^- \quad \overset{rapid}{\rightleftharpoons} \quad R_4P.O^- \quad + \quad H_2O \qquad (2)$$

$$R_4P.O^- \quad \overset{slow}{\longrightarrow} \quad R_3P=O \quad + \quad R^- \qquad (3$$

$$R^- \quad + \quad H_2O \quad \overset{fast}{\longrightarrow} \quad RH \quad + \quad OH^- \qquad (4$$
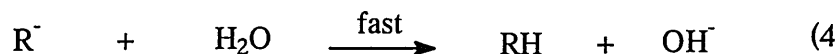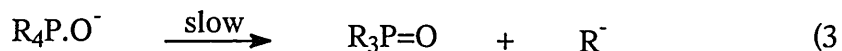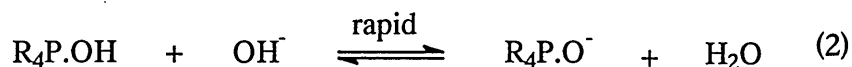
Scheme 9

Investigations into the kinetics of the above mechanism have established that a third order rate law is followed (rate α $[R_4P^+]$ $[OH^-]^2$). The relative ease of the departure of the R group (hydrocarbon) in the rate determining step (3) depends on its stability as a carbanion; the more stable the carbanion, the easier its departure. A benzyl group departs more easily than a phenyl,[34] methyl,[34] ethyl,[34] ferrocenyl[39] and a p-methoxybenzyl[39] group, but departs less easily than a m-bromobenzyl[35] or a p-chlorobenzyl[35] group.

Other factors that affect the rate of the reaction are the nature of the non-departing groups. Electron-withdrawing groups accelerate the reaction, whereas electron-donating substituents tend to retard the reaction, because of their inductive effects on the position of the equilibrium in steps (1) and (2).

The effects of thienyl, (and furyl) substituents on phosphonium salts have been investigated,[37,38] and it was seen that the rate of hydrolysis was markedly increased for both the 2-thienyl phosphonium salts **(36)** and **(37)**[38] and the 2-furyl phosphonium salts **(38)** and **(39)**[38] compared to the triphenylphosphonium salt analogues.
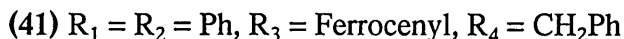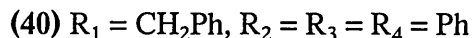
| X = S **(36)** | X = S **(38)** |
| X = O **(37)** | X = O **(39)** |

In the hydrolysis of the triheteroarylphosphonium salts (36-39), the heteroaryl entity was the leaving group, forming the hydrocarbons thiophene and furan, but in the case of the triphenylphosphonium salt analogues, benzyl was the leaving group forming toluene and triphenylphosphine oxide. Due to the increased rate of hydrolysis for (36-39), and the course of the reaction compared to the triphenylphosphonium salt analogues, it was seen that the 2-thienyl and 2-furyl carbanions are more stable than the benzyl carbanion. The very rapid hydrolysis of the salts shows that the two heteroaryl groups have a powerful electron withdrawing character due to the electronegative sulphur and oxygen atoms.

The 2-thienyl (methyl) phosphonium salt (36) and the 2-thienyl (benzyl) phosphonium salt (37) hydrolysed respectively 1.45×10^8 and 2.5×10^5 times more rapidly than the triphenylphosphonium salt analogues. The 2-furyl phosphonium salts (38) and (39) were found to hydrolyse $10^2 - 10^3$ times faster than the 2-thienyl analogues (36) and (37), this being due to the greater electron withdrawing capacity of furan compared to thiophene.

McEwen *et al* have investigated the effect of ferrocenyl groups on the decomposition of quaternary phosphonium hydroxides.[39] It was seen that a slower rate of alkaline hydrolysis was observed for the ferrocenyl phosphonium salts (41-43) compared to the rates of hydrolysis of typical phenyl phosphonium salt (40).

$$
\begin{array}{c}
R_1 \\
| \\
P^+ \quad\quad I^- \\
R_2 \diagup \; | \; \diagdown R_4 \\
R_3
\end{array}
$$

(40) $R_1 = CH_2Ph$, $R_2 = R_3 = R_4 = Ph$

(41) $R_1 = R_2 = Ph$, $R_3 = $ Ferrocenyl, $R_4 = CH_2Ph$

(42) $R_1 = Ph$, $R_2 = R_3 = $ Ferrocenyl, $R_4 = CH_2Ph$

(43) $R_1 = R_2 = R_3 = $ Ferrocenyl, $R_4 = CH_2Ph$
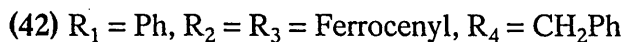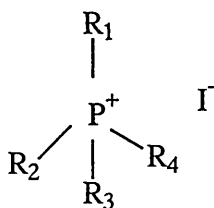
It has been proposed that the addition of the hydroxide ion to the phosphonium atom in the first step is inhibited due to some type of stabilising interaction between the ferrocenyl group and the cationic phosphorus which decreases the electrophilic

reactivity of the phosphonium atom. It was thought that this stabilising interaction was caused by the overlap of the nonbonding electrons of the ferrocenyl group with the 3d orbitals of the phosphorus atom and that the relatively slow rate of alkaline hydrolysis of ferrocenyl phosphonium salts is due to steric effects rather than to electronic effects has been ruled out.[40,41] It was also observed that the hydrolysis reactions were slower with an increase in the number of ferrocenyl moieties attached to the phosphorus atom. For example, salt (41), with only one ferrocenyl moiety attached to the phosphorus atom, hydrolyses approximately five times faster than salt (43) with three ferrocene moieties.

Only the benzyl and the phenyl groups were seen to leave on the hydrolysis of the salts (40-43) producing benzene and toluene as the hydrocarbons respectively. Far more toluene was formed compared to benzene, showing benzyl to be a more favourable leaving group (i.e. more stable carbanion) compared to phenyl. As ferrocene was not formed in any of the hydrolysis experiments, the ferrocenyl carbanion is not as stable as benzyl or phenyl carbanions.

For compounds (1&2) in the present study, even though the ferrocene and the thiophene moieties were not directly attached to the phosphorus atom as with (41-43) and (36) and (38), it was interesting to see the effect of these moieties on the stability of the carbanion derived from the substituent directly attached to the phosphorus. If the anion was more stable than the phenyl carbanion very little phosphine oxide would be formed and the product reaction mixture would consist mainly of the hydrocarbon (44-47) and triphenylphosphine oxide. Kinetic studies of these reactions were not carried out, as this was not the prime aim of the research but could be of interest in terms of identifying electronic effects of substituents on the mechanism.

The hydrolysis of the phosphonium salts (1-4) gave a mixture of products, which were investigated by TLC and GCMS. The phosphine oxides (6-9) (and benzene) were formed as principal products, together with smaller quantities of the hydrocarbons (44-47) (and triphenylphosphine oxide).

R =

	Hydrocarbon	Phosphine oxide
Ferrocenyl	(44)	(6)
Thienyl	(45)	(7)
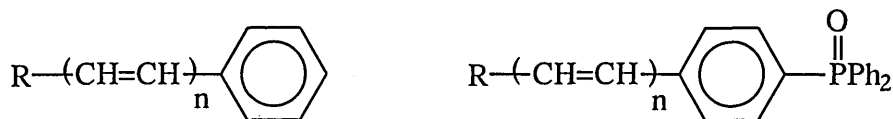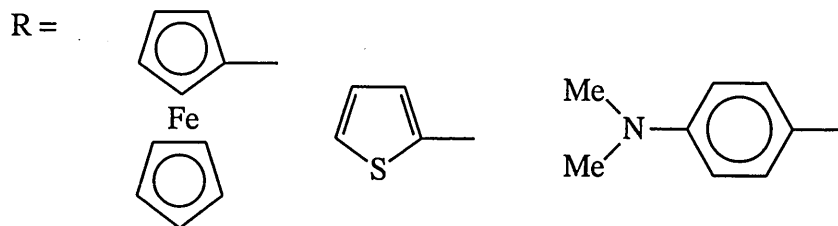
Hydrocarbon   (44)   (45)   n = 1 (46) n = 2 (47)

Phosphine oxide   (6)   (7)   n = 1 (8) n = 2 (9)

The ferrocenyl phosphine oxide (6) was obtained as a pale orange solid in comparison to the purple salt (1). The thienyl phosphine oxide (7) was obtained as a very pale yellow solid, similar to the salt (2). The dimethylaminostilbene phosphine oxide (8) (n = 1) was a yellow solid, and the most drastic colour change was seen for (9) (n = 2) where the bright red salt (4) turned bright yellow instantly on the addition of sodium hydroxide to the reaction mixture.

4.4 Characterisation of the phosphonium salts.

The ^{31}P NMR spectrum of each of the triphenylphosphonium salts (1-4) consisted of a single resonance peak in the region expected for tetraarylphosphonium salts, as shown in table 1.

Salt	Chemical Shift (ppm)
(1)	22.42
(2)	22.35
(3)	22.25
(4)	22.29

Table 1 ^{31}P NMR signals for salts (1-4) in $CDCl_3$.

The proton NMR spectra were also consistent with the expected structures. All the salts exhibited the required molecular cation by accurate mass (FAB) spectrometry.

4.5 Characterisation of the phosphine oxides.

The phosphine oxides (6-9) were all obtained in their crude form. GCMS studies showed all the phosphine oxides to contain the respective hydrocarbon impurities (44-47) and triphenylphosphine oxide in varying amounts, but some of the phosphine oxides themselves were not observable by GCMS as they were too involatile. In these cases,

193

electron impact mass spectrometry gave evidence of the formation of the phosphine oxides.

TLC of the crude solids showed all of the phosphine oxides to contain a small amount of the related hydrocarbon, and the intense bullet shaped spots (less polar than the original salt spot) were at the same r.f. value as triphenylphosphine oxide in all solvent systems tested. This led to a problem in the purification process; the hydrocarbons were easily and successfully isolated, but separating the phosphine oxides from triphenylphosphine oxide proved difficult. However, after repeated column chromatography, (6-9) were isolated as the pure phosphine oxides.

All the hydrocarbons (44-47) were characterised to some extent, depending on the amount of hydrocarbon isolated.

Each of the phosphine oxides gave a single sharp resonance in the ^{31}P NMR spectrum as shown in table 2, and have a very similar chemical shift to that of triphenylphosphine oxide.

| Phosphine oxide	Chemical Shift (ppm)
(6)	29.02
(7)	28.63
(8)	29.17
(9)	28.80
Triphenylphosphine oxide	28.76

Table 2 ^{31}P NMR data for phosphine oxides (6-9) in CDCl$_3$.

^{1}H NMR spectra of the phosphine oxides (6-9) [and the related hydrocarbons (44-47)] were also consistent with their proposed structures. Accurate mass (EI) spectrometry of the phosphine oxides confirmed the composition of the molecular ion.

4.6 Solvatochromism studies.

UV/Visible studies were carried out on the salts (1-4) and the phosphine oxides (6-9) at room temperature and pressure using analytical grade (Aldrich) solvents. The results are shown in tables 3-10 for concentrations at *ca.* 1×10^{-4} mol l^{-1}.

The ferrocenyl phosphonium salt (1) showed essentially two absorption bands in the region 300-800 nm. The band at *ca.* 335 nm was a lot stronger than the band at *ca.* 485 nm, which could only be seen in more concentrated solutions. The only significant change in λ_{max} was observed in dichloromethane with a hypsochromic shift of 12-14 nm for the low-energy absorption band (from *ca.* 485 nm) and a hypsochromic shift of 4-6 nm (from *ca.* 335 nm) for the high-energy absorption band. However, this compound also shows reverse solvatochromism, exhibiting a bathochromic shift of 22 nm in going from dichloromethane to THF.
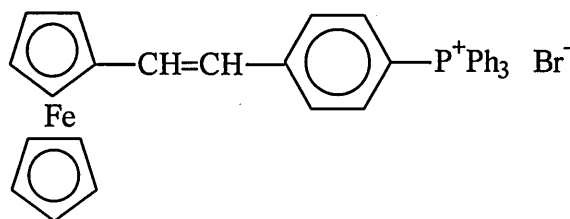
(1)

Solvent	Colour	Wavelength λ_{max} nm	$v_{max} \times 10^3$ cm^{-1} for λ_{max} *ca.* 485nm
Methanol	red	336, 486	20.58
Acetonitrile	"	334, 484	20.66
Acetone	"	336, 486	20.58
Dichloromethane	dark red	340, 498	20.08
Tetrahydrofuran	pale red*	336, 476	21.00
Δ (DCM-MeOH)		4 12	-0.5

$\Delta v = v_{nonpolar} - v_{polar}$ *not completely soluble

Table 3   Solvatochromism data for salt (1) in various solvents.

For the absorption properties of the ferrocenyl stilbene (12) ($Y = NO_2$) ($R_1 = H$) three bands in heptane were reported (320, 406, 462 nm) whereas in DMF only two bands were observed (340 and 492 nm).[9]

For the ferrocenylaldimine (14), where Y was a variety of acceptor groups, generally two bands were observed in the region between 300 nm and 750 nm.[14] Generally smaller shifts were observed in the position of the high-energy band (ca. 310 nm), whilst quite large solvatochromic shifts were observed for the low-energy band (ca. 450 nm). All the shifts for the low-energy band were bathochromic (except Y = CN or F) with (16) and (14) (Y = NO$_2$) having shifts of 19 nm and 13 nm respectively from diethyl ether to DMF. The absorption bands at ca. 310 nm only shifted by between 1-4 nm. Similarly two absorption bands for the triflate salt (13) were observed in acetonitrile at 362 nm and 551 nm.[11]

Calabrese et al reported the nonlinear optical properties of metallocenes of the form [M(C$_5$X$_5$)(C$_5$H$_4$-(CH=CH)$_n$-(C$_6$H$_4$Y-p)] (M = Fe or Ru, X = Me or H, n = 1 or 2, Y = CN or NO$_2$), for which the visible absorption spectra also showed two bands.[42] Using extended-Hückel molecular orbital calculations,[42] the lower energy transition of these metallocenes was assigned to metal to ligand charge-transfer and the higher energy transition was assigned to essentially π-π^* transitions (with some metal character).[42]

For the phosphonium salt (1), negative solvatochromism (from methanol to dichloromethane) suggests the stability of the ground state (48A) in polar solvents with respect to the quinoidal excited state (48B), and the reverse is true from dichloromethane to THF.

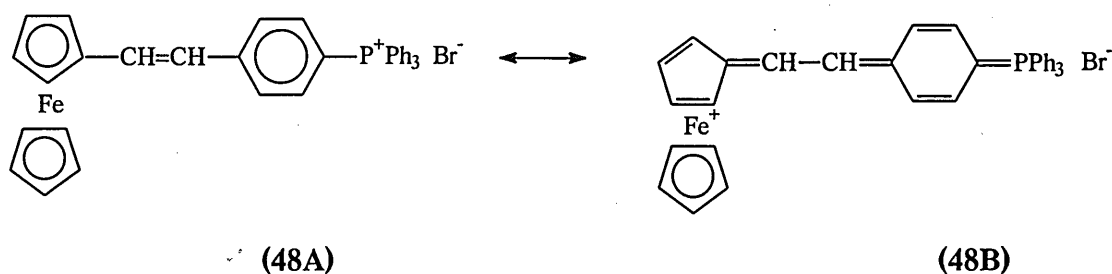
Figure 2

Salt (2) shows very little solvatochromism compared to (1), suggesting that the 2-thienyl system is not as an efficient electron-donor as ferrocenyl. As with (1), the wavelength only seems to change in dichloromethane for which a hypsochromic shift of only 6 nm is observed. This suggests that (49A) is more stable in polar solvents relative to the quinoidal structures (49B) and (49C).
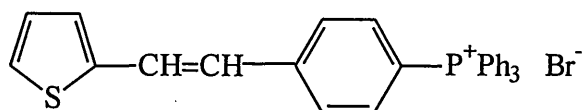
(2)

Solvent	Colour	Wavelength λ_{max} nm	$\nu_{max} \times 10^3$ cm^{-1}
Methanol	pale yellow	352	28.41
Acetonitrile	"	350	28.57
Acetone	"	352	28.40
Dichloromethane	"	358	27.93
Tetrahydrofuran	"*	354	28.23
Δ (DCM-MeOH)		6	-0.41

$\Delta \nu = \nu_{nonpolar} - \nu_{polar}$

* not completely soluble

Table 4 Solvatochromism data for salt (2) in various solvents.
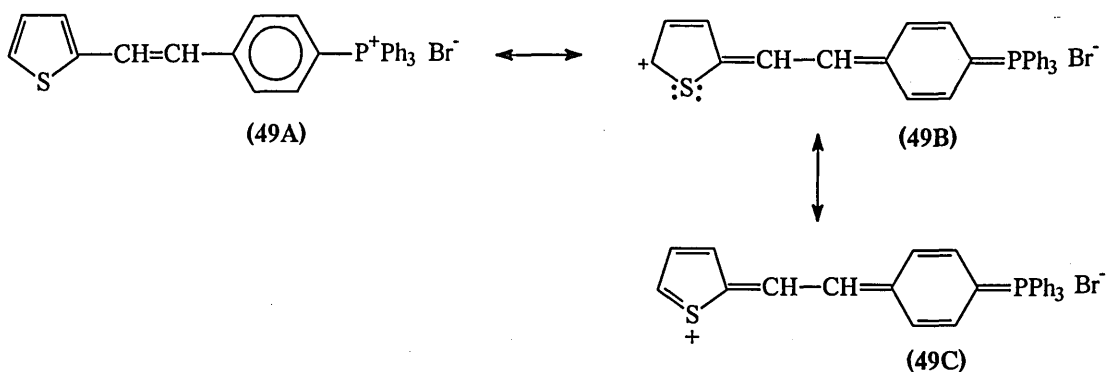
Figure 3

Similarly for salts (3) and (4), very little solvatochromism was also observed in passing from methanol to acetone; however a hypsochromic shift of 16 nm for (3) and 18 nm for (4) was observed in going from acetone to dichloromethane. A bathochromic shift of 14 nm was also observed on going from dichloromethane to THF for both (3) and (4). A red shift in the absorption band on increasing the extent of conjugation of the π-electron bridge. In dichloromethane and THF, the absorption maximum of (4) is

197

increased by 20 nm compared to that of (3). This red shift is between 16 nm and 18 nm for the other solvents.

$$Me_2N-\text{C}_6\text{H}_4-CH=CH-\text{C}_6\text{H}_4-P^+Ph_3 \quad Br^-$$

(3)

Solvent	Colour	Wavelength λ_{max} nm	ν_{max} x 10^3 cm^{-1}
Methanol	pale yellow	406	24.63
Acetonitrile	"	404	24.75
Acetone	"	406	24.63
Dichloromethane	"	422	23.70
Tetrahydrofuran	"*	408	24.51
Δ (DCM-MeOH)		16	-0.93

$\Delta\nu = \nu_{nonpolar} - \nu_{polar}$

* not completely soluble

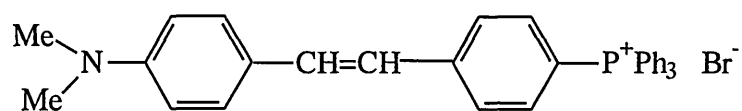**Table 5**   Solvatochromism data for salt (3) in various solvents.

198

$$Me_2N-C_6H_4-(CH=CH)_2-C_6H_4-P^+Ph_3 \quad Br^-$$
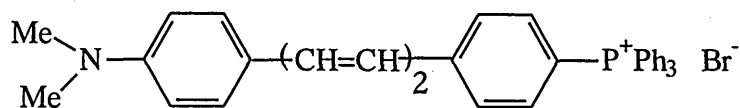
<div align="center">(4)</div>

Solvent	Colour	Wavelength λ_{max} nm	$\nu_{max} \times 10^3$ cm^{-1}
Methanol	gold	422	23.70
Acetonitrile	"	420	23.81
Acetone	"	424	23.58
Dichloromethane	"	442	22.62
Tetrahydrofuran	"*	428	23.36
Δ (DCM-MeOH)		20	-1.08

$\Delta\nu = \nu_{nonpolar} - \nu_{polar}$

* not completely soluble

<div align="center">Table 6   Solvatochromism data for salt (4) in various solvents.</div>

For both (3) and (4), the observation of negative solvatochromism from methanol to dichloromethane reflects the stabilisation of the ground state (50A) in the polar solvents relative to the excited state (50B). Positive solvatochromism from dichloromethane to THF shows the stabilisation of the quinoidal structure (50B) relative to (50A) in the nonpolar solvents.

$$Me_2N-C_6H_4-CH=CH-C_6H_4-P^+Ph_3 \quad Br^- \longleftrightarrow Me_2\overset{+}{N}=C_6H_4=CH-CH=C_6H_4=PPh_3 \quad Br^-$$

<div align="center">(50A)   (50B)</div>
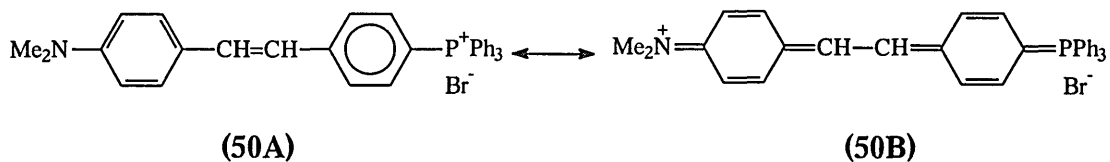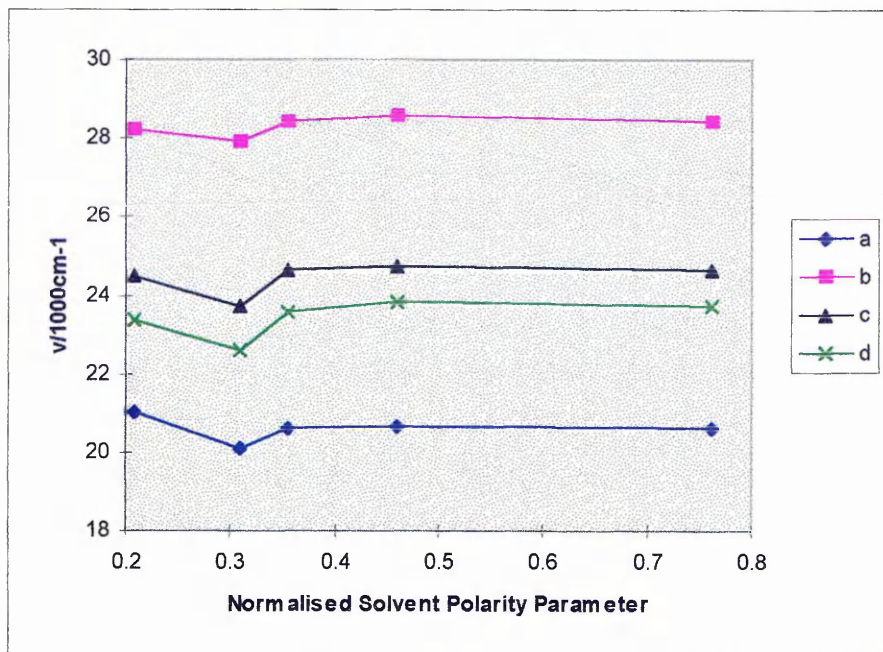
<div align="center">Figure 4</div>

A plot of wavenumber ν against the normalised empirical solvent polarity parameter E_T^N is shown in figure 5 for the phosphonium salts (1-4). The salts behave in an identical manner in all the solvents indicating that they are solvated in a similar manner in solution with respect to the ground and excited states.

<div align="center">199</div>

a = (1), b = (2), c = (3), d = (4)

Figure 5 Plot of longest wavenumber visible absorption band against the normalised solvent polarity parameter.

For the phosphine oxide (6) with ferrocene as the donor solvatochromism was not observed. Only one band was seen at *ca.* 320 nm (in methanol and THF), but an additional band 466 nm was observed in dichloromethane. On going from the salt (1) to the phosphine oxide (6) a blue shift was observed, where λ_{max} is at a lower wavelength by 18 nm (high-energy absorption band) and 32 nm (low-energy absorption band) respectively.

(6)
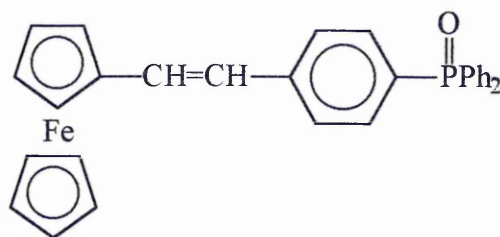
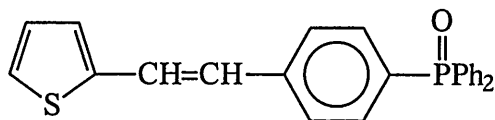| Solvent	Colour	λ_{max} nm
Methanol	Orange	322
Dichloromethane	"	324, 466
Tetrahydrofuran	"	322

Table 7 Solvatochromism data for phosphine oxide (6) in various solvents.

200

Essentially no solvatochromism is observed for the phosphine oxides **(7-9)**, (tables 8-10). This suggests that the neutral phosphine oxide is not as great an electron acceptor as the positive phosphonium moiety.
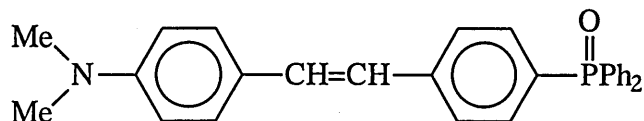

(7)

Solvent	Colour	λ_{max} nm
Methanol	Pale yellow	336
Dichloromethane	"	338
Tetrahydrofuran	"	338

Table 8 Solvatochromism data for phosphine oxide (7) in various solvents.

The phosphine oxide **(8)** also exhibits a blue shift compared to its related salt **(3)**. The UV/Visible data for compound **(8)** has been reported in the literature[3] and the λ_{max} are: cyclohexane 367.5 nm, dichloromethane 378 nm (and 484 nm), acetone 376 nm, DMF 379 nm and DMSO 383.5nm. All λ_{max} are very similar apart from in cyclohexane and DMSO, and a bathochromic shift of 16 nm was observed in the latter. A λ_{max} of 374 nm was observed in dichloromethane in the present study.

(8)

Solvent	Colour	λ_{max} nm
Methanol	Pale yellow	370
Dichloromethane	"	374
Tetrahydrofuran	"	370

Table 9 Solvatochromism data for phosphine oxide (8) in various solvents.

An increase in conjugation length of the π-electron bridge between the donor and acceptor of phosphine oxides **(8)** and **(9)** produced a red shift as with the

201

phosphonium salts (3) to (4). In the three solvents employed for the study the increase in the absorption maximum was *ca.* 20-26 nm. However, again no solvatochromic behaviour was observed.

$$Me_2N\text{—}C_6H_4\text{—}(CH=CH)_2\text{—}C_6H_4\text{—}PPh_2=O$$

(9)
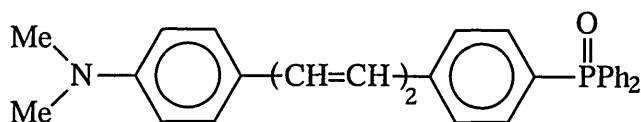
Solvent	Colour	λ_{max} nm
Methanol	Fluorescent yellow	394
Dichloromethane	"	396
Tetrahydrofuran	"	396

Table 10 Solvatochromism data for phosphine oxide (9) in various solvents.

4.7 Future Developments

It would be interesting to measure the first order hyperpolarisabilities (β) for the above compounds with a view to measuring any SHG properties.

In view of the results on the compounds discussed earlier in chapter 2 it might be useful to synthesise a range of naphthyl and anthracenyl analogues of the phosphonium salts (1-4) and phosphine oxides (6-9), as they would have a greater potential for the polarisability of the π-electron system. For systems (3) and (4) and the respective phosphine oxides (8) and (9) the naphthyl or anthracenyl unit could be at the donor end of the molecule as in the naphthyl system (51) or at the acceptor end of the molecule as in the anthracene system (52). Alternatively such units could be at both the donor and acceptor end of the molecule.

DONOR—CH=CH—ACCEPTOR

(51)

202
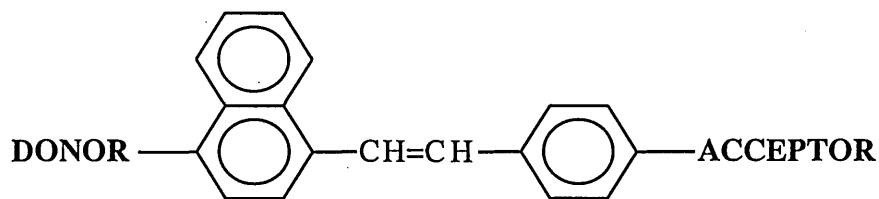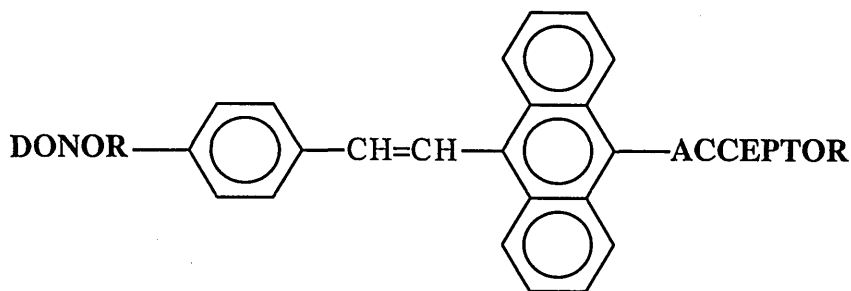
Donor = $(Me)_2N$ Acceptor = Ph_2PO or $Ph_3P^+ Br^-$

(52)

4-Dimethylaminonapthaldehyde is available commercially and so an analogue of **(51)** with a naphthyl unit at the donor end of the molecule could be very easily synthesised.

Concerning the ferrocenyl- **(1)** and the thienyl- phosphonium salts **(2)** and the respective phosphine oxides **(6)** and **(7)**, a naphthyl or anthracene unit would have to be employed at the acceptor end of the molecule as in **(53)**.
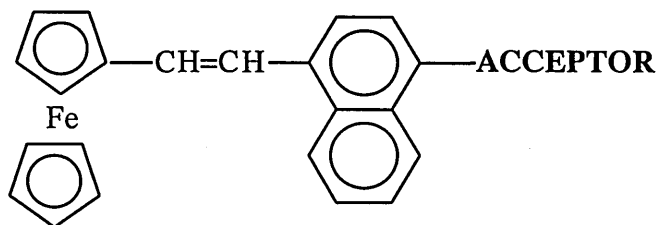
Acceptor = Ph_2PO or $Ph_3P^+ Br^-$

(53)

A theoretical study on naphthylphenylacetylenes has been reported,[43] together with some preliminary experimental data[44] and comparisons made with the well studied diphenylacetylenes. Theoretical calculations were carried out on **(54)**, varying the electron-acceptor and electron-donor groups, and altering the conjugation lengths (number of triple bonds). It was seen that the naphthyl systems had larger hyperpolarisabilities β compared to the diphenyl analogues, e.g. $D = NH_2$ and $A = NO_2$ (naphthyl) $\beta\mu = 39.2 \times 10^{-30}$ esu compared to (phenyl) $\beta\mu = 35.4 \times 10^{-30}$ esu. However the increase was not great, and it was thought that as far as charge-transfer was concerned the naphthyl ring may not be as efficient as the phenyl ring.

203

$$n = 1\text{-}5$$
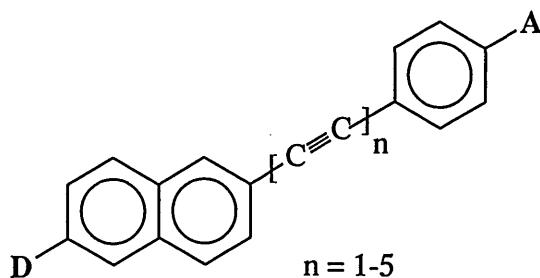
(54)

Another advantage of naphthyl systems over their phenyl counterparts is that the introduction of a naphthyl unit into the backbone would probably lead to a noncentrosymmetric structure, which is an essential condition for observation of second-order nonlinearity.

Increasing the conjugation length had a more dramatic effect on the hyperpolarisabilities of the naphthylphenylacetylenes. For example where $D = NH_2$ and $A = NO_2$ (n = 1) $\beta = 39.2$ x 10^{-30} esu compared to (n = 5) $\beta = 69.6$ x 10^{-30} esu. It would therefore be interesting to make the acetylene range of the phosphonium salts (1-4) and phosphine oxides (6-9), (both phenyl and naphthyl), e.g. (55) and investigate the effect of increasing the conjugation length.
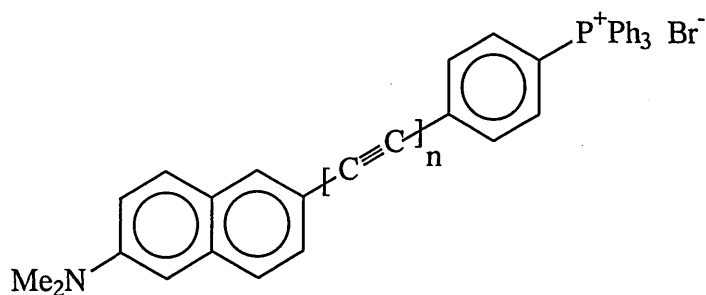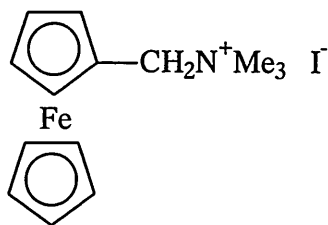

(55)

If the hyperpolarisabilities β of the phosphonium salts (phenyl or naphthyl) were to be measured in the future, it would be advantageous to vary the anion, as earlier work with compound (13) has shown.[11]

4.8 Experimental

### (28) Ferrocenylmethyltrimethylammonium iodide

(Dimethylaminomethyl)ferrocene (10 g, 0.004 mol) was stirred at room temperature in dry acetonitrile (50 ml). Methyl iodide (11.36 g, 0.08 mol) was added dropwise slowly and allowed to stir at room temperature for three hours, and then heated under reflux for a further hour. The solvent was evaporated in vacuo, and the residual solid triturated several times with fresh diethyl ether to afford a brown solid. Yield 15.15 g, 98 %.

mp 150-180 °C (decomp.)

^{1}H NMR (CDCl$_3$): δ 3.29(s, 9H, -Me$_3$), 4.29(s, 5H, cyclopentadienyl), 4.48(s, 2H), 4.88(s, 2H).

MS(FAB) (M$^+$ cation) 257.9.

(29) Ferrocenylmethyltriphenylphosphonium iodide
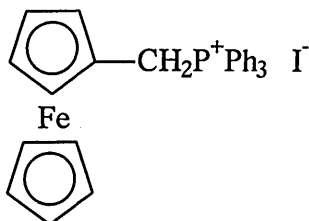
(28) (10 g, 0.026 mol) was allowed to react with triphenylphosphine (13.6 g, 0.052 mol) in acetonitrile under reflux (100 ml) for eight hours. The reaction mixture was allowed to cool and the acetonitrile evaporated in vacuo to afford a sticky solid. The solid was triturated with fresh diethyl ether several times to remove any unreacted triphenylphosphine. The solid was filtered to afford a beige-orange powder. Yield 12.66 g, 83 %.
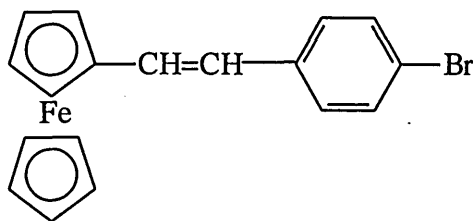
mp 150-180 °C (decomp.)

^{31}P NMR (CDCl$_3$): 18.87 ppm

^{1}H NMR (CDCl$_3$): δ 3.96 and 4.04(d, ferrocene), 4.33(s, ferrocene), 4.93(d, 2H, -P$^+$CH$_2$), 7.62-7.80(m, 15H, aromatic).

MS(FAB) (M$^+$ cation) 460.

(30) 1-Ferrocenyl-2-(4-bromophenyl)ethene

Phosphonium salt **(29)** (6.00 g, 0.01 mol) was allowed to stir with 4-bromobenzaldehyde (1.85 g, 0.01 mol) in dry THF (50 ml). Potassium tertiary butoxide (1.24 g, 0.011 mol) was added, whereupon the reaction mixture turned orange. The mixture was poured into a large volume of water, where a red oily solid precipitated out. The solid was filtered and allowed to dry. The product was isolated by column chromatography using dichloromethane as the eluting solvent. The dark orange solid was dried under reduced pressure. Yield 1.77 g, 48 % (*cis-trans* isomer mix).

Alternatively solvent extraction of the reaction mixture with diethyl ether (3 x 50 ml) and water (200 ml) was found to be a cleaner procedure to isolate the product. The organic layer was dried (MgSO$_4$) and the diethyl ether evaporated off in vacuo. A red oil remained which afforded pure **(30)** when triturated in methanol and filtered to give once more a dark orange solid. Yield 2.1 g, 52 % (*cis-trans* isomer mix).

mp 125-128 °C

^{1}H NMR (CDCl$_3$): δ 4.15(s, 5H, cyclopentadienyl), 4.30(s, 2H), 4.46(s, 2H), 6.60-6.67(d, 1H, olefinic, J = 17.58Hz), 6.85-6.91(d, 1H, olefinic, J = 15Hz), 7.28-7.32(d, 2H, aromatic, J = 10Hz), 7.44-7.47(d, 2H, aromatic, J = 1.54Hz).

MS (EI) (M$^+$) 364.9 and 366.9.
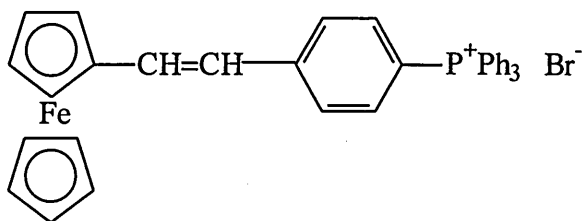
Exact mass calculated for C$_{18}$H$_{15}$^{79}Br^{56}Fe: 365.97064 Found: 365.97097

C$_{18}$H$_{15}$^{81}Br^{56}Fe: 367.96860 Found: 367.96697

C$_{18}$H$_{15}$BrFe requires: C, 58.90; H, 4.12%. Found: C, 58.82; H, 4.14%.

(4) 1-Ferrocenyl-2-(4-triphenylphosphoniophenyl)ethene bromide

The bromophenylalkene **(29)** (1.57 g, 0.0043 mol) was heated under reflux with triphenylphosphine (1.69 g, 0.0065 mol) and nickel (II) bromide (0.47 g, 0.0021 mol) in benzonitrile (37 ml) for four hours under nitrogen. The solution remained a deep red in colour instead of turning the usual bottle green. Once cooled, solvent extraction was carried out with dichloromethane and aqueous KBr (10 %). The organic layer was dried $(MgSO_4)$ and the solvent was evaporated in vacuo.

The remaining benzonitrile mixture was poured into diethyl ether and the solid precipitated was triturated many times with fresh diethyl ether. On filtering, the solid was found to be very hygroscopic, and therefore the salt **(4)** was purified and isolated as a red crystalline solid by column chromatography with an eluting solvent of dichloromethane/methanol. The solid was dried under reduced pressure. Yield 0.38 g, 14 %.

mp > 75 °C (decomp.)

^{31}P NMR $(CDCl_3)$: 22.42 ppm

^{1}H NMR $(CDCl_3)$: δ 4.16(s, 5H, cyclopentadienyl), 4.39(s, 2H), 4.53(s, 2H), 6.83-6.90(s, 1H, olefinic, J = 17.5Hz), 7.32-7.38, (1H, olefinic, J = 15Hz), 7.52-7.92(m, 19H, aromatic).

Accurate (FAB) Exact mass calculated for $C_{36}H_{30}FeP$: 549.09376. Found: 549.09369 (0.00 ppm).

(31) 2-Thienylmethyl(trimethyl)ammonium iodide
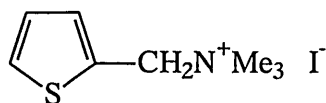
Methyl iodide (31 g, 0.22 mol) was added dropwise to 2-(dimethylaminomethyl)thiophene (15 g, 0.11 mol) in acetonitrile (100 ml) and stirred at room temperature overnight. The acetonitrile and the excess methyl iodide were evaporated in vacuo to leave a cream-yellow solid, which was triturated several times in

fresh diethyl ether to afford a pale yellow solid, which was dried under vacuum at room temperature. Yield 27.39 g, 88 %.

mp 145-147 °C

^{1}H NMR δ (CDCl$_3$): 3.24 and 3.46(brs and s, 9H, -Me$_3$), 5.14 and 5.32(bs and s, 2H, -CH$_2$), 6.91-7.64(m, 3H, thiophene)

MS (FAB) (M$^+$ cation) 155.8.

(32) Attempted synthesis of 2-Thienylmethyl(triphenyl)phosphonium iodide

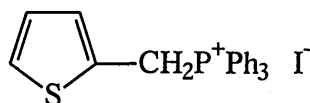The ammonium salt **(31)** (23.05 g, 0.08 mol) was heated under reflux with triphenylphosphine in acetonitrile (400 ml) for eight hours. The acetonitrile was evaporated off in vacuo and the pale cream solid triturated several times in fresh diethyl ether. Yield 22.18 g [recovered starting material **(31)**, with trace amount of **(32)**].

^{31}P NMR (CDCl$_3$): 21.28 ppm (very weak).

The recovered salt **(31)** was allowed to react with triphenylphosphine (41 g,) in acetonitrile (200 ml) for a further eight hours. [Salt **(31)** recovered unchanged].

The salt **(31)** (2 g, 0.007mol) was heated under reflux with triphenylphosphine (4.12 g, 0.0157 mol) in methanol (30 ml) for twelve hours. [The salt **(31)** was again recovered unchanged].

The salt **(31)** (1.84 g, 0.0065 mol) was heated under reflux with triphenylphosphine (3.40 g, 0.13 mol) in benzonitrile (50 ml) for twelve hours.
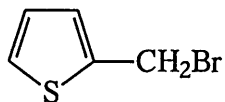
mp >210 °C (decomp.)

^{31}P NMR (CDCl$_3$): 21.29 ppm **(32)** and 21.18 ppm.

^{1}H NMR (CDCl$_3$): 5.42 - 5.47, (d, 2H, -CH$_2$), 6.7 - 7.8, (m, 18H, aromatic and thiophene).

MS(FAB) (M$^+$ cation) 358.2 (100%) , 277, 262, 183, 135, 96.

(33) 2-Bromomethylthiophene

2-Methylthiophene (5 g, 0.05 mol) was heated under reflux with NBS (recryst from H_2O) (8 g, 0.05 mol) and a crystal of AIBN for several hours in chloroform (100 ml). On cooling the insoluble succinimide was filtered, and the residual chloroform was evaporated off in vacuo. Crude (33) was used for the synthesis of (34) without purification.

(34) 2-Thienylmethyltriphenylphosphonium iodide
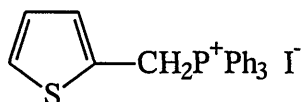
Crude (33) (8 g, 0.045 mol) was heated under reflux with triphenylphosphine (18 g, 0.07 mol) in acetonitrile (50 ml) for four hours under nitrogen. The solvent was evaporated off in vacuo, and the solid triturated with several portions of fresh diethyl ether to afford a cream solid. Yield 16.2 g, 74 %.

mp > 220 °C (decomp.)

^{31}P NMR ($CDCl_3$): 21.32 ppm.

^1H NMR ($CDCl_3$): δ 5.42-5.46(d, 2H, CH_2), 6.8-7.7(m, 18H, aromatic and thiophene).

MS (FAB) (M^+) cation 358.3 (base peak).

(35) 1-(4-Bromophenyl)-2-(2-thienyl)ethene
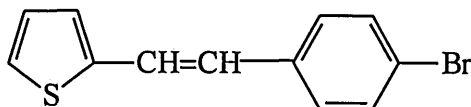
The salt (34) (9.79 g, 0.022 mol) was stirred with 4-bromobenzaldehyde (4 g, 0.022 mol) in dry THF (100 ml). Potassium tertiary butoxide (3.4 g, 0.03 mol) was added, and the reaction mixture stirred for four hours. The reaction mixture was poured into water (200 ml) and extracted with diethyl ether (3 x 50 ml). The yellow organic layer was dried ($MgSO_4$). The crude solid was washed with methanol until the washings went from pale yellow to colourless to afford a pale yellow solid. Yield 1.66 g, 28.5 %.

mp 144-146 °C

^{1} H NMR δ (CDCl$_3$): δ 6.83-7.49(m, 9H, aromatic and olefinic).

MS (EI) (M$^+$) 264 and 266.

C$_{12}$H$_9$SBr requires: C, 54.36; H, 3.42%. Found: C, 54.52; H, 3.50 %.

(2) 1-(2-Thienyl)-2-(4-triphenylphosphoniophenyl)ethene bromide
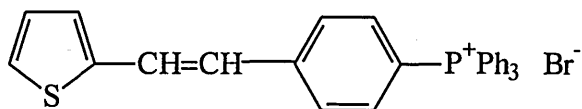
The bromo compound (35) (1.5 g, 0.0057 mol) was heated under reflux in benzonitrile (50 ml) with triphenylphosphine (3g, 0.01 mol) and nickel (II) bromide (0.63 g, 0.0029 mol) for eight hours under nitrogen to form a bottle green reaction mixture. The mixture was poured into aqueous KBr (10 %) (200 ml) and the product extracted with dichloromethane (3 x 50 ml). The yellow organic layer was dried (MgSO$_4$) and the solvent was evaporated in vacuo. The remaining benzonitrile mixture was poured into diethyl ether and triturated several times with fresh diethyl ether. The solid was filtered to afford a pale yellow powder. Yield 1.18 g, 60 %.

mp 310-312 °C (decomp.)

^{31}P NMR (CDCl$_3$): 22.35 ppm.

^{1}H NMR (CDCl$_3$): δ 6.50-6.55(d, 1H, olefinic, J = 12.5Hz), 6.75-7.89(m, 22H, aromatic and 1H olefinic).

MS (FAB) (M$^+$ cation -1) 446.

C$_{30}$H$_{24}$SPBr requires: C, 68.31; H, 4.59 %. Found: C, 68.02; H, 4.60 %.

(25) *p*-Bromobenzyltriphenylphosphonium bromide
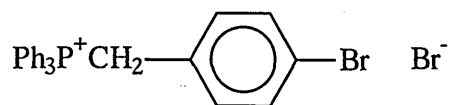
4-bromobenzylbromide (2 g, 0.008 mol) was allowed to react with triphenylphosphine (3.15 g, 0.012 mol) in acetonitrile (50 ml) at reflux for two hours. The solvent was evaporated in vacuo and the crude solid triturated several times with fresh diethyl ether, and filtered under suction to afford a white solid. Yield 4.1 g, 100 %.

mp 260-261 °C

^{31}P NMR (CDCl$_3$): 22.92 ppm

^{1}H NMR (CDCl$_3$): δ 5.5(d, 2H, -CH$_2$), 6.9-7.2(dd, 4H, aromatic), 7.5-7.8(m, 15H, aromatic).

MS (FAB) (M$^+$ cation) 430.8 and 431.8.

(26) 1-(4-Bromophenyl)-2-(4-dimethylaminophenyl)ethene
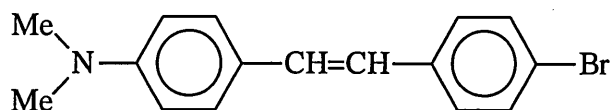
The salt (25) (10 g, 0.02 mol) was stirred with 4-dimethylaminobenzaldehyde (2.98 g, 0.02 mol) in dry THF (120 ml). Potassium tertiary butoxide (2.47 g, 0.022 mol) was added and the reaction mixture was left to stir overnight, during which time the reaction mixture turned from orange to pale yellow.

The reaction mixture was poured into water and the solid which precipitated out, was filtered under suction and recrystallised from dichloromethane or acetone to afford a pale yellow solid. (cis and trans isomers observed by GCMS). Yield 3.68 g, 61 %.

mp 224-230 °C

^{1}H NMR (CDCl$_3$): δ 2.90, ([weak], 6H, Me$_2$, Z-isomer), 3.03(s, 6H, Me$_2$, E-isomer), 6.65-7.12(m, 2H, olefinic), 7.31-7.62(m, 8H, aromatic).

MS (EI) (M$^+$) 300.9 and 301.9.

C$_{16}$H$_{16}$NBr requires: C, 63.59; H, 5.34; N, 4.63 %. Found: C, 63.53; H, 5.27; N, 4.42 %

(3) 1-(4-Dimethylaminophenyl)-2-(4-phenylphosphoniophenyl) bromide
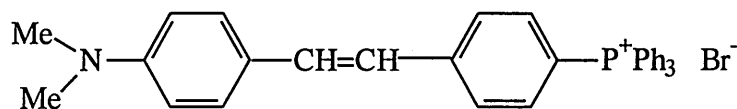
The bromostilbene (26) (3 g, 0.01 mol) was heated under reflux with triphenylphosphine (3.93 g, 0.015 mol) and nickel (II) bromide (1.09 g, 0.005 mol) in benzonitrile (70 ml) for four hours under nitrogen. The cooled reaction mixture was poured into aqueous KBr (10% w/v) (200 ml) and extracted with dichloromethane (3 x 50 ml). The combined organic layers were washed with KBr (aq), dried (MgSO$_4$), and the solvent was evaporated in vacuo. After repeated trituration of the oil with diethyl ether, a rusty-orange solid was obtained which was dried under vacuum. Yield 4.54 g, 94 %.

mp >70°C (decomp.)

^{31}P NMR (CDCl$_3$): 22.25 ppm.

^{1}H NMR δ (CDCl$_3$): δ 2.90(s [weak], 6H, Me$_2$, Z-isomer), 2.95(s, 6H, Me$_2$, E-isomer), 6.65-7.86(m, 25H, aromatic and olefinic).

^{13}C NMR (CDCl$_3$): 40.55, 112.13, 112.43, 117.53, 118.96, 121.1, 124.2,. 127.76, 127.76, 127.96, 129.02, 130.32, 131.04, 131.23, 134.54, 134.69, 135.31, 136.06, 146.34, 151.35 ppm

MS (FAB) Exact mass calculated for (M$^+$) cation C$_{34}$H$_{31}$NP: 484.219414. Found: 484.218048 (2.8 ppm).

C$_{34}$H$_{31}$NPBr.2H$_2$O requires: C, 68.00; H, 5.87; N, 2.33 %. Found: C, 67.84; H, 5.30; N, 2.32 %.

(27) 1-(4-Bromophenyl)-4-(4-dimethylaminophenyl)-1,3-butadiene
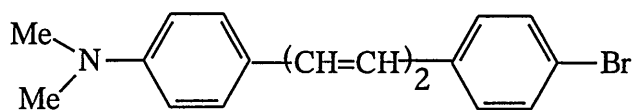
Salt **(25)** (16.6 g, 0.032 mol) was stirred with 4-dimethylaminocinnamaldehyde (5.68 g, 0.032 mol) in dry THF (120 ml) at room temperature. Potassium tertiary butoxide (4 g, 0.035 mol) was added, and left to stir overnight. The reaction mixture was poured into a large volume of water, and the solid filtered under suction. The crude solid was recrystallised from dichloromethane, and washed with a small amount of cold acetone to afford a pale yellow solid (*trans* isomer only from GCMS). Yield 2.1 g, 20 %.

mp 239-240 °C

^{1}H NMR (CDCl$_3$): δ 2.99(s, 6H, Me$_2$), 6.46-6.95(m, 4H, olefinic), 7.28-7.45(m, 8H, aromatic).

MS (EI) Exact mass calculated for (M$^+$) C$_{18}$H$_{18}$N^{79}Br: 327.06226 Found: 327.06000 (6.9 ppm).

C$_{18}$H$_{18}$NBr requires: C, 65.86; H, 5.53; N, 4.27 % Found: C, 65.74; H, 5.53; N, 4.21 %.

212

(4) 1-(4-Dimethylaminophenyl)-4-(4-triphenylphosphoniophenyl)-1,3-butadiene bromide
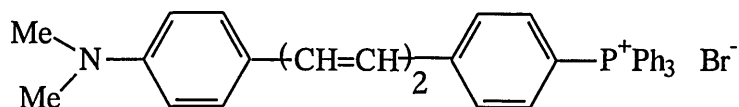
The diene **(27)** (2 g, 0.006 mol) was heated under reflux in benzonitrile (40 ml) with triphenylphosphine (2.36 g, 0.009 mol) and nickel (II) bromide (0.066 g, 0.003 mol) for four hours under nitrogen. The cooled reaction mixture was poured into aqueous KBr (10% w/v) (200 ml) and extracted with dichloromethane (3 x 50 ml). The combined organic layers were washed with KBr (aq), dried (MgSO$_4$) and the solvent was removed in vacuo. After repeated trituration of the oil with diethyl ether the filtered solid was found to be hygroscopic, and so was purified by flash chromatography using 10:90 MeOH:CH$_2$Cl$_2$ as the eluting solvent. A bright red crystalline solid was obtained. Yield 3.43 g, 97 %.

mp > 425 °C (decomp.)

^{31}P NMR (CDCl$_3$): 22.29 ppm.

^{1}H NMR (CDCl$_3$): δ 2.95(s, 6H, Me$_2$), 6.62-6.80(m, 4H, olefinic), 7.34-7.92(m, 23H, aromatic).

^{13}C NMR (CDCl$_3$): 40.59, 112.93, 118.93, 128.54, 131.04, 131.25, 134.57, 134.72, 136.07 ppm.

MS (FAB) Exact mass calculated for (M$^+$) cation C$_{36}$H$_{33}$NP: 510.235064. Found: 510.235002 (0.1 ppm).

C$_{36}$H$_{33}$NPBr.H$_2$O requires: C, 71.05; H, 5.80; N, 2.30 %. Found: C, 70.86; H, 5.72; N, 2.21 %.

(6) 1-(4-Diphenylphosphinoylphenyl)-2-(ferrocenyl)ethene
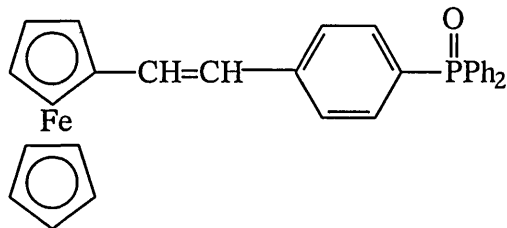
Phosphonium salt **(1)** (0.81 g, 1.6 mmol) was heated under reflux in ethanol (3 ml) for three hours with sodium hydroxide (1 M, 1.5 ml). After several hours the colour of the

reaction mixture turned from red to orange-brown. The cooled reaction mixture was poured into water and extracted with dichloromethane (3 x 20 ml) and washed with water. The combined organic layers were dried (MgSO$_4$), and the solvent evaporated in vacuo to afford the crude phosphine oxide as an orange powder.

The hydrocarbon (44) was isolated by column chromatography using dichloromethane as the eluting solvent. A mixture of dichloromethane and methanol were used to isolate the phosphine oxide (6).

Phosphine oxide (6)

Obtained as an orange solid. Yield 0.4 g, 52 %.

mp 154-157 °C

^{31}P NMR (CDCl$_3$): 29.02 ppm.

^{1}H NMR (CDCl$_3$): δ 4.11(s, 5H, cyclopentadienyl), 4.33(s, 2H), 4.49(s, 2H), 6.66-6.73(d, 1H, olefinic, J = 16.25 Hz), 6.97-7.04(d, 1H, olefinic J = 16.25 Hz), 7.19-7.97(m, 14H, aromatic).

MS (EI) Exact mass calculated for C$_{30}$H$_{25}$OP^{54}Fe: 486.10391. Found: 486.10211 (3.7 ppm) (7.19 %) C$_{30}$H$_{25}$OP^{56}Fe: 488.09924. Found: 488.10001 (-1.6 ppm) (100 %) C$_{30}$H$_{25}$OP^{57}Fe: 489.09970. Found: 489.10274 (-6.2 ppm) (35.97 %).

Hydrocarbon (44) 1-(Ferrocenyl)-2-(phenyl)ethene
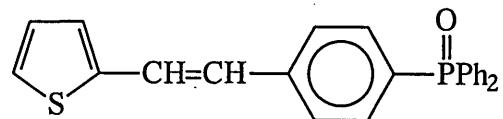
Obtained as a orange solid.

mp- not enough sample isolated to carry out a melting point.

^{1}H NMR (CDCl$_3$): δ 4.15(s, 5H, cyclopentadienyl), 4.22(s, 2H), 4.48(s, 2H), 6.67-6.73(d, 1H, olefinic, J = 16.25 Hz), 6.86-6.92(d, 1H, olefinic J = 16.25 Hz), 7.20-7.47(m, 5H, aromatic).

MS (EI) Exact mass calculated for C$_{18}$H$_{16}$^{56}Fe: 288.06015. Found: 288.05882 (4.6 ppm).

(7) 1-(4-Diphenylphosphinoyl)-2-(2-thienyl)ethene

Analogous to the procedure for (6), salt (2) (0.5 g, 0.95 mmol) was heated under reflux in ethanol with sodium hydroxide (1 M, 2 ml) for two hours. No colour change was observed during the reaction. After solvent extraction a pale yellow solid was obtained. The hydrocarbon (45) and the phosphine oxide (7) were isolated by column chromatography.

Phosphine oxide (7)

Obtained as a pale yellow solid. Yield 0.14 g, 27 %.

mp 156-160 °C

^{31}P NMR (CDCl$_3$): 28.63 ppm.

^{1}H NMR (CDCl$_3$): δ 6.95-7.73(m, 19H, aromatic).

MS (EI) Exact mass calculated for C$_{24}$H$_{19}$SOP: 386.08942. Found: 386.08705 (6.1 ppm).

Hydrocarbon (45) 1-Phenyl-2-(2-thienyl)ethene

Obtained as a very pale yellow solid.

MS (EI) 183.0 (M$^+$) (base peak).

Not enough sample isolated for other analysis.

(8) 1-(4-Dimethylaminophenyl)-2-(4-diphenylphosphinoylphenyl)ethene
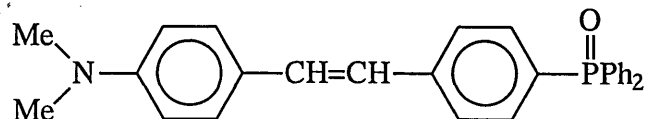
Analogous to the procedure for (6), salt (3) (0.11 g, 0.195 mmol) was heated under reflux in ethanol with sodium hydroxide (1 M, 0.5 ml) for two hours. No colour change was observed during the reaction and a pale orange solid was obtained. The hydrocarbon (46) and the phosphine oxide (8) were isolated by column chromatography.

<u>Phosphine oxide (8)</u>

Obtained as a yellow solid. Yield 0.05 g, 70 %.

mp 253-254°C (lit. 255 °C)[4]

^{31}P NMR (CDCl$_3$): 29.17 ppm.

^{1}H NMR (CDCl$_3$): δ 2.87(s, 6H, Me$_2$), 6.58-6.62(d, 1H, olefinic J = 10 Hz), 6.70-6.73(d, 1H, olefinic J = 7.5 Hz), 6.87-7.72(m, 18H, aromatic).

MS (EI) Exact mass calculated for C$_{28}$H$_{26}$ONP: 423.17520. Found: 423.17500 (0.5 ppm)

<u>Suspected hydrocarbon (46) 1-(4-Dimethylaminophenyl)-2-(phenyl)ethene</u>

Obtained as a yellow-orange solid.

No analysis carried out as a negligible amount isolated by column chromatography.

(9) 1-(4-Dimethylaminophenyl)-4-(4-diphenylphosphinoylphenyl)-1,3-butadiene
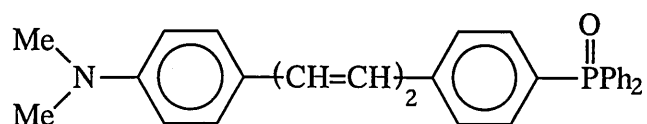
Analogous to the procedure for **(6)** salt **(4)** (0.5 g, 0.85 mmol) was treated with sodium hydroxide (1 M, 4 ml) under refluxing ethanol (3 ml). As soon as the base was added, a bright yellow solid precipitated out, which was left stirring under reflux for a further hour. A bright yellow waxy solid was obtained and the hydrocarbon **(47)** and the phosphine oxide **(9)** were isolated by column chromatography.

<u>Phosphine oxide (9)</u>

Obtained as a bright yellow waxy solid. Yield 0.2 g, 53 %.

mp 202-205 °C

^{31}P NMR (CDCl$_3$): 28.80 ppm.

^{1}H NMR (CDCl$_3$): δ 3.12(s, 6H, Me$_2$), 6.3-8.0(m, 22H, aromatic and olefinic).

MS (EI) Exact mass calculated for C$_{30}$H$_{28}$NOP: 449.19086. Found: 449.19026 (1.3 ppm).

Hydrocarbon (47) 1-(4-Dimethylaminophenyl)-4(phenyl)-1,3-butadiene

Obtained as a pale yellow-green solid. Yield 0.07 g.

mp 162-165 °C

^{1}H NMR (CDCl$_3$): δ 2.92(s, 6H, Me$_2$), 6.5-7.3(m, 13H).

MS (EI) 249.1 (M$^+$) (base peak).

Not enough sample was isolated for accurate mass spectrometry.

References

1. J. L. Oudar, *J. Chem. Phys.,* **67**, 1977, 446.

2. A. Dulcic, C. Flytzanis, C. L. Tang, D. Pépin, M. Fétizon and Y. Hoppiliard, *J. Chem. Phys.,* **74**, 1981, 1559.

3. K. Chane-Ching, M. Lequan, R.-M. Lequan, C. Runser, M. Barzoukas and A. Fort, *J. Mater. Chem.,* **5**(4), 1995, 649.

4. M. Lequan, R.-M. Lequan, K. Chane-Ching, P. Bassoul, G. Bravic, Y. Barrans and D. Chasseau, *J. Mater. Chem.,* **6**(1), 5.

5. K. Chane-Ching, M. Lequan, R.-M. Lequan and F. Kajzar, *Chem. Phys. Lett.,* **242**, 1995, 598.

6. P. A. Kranken, A. E. Hill and C. W. Peters, *Phys. Rev. Lett.,* **7**, 1961, 118.

7. C. Chen and G. Liu, *Annu. Rev. Mater. Sci.,* **16**, 1986, 203.

8. S. R. Marder, J. W. Perry, B. G. Tiemann and W. P. Schaefer, *Organometallics*, **10**, 1991, 1896.

9. M. L. H. Green, S. R. Marder, M. E. Thompson, J. A. Bandy, D. Bloor, P. V. Kolinsky and R. J. Jones, *Nature*, **330**, 1987, 360.

10. J. A. Bandy, H. E. Bunting, M. L. H. Green, S. R. Marder and M. E. Thompson, *Special Publication, R. Soc. Chem.,* **69**, 1989, 219.

11. S. R. Marder, J. W. Perry, W. P. Schaefer, B. G. Tiemann, P. C. Groves and K. J. Perry, *SPIE*, **1147**, 1989, 108.

12. G. Meredith in "Nonlinear Optical Properties of Organic and Polymeric Materials", *ACS Sypm. Ser.,* **233**, D. J. Williams, Ed., American Chemical Society, Washington, 1983, 30.

13. D. R. Kanis, M. A. Ratner and T. J. Marks, *J. Am. Chem. Soc.,* **114**, 1992, 10338.

14. A. Houlton, N. Jasmin, R. M. G. Roberts, J. Silver, D. Cunningham, P. McArdle and T. Higgins, *J. Chem. Soc., Dalton Trans.*, 1992, 2235.

15. H. Kersten and P. Boldt, *J. Chem. Research (S)*, 1994, 336.

16. M. E. Wright, E. G. Toplikar, R. F. Kubin and M. D. Seltzer, *Macromolecules*, 25, 1992, 1838.

17. M. E. Wright and E. G. Toplikar, *Macromolecules*, 25, 1992, 6050.

18. M. E. Wright, E. G. Toplikar, H. S. Lackritz and J. T. Kerney, *Macromolecules*, 27, 1994, 3016.

19. A. Abbotto, S. Bradamante, A. Facchetti and G. A. Pagani, *J. Org. Chem*, 62, 1997, 5755.

20. F. Effenburger and F. Würthner, *Angew. Chem. Int. Ed. Engl.*, 32(5), 1993, 719.

21. J. X. Zhang, P. Dubois and R. Jérôme, *J. Chem. Soc., Perkin Trans. 2*, 1997, 1209.

22. K. J. Drost, V.Pushkara Rao and A. K.-Y. Jen, *J. Chem. Soc., Chem. Commun.*, 1994, 369.

23. C.-F. Shu, W. J. Tsai, J.-Y. Chen, A. K.-Y. Jen, Y. Zhang and T.-A. Chen, *J. Chem. Soc., Chem., Commun.*, 19, 1996, 2279.

24. S. Bradamante, A. Facchetti and G. A. Pagani, *Journal of Physical Organic Chemistry*, 10, 1997, 514.

25. S. Bradamante and G. A. Pagani, *Pure Appl. Chem.*, 61, 1989, 709.

26. A. Berlin, S. Bradamante and R. Ferraccioli, *J. Chem. Soc., Perkin Trans. 2*, 1988, 1525.

27. A. Abbotto, V. Alanzo, S. Bradamante and G. A. Pagani, *J. Chem. Soc., Perkin Trans. 2,* 1991, 481.

28. M. Charton, *Prog. Phys. Org. Chem.*, 13, 1981, 119.

29. D. D. Cunningham, L. Laguren-Davidson, H. B. J. Mark, C. V. Pham and H. Zimmer, *J. Chem. Soc., Chem. Commun.*, 1987, 1021.

30. A. F. Diaz, J. Crowly, J. Bargon, G. P. Gardini and J. B. Torrance, *J. Electroanal. Chem.*, 121, 1981, 355.

31. G. P. Gardini, *Adv. Heterocycl. Chem.*, 15, 1973, 67.

32. L. Horner, G. Mummenthey, H. Moser and P. Beck, *Chem. Ber.*, 99, 1966, 2782.

33. M Zanger, C. A. VanderWerf and W. E. McEwen, *J. Am. Chem. Soc.*, 81, 1959, 3806.

34. W. E. McEwen, K. F. Kumli, A. Blade-Font, M. Zanger and C. A. VanderWerf, *J. Am. Chem. Soc.*, **86**, 1964, 2378.

35. W. E. McEwen, G. Axelrad, M. Zanger and C. A. VanderWerf, *J. Am. Chem. Soc.*, **87**(17), 1965, 3948.

36. S. J. Turner and R. D. Harcourt, *Chem. Commun.*, **1**, 1967, 63.

37. D. W. Allen, *J. Chem. Soc.(B)*, 1970, 1490.

38. D. W. Allen, B. G. Hutley and M. T. J. Mellor, *J. Chem. Soc., Perkin II*, 1972. 63.

39. A. W. Smalley, C. E. Sullivan and W. E. McEwen, *Chem. Commun.*, **1**, 1967, 5.

40. G. Aksnes and J. Songstad, *Acta. Chem. Scand.*, **16**, 1962, 1426.

41. G. Aksnes and L. I. Budvik, *ibid*, **17**, 1963, 1616.

42. J. C. Calabrese, L. Cheng, J. C. Green, S. R. Marder and W. Tam, *J. Am. Chem. Soc.*, **13**, 1991, 7227.

43. B. V. V. S. N. Prabhakara Rao, S. C. Mathur, D. C. Dube, D. P. Tewari and M. Banerjee, *Can. J. Chem.*, **75**, 1997, 1041.

44. A. Z. Al-Ansari, *Journal of Physical Organic Chemistry*, **10**, 1997, 687.

CHAPTER 5

Preliminary Investigations of Multi-Chromophoric Systems

5.0 Introduction

As seen in chapter 2, the quinolinium betaine **(1)** and the pyridinium betaine **(2)**[1] have been shown to exhibit a large degree of negative solvatochromism. It was thought that it would be interesting to make dipolar systems that contained more than one of these solvatochromic chromophores, and initially to observe the effects (if any) on the degree of solvatochromism. The nonlinear optical properties of such systems would also be of interest.

(1)

(X=Cl, Br)

(2)

(X = Cl, Br, Bu^t)
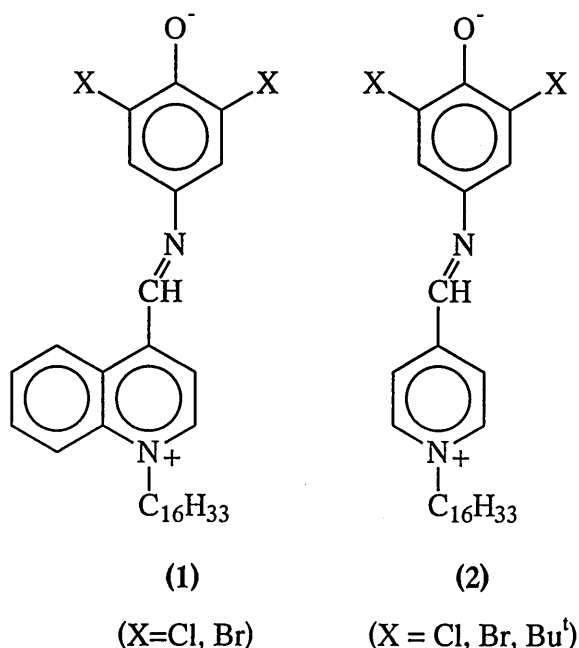
As discussed earlier (chapter 2), Lambert *and coworkers* have synthesised two three-dimensional phosphonium ion chromophores and the analogous one-dimensional system.[2] The charged phosphonium centre was connected to one [**(10)** in chapter 2], three [**(8)** in chapter 2] or four [**(9)** in chapter 2] azobenzene subchromophores. It was seen that the nonlinear properties were substantially enhanced in the three-dimensional systems.

The solvatochromism of the bis-chromophoric cyanine dye **(3)** has been studied,[3] and found to exhibit reverse solvatochromism. Analysis of the solvatochromism shows that with an increase in the length of the methylene chain spacer, v_{max} was increased for both *ortho* and *para* analogues. However, to date the nonlinear properties of this bis-chromophoric dye do not appear to have been studied.

HO—⟨benzene⟩—CH=CH—⟨pyridinium⟩N$^+$—(CH$_2$)$_n$—$^+$N⟨pyridinium⟩—CH=CH—⟨benzene⟩—OH

2Br$^-$

n = 2-6

(3)
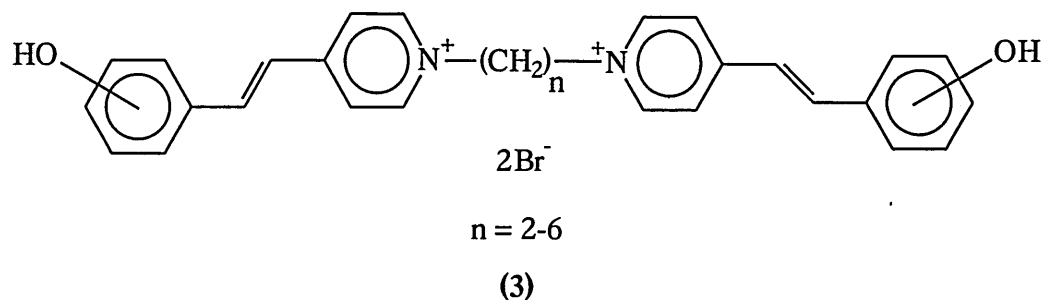
Octupolar molecules were introduced in the early 1990's into the area of second-order nonlinear optics by Zyss *and coworkers*. These *nonpolar* systems combine second-order nonlinear optical properties with a strict cancellation of all vector-like observables such as the ground and excited state dipole moment.[4]

There are several advantages of using these types of molecules in the area of nonlinear optics which include:-

- Easier crystallisation in a non-centrosymmetric manner, (essential for SHG).

- No dipolar (aggregate) interactions.

- Improved efficiency-transparency trade-off.

A recent example of an octupolar system is the cation (4) which exhibits considerable nonlinear optical properties with a hyperpolarisability of $\beta(0) = 470 \times 10^{-30}$ esu.[5] An octupolar structure that displays one of the largest hyperpolarisabilities ($\beta(0) = 1200 \times 10^{-30}$ esu) is a tri-substituted ruthenium complex due to an intense multidirectional metal-to-ligand charge-transfer.[6]

$N(CH_3)_2$

C^+

$(H_3C)_2N$ $N(CH_3)_2$

(4)
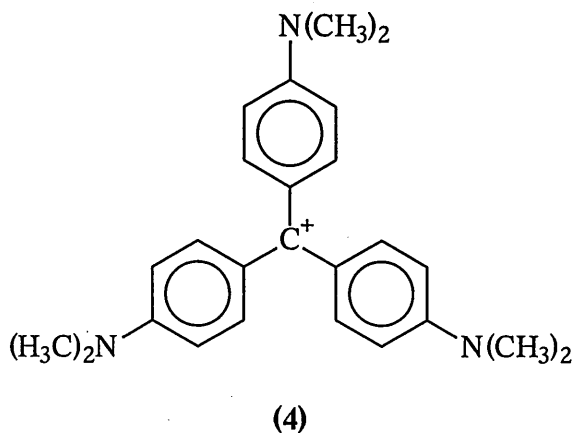
The tris-chromophoric pyridinium betaine system (5) is therefore of interest for its potential nonlinear optical properties and was thought to be easily accessible from the synthon (6) which was easily prepared from mesitylene.[7] However, in the time

222

available the respective tris-salt of (5) could not be synthesised and only the mono-salt of the respective betaine (7) was synthesised from the synthon (8) primarily as a comparison with the desired tris-analogue.
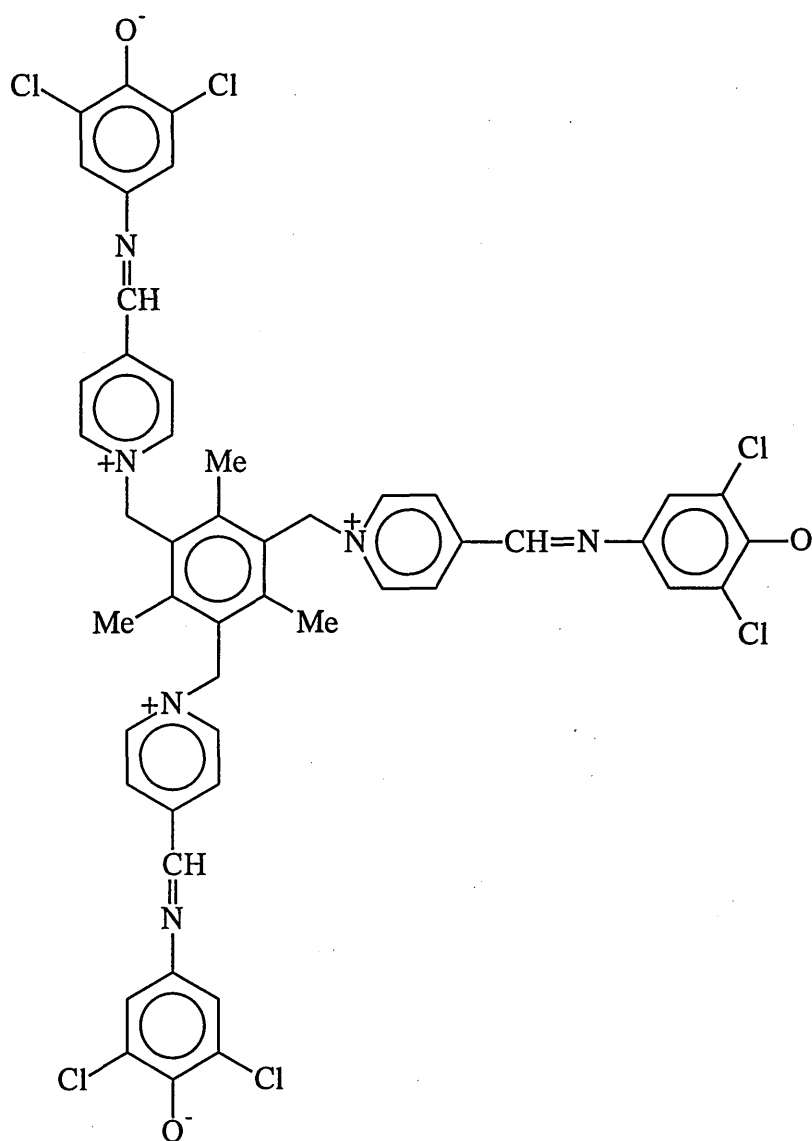
(5)
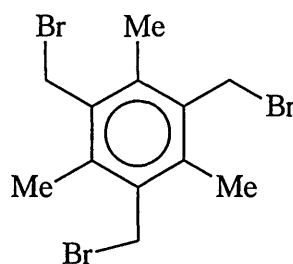
(6)

(7)
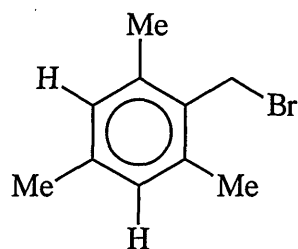
(8)

The synthesis of the bis-chromophoric systems (9) and (10) and (11) was attempted from the commercially available xylenes (12) and (13).
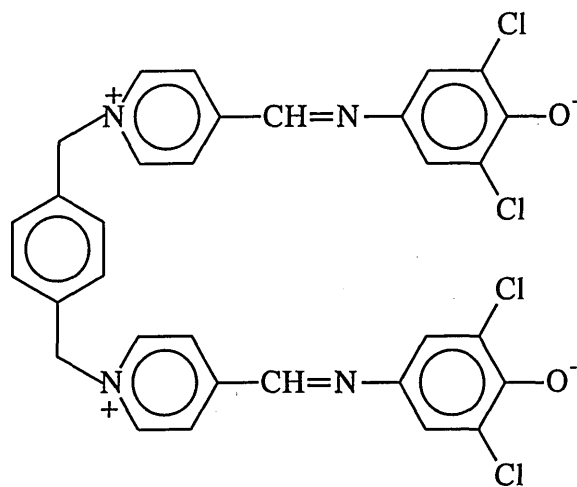
(9)
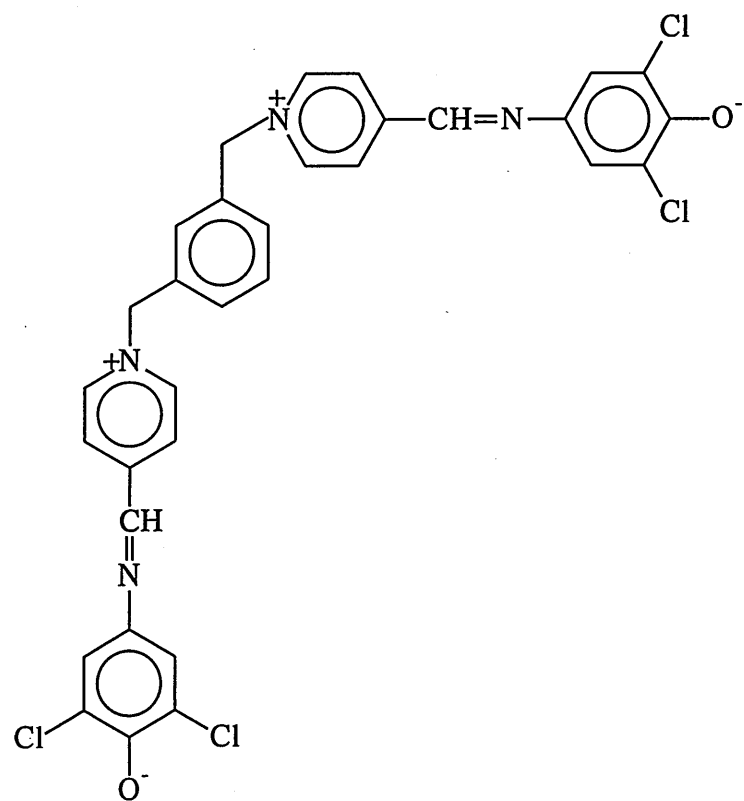
(10)
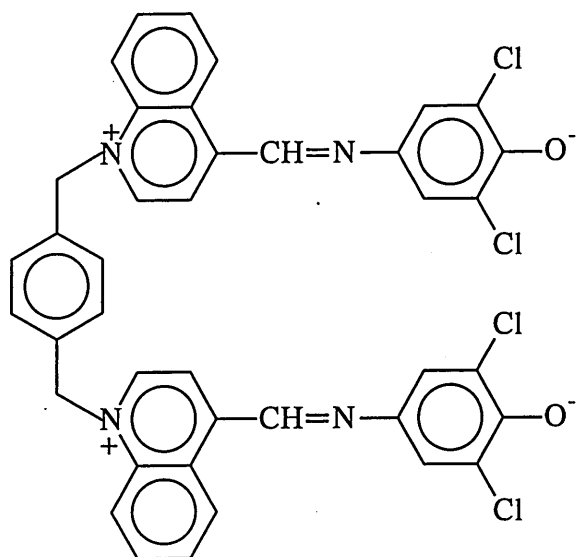
(11)
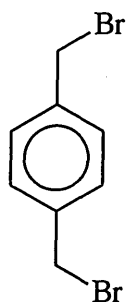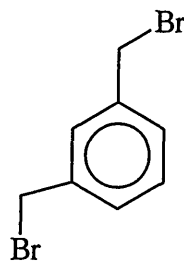
(12)   (13)

5.1 Synthesis of the pyridine and quinoline imines.

The imines **(14)** and **(15)** were easily synthesised by treating the appropriate aldehyde with 4-amino-2,6-dichlorophenol in refluxing ethanol for several hours under nitrogen. This has already been discussed in chapter 2 in more detail.
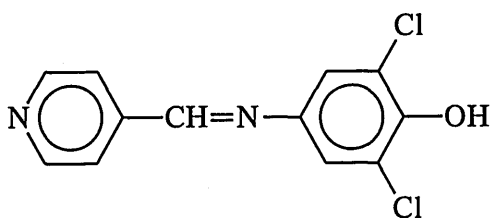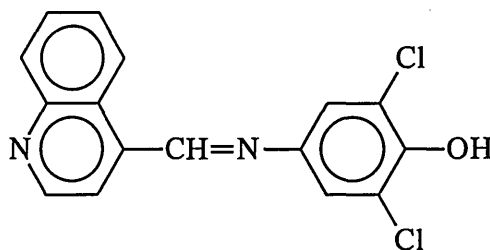
(14)   (15)

5.2 Synthesis of the bromomethylated precursors.

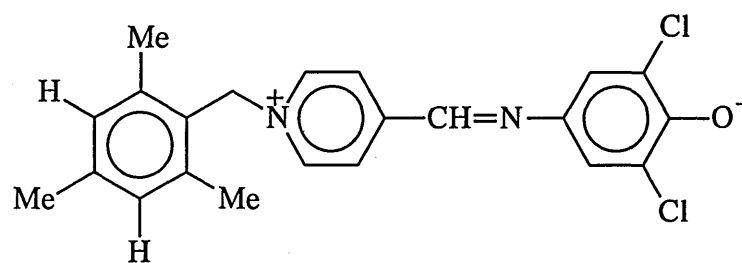The tris-bromomethylated precursor **(6)** and the mono-bromomethylated precursor **(8)** were easily synthesised from a recent literature procedure[7] as shown in scheme 1. The bis-bromomethylated compound **(16)** was also synthesised but this was not used to make a bis-substituted pyridinium betaine system due to lack of time. The degree of bromomethylation depended upon the concentrations of paraformaldehyde, and hydrogen bromide used, the temperature of the reaction mixture and the reaction time.

$$R_1 = R_2 = R_3 = CH_2Br \ (6)$$

$$R_1 = R_2 = H, \ R_3 = CH_2Br \ (8)$$

$$R_1 = H, \ R_2 = R_3 = CH_2Br \ (16)$$
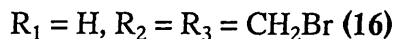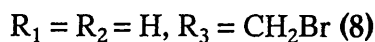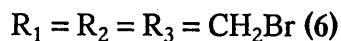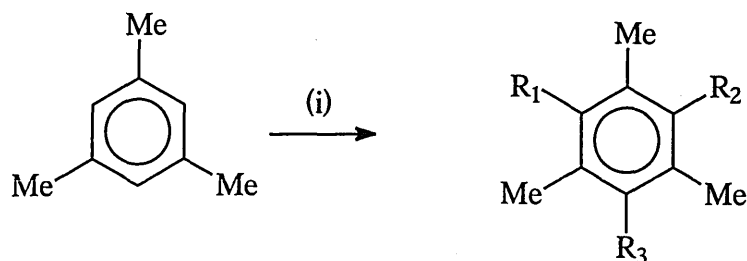
(i)   Paraformaldehyde, glacial acetic acid, HBr (31 %wt) /glacial acetic acid; (6) 12hrs, 95 °C; (8) 2hrs, 50 °C; (16) 8hrs, 80 °C.

Scheme 1

5.3 Characterisation of the bromomethylated precursors.

The ^{1}H and the ^{13}C NMR spectra of (6), (8) and (16) showed that they were bromomethylated to the required degree. The compounds were shown to be pure by GCMS, and that no mixed bromomethylated products had been obtained. Electron impact mass spectrometry gave the characteristic molecular ion and the melting points were in the correct range to those reported in the literature.

It was extremely important that (6), (8) and (16) were pure before synthesising the salts, as otherwise mixed mono-, bis-, and tris-salts would have been obtained which would have been impossible to separate.

5.4 Synthesis of the mono- and tris-chromophoric salts.

Synthesis of the tris-salt (17) and the mono-salt (18) was attempted by refluxing (6) and (8) with three moles and one mole equivalent of the pyridinium imine (14), respectively, in acetonitrile (scheme 2). All the starting materials dissolved upon reflux and an orange (17) or yellow (18) solid precipitated out almost immediately; however the reaction mixture was refluxed for a further twenty four hours with stirring. After cooling the reaction mixture slightly, the insoluble salts were filtered and washed with copious amounts of cold acetonitrile and then cold diethyl ether, and the salts were then dried under vacuum.

227

5.5 Synthesis of the bis-chromophoric salts.

The pyridinium salts **(19)** (*para* analogue) and **(20)** (*meta* analogue) and the quinolinium salt **(21)** (*para* analogue) were prepared in a similar manner to the salts **(17)** and **(18)** (scheme 2), using two moles equivalent of the pyridinium imine. Upon reflux the suspected pyridinium salts **(19)** and **(20)** precipitated out of solution almost immediately as yellow **(19)** or orange **(20 and 21)** solids. However the quinolinium salt **(21)** precipitated out of solution very slowly due to the insolubility of the quinoline starting material **(15)** in acetonitrile (insolubility of **(15)** has already been discussed in chapter 2).

(6), (8), (12) or **(13)** + **(14)** or **(15)** $\xrightarrow{\text{(i)}}$

(17), (18)

XBr⁻

(19), (20), (21)

2Br⁻
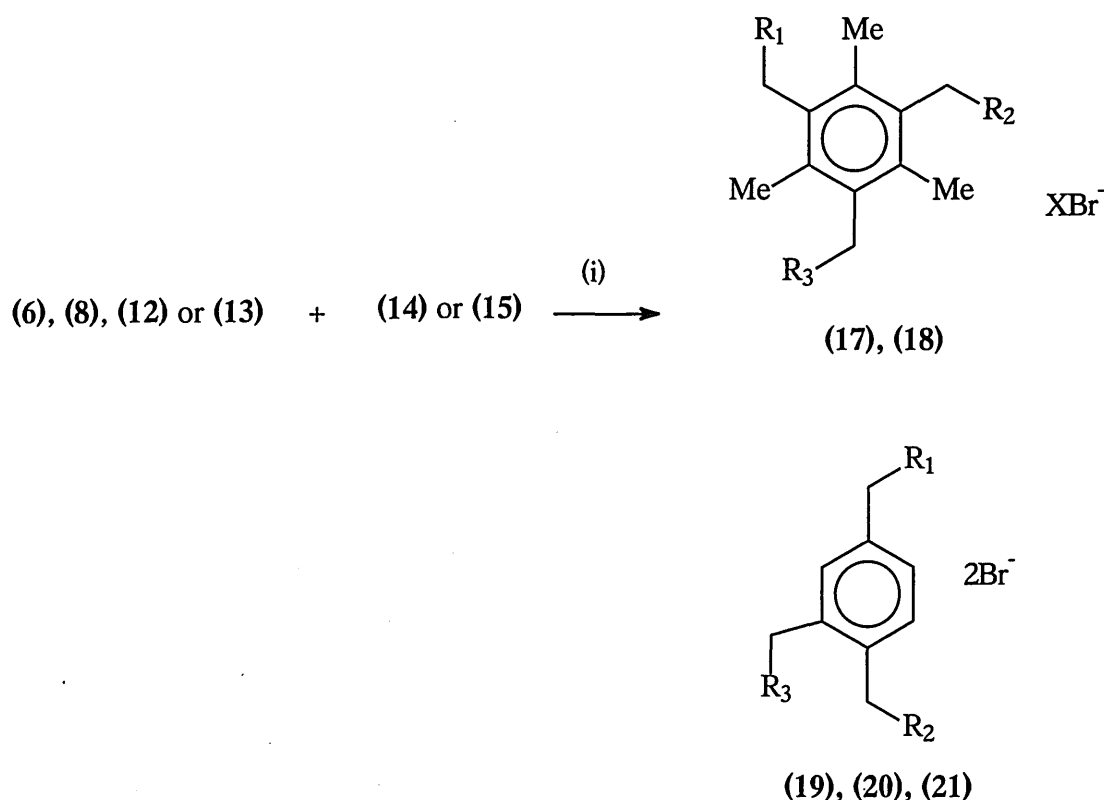
$\quad$ **(17)**; $R_1 = R_2 = R_3$ = pyridinium moiety, X = 3

(18); R_1 = pyridinium moiety, $R_2 = R_3$ = H, X = 1

(19); $R_1 = R_2$ = pyridinium moiety, R_3 = H

(20); $R_1 = R_3$ = pyridinium moiety, R_2 = H

(21); $R_1 = R_2$ = quinolinium moiety, R_3 = H

(i) MeCN, reflux, 24hrs

Scheme 2

The tris-salt **(17)** and the bis-salts **(19)**, **(20)** and **(21)** were found to be very insoluble, and could only be dissolved in methanol and DMF at room temperature. They were also partially soluble in cold ethanol. The above salts were completely insoluble in refluxing acetonitrile, acetone and dichloromethane. The mono-salt **(18)** was slightly more soluble, being partially soluble in acetone and hot dichloromethane.

For all the pyridinium salts a strange effect was observed in water; the salts were completely insoluble in this solvent; however, the orange or yellow solids turned deep red-purple instantly when immersed in the liquid. It is thought that there is some kind of interaction between the outer surface of the salt and the water molecules, probably converting the salt to the betaine. This colour change was not observed in any other solvents in which the salts were insoluble, and the solids remained yellow-orange in colour. The same effect was observed for the quinolinium salt, in which the solid turned from orange to green in water, however the colour change was not immediate, unlike for the pyridinium salts.

The high degree of polarity of the salts was also observed by thin layer chromatography. All of the salts discussed in chapters 2-4, are observed in TLC studies as bullet shaped spots using the eluting solvent methanol (5-10 %) in dichloromethane. Salts **(17)** and **(19-21)** would only develop using the eluting solvent containing methanol (40 %) in dichloromethane. However the mono-salt **(18)** was resolved using methanol (20 %) in dichloromethane.

5.6 Characterisation of the salts.

The high degree of insolubility of the salts was initially thought to be due to their high degree of polarity due to the presence of two or three positive charges on the nitrogen and the two or three bromide anions. However the FAB mass spectra of the suspected multi-chromophore salts strongly suggested that the tris- and bis-salts had not been prepared.

The FAB mass spectrum of the mono-salt **(18)** gave the required characteristic molecular cation at m/z 400, but for the proposed tris-salt **(17)** the required molecular cation at m/z 960 was not observed. A few selected mass ions observed in the mass spectrum are shown in table 1, and it can be presumed that possibly a small amount of the bis-salt **(22)** and the mono-salt **(23)** had been obtained, although the intensities of these mass peaks are negligible. The mass for the pyridine imine **(14)** was also observed

which could indicate that maybe the tris-salt had been obtained, yet fragmented very easily in the mass spectrometer.

(22)   (23)
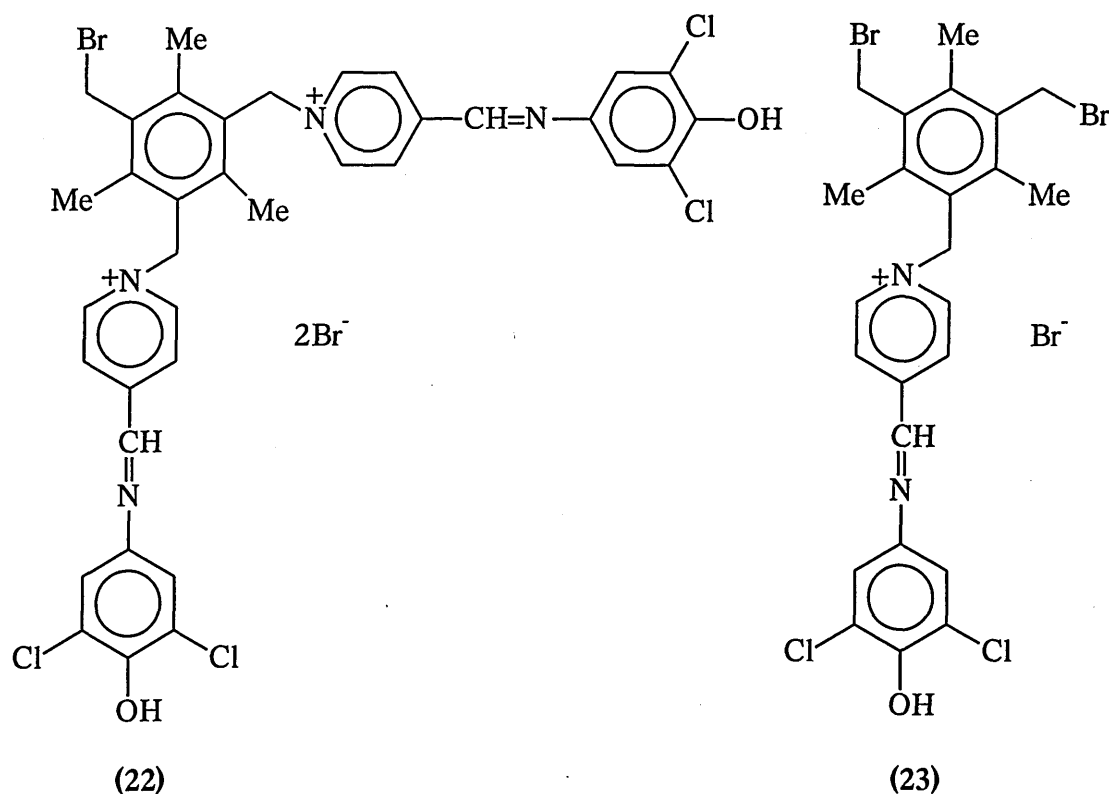
m/z	Fragment Ion	Intensity of Peak
680	Cation of (22) – CH$_2$Br	Very weak
508	Cation of (23) – Br	Very weak
491	Cation of (23) – CH$_2$Br	Very weak
267	(14)	Medium

Table 1   FAB MS data for suspected salt (17).

The bis-pyridinium salts (19) and (20) gave the required molecular ion but at negligible intensities. The molecular cations for the mono-salts (24) and (25) were also observed at negligible intensities (tables 2 and 3).

230

(24)   (25)
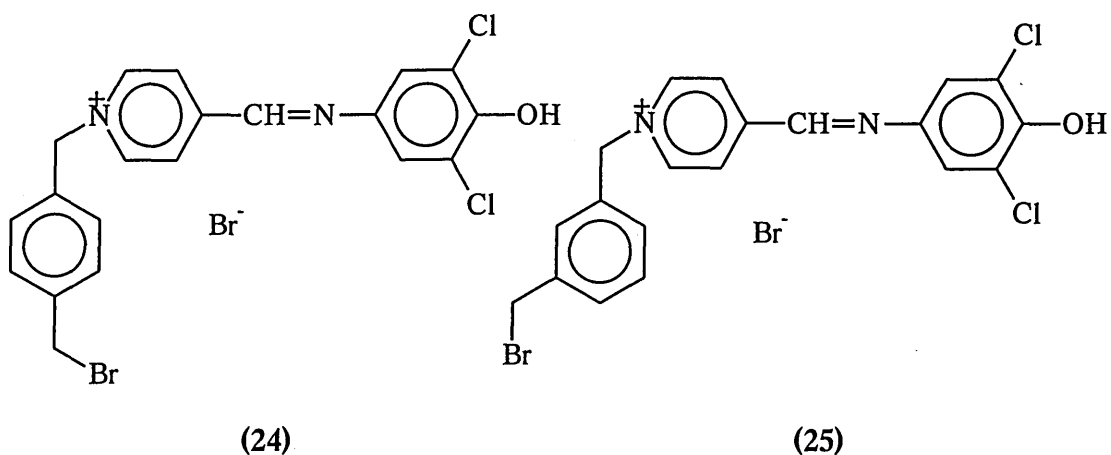
m/z	Fragment Ion	Intensity of Peak
638	Cation of (19)	Very weak
451	Cation of (24)	Very weak
370	Cation of (24) –Br	Weak-medium
267	(14)	Medium

Table 2   FAB MS data for suspected salt (19).

m/z	Fragment Ion	Intensity of Peak
638	Cation of (20)	Very weak
451	Cation of (25)	Very weak
370	Cation of (25) –Br	Very weak
267	(14)	Strong

Table 3   FAB MS data for suspected salt (20).

The FAB mass spectrum for the proposed quinolinium salt (21) only gave the cation for the mono-salt (26) at m/z 501, which was observed at a reasonable intensity. The molecular ion for the quinoline imine (15) was also observed.
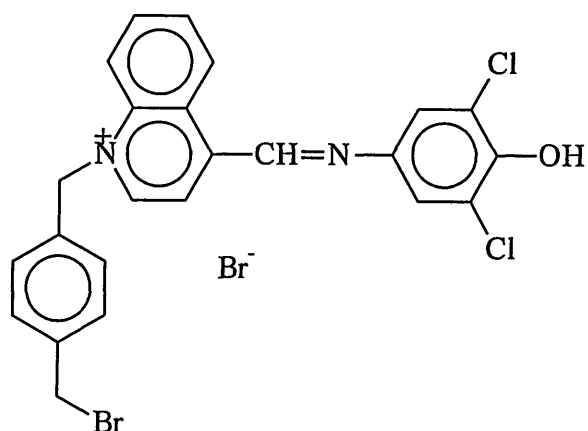
(26)

The proton NMR spectra of the salts are very complex, especially in the aromatic region, and do not confirm the exact structure of the products.

An interesting point to note is that especially for the suspected tris-salt **(17)** the yield obtained is consistent with the tris-salt being produced. The yield is too high for the product to be solely the mono-or the bis-salt, or a mixture of the two, and the starting materials are not present as impurities as the salt products were washed with solvents in which the starting materials are soluble until the washings were clear. However, the mono-analogues of the proposed bis-salts **(19)** and **(20)** seem to have been made according to the yields recorded.

If there is a lower degree of chromophore substitution than expected there are two possible reasons for this. The first is from a steric point of view especially for the tris-salt **(17)** and possibly the *meta* bis-pyridinium salt **(20)**. The other possibility is that the mono-salt is being formed in each case, and instantly precipitates out of solution, before substitution of the second or third chromophore. A possible way of overcoming the latter problem is to slowly add one of the reagents dropwise.

Additionally the high degree of insolubility seems very strange if the mono salts **(23)**, **(24)**, **(25)** and **(26)** have been made; the mono-salt **(18)** is fairly insoluble in most high polarity solvents, but not to such a large degree as the other salts.

The salts should also be analysed by matrix-assisted laser desorption/ionisation-time of flight (MALDI-TOF) mass spectrometry, as this method causes little or no fragmentation of the molecular ion. In positive mode MALDI if the tris- or bis- salts have been made the $[M+H]^+$ cation should be observed.

232

At the time of writing microanalytical data (C, H, N) had not been obtained, but this is essential as it would show the degree of chromophore substitution.

5.7 Synthesis of the betaines.

In spite of the uncertainties in the composition of the salts, attempted conversion to the betaine systems was conducted by stirring the suspected salt with the appropriate number of moles of base, even though at the present time the degree of chromophore substitution is unknown for the salts **(17)**, **(19)** and **(20)**.

Due to the complete insolubility of the salts **(17-21)** in most solvents, conversion to, and isolation of the betaine was found to be difficult by the usual routes employed. Dissolving the salts in dichloromethane and shaking with aqueous sodium hydroxide or stirring the salt in acetonitrile or dichloromethane with an excess of potassium carbonate proved impossible.

Stirring the salt **(17)** in methanol with an excess of aqueous sodium hydroxide instantly turned the yellow-orange solution to deep purple. A large amount of water was added as it was thought that the betaine would precipitate out, but this was not the case. A small amount of this solution was poured into a further amount of water, and a small amount of purple solid precipitated out. This is an inappropriate way of isolating the betaine **(5)**.

The salt **(17)** was stirred with a large excess of anhydrous potassium carbonate in methanol, again the solution turned deep purple instantly. After filtering off the insoluble solid the solvent was evaporated off to leave a red-brown oil, but trituration with diethyl ether and various other solvents did not afford a solid.

To date an appropriate method of isolating the betaines has not been found, although anion exchange chromatography is a possible solution.

5.8 Solvatochromism studies.

Preliminary solvatochromic studies were carried out on salts (17) and **(19-21)** in methanol and ethanol, and on salt **(18)** in acetone and THF in addition to methanol and ethanol. The betaines were formed *insitu* using sodium hydroxide dissolved in methanol or ethanol or aqueous sodium hydroxide, or by adding a small amount of potassium carbonate to the salt solution. The studies were carried out at room temperature and pressure and the concentrations of the solutions could not be measured due to the partial solubility of the salts.

A comparison of these systems is made with the long chain pyridinium (2),[1] the long chain quinolinium (1) and the methyl pyridinium betaine (27) which has also been reported in the literature.[1]

$$CH_3-\overset{+}{N}\!\!\bigcirc\!\!-CH=N-\bigcirc-O^-$$

(with Cl substituents ortho to the O^- group)
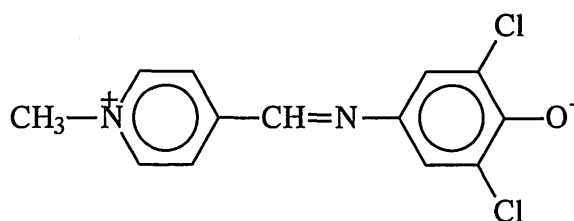
(27)

Selected solvatochromic data of betaines (1), (2), and (27) is given in table 4. UV/Visible data for the respective salts has not been studied.

Solvent	(2)	(27)	(1)
Methanol	516	510	582
Ethanol	544	540	N/A
Acetone	606	578	N/A
Tetrahydrofuran	648	590	N/A

Table 4 Solvatochromism data for the betaines (1), (2), and (27).

The suspected tris-betaine (5) has a λ_{max} of 524 nm compared to that of *ca.* 510 nm for the pyridinium betaines (2) and (27) in methanol, however in ethanol the values are very similar (table 5). For conversion to this betaine using potassium carbonate there is also an additional band at 450 nm, which is not due to the salt. This could be due to some other compound being formed, and is most likely why the proposed betaine (5) could not be made (as discussed earlier).

234

Solvent	Reagent for *in situ* conversion to the betaine	Colour	λ_{max} nm
Methanol	-	Yellow	390
	NaOH	Deep red	524
	K_2CO_3	Deep red	450 526
Ethanol	-	Yellow	394
	NaOH	Deep red	540
	K_2CO_3	Deep red	546

Table 5 Solvatochromism data for the proposed salt (17) and the respective betaine (5).

The mono-betaine (7) again had a longer λ_{max} than the corresponding pyridinium betaines (2) and (27) in methanol (table 6). In ethanol the salt (18) showed evidence of the betaine in solution as the λ_{max} of the betaine was present at the same intensity as that of the salt and the solution was deep red in colour instead of yellow. In ethanol betaine (7) had a λ_{max} of 554 nm compared to *ca.* 540 nm for (2) and (27).

The salt was only partially soluble in acetone and THF; in acetone the salt showed evidence of the betaine and the solution was green in colour instead of the expected yellow. The betaine showed a slightly longer λ_{max} than the pyridinium betaines (2) and (27) in acetone. In THF two absorption bands were observed at *ca.* 544 nm and 658 nm. The splitting of bands was also observed for the pyridinium analogues (2) and (27),[1] however, only the longest wavelength absorption band was reported in each case at 648 nm and 590 nm, respectively.

Solvent	Reagent for *in situ* conversion to the betaine	Colour	λ_{max} nm
Methanol	-	Yellow	390
	NaOH	Deep red	520
	K_2CO_3	Deep red	520
Ethanol	-	Deep red	398 520
	NaOH	Deep red	554
	K_2CO_3	Deep red	552
Acetone	-	Green	382 614
	NaOH	Blue	614
	K_2CO_3	Blue	614
Tetrahydrofuran	-	Yellow	370
	NaOH	Blue	544 654
	K_2CO_3	Blue	548 658

Table 6 Solvatochromism data for salt (18) and the respective betaine (7).

The proposed bis-betaines (9) and (10) behaved identically in the solvents, exhibiting very similar wavelengths to the mono-betaine (7).

Solvent	Reagent for *in situ* conversion to the betaine	Colour	λ_{max} nm
Methanol	-	Yellow	392
	NaOH	Deep red	526
	K_2CO_3	Deep red	522
Ethanol	-	Yellow	398
	NaOH	Deep red	556
	K_2CO_3	Deep red	554

Table 7   Solvatochromism data for salt the proposed salt (19) and the respective betaine (9).

Solvent	Reagent for *in situ* conversion to the betaine	Colour	λ_{max} nm
Methanol	-	Yellow	388
	NaOH	Deep red	526
	K_2CO_3	Deep red	
Ethanol	-	Yellow	398
	NaOH	Red-purple	552
	K_2CO_3	Red-purple	554

Table 8   Solvatochromism data for the proposed salt (20) and the respective betaine (10).

The quinolinium betaine, which is most probably the respective betaine of the mono-substituted salt (26) was only studied in methanol and gave a charge-transfer band at 600 nm compared to 582 nm for the long chain quinolinium betaine (1).

Solvent	Reagent for *in situ* conversion to the betaine	Colour	λ_{max} nm
Methanol	-	Yellow	420
	NaOH	Blue	600

Table 9   Solvatochromism data for salt (26) and the respective betaine.

237

For the monosubstituted betaine (7) and suspected tris-betaine (5) the solvatochromic data is not that disimilar to the data for that of the betaines (2) and (27). However this does not definitely confirm that the tris-betaine (5) has not been synthesised as the solvatochromic properties may not have been that different to the mono-chromophoric system anyhow. The attachment of the pyridinium chromophore to the methylated aromatic ring does, however, shift the λ_{max} to a slightly longer wavelength.

The unconfirmed bis-chromophoric betaine systems (10) and (11) are also very similar in their solvatochromic behaviour to (2) and (27). However, the absorption maximum of the mono-chromophoric quinolinium betaine has a slightly longer wavelength than that of the long chain quinolinium betaine (1).

5.9 Attachment of a chromophore to a polymer.

It was also of interest to explore the attachment of the chromophore units to a polymer, as such a potentially solvatochromic material would be of interest as a sensor component, having been solvent cast as a thin film.

The quinoline imine [(51) in chapter 2] was attached to soluble chloromethylated polystyrene (28) which itself was synthesised by a recommended literature procedure,[8] to produce the polymer system (29).
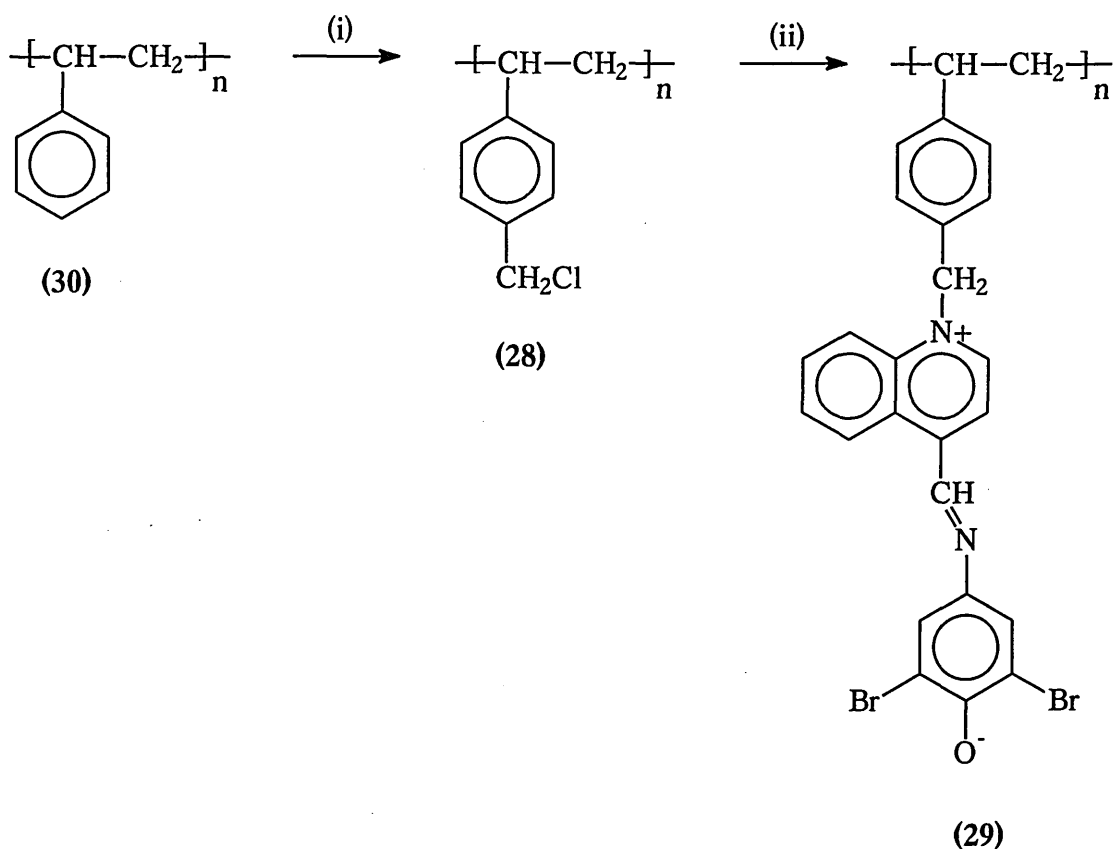
Scheme 3

(i)   Dimethoxymethane, thionyl chloride, $ZnCl_2$

(ii)   [(51) in Chapter 2], silver-p-toluene sulphonate, DMF, 80 °C, N_2

Soluble polystyrene (30) was allowed to react with dimethoxymethane and thionyl chloride with zinc chloride as the Lewis acid catalyst to produce chloromethylated polystyrene (28) scheme 3. Chloromethyl methyl ether is produced *in situ*, this having the advantage that this carcinogenic compound does not have to be handled directly. Zinc chloride was chosen rather than stannic chloride as there was less chance of cross-linking occurring (causing insolubility of the chloromethylated polymer). The ^{13}C NMR spectrum of the chloromethylated polymer showed no signal at 65.1 ppm due to the hydroxy methyl group, (a possible side product of polymer work up).

The polymer bound betaine (29) was obtained by the treatment of the quinoline imine with chloromethylated polystyrene (28) with one mole equivalent of silver-p-toluene sulphonate in DMF. The reasons for this method were discussed for the quinolinium betaine systems (54) and (55) in chapter 2.

239

The microanalytical data obtained for the chloromethylated polystyrene (28) indicated that one in every nine monomer units were chloromethylated. The microanalytical data for the polymer bound betaine (29) indicated that *all* of the possible chlorine sites had been N-alkylated.

The molecular weight of polymer (29) was calculated from the original molecular weight of the soluble polystyrene used for the chloromethylation step, and was found to be approximately 65,000. This is assuming that no alteration in chain length occurred during the chloromethylation and N-alkylation steps.

The UV/Visible spectrum of (29) could only be obtained in dichloromethane, due to the insolubility of the polymer in other solvents. The longest wavelength absorption band was observed at 728 nm; the same wavelength as that observed for the quinolinium betaine (55) in chapter 2.

The formation of an LB film of the polymer bound betaine (29) was studied at Cranfield University, however attempts to attach such films to a gold layer for SPR studies were unsuccessful.

5.10 Future Developments

It is necessary to carry out MALDI-TOF mass spectrometry and to obtain microanalytical data on these salt systems to determine what degree of chromophoric substitution has occurred. If a lower degree of substitution has been obtained than expected, the problematic synthesis of the salts should be investigated further. Additionally isolation of the betaines is of utmost importance for any NLO investigations to be performed.

5.11 Experimental

### (14) N-(4-Pyridinylmethylidene)-4-amino-2,6-dichlorophenol
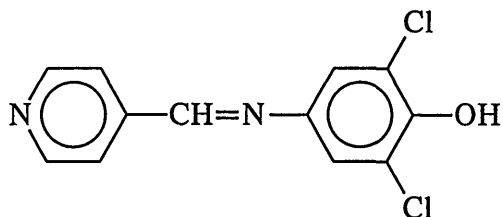
Pyridine-4-carboxaldehyde (4 g, 0.037 mol) and 4-amino-2,6-dichlorophenol (6.65 g, 0.037 mol) were heated under reflux in ethanol (30 ml) for two hours. The solid, which precipitated out of solution on cooling was filtered and washed with cold ethanol. The product was obtained as a green-brown solid. Yield 5.86 g, 59 %.

m.p. 221-223 °C (lit. 222-224 °C)[1]

^{1}H NMR (CD$_3$OD): δ 6.8(s, 2H, aromatic), 8.05 and 8.20(dd, 4H, aromatic), 8.7(s, 1H, CH=N).
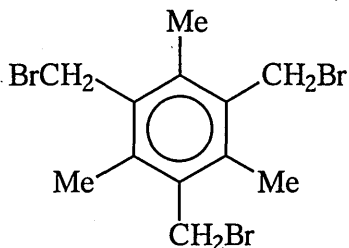
MS (EI) 266.0 and 268.0 (M$^+$) base peak.

(15) N-(4-Quinolinylmethylidene)-4-amino-2,6-dichlorophenol
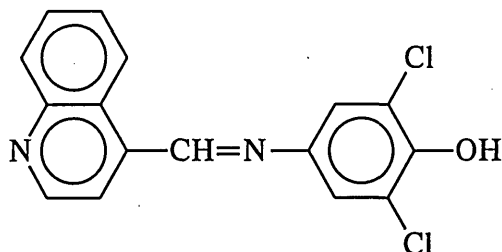
For details of synthesis refer to experimental section chapter 2.

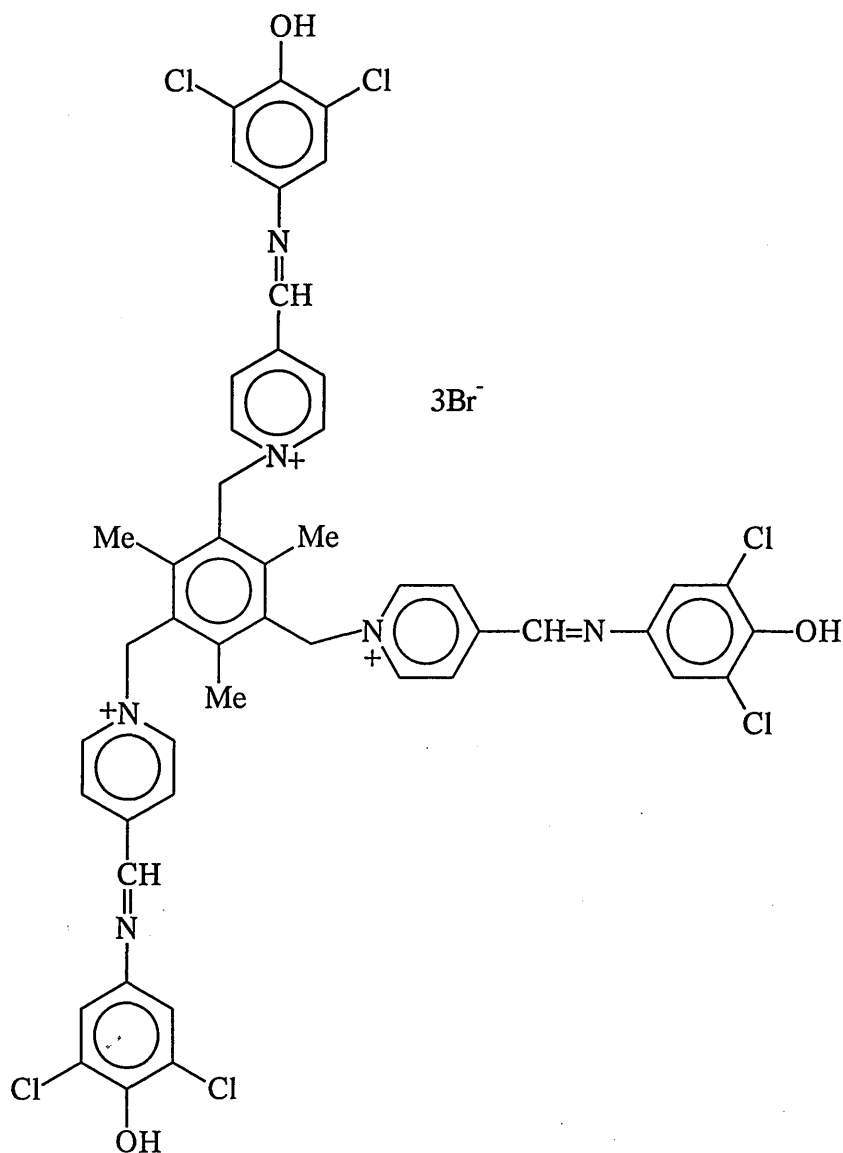### (6) 1,3,5-Tris(bromomethyl)-2,4,6-trimethylbenzene

To a mixture of mesitylene (6 g, 0.05 mol), paraformaldehyde (5 g, 0.165 mol) and 25 ml of glacial acetic acid, was added 35 ml of a 31 % HBr/acetic acid solution. The mixture was kept for twelve hours at 95 °C and then poured into 100 ml of water. The

product was filtered off under suction and washed with copious amounts of water. The product was obtained as a white powder, and dried under vacuum. Yield 17.85g, 100 %. m.p. 186-189 °C (lit. 186 °C)[7]

^{1}H NMR (CDCl$_3$): δ 4.57(s, 6H, -CH$_2$Br), 2.46(s, 9H, -CH$_3$).

MS (EI) 397.4 and 399.4 (M$^+$), 318.6 (M$^+$ - Br).

(17) Attempted synthesis of the tris-pyridinium salt

Tris-(bromomethyl)mesitylene (6) (1 g, 0.0025 mol) was heated under reflux with the pyridine imine (14) (2.34 g, 0.00875 mol) in acetonitrile (40 ml) for twenty four hours. Upon reflux an orange solid precipitated out immediately. The reaction mixture was cooled slightly and filtered under suction, and washed with acetonitrile, and then diethyl ether. Yield 2.74 g, 91 % (assuming (17) has been made).

m.p. 210-240 °C (decomp.)

MS (FAB) 680 (22) (M^+ cation), 508 (23) (M^+ cation – Br), 491 (23) (M^+ cation – CH_2Br).

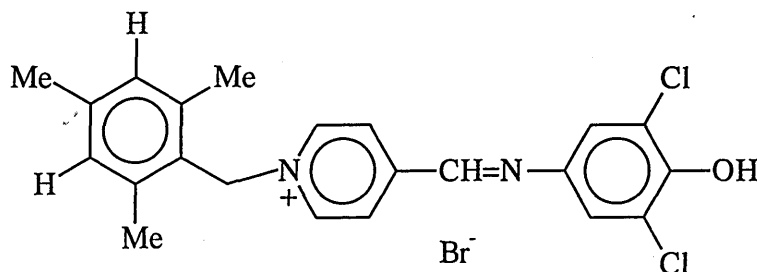## (8) 1-(Bromomethyl)-2,4,6-trimethylbenzene
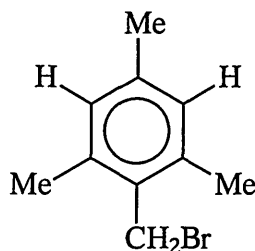
To a mixture of mesitylene (6 g, 0.05 mol), paraformaldehyde (1.54 g, 0.05 mol) and 25 ml of glacial acetic acid, was added 10 ml of a 31 % HBr/acetic acid solution. The mixture was kept for two hours at 50 °C and then poured into 100 ml of water. The product was filtered off under suction and washed with copious amounts of water. The product was obtained as a white powder and dried under vacuum. Yield 9.10 g, 85 %.

m.p. 49 °C (lit. 49 °C)[7]

^{1}H NMR ($CDCl_3$): δ 6.95(s, 2H, phenyl), 4.57(s, 2H, -CH_2Br), 2.47(s, 6H, -CH_3), 2.36(s, 3H, -CH_3).

MS (EI) 211.9 and 213.9 (M^+).

(18) The mono-pyridinium salt

Mono(bromomethyl)mesitylene (8) (2 g, 0.0094 mol) was heated under reflux with the pyridine imine (14) (2.56 g, 0.0096 mol) in acetonitrile (45 ml) for twenty four hours. An orange solid precipitated out almost immediately upon reflux. After cooling slightly, the insoluble solid was filtered under suction and washed with acetonitrile and then diethyl ether. The salt (18) was obtained as an orange solid. Yield 3.74 g, 83 %.

243

MS (FAB) 399 (M$^+$ cation).

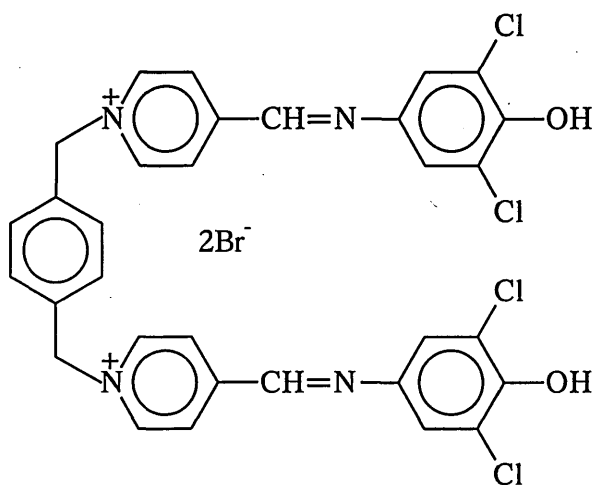### (16) 1,3-Bis(bromomethyl)-2,4,6-trimethylbenzene
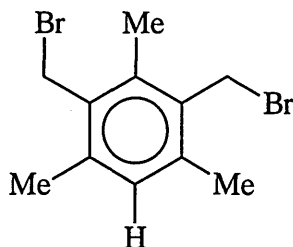
To a mixture of mesitylene (6 g, 0.05 mol), paraformaldehyde (3.075 g, 0.1 mol) and 25 ml of glacial acetic acid, was added 20 ml of a 31 % HBr/acetic acid solution. The mixture was kept for eight hours at 80 °C and then poured into 100 ml of water. The product was filtered off under suction and washed with copious amounts of water. The product was obtained as a white powder and dried under vacuum. Yield 15.20 g, 92 %.

m.p. 130-132 °C (lit. 133-134 °C)[7]

^{1}H NMR (CDCl$_3$): δ 6.90(s, 1H, phenyl), 4.57(s, 4H, -CH$_2$Br), 2.44(s, 3H, -CH$_3$), 2.38(s, 6H, CH$_3$).

MS (EI) 305.9 and 306.9 (M$^+$).

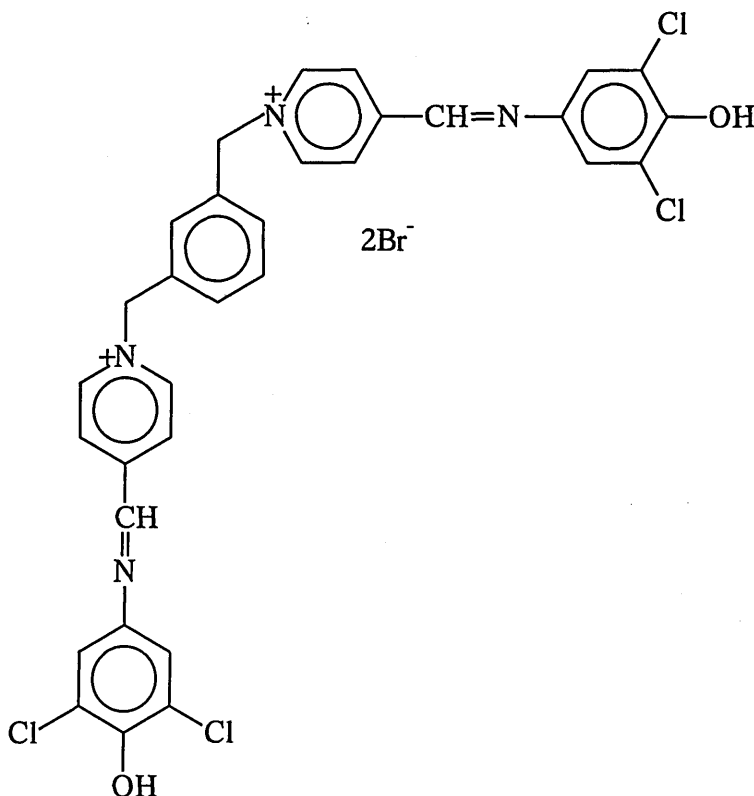### (19) Attempted synthesis of the bis-pyridinium salt *(para)*

α,α'-Dibromo-*p*-xylene (1.43 g, 0.0054 mol) and the pyridine imine (14) (3.4 g, 0.013 mol) were heated under reflux in acetonitrile (50 ml) for twenty four hours. Upon reflux

a bright yellow solid precipitated out immediately, which was filtered under suction after slightly cooling the reaction mixture. The solid was washed with acetonitrile and then diethyl ether. The product was obtained as a bright yellow solid. Yield 2.21 g, 51 % (if (19) made), 79 % (if (24) made).

MS (FAB) 638 (19) (M^+ cation), 451 (24) (M^+ cation), 491 (24) (M^+ cation $-$ Br).


(20) Attempted synthesis of the bis-pyridinium salt *(meta)*

α,α'-Dibromo-*m*-xylene (1.43 g, 0.0054 mol) and the pyridine imine (14) (3.4 g, 0.013 mol) were heated under reflux in acetonitrile (50 ml) for twenty four hours. An orange solid precipitated out after an hour of reflux, unlike the *para* analogue (19). After cooling the reaction mixture slightly, the solid was filtered under suction and washed with acetonitrile and diethyl ether. The product was obtained as an orange solid. Yield 2.41 g, 56 % (if (20) made), 86 % (if (25) made).

MS (FAB) 680 (20) (M^+ cation), 508 (25) (M^+ cation), 491 (25) (M^+ cation $-$ Br).

## (21) Attempted synthesis of the bis-quinolinium salt *(para)*
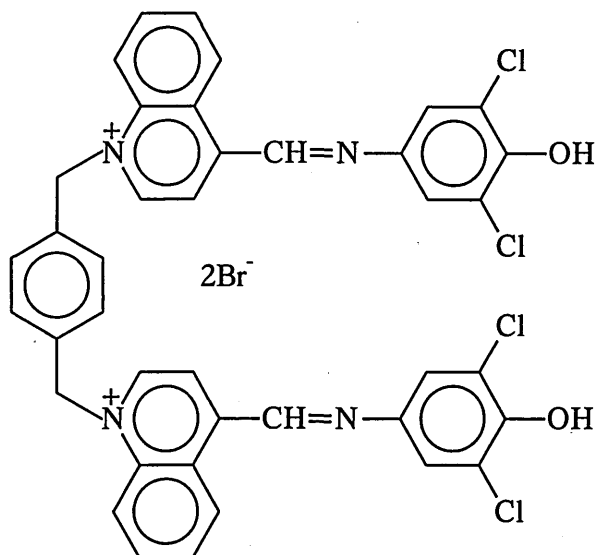
The quinoline imine **(15)** (2.47 g, 0.0078 mol) and α,α'-dibromo-*p*-xylene (0.83 g, 0.0032 mol) were heated under reflux in acetonitrile (35 ml) for twenty four hours. The quinoline imine **(15)** did not dissolve upon reflux, but went slowly into solution, as the salt slowly precipitated out of solution. The cooled reaction mixture was filtered and washed with cold acetonitrile and then with diethyl ether to afford an orange solid which was found to be the mono-salt **(26)**. Yield 1.82 g, 99 %.

mp > 190 °C (decomp.)

MS (FAB) 501 (M$^+$ cation).

(28) Chloromethylated polystyrene
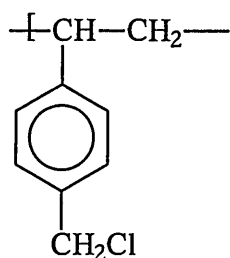
In a flask flushed with nitrogen, soluble polystyrene **(30)** (Aldrich, M$_w$ ≈ 45,000)   (5.0 g) was dissolved in dimethoxymethane (25 ml, 0.28 mol) which took four hours for complete dissolution. The mixture was cooled to 0 °C and thionyl chloride (9.2 ml, 0.13 mol) was added dropwise. The reaction mixture was allowed to warm to ambient temperature over forty five minutes. The reaction mixture was cooled to 0 °C and ZnCl$_2$ (0.2 ml in 1.0 M diethyl ether) was added and then the solution was allowed to stir at

40 °C for nineteen hours. The reaction mixture was then poured into methanol (10 ml/2 ml reaction mixture) where a beige solid precipitated out. This was repeated three times (by dissolving in dichloromethane first). The white solid obtained was dried at 60 °C. Yield 3.3 g.

Anal. Found: Cl, 3.6 %.

^{1}H NMR (CDCl$_3$): δ 1.0-3.0 (br t, -CH$_2$-CH) 4.5–4.8(br s, CH$_2$-Cl), 6.5-8.0(br d, aromatic).

(29) The betaine-functionalised polystyrene
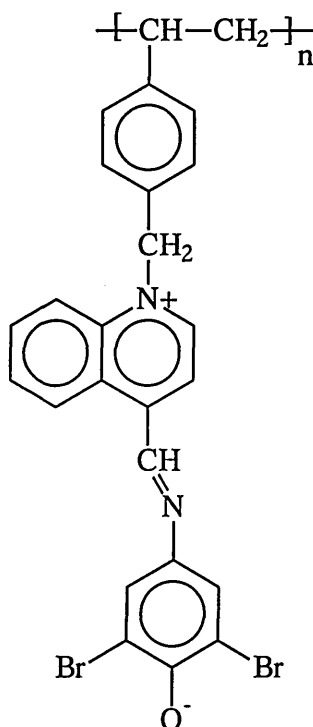
Chloromethylated polystyrene (28) (0.43 g, 0.00047 mol of Cl) was stirred in dry DMF (30 ml) with the dibromo quinoline imine (0.19 g, 0.00047 mol) and silver-*p*-toluene sulphonate (0.13 g, 0.00047 mol) for two days under nitrogen in the dark. The work up procedure was analogous to that of the synthesis of betaine (55) in chapter 2.

After rotary evaporation methanol was added to the dark blue oil that remained and silver iodide was added to the cloudy solution in order to flocculate the solid. The solid was filtered under suction, washing with methanol, and then dried under vacuum. A dark blue solid was obtained. Yield 0.2 g.

Anal. Found: C, 86.03; H, 7.14; N, 2.19 %.

References

1. D. W. Allen and X. Li, *J. Chem. Soc., Perkin Trans. 2*, 1997, 1099.

2. C. Lambert, E. Schmälzlin, K. Meerholz and C. Bräuchle, *Chem. Eur. Journal*, 4(3), 1998, 512.

3. B. K. Mishra, M. Kuanar, A. Mishra and G. B. Behera, *Bull. Chem. Soc. Jpn.*, **69**, 1996, 2581.

4. J. L. Brédas, F. Meyers, B. M. Pierce and J. Zyss, *J. Am. Chem. Soc.*, **114**, 1992, 4928.

5. T. Verbiest, K. Clays, C. Samyn, J. Wolf, D. Reinhoudt and A. Persoons, *J. Am. Chem. Soc.*, **116**, 1994, 9320.

6. C. Dhenaut, I. Ledoux, I. D. W. Samuel, J. Zyss, M. Bourgault and H. Le Bozec, *Nature*, **374**, 1995, 339.

7. A. W. van der Made and R. H. van der Made, *J. Org. Chem.*, **58**, 1993, 1262.

8. M. E. Wright, E. G. Toplikar and S. A. Svejda, *Macromolecules*, **24**, 1991, 5879.

CHAPTER 6

Conclusions and Overview

6.0 Conclusion and Overview

A range of novel Donor-π-Acceptor systems has been synthesised and their solvatochromic properties studied. Many solvatochromic dyes have been proposed as solvent polarity indicators over the years, although the prime aim of the present research was to use solvatochromism as an initial indicator for nonlinear optical (NLO) properties (second harmonic generation). Research into organic and organometallic NLO materials has increased dramatically over the last few decades, as they have many advantages over their inorganic counterparts, which were initially studied as NLO materials for a wide variety of applications, such as telecommunication systems and frequency doubling devices.

A series of long chain phosphoniophenyl imino-phenolate (1) and -imidazolide (2) betaines were synthesised and characterised with a view to studying the formation of Langmuir Blodgett (LB) films as ordered systems. These are the first LB films of phosphonium betaine systems to be characterised; however these betaines absorbed strongly at the second harmonic wavelength (532 nm) of the Nd:YAG laser (1064 nm) used to study their NLO properties at Cranfield University, and therefore further investigation of these compounds was not possible.

CH=N, X, O⁻, P⁺Ph₂, C₁₆H₃₃

Ph₂P⁺, C₁₆H₃₃, N, R
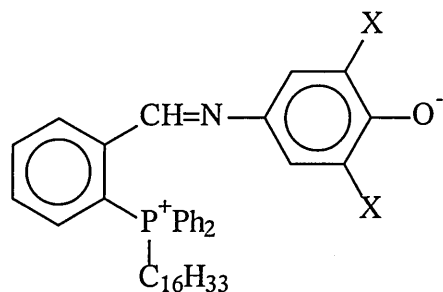
X = Cl, Br, Ph

(1)
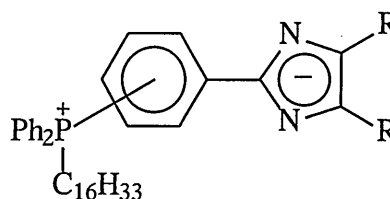
R = Ph, phenanthryl

(2)

However, as the above phosphoniophenyl betaines were still of interest in the area of nonlinear optics, the related triphenyl phosphonionaphthyl analogues of the above systems were subsequently synthesised, to study the effect of annelation which was expected to move the charge transfer absorption band to a longer wavelength, in order that the betaine systems would not absorb at 532 nm.

In observing a fairly large bathochromic shift away from 532 nm with the formation of (3), it would now be interesting to synthesise a long chain analogue so that

LB film formation could be studied, and any potential NLO properties investigated. Unfortunately the wavelength of the charge transfer bands of the naphthyl phosphonium imidazolide systems (4) and (5) were still not shifted far enough away from the second harmonic wavelength of the laser, as the original phosphoniophenyl systems initially absorbed at shorter wavelengths compared to the imino-phenolate systems. Thus further annelation of these systems is required, (i.e. perhaps by forming the anthracene analogues) in order to achieve the desired absorption wavelength before the long chain analogues can be prepared for study of NLO properties of these systems.
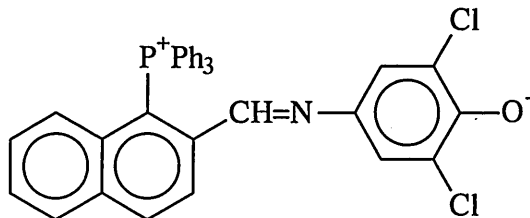
(3)
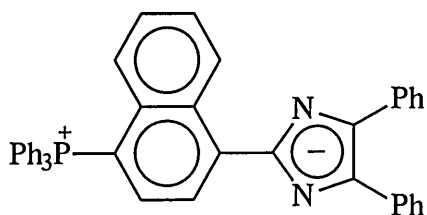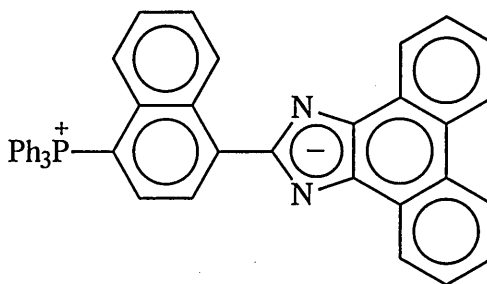
(4)   (5)

Even so, for all of the naphthyl systems prepared, as well as the charge transfer band shifting to a longer wavelength as expected, the degree of solvatochromism was increased, which implies that the first hyperpolarisability β of the betaines will also be increased.

A series of quinolinium betaine systems (6) was prepared and the degree of solvatochromism was found to be greater than that for the pyridinium analogues (7) already reported in the literature.[1] LB films of the quinolinium betaine (6, X = Cl) were prepared and studied for NLO properties, and surface plasmon resonance (SPR) experiments were conducted to explore possible sensor properties. Investigations of these are still being carried out at Cranfield University at the present time and betaine (6, X = Br) is similarly being investigated.

O⁻ ... X ... X ... N ... CH ... N+ ... $C_{16}H_{33}$
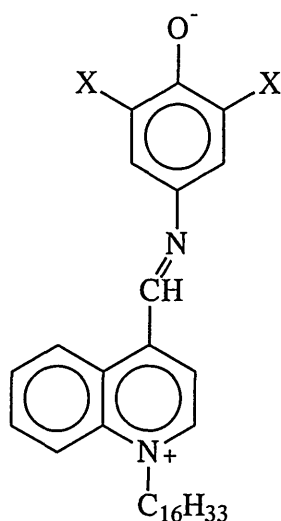
X = Cl, Br

(6)
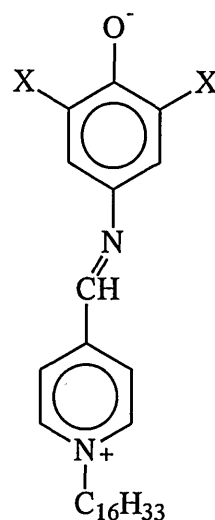
X = Cl, Br, Ph, Buᵗ

(7)

As the phosphonium iminophenolate betaine systems will probably have more potential in the fields of NLO and sensor-science due to their larger degree of solvatochromism compared to that of the phosphonium imidazolide betaine systems, it was decided to restrict further studies to (8, E = P). The positive phosphonium acceptor moiety in these compounds was replaced by the related triaryl arsonium (8, E = As) and stibonium moieties (8, E = Sb), employing a new synthetic procedure. These are the first solvatochromic arsonium and stibonium betaine systems and they exhibit essentially the same degree of solvatochromism as their phosphonium counterparts. This implies that the arsonium and stibonium moieties are just as efficient electron acceptors as the phosphonium moiety, even though their ability to accept an electron pair would expected to decrease from phosphorus to antimony, as the electronegativity decreases down the group, and as the size and energy of the appropriate acceptor d orbitals increases.
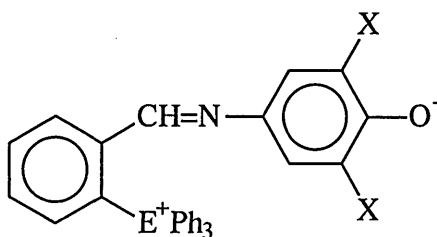
$$E = P, As, Sb$$
$$X = Cl, Br, Ph$$

(8)

This also indicates that upon excitation of the phosphonium iminophenolate betaines, phosphorus does not become involved in d_π-bonding to a significant extent, as the solvatochromic properties of these compounds are comparable to those of the arsonium and stibonium systems. In these systems it would be expected that the d_π-bonding would essentially be non-existent due to the increase in size and energy of the d orbitals which occurs from phosphorus (3d) to arsenic (4d) to antimony (5d).

If significant d_π-bonding had been involved in the phosphonium iminophenolate betaines, then it would have been expected that these compounds would have shown a greater degree of solvatochromism than the arsonium and stibonium analogues, because such bonding would have resulted in a less polar excited state, and hence a larger difference in the dipole moments of the dipolar ground state and the less polar excited state. In contrast, where d_π-bonding is not involved, the difference in the dipole moment between the polar ground state and the slightly less polar ylidic excited state is not so large and such situations would exhibit a smaller degree of solvatochromism.

The arsonium betaines are slightly less solvatochromic than the phosphonium and the stibonium analogues, which was unexpected. If anything, the stibonium betaines would be expected to exhibit the smallest degree of solvatochromism of the three. However, the reduced solvatochromism of the arsonium compounds may be due to a strange anomaly in the chemistry of the elements of the third period, which is also observed for bromine. Arsenic (and bromine) are both reluctant to become five valent which is demonstrated by the well established existence of PCl_5 and $SbCl_5$, in contrast to the recent synthesis of $AsCl_5$,[2] which is much less stable.

In addition to the slightly reduced solvatochromism of the arsonium betaines, further evidence for this anomaly is provided from X-ray structural studies of stibonium

253

(9) and arsonium **(10)** salts by the stronger interaction of antimony with nitrogen compared to arsenic with nitrogen, to form the stiborane and arsorane species respectively. It might have been expected that the antimony–nitrogen distance would have been longer, as a result of size effects.
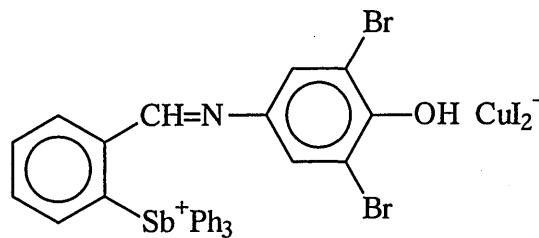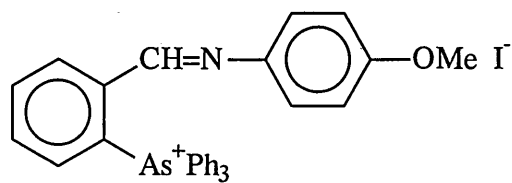
$$\text{(9)} \qquad\qquad \text{(10)}$$

A range of push-pull phosphonium salts was also synthesised, involving the positive phosphonium moiety as the acceptor group and the electron rich ferrocene, thiophene and dimethylaminophenyl moieties as the donor groups. It was anticipated that these systems would show a fair degree of solvatochromism as the phosphonium moiety has been shown to be a good electron pair acceptor in the systems discussed previously. These donor groups have also shown to be efficient in other push-pull systems.[3] However, in the present study these systems showed negligible solvatochromism and furthermore changing the acceptor group to a phosphine oxide moiety also resulted in a lack of solvatochromism. Clearly, in the design of such push-pull systems, there is a need for a much more subtle match of donor and acceptor centres.

The one-dimensional (1-D) pyridinium and quinolinium iminophenolate betaine systems were found to exhibit a larger degree of solvatochromism than the respective phosphonio-phenyl and -naphthyl betaines, (probably due to the reluctance of phosphorus to become involved in d_π-bonding). In consequence, the investigation was extended to explore the systems of related three-dimensional (3-D) pyridinium and quinolinium betaine systems, as it has already been shown that first hyperpolarisabilities increase in the 3-D systems compared to the 1-D analogues.[4] A comparison of the solvatochromism of the 3-D system with the 1-D system could give an initial indication of an increase in the NLO properties. However, the synthesis of these systems has proved difficult, and, at present the degree of chromophore substitution is unknown.

References

1. G.J. Ashwell, K. Sjonnemand, M.P.S. Roberts, D.W. Allen and X. Li, *Colloids and Surfaces A: Physiochem. Eng. Aspects*, in press.

2. W. E. Dasent, *"Nonexistent Compounds"*, M. Dekker, Inc., New York., 1965, pp117.

3. M. J. Long, *Angew. Chem. Int. Engl.*, **34**, 1995, 21.

4. C. Lambert, E. Schmälzlin, K. Meerholz and C. Bräuchle, *Chem. Eur. Journal*, 4(3), 1998, 512.

A copper(I)-catalysed template synthesis of solvatochromic aryl-arsonium and -stibonium systems and a synchrotron structural study of a tetraarylstibonium di-iodocuprate

David W. Allen,[*a] Joanne P. L. Mifflin[a] and Simon Coles[b]†

[a] Division of Chemistry, Sheffield Hallam University, Sheffield, UK S1 1WB
[b] Department of Chemistry, University of Wales, Cardiff, Cardiff, UK CF1 3TB

A route to solvatochromic tetraaryl-arsonium and -stibonium phenolate betaines is described, together with a synchrotron structural study of a precursor arylstibonium di-iodocuprate salt in which both cation and anion have unusual geometries.

Methods for the synthesis of aryl-arsonium or -stibonium salts from tertiary arsines or stibines and aryl halides are limited, the usual route being the reaction of the tertiary arsine or stibine, commonly the triphenyl derivative, and an aryl halide, in the presence of aluminium chloride at >200 °C.[1] We have shown that tertiary phosphines react with aryl halides bearing appropriate donor atoms in the *ortho* position to the halogen in the presence of catalytic quantities of nickel(II) or copper(II) compounds under mild conditions in refluxing ethanol,[2] and were interested in exploring similar template-assisted reactions of triaryl-arsines and -stibines. As triaryl-arsines and -stibines coordinate readily to copper(I) halides to form complexes which are labile in solution,[3] we have investigated their reactions with a series of template aryl halides in the presence of copper(I) iodide, in acetonitrile, and wish to report the formation of tetraaryl-arsonium and -stibonium systems in high yield under these remarkably mild conditions. We have also applied this procedure in the synthesis of the first solvatochromic tetraaryl-arsonium and -stibonium iminophenolate betaines, the properties of which are compared with those of the related phosphonium system. A synchrotron structural study of one tetraarylstibonium salt is also reported, which reveals a significant intramolecular coordinative interaction between the onium centre and the donor atom in the *ortho* position of the template system, and also the presence of a di-iodocuprate(I) anion which interacts with a second di-iodocuprate anion *via* a short copper–copper interaction to give a dinuclear anion.

The reaction of the aryl halides **1** (X = H, Z = OMe; X = Cl, Br, or Ph, Z = OH) with triphenylarsine and copper(I) iodide in acetonitrile under reflux for several hours gave, after pouring into aqueous potassium iodide solution and solvent extraction into dichloromethane, the tetraarylarsonium salts **2** (E = As, Y = I or CuI$_2$) as yellow-brown crystalline solids. ^{1}H and ^{13}C NMR spectra were consistent with the proposed structures. Under FABMS conditions, the arsonium salts gave a characteristic molecular ion for the cation present. The structure of the salt **2** (X = H, Z = OMe, E = As, Ar = Ph, Y = I) was also confirmed by a full X-ray crystallographic study.[4] Similarly, treatment of the aryl halides **1** (X = H, Z = OMe; X = Cl, Br, or Ph, Z = OH) and **3** with triphenyl- or tri-p-tolyl-stibine and copper(I) iodide in acetonitrile under reflux gave the related arylstibonium salts **2** (E = Sb; Ar = Ph or p-tolyl, Y = CuI$_2$) and **4** (Ar = Ph or p-tolyl, Y = CuI$_2$). Again, ^{1}H and ^{13}C NMR spectra were consistent with the proposed structures, and under FABMS conditions, each stibonium salt gave a characteristic molecular ion for the cation present. The nature of the anion present was confirmed by negative ion mass spectrometry. The stibonium salts formed more quickly than the related arsonium salts under the same conditions. Attempts to prepare the related

phosphonium salts using copper(I) iodide as catalyst in acetonitrile were unsuccessful. Clearly, the group 15 ligand must influence crucial stages of the reaction, for which the mechanism is uncertain. A kinetic study of related nickel(II)-catalysed reactions of phosphines with template aryl halides supported a mechanism in which oxidative insertion of an intermediate phosphine–nickel complex into the carbon–halogen bond was the key step, followed by reductive elimination of the arylphosphonium salt and regeneration of the effective catalyst.[5] It is likely that a similar mechanism applies in the above reactions, perhaps involving a copper(I)–copper(III) redox cycle, in which the triaryl-arsine and -stibine ligands are able to stabilise intermediate organometallic species more effectively than the related triarylphosphines.

1 **2** **3** **4**
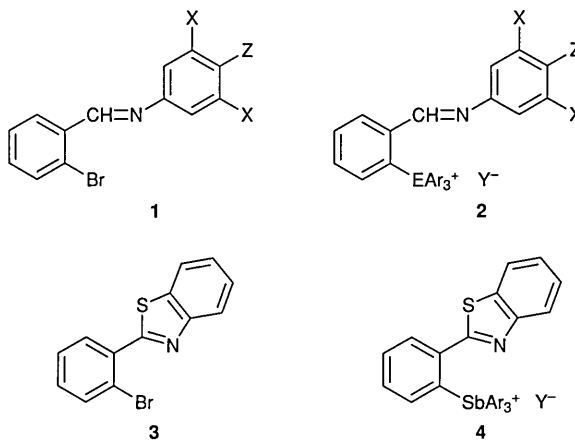
A structural study‡ has been made of the stibonium salt **2** (E = Sb; Ar = Ph; X = Br; Z = OH, Y = CuI$_2$). Routine investigations, using a rotating anode X-ray source, failed to provide data of sufficient intensity to produce a fully refinable structure. Data were therefore collected, upon a crystal of dimensions 200 × 20 × 20 μm, using station 9.8 of the Daresbury SRS.[6] The cation of the observed structure is displayed in Fig. 1 (together with selected bond lengths and angles for both cation and anion). Significant points of interest are the close intramolecular approach of the imino nitrogen to the stibonium centre, the antimony–nitrogen distance (2.65 Å), lying well within the sum of the van der Waals' radii (3.75 Å),[7] and the consequent distortion of the bond angles at antimony from the idealised tetrahedral angle towards a five-coordinate arrangement, consistent with an intramolecular coordinative interaction from nitrogen to antimony to form a five-membered ring. Tetraarylstibonium halides also show considerable distortion from idealised tetrahedral geometry as a result of weak interactions of the stibonium centre with the halide ion, resulting in essentially trigonal bipyramidal structures in which the antimony–halogen bond is unusually long.[8,9] The structure co-crystallises with a 50% occupied CH$_2$Cl$_2$ solvent and the counter-ion, which was found to be di-iodocuprate(I). The CuI$_2$
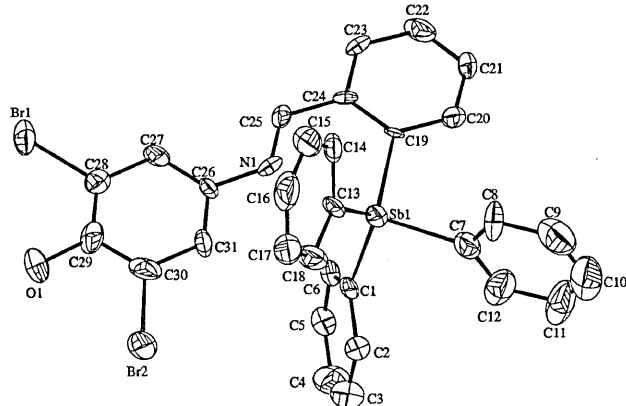
Fig. 1 Structure of the tetraarylstibonium cation with selected bond lengths (Å) and angles (°) for cation and di-iodocuprate anion: Sb–N1 2.65(4), Sb–C1 2.09(2), Sb–C7 2.13(2), Sb–C13 2.13(2), Sb–C19 2.114(14), C25–N1 1.28(2), Cu1–I1 2.508(2), Cu1–I2 2.576(2), Cu–Cu 2.732(4); C1–Sb–C7 106.7(7), C1–Sb–C13 119.2(6), C1–Sb–C19 113.6(6), C7–Sb–C13 102.0(7), C7–Sb–C19 101.4(6), C13–Sb–C19 115.9(6), C19–C24–C25 121.2(14), N1–C25–C24 118.9(13), N1–Sb–C1 83.9(7).

moiety shows a considerable distortion from the expected linear arrangement as a result of a very short copper–copper interaction (2.73 Å) with a second di-iodocuprate anion in the lattice. The stabilisation of poly[dihalocuprate(I)] anions by large phosphonium cations has been documented,[10,11] but the only stibonium salt involving a related anion is that of the copper(II) complex, $(SbPh_4)_2 \cdot Cu_2Cl_6$.[12] However the Cu–Cu separation in this structure is much greater (3.394 Å) than that in the di-iodocuprate(I) counter-ion discussed here. Comparison with other di-iodocuprate(I) anions crystallizing in the same manner shows the Cu–Cu separation to be somewhat greater than in our example (average = 2.95 Å).[13,14]

Treatment of the salts **2** (E = As or Sb; Ar = Ph; X = Cl, Br, or Ph), dissolved in dichloromethane, with aqueous sodium hydroxide solution, resulted in a marked colour change from yellow to red-purple with formation of the related betaines **5**,

5
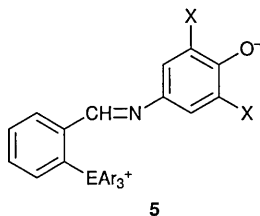
which were subsequently isolated and purified by trituration with diethyl ether. Again, ¹H and ¹³C NMR spectra were consistent with the proposed structures, showing some significant chemical shift changes compared to the parent salts. Under FABMS conditions, cationic molecular ions were again observed. Conversion to the betaines resulted in a significant shift of the visible absorption maximum to longer wavelength. Thus, e.g. λ_{max} for the salt **2** (E = Sb; Ar = Ph; X = Cl, Y = CuI_2) in dichloromethane was observed at 358 nm, whereas for the related betaine **5** in the same solvent, λ_{max} = 536 nm. Significantly, in view of the potential link with non-linear optical properties, the betaines exhibited negative solvatochromism, the visible absorption maximum moving to longer wavelength on moving to a solvent of lower polarity. In the case of the above betaine, λ_{max} moved from 536 nm in dichloro-

methane to 576 nm in THF. The solvatochromic behaviour of the arsonium and stibonium betaines is almost identical to that of the related phosphonium betaines **5** (E = P, Ar = Ph; X = Cl, Br, or Ph) which we reported recently.[15] There is currently growing interest in the optical properties of organic derivatives of the main group 15 elements.[16,17]

Notes and References

† Author to whom crystallographic enquiries should be addressed.
‡ *Crystal data*: $C_{31.5}H_{23}NOClSbBr_2 \cdot CuI_2$, M_r = 1065.87, monoclinic, space group $P2_1/n$, a = 9.259(5), b = 24.785(11), c = 15.100(7) Å, β = 98.998(2)°, U = 3422.6(3) Å³, Z = 4, D_c = 2.069 g cm⁻³, μ = 5.653 mm⁻¹, $F(000)$ = 2000, crystal size 0.2 × 0.02 × 0.02 mm. Data were collected at 160 K, with a wavelength of 0.6875 Å, on a Bruker (formerly Siemens) SMART CCD area detector diffractometer, equipped with a silicon(111) crystal monochromator and a palladium coated focussing mirror on station 9.8 of the Daresbury SRS. ω scans, with a frame increment of 0.3°, were used to cover a hemisphere of reciprocal space, giving θ_{min} = 1.54° and θ_{max} = 20.00° (index ranges $-11 \leqslant h \leqslant 12$, $-26 \leqslant k \leqslant 32$, $-18 \leqslant l \leqslant 19$). Corrections were applied to account for incident beam decay and absorption effects. A solution was obtained *via* direct methods and refined by full-matrix least-squares on F^2. 3520 unique data were produced from 11707 measured reflections (R_{int} = 0.0882). 389 parameters refined to R_1 = 0.0573 and wR_2 = 0.1253 [$I > 2\sigma(I)$] with s = 1.057 and residual electron densities of 0.967 and -1.124 e Å⁻³. CCDC 182/984.

1 J. Chatt and F. G. Mann, *J. Chem. Soc.*, 1940, 1192; G. Doak and L. D. Freedman, *Organometallic Compounds of Arsenic, Antimony, and Bismuth*, Wiley Interscience, 1970, and references therein.
2 D. W. Allen, P. E. Cropper, P. G. Smithurst, P. R. Ashton and B. F. Taylor, *J. Chem. Soc., Perkin Trans. 1*, 1986, 1989; D. W. Allen, I. W. Nowell, L. A. March and B. F. Taylor, *J. Chem. Soc., Perkin Trans. 1*, 1984, 2523; D. W. Allen and P. E. Cropper, *Polyhedron*, 1990, **9**, 129.
3 N. R. Champness and W. Levason, *Coord. Chem. Rev.*, 1994, **133**, 115; G. A. Bowmaker, R. D. Hart, E. N. de Silva, B. W. Skelton and A. H. White, *Aust. J. Chem.*, 1997, **50**, 553; G. A. Bowmaker, R. D. Hart and A. H. White, *Aust. J. Chem.*, 1997, **50**, 567.
4 D. W. Allen, J. P. L. Mifflin, M. B. Hursthouse and K. M. A. Malik, to be published.
5 D. W. Allen and P. E. Cropper, *J. Organomet. Chem.*, 1992, **435**, 203.
6 R. J. Cernik, W. Clegg, C. R. A. Catlow, G. Bushnell-Wye, J. V. Flaherty, G. N. Greaves, I. D. Burrows, D. J. Taylor, S. J. Teat and M. Hamichi, *J. Synchrotron Rad.*, 1997, **4**, 279.
7 A. Bondi, *J. Phys. Chem.*, 1964, **68**, 441.
8 G. Ferguson, C. Glidewell, D. Lloyd and S. Metcalfe, *J. Chem. Soc., Perkin Trans. 2*, 1988, 731.
9 L-J. Baker, C. E. F. Rickard and M. J. Taylor, *J. Chem. Soc., Dalton Trans.*, 1995, 2895.
10 S. Andersson, M. Hakansson and S. Jagner, *Inorg. Chim. Acta*, 1993, **209**, 195.
11 A. Pfitzner and D. Schmitz, *Z. Anorg. Allg. Chem.*, 1997, **623**, 1555.
12 A. Bencini, D. Gatteschi and C. Zanchini, *Inorg. Chem.*, 1985, **24**, 704.
13 H. Hartl, I. Brudgam and F. Mahdjour-Hassan-Abadi, *Z. Naturforsch., Teil B*, 1985, **40**, 1032.
14 M. Hofer and H. Hartl, *Z. Anorg. Allg. Chem.*, 1992, **45**, 612.
15 D. W. Allen and X. Li, *J. Chem. Soc., Perkin Trans. 2*, 1997, 1099.
16 C. Lambert, S. Stadler, G. Bourhill and C. Brauchle, *Angew. Chem., Int. Ed. Engl.*, 1996, **35**, 644.
17 C. Lambert, E. Schmalzlin, K. Meerholz and C. Brauchle, *Chem. Eur. J.*, 1998, **4**, 512.

Received in Cambridge, UK, 23rd July 1998; 8/05759A